Development of Novel Slow-Release Micronutrient Fertilizers Using Mechanochemical Synthesis

Bo Zheng

B.Sc. (Hons.) Agricultural Sciences (Soil science)

Fertilizer Technology Research Centre

School of Agriculture, Food and Wine

The University of Adelaide

A thesis submitted in fulfilment of the requirements for the degree of

Doctor of Philosophy

May 2023

Abstract

This thesis investigated the possibility of applying a green mechanochemical synthesis method for the formulation of boron (B) and molybdenum (Mo) fertilizers. More generically, the aim was to combine sustainable engineering and fertilizer manufacturing. The thesis consists of 6 chapters, including an overview of the literature relevant to this project (Chapter 1). Subsequent chapters describe the development of B and Mo fertilizers using mechanochemistry with the aim to produce micronutrient fertilizers or micronutrient-enriched macronutrient fertilizers which would display a range of solubilities of B and Mo and reduce wasteful losses of these nutrients through leaching in high-rainfall environments.

Formulations were developed using a range of manufacturing variables, such as reactant species, reactant concentrations and ratios, milling time and post-milling activation treatments (e.g. water assisted reaction). Formulations were characterized by various chemical and spectroscopic techniques, and these characteristics were related to solubility determined in batch and kinetic tests. Finally, agronomic evaluation of the most promising products was undertaken in pot trials using protocols to simulate high leaching environments.

Three different types of micronutrient fertilizer were synthesized using mechanochemistry. Firstly, a sparingly soluble zinc borate was successfully synthesized using ZnO and B_2O_3 as raw materials by a simple mechanochemical process that, when scaled up, would be energy efficient and have a low environmental footprint. Mechanochemical synthesis of zinc borate was compared with conventional wet or hydrothermal methods in terms of waste generation using a sustainability metric called the E(nvironmental) Factor. The E factor for mechanochemically synthesized zinc borate was 1.7 kg waste/kg product compared to 77.5-250 kg waste/kg product for conventional synthesis methods. Secondly, a slow-release Mo fertilizer with a layered structure was mechanochemically synthesized from ZnO, $ZnSO_4 \cdot 7H_2O$ and MoO_3, with the final formulation containing zinc hydroxide sulfate (ZHS), together with low solubility zinc molybdenum oxide hydrate ($Zn_5Mo_2O_{11}.5H_2O$) and its less hydrated analogue. Thirdly, a different type of slow-release Mo-Zn fertilizer was synthesized by mechanochemical treatment of ZnO and MoO_3. Using these compounds, micronutrient-enriched macronutrient fertilizers were produced by coating or co-compaction. The Mo-containing compounds were not assessed using the E-factor, as no comparable methods which synthesize the same compounds were identified in the literature. However, the mechanochemical procedure used to synthesize the formulations did not generate any waste streams. In addition, the treatment with mechanochemically treated 4% Mo-Zn fertilizer showed significantly less leaching than the control without ball milling and the DAP co-compacted with 4% Mo had a higher plant Mo update compare to other Mo sources.

Mechanochemical synthesis methods were successful in producing formulations that demonstrated slow-release characteristics for B or Mo using highly soluble raw materials. The environmental footprint of the proposed mechanochemical synthesis methods was smaller than traditional synthesis techniques. Mechanochemistry therefore offers an opportunity to transform micronutrient fertilizer manufacturing methods. The products made need to be evaluated not only for their manufacturing footprint but also for their agronomic and environmental performance and their compatibility with current nutrient delivery systems.

Table of Contents

Declaration

I certify that this work contains no material which has been accepted for the award of any other degree or diploma in my name, in any university or other tertiary institution and, to the best of my knowledge and belief, contains no material previously published or written by another person, except where due reference has been made in the text. In addition, I certify that no part of this work will, in the future, be used in a submission in my name, for any other degree or diploma in any university or other tertiary institution without the prior approval of the University of Adelaide and where applicable, any partner institution responsible for the joint award of this degree.

The author acknowledges that copyright of published works contained within the thesis resides with the copyright holder(s) of those works. I give permission for the digital version of my thesis to be made available on the web, via the University's digital research repository, the Library Search and also through web search engines, unless permission has been granted by the University to restrict access for a period of time.

I acknowledge the support I have received for my research through the provision of an Australian Government Research Training Program Scholarship acknowledge the support

Bo Zheng

May 2023

Preface

This project investigated the possibility of applying the green synthesis method - mechanochemistry to the formulation and agronomic application of B and Mo micronutrient fertilizers. The thesis consists of 6 chapters, including an overview of the literature relevant to this project (Chapter 1). Chapter 6 summarizes the main contribution of the thesis and recommendations for future work.

The remaining chapters are in publication format (Chapters 2, 3, 4 and 5) which include

- Published manuscript - Chapter 2

  Mechanochemical Synthesis of Zinc Borate for Use as a Dual-release B Fertilizer

  ACS Sustainable Chem. Eng. 2021, 9, 47, 15995–16004.
  https://doi.org/10.1021/acssuschemeng.1c07111

- Manuscript accepted for publication by the Journal of Soil Science and Plant Nutrition - Chapter 3

  Agronomic Comparison of Mechanochemically Synthesized Zinc borate and Other Boron Sources Granulated with Macronutrient Fertilizers.

- Manuscripts prepared for submission - Chapters 4 and 5

  Chapter 4 - Mechanochemical Synthesis of Layered Zn-Mo Compounds as Slow-release Mo Fertilizers.

  Chapter 5 - Co-granulation of Mechanochemically Processed MoO3-ZnO Mixtures with Macronutrient Fertilizer Affects Mo Supply to Plants-

Acknowledgements

I wish to show my gratitude to all the people fighting for human and humanity in the COVID-19 pandemic.

It has been a very different, challenging but fruitful life journey over the past years since 24th August 2017 I commenced my PhD candidature. My deepest and sincere gratitude goes to my principal supervisor Mike McLaughlin for taking me as his student when I am truly lost. Mike has offered me unlimited support and unconditional guidance during my PhD journey. During the COVID pandemic, I couldn't continue my PhD work for more than 18 months. Mike has provided all the help and support academically and mentally. Mike has shown me what an intelligent scientist and outstanding person looks like. I hope, someday, I could have my own group of students and be a person like him. My gratitude extends to my Co-Supervisor Fien Degryse for invaluable advice, continuous support, and patience every time I knocked on her door. Her immense knowledge and plentiful experience have encouraged me in all the time of my academic research as a female scientist.

I am deeply grateful to Ivan Andelkovic and Roslyn Baird who have provided fruitful discussion, valuable guidance and encouragement throughout the project. A special thanks to Shervin Kabiri and Rodrigo da Silva for all the mentoring and support and I couldn't make it to this stage without any of you. I would like to pay respect to all the technical staff in Mike's group, with special thanks to Colin Rivers, Bogumila Tomczak, Ashleigh Broadbent and Andrea Paparella. You all have provided all the help and support as both technical staff and friends.

Thank you to the University of Adelaide, for awarding me with a scholarship to complete this life journey. I am grateful for the one-year scholarship from the School of Agriculture, Food and Wine. I also want to thank all the staff from the University of Adelaide who provided me with help and support.

To my friends, Xueying Feng is one of the nicest people I know on earth, a dog person, and a fascinating soul. It was the best friendship I gain during this journey. Thanks for always being there for me. I want to acknowledge all my friends I meet during this long journey, Jinchen Li, Danchen Zhu, Chen Rao, and Cathy Xiao. I also want to thank all my officemates and friends, Jacinta Dockerill and Emma Knight for all the laughs, support and cake time we had together.

To my family. My deepest respect, appreciation and love to my parents, thank you for believing in me and supporting me every step of the way. Like you hold my hands when I was little, I hope to hold yours as long as I can. I would like to dedicate my thesis to my grandparents, all the good things in me are from you and your unconditional love. I want to acknowledge Yuanlin Qi, who has loved me like my family.

List of Abbreviations

AMT	Ammonium molybdate tetrahydrate	**LDH**	Layered double hydroxide
ANOVA	Analysis of variance	**LHS**	Layered hydroxide salts
ARW	Artificial rain water	**MAP**	Monoammonium phosphate
ATP	Adenosine triphosphate	**MC**	Mechanochemistry
ATR	Attenuated total reflectance	**MOP**	Muriate of Potash
BPR	Ball-to-power ratio	**OM**	Organic matter
CEC	Cation Exchange Capacity	**P**	Probability
CRF	Control release fertilizer	**pH**	The negative log of hydrogen ion activity, (-log[H^+])
DAP	Diammonium phosphate	**RO**	Reverse Osmosis
DI	Deionized water	**SRF**	Slow release fertilizer
DTG	Derivative Thermogravimetry	**TGA**	Thermogravimetric analysis
FE-SEM	Field emission scanning electron microscopy	**WAR**	Water assisted reaction
FTIR	Fourier transform infrared	**XRD**	X-ray diffraction
GHG	Greenhouse gas	**ZHS**	Zinc hydroxide sulphate
ICP-OES	Inductively coupled plasma - optical emission spectroscopy		

Chapter 1 Literature Review

1.1 BACKGROUND

Mechanochemistry is the use of mechanical force to drive chemical transformations without the need for bulk dissolution. The use of mechanochemistry for the synthesis of slow-release fertilizers can offer several advantages over conventional wet chemical methods. With the increasing cost of electricity generation and slow uptake of renewable energy, fast fertilizer synthesis employing purely mechanochemical processing is more sustainable than solvent-based methods as it generates less waste, obtains high conversion rates with shorter reaction times and requires no heating or high pressure. Mechanochemistry can also create unique and novel compounds that cannot be synthesized using solution-based processes. The nutrient release rate of mechanochemical synthesized fertilizers can be simply manipulated by adjusting the stoichiometric ratio of reactants or the force applied during synthesis. This thesis explores the use of mechanochemistry for synthesis of micronutrient fertilizers, specifically boron (B) and molybdenum (Mo) fertilizers.

1.2 ESSENTIAL NUTRIENTS AND MICRONUTRIENTS FERTILIZERS

1.2.1 Essential nutrients

Carbon, hydrogen and oxygen are the structural elements of plants that can easily be accessed from air and water, however, access to other mineral nutrients required for plant metabolism is frequently limited by the nature of the soil. The definition of “essential” is based on the responses of plants when a given nutrient is low in concentration or absent.

The widely accepted criteria for an essential nutrient are a) plants cannot complete their life cycle without this nutrient; b) this nutrient is involved in a metabolic process; c) this nutrient is not replaceable (Mengel et al., 2001b). The nutrients can be further divided into two major groups, the macronutrients that are required in higher concentrations in plants and the micronutrients that are required in relatively low concentrations but are equally important for plants (Kirkby, 2012).

Intensive farming depletes the soil of essential nutrients if they are not resupplied through fertilizers. Mineral fertilizers have been the most significant contributors to modern agriculture and have increased crop yields by around 50% during the 20th century (Borlaug, 1994, Fageria et al., 2008). Mineral fertilizer inputs of crop nutrients are essential to secure the global food demand with increasing world populations. The prediction is that medium population growth will result in 9.4-10.2 billion people by 2050 with an increase of around 35 million per year (UN, 2012). Moreover, there are 815 million undernourished people around the world and 151 million children under age 5 are suffering stunting (UN, 2017). Furthermore, continued urbanization may decrease the area of land available for agriculture thus putting more stress on the existing land for food production (UN, 2015). A meta-analysis from Ray et al. (2013) shows insufficient crop production by 2050 according to current yield trends for important crops. Considering urbanization and nature conservation, it is not ideal to increase the amount of agricultural land, instead, the projected food production must be achieved by sustainable intensification, which includes more efficient fertilizer management (Balmford et al., 2005). With more intense farming practices, more and more areas observe micronutrient deficiency and related risks to livestock and human health. In addition, different micronutrients behave very differently in soil and some of them have a very small window between deficiency and toxicity. More precise and efficient micronutrient application is required to effectively increase crop yield and avoid unnecessary accumulation in soil.

1.2.2 Micronutrients

Micronutrients are only required by crops in very small amounts, however, plants will fail to achieve optimum yields if one of the nutrients is deficient. Copper (Cu), iron (Fe), manganese (Mn), Mo, zinc (Zn) and nickel (Ni) are metals or transition metals that are essential micronutrients for plant metabolism. Molybdenum is needed by different enzymes of plants to perform redox-reactions, in particular molybdopterin, which is required by many enzymes involved in N fixation, nitrate reduction and nitrogen transport at their catalytic sites (Mengel et al., 2001b, Barker and Pilbeam, 2006, Broadley et al., 2012, Hawkesford et al., 2012). Zinc is present in the soil as a cation and is commonly deficient in calcareous soils (Alloway, 2009). Zinc deficiency remains a global health problem that is estimated to affect 17% of the global population (Myers et al., 2015).

Other micronutrients are non-metallic elements which include B and chlorine (Cl). Chorine is involved in photosynthesis and osmotic regulation. The physiological and metabolic behavior of B in plant growth and function is still not clear and is least understood among all other nutrients. Unlike other micronutrients, B is neither a constituent nor an activator of an enzyme. The clearest role of B in plant growth is as a cross-linkage for a compound associated with primary cell wall development. Other functions involving B are sugar transport, reproduction, phytohormone regulation, nucleic acid metabolism and tissue structure.

1.2.3 Interactions with soil and leaching risk of micronutrients

The interactions of nutrients with soil particles, soil solution, and air can significantly influence or even limit the availability of nutrients to plants. Adsorption is a process that retains nutrients in or on the solid soil phase. Clay particles, organic matter (OM), and metal oxide or hydroxides are responsible for controlling the soil surface charge, and in turn, influence sorption and desorption of nutrients. The negative charge on a clay mineral is generally caused by the isomorphic substitution of Si^{4+} by Al^{3+} in the tetrahedral and Al^{3+} by Mg^{2+} and Fe^{2+} in octahedral layered silicates. The isomorphic reactions induce a permanent negative charge, which is always neutralized by interlayer cations (Essington, 2015). The other charges within the soil are called pH-dependent charges which depend on both mineral and OM surfaces and environmental conditions. In general, nutrients need to be transported by soil solution through mass-flow and diffusion. As a result, the transport from soil to plant is generally faster when the concentration of nutrients in soil solution is higher, but the amount of nutrients that are present in soil solution is generally low compared with the actual amount of nutrients required by the plant (Mengel et al., 2001b). The ability of soil to maintain the nutrient concentrations in the soil solution (nutrient buffer capacity) varies with soil characteristics, such as soil texture, soil structure, soil OM content and soil pH.

Micronutrient fertilizers have been largely involved in agricultural practice since the last century. Most of the micronutrients (Cu, Fe, Mn, Ni and Zn) are present in the soil as metallic cations and show relatively strong adsorption to soil. Thus, soluble forms of these fertilizer are generally preferred. However, some of the micronutrients are harder to manage in practice, as the major or plant available form in the soil solution is mostly in an unionized form (B) or anion (Mo). As a result, adsorption is weak in most soils and there is therefore a higher risk of leaching and runoff than with other micronutrients. Boron deficiency is a worldwide problem, as the predominant form of B in soil solution is boric acid (H_3BO_3), which is an unionized form with little retention in soil (Mengel et al., 2001a). Most B deficiency occurs in soils that are highly weathered, have good drainage, are in high rainfall regions and are under regular cropping (Shorrocks, 1997a). Further, the mobility of B in phloem is very limited in many crops (Raven, 1980), while B is constantly required by the plant for cell wall growth (O'Neill et al., 2001), thus B needs to be available for plant uptake throughout the whole growing season. However, the optimum soil solution concentration is very narrow with a small difference between sufficiency and toxicity (0.3 to 1 mg B L^{-1}) (Asad et al., 2001). Therefore, the management of B fertilizer application is very challenging, with the aim to continue supply of enough B throughout the crop growth cycle but not cause seedling toxicity. Slow-release B fertilizer that can provide a B supply over the whole growing season is ideal to consider as a B fertilizer for more effective management.

On the other hand, Mo deficiency is mostly caused by Mo fixation in acidic soils. Molybdenum occurs mainly as molybdate (MoO_4^{2-}) in soil solutions with pH>4.2 and can be adsorbed on oxide surfaces in acid soils. Molybdenum deficiency therefore generally occurs in highly weathered acidic, well-drained, and frequently cropped soils (Jones and Belling, 1967). If Mo content in soil is high enough, liming of the soil decreases the adsorption and hence increases the availability (Kamprath and Foy, 1985). On the other hand, a high concentration of water-soluble Mo in alkaline soils might be lost through soil leaching. Molybdenum is also continuously required by plants to maintain metabolism with various types of molybdoenzymes. Particularly, legumes are more sensitive to Mo deficiency as the molybdoenzymes are the key enzymes for inorganic N assimilation. (Mendel and Hänsch, 2002, Kaiser et al., 2005). For non-legume plants, molybdoenzymes are associated with the catabolism of sulfur-containing amino acids (Williams and Fraústo da Silva, 2002). In contrast to B, crop yield decrease due to Mo toxicity is rare; however, high Mo concentration in plants are a concern with regards to animal health, as excessive intake can cause molybdenosis in grazing animals (Miller et al., 1991). Therefore, slow or controlled-release Mo fertilizer with a low risk of leaching and build-up is required, particularly for pasture legumes.

1.2.4 Conventional micronutrient fertilizers and environmental concerns

The consumption of major fertilizer nutrients is predicted to reach 223.1 million tons by the end of 2030 (Albino et al., 2012). However, there is increased environmental concern regarding fertilizer inputs in terms of greenhouse gas (GHG) emissions (Akiyama et al., 2010), groundwater eutrophication or contamination (Badruzzaman et al., 2012; Daniel et al., 1998), accumulation of potentially toxic trace elements (Jiao et al., 2012), and soil degradation (Shaviv and Mikkelsen, 1993). These concerns are due, for the most part, to excessive nutrient accumulation in soils (Shaviv, 2001) or asynchrony in the nutrient application and plant uptake leading to nutrient leaching, runoff or emissions of GHG to the atmosphere (Timilsena et al., 2015).

Most soils have a sufficient total content of most metal micronutrients; however, the bioavailability of the nutrient is often insufficient for regular cropping practice (Mikula et al., 2020). Both deficiency and toxicity are regularly observed during agricultural practice when precise application cannot be achieved with conventional fertilizers. Most micronutrients are directly applied as soluble salts to soil, to foliage or to seeds, or applied with pesticides or macronutrients (Mortvedt, 1985). Soluble micronutrient fertilizer is the most common form applied in agricultural practice, as they can quickly compensate for the deficiency. However, the use of soluble fertilizer can have several disadvantages: a) they can easily leach or run off from soil; b) they can precipitate with other nutrients in soil solution; c) they can be adsorbed by soil particles; d) they can cause stress or toxicity to seed or plants; and e) they can be deficient later in the season due to losses or excessive uptake early in the season. For some micronutrients (Cu, Fe, Zn), the long-term build up might induce phytotoxicity (Chaney and Giordano, 1977) and even stimulate oxidative stress (Blasco et al., 2018). For grazing practice, micronutrient application needs even more precise application, as the accumulation of micronutrients might harm the health of animals (Gupta, 2019; Gupta et al., 2008). Foliar application can correct deficiency efficiently with small and accurate amounts of nutrients, however, the uptake and transport from leaves to other parts of the plants vary widely between plant species, growth stages and physical characters of the plant leaves (Fernandez and Brown, 2013). Moreover, careful application with intensive labor is required. High concentrations might cause leaf burn, while if the concentration is too low, multiple applications are required to correct the deficiency. Moreover, there are no residual effects of foliar application (Fageria et al., 2002).

With rising awareness regarding “precision” and “sustainable agriculture, there is a shift in recent years that agriculture practice should aim to obtain optimum yield with minimal input (Capmourteres et al., 2018). Therefore, fertilizers which are environmental-friendly, economical, and sustainable are needed to address these challenges. To ensure that the proper use of fertilizer is beneficial for crop production and to reduce environmental aspects associated with their use, researchers and the fertilizer industry are continually seeking to improve fertilizer nutrient use efficiency and minimize environmental threats (Chien et al., 2009). Moreover, to achieve more precise cropping practice, the plant's access to optimum micronutrients through all growth stages needs to be ensured when considering new fertilizer formulations (Mikula et al., 2020). Therefore, slow and controlled-release fertilizers (SRFs/CRFs) are a promising strategy for reducing environmental threats related to fertilizer use.

1.2.5 Existing slow-release micronutrient fertilizers

Slow and controlled-release fertilizers (S/CRFs) have been extensively studied as a better approach to improve nutrient use efficiency. These fertilizers can potentially produce more food without harming the environment. In general, S/CRFs can be classified in three groups (Shaviv and Mikkelsen, 1993; Shaviv, 2001): a) fertilizers with a physical barrier controlling nutrient release; b) low solubility inorganic compounds; c) degradable organic compounds with low solubility. Fertilizers and substances with the criteria described above are expected to better supply nutrients in synchrony with plant demand, resulting in a higher use efficiency and fewer environmental effects. Compared to NPK fertilizers, the area of developing slow/controlled released micronutrients has not been explored in depth. Existing slow/controlled release micronutrient fertilizers applied in the agriculture practice are summarized in Table 1.1.

Table 1.1 Examples of slow-release micronutrient fertilizers used in agricultural practice (summarized from Hignett and McClellan (1985), Mortvedt (1991), Mortvedt (1994)).

Forms	**Elements**	**Examples**
Partially soluble	Cu, Mn, Ca, Zn, Mo, B	$CuSO_4 \cdot 3Cu(OH)_2 \cdot H_2O$, CuO, $MnCO_3$, MnO, $CaMoO_4$, ZnO, $ZnCO_3$, Colemanite, Mn oxysulfate, MoO_3, $ZnSO_4 \cdot 4Zn(OH)_2$, Zn oxysulfate
Frits	Fe, B	Fritted Fe, Fritted B
Fine metal particles	Cu, Zn	Cu, Zn alloys
Organic fertilizers	Zn, Fe, Cu, Mn	Digest liquors, phenols
Coated fertilizer	Mn Zn, Fe	Sulfur coated Fe/Mn/Zn

Two types of low-solubility micronutrient products have been used by the fertilizer industry: a) low solubility inorganic compounds; and b) degradable organic compounds. The inorganic low-solubility or partially soluble micronutrient fertilizers are the earliest micronutrient S/CRFs applied in practice. Low-solubility micronutrients are generally cheaper than organic micronutrient fertilizers. Their plant availability can be adjusted by particle size and methods of application such as powdered or bulk blended with macronutrients. Similarly, the effectiveness of the frit products is also controlled by the particle size, and as these tend to be very slow releasing, they are usually only applied in sandy soils under high rainfall (Mortvedt, 1985). Most frits applied in practice are B frits, as B is the micronutrient that is most prone to leaching losses (Mortvedt, 1994). Both frits and fine metallic particles are used to maintain the micronutrient level rather than correct severe deficiencies, as the solubility and bioavailability are very limited in most cropping systems.

1.2.6 Novel technologies for micronutrient fertilizers

In recent decades, new technologies for micronutrient fertilizer synthesis have emerged including: a) newly formulated low solubility inorganic compounds; b) nano-fertilizers; c) layered materials onto which micronutrients are loaded; d) newly formulated organic compounds. One of the examples of low solubility inorganic compounds is phosphate or polyphosphate products. The polyphosphate can be prepared by heating phosphoric acid at 200-300 °C with multiple micronutrients, such as Fe (Chandra et al., 2009), Zn-Fe-Mn-Cu (Bandyopadhyay et al., 2014), Fe-Mn (Bhattacharya et al., 2007), Mo (Bandyopadhyay et al., 2008a) to attach the micronutrient to polyphosphate, and B (Abat et al., 2015d, Abat et al., 2015a, Abat et al., 2015c) to synthesize boron phosphate. To complete the synthesis of phosphate or polyphosphate, some of the studies followed the phosphoric acid treatment by a neutralization and drying procedure.

Mineral-based nanocomposites have been proposed to be used as a more sustainable carrier for micronutrients delivery, where the minerals are compounds that generally exist in nature such as montmorillonite-Fe (Gharekhani et al., 2018), zeolite-Fe-Zn-Cu (Lateef et al., 2016) and clay-added hydrogel-B (Bortolin et al., 2016).

Another major body of proposed micronutrient fertilizers are loading micronutrients (B, Zn, Cu and Fe) into biodegradable materials such as chitosan, cellulose, starch alginate (Knijnenburg et al., 2021, Akalin and Pulat, 2019, Kumar et al., 2018), and modified biochar (Yao et al., 2013, Khan et al., 2021).

Layered structures such as layered double hydroxides (LDHs) and graphene-based materials have been investigated as micronutrient carriers in recent years. The widely accepted formula for these LDHs can be $[M^{2+}_{1-x}M^{3+}_{x}(OH)_2][A^{n-}]_{x/n}\cdot zH_2O$, where M^{2+} is a divalent cation such as Mg^{2+}, Ca^{2+}, Zn^{2+} or Ni^{2+}, M^{3+} is a trivalent cation such as Al^{3+},

Fe^{3+} or Mn^{3+}, and A^{n-} is the exchangeable inorganic or organic anion which can be released or adsorbed between the layers ("guest anion"). Other possible structures with different valences of metallic cations have also been proposed such as Ti^{4+}, Sn^{4+}, Li^{+} and Mo^{6+} (Qu et al., 2016; Wang and O'Hare, 2012). LDHs have been proposed as slow-release fertilizers for micronutrients, with B and Mo serving as the guest anions (Everaert et al., 2021b, Songkhum et al., 2018, Castro et al., 2020).

1.2.7 Water use efficiency, carbon footprint and agricultural sustainability

The fertilizer industry is always facing environmental concerns and these concerns have been linked to many associated agricultural changes. Besides introducing more efficient fertilizer products, many chemical fertilizer manufacturers have started to design and construct their plants more sustainably or effectively. Large amounts of effluent containing N, P, K, S, F, Si and other trace elements are produced during fertilizer manufacturing. Several efforts have been made in the fertilizer industry to minimize the adverse effects of pollutants: a) new technologies for acid absorption; b) new technologies for gas absorption; c) avoiding raw materials with high pollutant content; d) better effluent recirculation; e) engineering evolution for infrastructure; and f) non-pollutant innovative processing approaches (Hodge, 1994). A new carbon footprint assessment in the fertilizer industry has been proposed to count both direct and indirect emissions related to processing, energy consumption and waste or wastewater as CO_2 equivalent for a given fertilizer. To minimize the environmental effects of fertilizer production, a more sustainable manufacturing approach should be considered. In recent years, many engineered materials have been proposed with a more sustainable manufacturing process, such as recovering N, P, K and heavy metals from the wastewater of the fertilizer industry (Maine et al., 2019, Sabiha et al., 2009, Cánovas et al., 2017, Gouider et al., 2014). However, most of the recovery processes lack energy/cost analyses and atom efficiency of the procedure (Beckinghausen et al., 2020). Compared to the treatment of the effluents, it could be more beneficial to consider more sustainable manufacturing with less effluents production. One of the concepts introduced in 1991 as a green metric for the chemical industry was the E Factor. The E factor is defined as the mass ratio of waste to the final products, which included all of the auxiliary components such as water and solvent for washing. Roschangar et al. (2015) suggested the calculation of a simple E factor (sEF) and a complete E factor (cEF) as full-scale manufacturing E factors generally fall between these two metrics. In a recent survey, water usage was the most used metric to assess green chemistry in commercial manufacturing (Giraud et al., 2014).

1.3 HISTORY, MECHANISM AND INDUSTRIAL APPLICATION OF MECHANOCHEMISTRY

1.3.1 Definition and history of mechanochemistry

The official definition of a mechanochemical reaction from IUPAC (Horie et al., 2004) is "a chemical reaction that is induced by the direct absorption of mechanical energy". Mathew Carey Lea was the first person who separated mechanochemical reactions from thermochemical reactions in the 1890s, when silver and mercuric chloride were decomposed by grinding while they remained undecomposed under heating (Takacs, 2004). Current studies have separated thermal- and mechano-chemistry through the reaction pathways and product classification for both inorganic and organic materials (Konôpka et al., 2008, Hernandez and Bolm, 2017). The earliest model and theory of mechanochemistry can be found during the mid-20th century, known as the hot-pot theory and magma-plasma model (Bowden and Yoffe, 1958, Thiessen et al., 1967, Baláž et al., 2013). The hot-pot theory and magma-plasma model were developed by considering frictional heating and associated free energy release (Baláž et al., 2013). Presently, mechanochemistry is recognized as a sub-discipline of physical chemistry that is at the same level as thermochemistry, electrochemistry and photochemistry, and has been linked to quantum chemistry in the last two decades (Stauch and Dreuw, 2016).

Mechanical activation is a fundamental term in mechanochemistry. Solids exposed to mechanical activation will experience four processes to achieve activation: a) decreasing particle size and accumulating defects, b) plastic deformation and amorphization, c) formatting of metastable polymorphous forms; and d) completion of chemical reactions (Juhasz, 1998; Boldyrev and Tkáčová, 2000; Baláž, 2008a). Specifically, the defects accumulated in the first process can be point defects, dislocations, the disordering of grain boundaries, and the increasing of amorphous regions and two-phase regions. Further, the metastable forms are achieved by structural relaxation of which several different channels are available according to the nature of reactants such as heating, new interfaces, aggregation, recombination, adsorption, imperfection and the chemical reaction between adjoining particles, etc. (Boldyrev, 2006, Baláž, 2008b).

Structure relaxation is a vital part of mechanical activation because it determines the reactivity of the activated solid, some being short-lived states or others long-lived states. The short-lived states might only temporarily occur in mechanochemical reactions (Boldyrev, 2006, Baláž, 2008b). Overall, mechanochemical activation firstly increases substance reactivity by increasing surface free energy and surface area, and decreases the cohesive energy of solids. In the activated system during milling or after milling, spontaneous processes may occur such as aggregation and agglomeration with a decreased surface area (small particles aggregated as a larger particle), wetting and recrystallization with an ordered internal structure, or mechanochemical reactions (Juhasz, 1998).

Mechanical alloying in industry existed long before the understanding of mechanochemistry. This process involves deformation, cold welding, fracturing and rewelding of powder particles in a high-velocity ball mill. J.S. Benjamin invented this method around the mid-1960s and work thrived in the 1980s (Suryanarayana et al., 2001). Later, mechanochemical activation was used to produce oxide dispersion-strengthened Ni and Fe-based superalloys for the aerospace industry (Benjamin and Shingu, 1992). Nowadays, mechanical alloys are produced through mills with more than 1,000 kg capacity for commercial purposes (Baláž et al., 2013). Another early development of industrial mechanochemistry was in the building industry for the production of silicate concrete through the mechanochemical activation of quartz (Juhász and Opoczky, 1982, Baláž and Dutková, 2009). In the hydrometallurgical industry, the earliest application of mechanochemistry on an industrial scale was in Austria in which a pilot plant of Lurgi-Mitterberg tested the leaching of mechanically-activated chalcopyrite by flotation (Biangardi and Pietsch, 1976). Mechanical activation in this pilot plant achieved 95% Cu extraction (Baláž and Dutková, 2009). Later, Australians invented the active process where ultra-fine milling was involved and where recovery rates of 98.2%, 88.3% and 82.9% of Ni, Co and Cu from ores were achieved, respectively (Palmer and Johnson, 2005). In the material industry, diborane (B_2H_6) has been mechanochemically synthesized in solvent-free conditions for the semiconductor industry (Anderson, 2001). In the pharmaceutical industry, acetylsalicylic acid salts were produced by conventional methods with a complex and expensive purifying process on a small scale. Later, an anti-inflammatory drug with β-cyclodextrin was also synthesized by high-energy milling for production-scale in Italy (James et al., 2012b). Mechanochemistry was also applied in the waste management industry for asbestos fiber destruction in Germany (Baláž and Dutková, 2009).

1.3.2 Milling equipment and process parameters

Mechanochemistry requires high-energy inputs to accumulate solid-phase defects for further activation and synthesis. The mechanical devices provide single or combined mechanical stress as summarized in Table 1.2.

Table 1.2 The common mechanical stress provided by different devices (summarized and adopted from Boldyreva (2013)).

Mechanical stress	Mechanical devices
Impact 	Pin mill, jet mill
Shear 	Rollers
Impact & Shear 	Ball mill, attritor, vibration mill, planetary mill

Baláž et al. (2013) summarized the variables that could influence the milling process as: a) type of mill, b) material of milling media (chamber, vial and balls), c) ball-to-powder ratio, d) extent of filling of the milling chamber, e) milling atmosphere, f) milling speed, and g) milling time. Depending on the physical and chemical properties of the reactants, such as size, phase and oxidation state, several different mills in Table 1.2 can be used to perform mechanochemical reactions. For example, wet milling generally will not be performed in a vibration mill and changes in atmospheric conditions can only be performed in certain mills. On the laboratory scale, mills like SPEX shaker mills with high energy input and low capacity are ideal for research purposes.

Ball-to-powder ratio (BPR), also defined as charge ratio, is the ratio of the weight of balls to the reactants powder which can range from 1:1 to 220:1. The typical ratio for small-scale milling is 10:1, while the ratio for large or commercial-scale milling can go up to 100:1. Collisions per unit time increase with increasing BPR ratio, which can increase the energy transferred to reactants and thus may shorten the required reaction time (Suryanarayana et al., 2001). The amount of free space in the milling vial for the balls and reactants is necessary to consider as it will influence the conversion rate. The generally recommended loading rate is less than 50% of the vial volume for most type of mills (Suryanarayana et al., 2001) and 20-30% for attritor mills (Baláž, 2008b). The milling atmosphere is an essential variable because of possible product contamination and effects on the form of final products (Lee and Koch, 1987, Ogino et al., 1990), particularly in the alloying industry. Products requiring high-purity or those sensitive to air are generally milled in evacuated conditions, in argon or helium charged containers (Suryanarayana et al., 2001).

Increasing the milling speed generally can increase the ball movement within the chamber, thus increasing the energy input to the reactants. However, there will be a maximum speed for a given mill, higher than which the ball will pin to the inner walls of the chamber. Further, higher speed generally can cause higher temperatures thus potentially influencing the reactants by thermal heating (Suryanarayana et al., 2001). It is important to notice that both mechanical and thermal forces together may induce different relaxation mechanisms which potentially can influence the form of the final products. For example, Calka and Radlinski (1991) investigated the reaction pathway of Ni-Zr, Mg-Zn and Al-based alloy formation with high or low milling speeds. They found high melting point materials like Ni-Zr alloy generally can directly form an amorphous phase by high-speed milling, while low-speed milling will form the intermetallic phases initially and slowly change to a mixed form of an amorphous and crystalline phase. Milling time is also a critical variable for products to achieve the desired form, but it varies with the mill type, ball-to-powder ratio and the thermal effects during the milling process. The contamination rate can increase with milling time so that an optimum milling time may apply for a specific reaction (Suryanarayana et al., 2001).

1.4 MECHANOCHEMICALLY SYNTHESIZED FERTILIZERS

Mechanochemically synthesized fertilizers synthesized to date are summarized in the following table (**Error! Reference source not found.**).

Table 1.3 A summary of mechanochemical synthesized fertilizers.

Reference	**Reactants fertilizer nutrients**	**Reactants-structure**	**Stoichio-metric ratio**	**Products**	**Equipment**	**Type of balls/ Rotation time and speed**
N fertilizers						
Honer et al. (2017a)	Urea ($CO(NH_2)_2$)	$CaSO_4 \cdot 2H_2O$ $Ca(H_2PO_4)_2$ $Ca(NO_3)_2 \cdot 4H_2O$ $MgSO_4 \cdot H_2O$ $Mg(H_2PO_4)_2 \cdot 2H_2O$ $Mg(NO_3)_2 \cdot 6H_2O$	4:1	$CaSO_4 \cdot 4CO(NH_2)_2$ $Ca(H_2PO_4)_2 \cdot 4CO(NH_2)_2$ $Ca(NO_3)_2 \cdot 4CO(NH_2)_2$ $MgSO_4 \cdot 6CO(NH_2)_2 \cdot 0.5H_2O$ $Mg(H_2PO_4)_2 \cdot 4CO(NH_2)_2$ $Mg(NO_3)_2 \cdot 4CO(NH_2)_2 \cdot xH_2O$	Retsch MM300 mixer mill	3*8 mm balls 10 min 26Hz
Honer et al. (2018a)	Solid urea inorganic acid adducts $CO(NH_2)_2 \cdot H_2SO_4$ $CO(NH_2)_2 \cdot H_3PO_4$ $CO(NH_2)_2 \cdot HNO_3$	MgO $Mg(OH)_2$ $MgCO_3$ CaO $Ca(OH)_2$ $CaCO_3$	4:1	$CaSO_4 \cdot 4CO(NH_2)_2$ $Ca(H_2PO_4)_2 \cdot 4CO(NH_2)_2$ $Ca(NO_3)_2 \cdot 4CO(NH_2)_2$ $MgSO_4 \cdot 6CO(NH_2)_2 \cdot 0.5H_2O$ $Mg(H_2PO_4)_2 \cdot 4CO(NH_2)_2$ $Mg(NO_3)_2 \cdot 4CO(NH_2)_2 \cdot 2H_2O$	Retsch MM300 mixer mill	3*8 mm balls 10 min 26Hz

Table 1.3 Continued

Barčauskaitė et al. (2020)	Urea	$CaSO_4 \cdot 2H_2O$	1:4	$CaSO_4 \cdot 4$ urea cocrystal	Laboratory ball mill (Tinius Olsen TO-441-03)	5 h at 60 rpm dried at 50 ± 5 °C for 24 h
Elhadj and Perrin (2021)	Urea	kaolinite	1:3 1:1 2:1 4:1	Kaolinite-urea intercalates	Restch, planetary ball mill PM-100, Germany	30*10 mm 400 rpm 5, 10, 25, 60, 120 min dried at 40 °C for 48 h
Tongamp et al. (2008)	$Mg(OH)_2$, $Al(OH)_3$	$Mg(NO_3)_2.6H_2O$	2.4-2.7: 1: 0.3-0.6	Mg–Al–NO_3 layered double hydroxides (LDH)	Pulverisette-7 planetary ball mill	1:40 7*15 mm balls 60 min+120 min 700 rpm
P fertilizers						
Minjigmaa et al. (2007)	Fluorapatite $Ca_5(PO_4)_3F$		-	Partially amorphous fluorapatite	VM-4 vibration mill	100:1 5-27 mm balls 60-90 min
Chen et al. (2018)	Apatite $Ca_5(PO_4)_3(OH,F)$	Ammonium sulfate $(NH_4)_2SO_4$: Sulfuric acid H_2SO_4	1:1.5:3.5 1:1.5:3.6 1:1.5:4		Pulverisette-7 planetary ball mill	7*15 mm balls Up to 180 min 200-600 rpm
K fertilizers						
Said et al. (2018)	Grounded phlogopite Power (<150μm) $KMg_3AlSi_3O_{10}(F,OH)_2$	-	-	$KMg_3 [Si_3AlO_{10}] (OH)_2$	Pulverisette-7 planetary ball mill	7*15 mm balls 120 min, 0-700 rpm
Yuan et al. (2014)	KOH	SiO_2: CaO	1: 1-6: 1	K-Si-Ca-O $mK_2O \cdot CaO \cdot nSiO_2$	Pulverisette-7 planetary ball mill	7*11 mm balls 120 min 100-700 rpm

Table 1.3 Continued

NPK, NP, KP fertilizers						
Solihin et al. (2010a)	KH_2PO_4 $NH_4H_2PO_4$	$Mg(OH)_2$	1: 1	$KMgPO_4$ NH_4MgPO_4	Pulverisette-7 planetary ball mill	7*15 mm balls 120 min 100-700 rpm
Borges et al. (2017a)	K_2HPO_4	Montmorillonite Talc	1: 2 1: 1 2: 1	Montmorillonite- K_2HPO_4 Talc- K_2HPO_4-K-struvite-$MgKPO_4·6H_2O$ (amorphous)	Pulverisette-2 planetary disk mill	Disk 3-12h 70rpm
Solihin et al. (2011)	KH_2PO_4 $NH_4H_2PO_4$	Kaolin ($Si_2Al_2O_5(OH)_4$)	1: 1	Kaolin-KH_2PO_4 Kaolin-$NH_4H_2PO_4$ (amorphous)	Pulverisette-7 planetary ball mill	7*15 mm balls 120 min 100-700 rpm
Zhang and Saito (2009)	KH_2PO_4 $NH_4H_2PO_4$	$Al(OH)_3$ heating for 3h at 600 °C γ-Al_2O_3	2: 1-3	KH_2PO_4-Al_3O_3 $NH_4H_2PO_4$-Al_2O_3	Pulverisette-7 planetary ball mill	7*11 mm balls 120 min 300-600 rpm
Borges et al. (2015)	KH_2PO_4 $NH_4H_2PO_4$	Kaolin ($Si_2Al_2O_5(OH)_4$)	1: 1	Kaolin-KH_2PO_4 Kaolin-$NH_4H_2PO_4$	Pulverisette-5 high energy ball mill	15*10 mm balls 1-3 h 100-400 rpm
Borges et al. (2018)	K_2HPO_4	Chrysotile $Mg_3Si_2O_5(OH)_4$	1: 2 2: 1 1.5: 1.5	$MgKPO_4·6H_2O$ $MgKPO_4·H_2O$ SiO_2-MgO (amorphous)	Pulverisette-2 planetary disk mill Pulverisette-5 high energy ball mill	Disk 15*10 mm balls 6-24 h D-70rpm B-200-600 rpm
Al-Rawajfeh et al. (2019)	$(NH_4)_2HPO_4$. KH_2PO_4	kaolinite	25:75, 50:50, 75:25	kaolinite–KH_2PO4 kaolinite–$(NH_4)_2HPO_4$	Pulverisette-7 planetary ball mill	6*15 mm balls 120 min 600 rpm

Table 1.3 Continued

Tan et al. (2021)	$(NH_4)_2HPO_4$ $CaHPO_4$	Chrysotile	3:3:1	$NH_4MgPO_4·6H_2O$ $CaSiO_3$	Restch, planetary ball mill PM-100, Germany	1*17 mm 4*15 mm 20*5 mm 120 min 600 rpm
Tan et al. (2020)	$NH_4H_2PO_4$	talc	3:1	$NH_4MgPO_4·6H_2O$	Restch, planetary ball mill PM-100, Germany	1*17 mm 4*15 mm 20*5 mm 60 min 600 rpm
Borges et al. (2022)	KH_2PO_4	Asbestos	3:1, 2:1, 1:1, 1:2 1:3	Amorphous Ca/Mg-P-K compounds	Pulverisette-7 planetary ball mill	5*10 mm 0, 0.5, 1, 2, 3, 4, 5, 6, 7 h 600 rpm
Micronutrient fertilizers						
Li et al. (2017)	$FeSO_4·7H_2O$ $ZnSO_4·7H_2O$	$CaCO_3$	1: 1: 2.6	$FeCO_3$-$ZnCO_3$-$CaSO_4$ (with a mix of $FeSO_4$-$ZnSO_4$-$CaCO_3$)	Pulverisette-7 planetary ball mill	7*15 mm balls 120 min 200-700 rpm

1.4.1 Use of mechanochemistry to synthesize macronutrient fertilizers

1.4.1.1 Nitrogen (N)

The earliest investigation of N fertilizer synthesis by mechanical forces was performed by Malinowski et al. (2007). They produced a calcium sulfate and urea ($CO(NH_2)_2$) adduct by grinding reactants in agate or compacting them under pressure. The urea conversion percentage was influenced by the crystalline water content of the calcium sulfate and the stoichiometric ratio of the two reactants. Recently, Honer et al. (2017) produced a stable urea fertilizer based on ionic co-crystal synthesis by ball milling urea with magnesium and calcium salts for 10 min. They also performed an NH_3 emission test over 48h in a chamber on top of the soil surface. They found $CaSO_4 \cdot 4CO(NH_2)_2$ largely delayed or decreased NH_3 emission. They concluded that the ionic co-crystal products could inherit the stable characteristics from the inorganic parent compounds and thus keep urea from hydrolysis for a more extended period. Later, the same group agronomically assessed mechanochemically synthesized urea co-crystals with waste gypsum through a leaching and field experiment (Barčauskaitė et al., 2020). They concluded that improved N and S availability was observed at early stages of the maize growth when the urea co-crystals were applied in the field. Other approaches to mechanochemically synthesize N fertilizers are combining layered structured materials such as LDH and clay minerals with N to slow down N release. For example, Tongamp et al. (2008) proposed a two-step (dry and wet grinding) method to synthesize Mg-Al LDHs with nitrate as a guest molecule. The reactants, $Mg(OH)_2$, $Al(OH)_3$ and $Mg(NO_3)_2 \cdot 6H_2O$, were milled in a planetary ball mill, firstly with the hydroxides and then with nitrate and water. The nitrate in the final products showed a slower release pattern in a leaching test compared to the nitrate salts alone. Elhadj and Perrin (2021) adjusted the parameters (time and urea content) of mechanochemically intercalated kaolinite and urea. They concluded that a high content of urea in the milling process is more efficient.

1.4.1.2 Phosphate

Phosphate rock was the first fertilizer raw material processed by mechanochemical processes on an industrial scale. Traditionally, P fertilizers are prepared by decomposing phosphate rock in sulfuric acid and/or phosphoric acids (Bolan et al., 1993). The earliest studies found that volcanic rocks (apatite) and sedimentary rocks (phosphorites) can be mechanically activated (Baláž, 2008b). This method was explored further with a commercial vibration mill to investigate the solubility of fluorapatite ($Ca_5(PO_4)_3F$) after mechanochemical treatment (Minjigmaa et al., 2007). Using XRD and thermal analysis, they found increasing solubility of the fluorapatite is associated with the amorphization and lattice strain achieved by mechanical activation rather than the transformation into a new crystalline phase. Chen et al. (2018) reported a high conversion method for soluble P by adding extra sulfuric acid and ammonium sulfate into the reaction with apatite using ball milling. The increased solubility of the natural phosphate rock activated by mechanochemistry is more likely due to the increased defects (high energy accumulation) and nanostructure generation rather than the decreased surface area (Suryanarayana, 2001). Moreover, the solubility of apatite (a phosphate rock) can be largely increased by milling with a small amount of SiO_2. This is due to the reaction of apatite with SiO_2 volatilizing the F as SiF_4 from the structure and thus further degrading the apatite. Suryanarayana (2004) compared several process characteristics of traditional and mechanochemical methods of producing phosphate fertilizer (Table 1.3). Compared to traditional methods, the mechanochemical method had low chemical input and high time efficiency and environmental benefits such as no release of fluorine into the atmosphere.

Table 1.3 Comparison of traditional and mechanochemical methods for the production of phosphate fertilizers (adapted from Suryanarayana (2004)).

Process characteristics	**Traditional methods**	**Mechanochemical method**
Ammonium citrate	60 %	40-50 %
Duration of the production process	20 d (periodical)	20-24 h (continuous)
Consumption of energy per ton	450 kWh/t	500 kWh/t
Consumption of reagent per ton	0.7t H_2SO_4 (60%)	-
Duration of agrochemical action of the fertilizer	1-2 years	5-7 years
Release of fluorine into the atmosphere	Yes	No
Increase of acidity of soils	Yes	No
Possibility to use for small deposits (<1 million tons) of phosphate rock	No	Yes

1.4.1.3 Potassium

Similarly to the application to the P minerals, Said et al. (2018) mechanically activated phlogopite ($KMg_3AlSi_3O_{10}(F, OH)_2$) to produce a slow-release K fertilizer by increasing the K release rate in the mineral. Recently, the same group synthesized a K-Si-Ca-O compound as a slow-release K fertilizer in a glass phase by using KOH, CaO and SiO_2 as the reactants with different amounts of SiO_2 and different milling speeds (Yuan et al., 2014). The K release rate decreased with increasing SiO_2 content. Increased milling speeds decreased the release rate of K. Again, these experiments were generally designed based on material science rather than agricultural practice, that is, the content of other elements in the final product was much higher than the target nutrients and therefore more transport costs would result. Further, this structure may not suit a wide range of soil pH conditions as they only tested the nutrient release pattern in distilled water.

1.4.1.4 NPK, NP, KP fertilizers

Three methods were proposed by the same group to mechanochemically synthesize combined P and K or N fertilizers (Zhang et al., 2004, Solihin et al., 2010a). The final products of these methods are glass-phase products, struvite-structure products and clay mineral complexes. They used $NH_4H_2PO_4$ and KH_2PO_4 as NP and KP sources and γ-Al_2O_3 (glass), $Mg(OH)_2$ (forming struvite) and kaolin (clay mineral) as structural reactants. They found the amount of nutrients released from the final products decreased with increasing stoichiometry ratio of structural reactants. Another group also investigated the mechanochemical processing of K-P fertilizers (K_2HPO_4) with three clay minerals, kaolinite, montmorillonite and talc (Borges et al., 2017a, Borges et al., 2015). The major structural elements in these are Al-Si, Al-Mg-Si and Mg-Si. All final products achieved amorphization and showed the characteristics of SRFs. They also found the release time was significantly influenced by mill rotation speed rather than milling time. Notably, the release pattern was also influenced by the type of clay mineral, with talc showing the slowest release pattern. Recently, the same group introduced a waste management-based mechanochemical method to make use of chrysotile asbestos fibers, by producing a slow release K-P fertilizer ($MgKPO_4{\cdot}H_2O$ and $MgKPO_4{\cdot}6H_2O$) (Borges et al., 2018, Borges et al., 2022). Two mills, a planetary mill and a high-energy ball mill, were used to grind the chrysotile ($Mg_3Si_2O_5(OH)_4$) and K_2HPO_4 with different stoichiometric ratios, milling times and rotation speeds. They pointed out that the hazardous reactant can be transformed entirely to dittmarite, struvite and amorphous SiO_2/MgO when applying an appropriate stoichiometric ratio. Additionally, the type of mill also influenced the rate of nutrient release. In this study, products from a planetary mill showed a slower release rate compared to products made with a high-energy ball mill.

In the study mentioned above, the release of K, N and P from the synthesized kaolin-nutrients system is controlled by the kaolin content (Solihin et al., 2011). In addition, the synthesis of struvite combined with clay minerals lowered the solubility of the K and P in comparison with the clay mineral alone (Borges et al., 2017a). Further, mechanochemical reactions allow the constituents to form in different stoichiometric ratios (Trask et al., 2005), and in turn may change the properties or stability of the products (Karki et al., 2009, Thakuria et al., 2013). In addition, when mechanochemical activation creates enough defects to form highly active amorphization, defects gradually anneal or recrystallize with increasing temperature, so the solubility of the product decreases with an increased rate of recrystallization (Baláž, 2008b). Low solubility structures such as struvite and some carbonates may slow down the nutrient release rate by the process of recrystallization from mechanochemically activated amorphization (Borges et al., 2017a, Leukel and Tremel, 2018) which can be used to combine with high solubility products to synthesis S/CRFs.

1.4.2 Use of mechanochemistry to synthesize micronutrient fertilizers

To date, only one study has used a mechanochemical approach to synthesize micronutrients. Li et al. (2017) proposed a mechanochemical method whereby ferrous sulfate waste from titanium dioxide production was used to synthesize the desired SRFs. They milled the sulfates ($FeSO_4 \cdot 7H_2O$ and $ZnSO_4 \cdot 7H_2O$), low-cost calcium carbonate and a small amount of water together in a planetary ball mill. Like other studies, they also found milling speed can influence the conversion rate of the raw materials, and the final product became less soluble in water when the rotation speed reached a certain level, while solubility in citric acid (2%) was less influenced by the rotation speed.

1.4.3 The need for mechanochemically synthesized B and Mo fertilizer

Numerous studies have focused on slow-release NPK fertilizers as these nutrients are required by plants in large amounts. In contrast, the recommended B fertilizer application rate ranges from 0.5-4 kg ha^{-1} depending on the soil and crop type (Mortvedt, 1991). Boron primarily exists in soil solution as boric acid ($B(OH)_3$), which is only weakly bonded to clays, hydrous oxide surfaces and OM, and is subject to leaching particularly on coarse-textured soils (Shorrocks, 1997a). For example, in a 15-year study with repeated B applications on three different soils, 40-60% of applied B was leached from the topsoil (Eguchi and Yamada, 1997). Low solubility B sources (e.g. colemanite) have become more popular in high rainfall production systems. Broschat (2008) investigated the release rate of nine B sources with different solubilities in sand-leaching columns. The results indicated that slowest B sources, such as colemanite and sodium calcium borates, were retained in sand much longer than fast-release B sources such as Solubor (disodium octaborate tetrahydrate ($Na_2B_8O_{13}.4H_2O$) and boric oxide. Similarly, Saleem et al. (2011) observed a greater leaching potential of borax than colemanite and found, as expected, that the solubility of colemanite increased with decreasing particle size. Later, the same group applied borax and both powdered and granular colemanite to rice crops in the field, where they found the release rate of B from granular colemanite was too slow to effectively supply B to crops compared with the other two forms. In other words, optimum solubility might be required for production in the field (Broschat, 2008). Abat et al. (2015d) proposed to incorporate B phosphate (BPO_4) into a MAP fertilizer to produce a co-granulated B source as a more seedling-safe fertilizer (Abat et al., 2015a) and further proved a better crop response and lower leaching potential in a simulated leaching experiment (Abat et al., 2015c). More recently a novel potash fertilizer containing slow and fast-releasing sources of B was proposed where the release pattern of B better matched crop B demand during growth (da Silva et al., 2018b).

Molybdenum is primarily present in the soil as MoO_4^{2-} when the soil pH is above 4.2. The Mo-oxyanion is similar to phosphate, as the adsorption of Mo is mainly onto positively charged metal oxides and clay, and organic material particularly when pH is low (Bell and Dell, 2008). In acidic Australian soils, about 10% of applied Mo is leached through the soil as most Mo is absorbed by soil minerals and OM (Riley et al., 1987). However, Mo can easily be leached through neutral to alkaline soils (Carroll et al., 2006). The recommended Mo fertilizer application rate is the lowest among all micronutrients and ranges from 0.03 to 0.2 kg ha^{-1} (Mortvedt, 1991). Deficiency of Mo has been reported in several agricultural regions (Davies, 1945, Stout and Johnson, 1956, Kaiser et al., 2005). However, only a small number of studies have been performed on S/CRF Mo fertilizers. For example, Bandyopadhyay et al. (2008a) prepared a slow-released Mo fertilizer using a long-chain polyphosphate. They also tested this Mo fertilizer in the field where they found an 80% increase in yield and a 161% increase in nodulation in green gram (mung bean). Recently, Everaert et al. (2021b) loaded molybdate anion into a Zn-Al LDH at different Zn/Al ratios using co-precipitation and anion exchange. The optimum Mo-Zn_2Al LDH compound could be incorporated with urea as a potential slow-release Mo fertilizer. Mo-biochar was also proposed to be used as a slow-release fertilizer and was observed to enhance N assimilation and plant growth compared to a Mo basal application (Huang et al., 2022).

Notably, potential methods for slowing or controlling the release of B and Mo remain rare in comparison to other nutrients. This is mainly due to the chemical nature of these nutrients and the recognition before the occurrence of deficiency. The process of using wet chemistry to formulate the S/CRFs is time-consuming and can be more expensive than using mechanochemistry. Further, mechanochemistry may also be able to synthesize compounds that cannot be formulated through wet chemistry and could allow adjustment of the release rate of the micronutrients simply through altering the stoichiometric ratio of reactants. My hypothesis is that mechanochemistry could produce more sustainable slow-release B and Mo fertilizers with higher nutrient use efficiency by reducing leaching or improving plant growth compared to traditionally manufactured products.

1.5 RESEARCH GAP

Mechanochemical synthesis of fertilizers is in its infancy, with the first reports in the scientific literature only appearing in the last 10 years. The accumulated amount of studies explored the mobility and agronomical effectiveness of micronutrients such as B and Mo in soils, and concluded that plant growth could benefit from slow-release However, for new products using novel synthesize methods such as mechanochemistry, studies to date have generally focused on slow-release character rather than agronomical effectiveness. Fertilizer manufacturing should take into account the possible adverse effects of added elements; particularly those that may cause contamination and toxicity to soil or crops. There is an opportunity to mechanochemically formulate micronutrient fertilizers and assess their effectiveness from an agronomic perspective. Three major gaps could be identified from the literature: a) mechanochemistry has not been used to synthesize B and Mo micronutrient fertilizers; b) the effects of mechanochemical synthesis on the release behaviour of B and Mo micronutrients have not been assessed in the literature; and c) there is a lack of agronomic comparison of existing micronutrient fertilizers with mechanochemically synthesized fertilizers.

1.6 AIMS AND OBJECTIVES OF THE PROJECT

The overall aim of this thesis was to formulate and synthesize novel slow/controlled Mo and B fertilizers using mechanochemistry. The specific objectives of this project were to:

i. Formulate and identify slow/controlled release Mo and B fertilizers using mechanochemistry;

ii. Evaluate the release behaviour and identify suitable macronutrient carriers for mechanochemically synthesized B and Mo fertilizers; and

iii. Assess the agronomic effectiveness of the synthesized materials through leaching and pot studies in comparison with existing/commercial B and Mo fertilizers.

1.7 REFERENCES

Abat, M., Degryse, F., Baird, R., McLaughlin, M.J., 2015a. Boron Phosphates (BPO4) as a Seedling-safe Boron Fertilizer Source. Plant and Soil 391(1), 153-160.

Abat, M., Degryse, F., Baird, R., McLaughlin, M.J., 2015b. Responses of Canola to the `Application of Slow-Release Boron Fertilizers and Their Residual Effect. Soil Science Society of America Journal 79(1), 97-103.

Abat, M., Degryse, F., Baird, R., McLaughlin, M.J., 2015c. Slow-release Boron Fertilizers: Co-granulation of Boron Sources with Mono-ammonium Phosphate (MAP). Soil Research 53(5), 505-511.

Akiyama, H., Yan, X., Yagi, K., 2010. Evaluation of Effectiveness of Enhanced-Efficiency Fertilizers as Mitigation Options for N_2O and NO Emissions from Agricultural Soils: Meta-analysis. Global Change Biology 16(6), 1837-1846.

Al-Rawajfeh, A.E., AlShamaileh, E.M., Alrbaihat, M.R., 2019. Clean and Efficient Synthesis Using Mechanochemistry: Preparation of Kaolinite–KH_2PO_4 and Kaolinite–$(NH_4)_2HPO_4$ Complexes as Slow Released Fertilizer. Journal of Industrial and Engineering Chemistry 73, 336-343.

Albino, M., Jean-paul, M., Anne-katrin, B., Hugh, E., Fabiana, S., Helena, R.F., 2012. NPK: Will There Be Enough Plant Nutrients to Feed a World of 9 Billion in 2050?

Alloway, B.J., 2009. Soil Factors Associated with Zinc Deficiency in Crops and Humans. Environmental Geochemistry and Health 31(5), 537-548.

Anderson, N.G., 2001. Practical Use of Continuous Processing in Developing and Scaling Up Laboratory Processes. Organic Process Research and Development 5(6), 613-621.

Asad, A., Bell, R.W., Dell, B., 2001. A Critical Comparison of the External and Internal Boron Requirements for Contrasting Species in Boron-buffered Solution Culture. Plant and Soil 233(1), 31-45.

Badruzzaman, M., Pinzon, J., Oppenheimer, J., Jacangelo, J.G., 2012. Sources of Nutrients Impacting Surface Waters in Florida: A Review. Journal of Environmental Management 109, 80-92.

Baláž, P., 2008. Mechanochemistry and Nanoscience, Mechanochemistry in Nanoscience and Minerals Engineering. Springer Berlin Heidelberg, Berlin, Heidelberg, pp. 1-102.

Baláž, P., Achimovičová, M., Baláž, M., Billik, P., Cherkezova-Zheleva, Z., Criado, J.M., Delogu, F., Dutková, E., Gaffet, E., Gotor, F.J., Kumar, R., Mitov, I., Rojac, T., Senna, M., Streletskii, A., Wieczorek-Ciurowa, K., 2013. Hallmarks of Mechanochemistry: from Nanoparticles to Technology. Chemical Society Reviews 42(18), 7571-7637.

Baláž, P., Dutková, E., 2009. Fine Milling in Applied Mechanochemistry. Minerals Engineering 22(7), 681-694.

Balmford, A., Green, R.E., Scharlemann, J.P.W., 2005. Sparing Land for Nature: Exploring the Potential Impact of Changes in Agricultural Yield on the Area Needed for Crop Production. Global Change Biology 11(10), 1594-1605.

Bandyopadhyay, S., Bhattacharya, I., Ghosh, K., Varadachari, C., 2008. New Slow-Releasing Molybdenum Fertilizer. Journal of Agricultural and Food Chemistry 56(4), 1343-1349.

Bandyopadhyay, S., Ghosh, K., Varadachari, C., 2014. Multimicronutrient Slow-Release Fertilizer of Zinc, Iron, Manganese, and Copper. International Journal of Chemical Engineering 2014, 327153.

Barčauskaitė, K., Brazienė, Z., Avižienytė, D., Silva, M., Drapanauskaite, D., Honer, K., Gvildienė, K., Slinksiene, R., Jancaitiene, K., Mazeika, R., Staugaitis, G., Dambrauskas, T., Baltakys, K., Baltrusaitis, J., 2020. Mechanochemically Synthesized Gypsum and Gypsum Drywall Waste Cocrystals with Urea for Enhanced Environmental Sustainability Fertilizers. Journal of Environmental Chemical Engineering 8(4), 103965.

Barker, A.V., Pilbeam, D.J., 2006. Handbook of Plant Nutrition. CRC, Hoboken, pp 351374Lalibert E, Turner BL, Costes T, Pearse SJ, Wyrwoll KH, Zemunik.

Beckinghausen, A., Odlare, M., Thorin, E., Schwede, S., 2020. From Removal to Recovery: An Evaluation of Nitrogen Recovery Techniques from Wastewater. Applied Energy 263, 114616.

Bell, R.W., Dell, B., 2008. Micronutrients for Sustainable Food, Feed, Fibre and Bioenergy Production. International Fertilizer Industry Association (IFA).

Benjamin, J.S., Shingu, P.H., 1992. Mechanical Alloying. 88(90), 1-1.

Bhattacharya, I., Bandyopadhyay, S., Varadachari, C., Ghosh, K., 2007. Development of a Novel Slow-Releasing Iron−Manganese Fertilizer Compound. Industrial and Engineering Chemistry Research 46(9), 2870-2876.

Biangardi, S., Pietsch, H., 1976. Verarbeitung sulfidischer Kupfererze nach dem Lurgi-Mitterberg (LM)-Verfahren. Erzmetall 29, 73-76.

Blasco, B., Navarro-León, E., Ruiz, J.M., 2018. Chapter 10 - Oxidative Stress in Relation With Micronutrient Deficiency or Toxicity, in: Hossain, M.A., Kamiya, T., Burritt, D.J., Phan Tran, L.-S., Fujiwara, T. (Eds.), Plant Micronutrient Use Efficiency. Academic Press, pp. 181-194.

Bolan, N.S., Hedley, M.J., Loganathan, P., 1993. Preparation, Forms and Properties of Controlled-release Phosphate Fertilizers. Fertilizer research 35(1), 13-24.

Boldyrev, V.V., 2006. Mechanochemistry and Mechanical Activation of Solids. Russian Chemical Reviews 75(3), 177-189.

Boldyrev, V.V., Tkáčová, K., 2000. Mechanochemistry of Solids: Past, Present, and Prospects. Journal of Materials Synthesis and Processing 8(3), 121-132.

Boldyreva, E., 2013. Mechanochemistry of Inorganic and Organic Systems: What is Similar, What is Different? Chemical Society Reviews 42.

Borges, R., Baika, L.M., Grassi, M.T., Wypych, F., 2018. Mechanochemical Conversion of Chrysotile/K_2HPO_4 Mixtures into Potential Sustainable and Environmentally Friendly Slow-release Fertilizers. Journal of Environmental Management 206, 962-970.

Borges, R., Brunatto, S.F., Leitão, A.A., de Carvalho, G.S.G., Wypych, F., 2015. Solid-state Mechanochemical Activation of Clay Minerals and Soluble Phosphate Mixtures to Obtain Slow-release Fertilizers. Clay Minerals 50(2), 153-153.

Borges, R., Giroto, A.S., Guimarães, G.G.F., Reis, H.P.G., Farinas, C.S., Ribeiro, C., 2022. Asbestos Cement Waste Treatment through Mechanochemical Process with KH_2PO_4 for Its Utilization in Soil pH Correction and Nutrient Delivery. Environmental Science and Pollution Research 29(19), 28804-28815.

Borges, R., Prevot, V., Forano, C., Wypych, F., 2017. Design and Kinetic Study of Sustainable Potential Slow-Release Fertilizer Obtained by Mechanochemical Activation of Clay Minerals and Potassium Monohydrogen Phosphate. Industrial and Engineering Chemistry Research 56(3), 708-716.

Borlaug, N.E., 1994. Feeding a Human Population that Increasingly Crowds a Fragile Planet.

Bortolin, A., Serafim, A.R., Aouada, F.A., Mattoso, L.H.C., Ribeiro, C., 2016. Macro- and Micronutrient Simultaneous Slow Release from Highly Swellable Nanocomposite Hydrogels. Journal of Agricultural and Food Chemistry 64(16), 3133-3140.

Bowden, F.P., Yoffe, A.D., 1958. Fast Reactions in Solids. Butterworth's Scientific Publications.

Broadley, M., Brown, P., Cakmak, I., Rengel, Z., Zhao, F., 2012. Chapter 7 - Function of Nutrients: Micronutrients, in: Marschner, P. (Ed.) Marschner's Mineral Nutrition of Higher Plants (Third Edition). Academic Press, San Diego, pp. 191-248.

Broschat, T.K., 2008. Release Rates of Soluble and Controlled-release Boron Fertilizers. HortTechnology hortte 18(3), 471-474.

Calka, A., Radlinski, A.P., 1991. Universal High Performance Ball-milling Device and Its Application for Mechanical Alloying. Materials Science and Engineering A 134(C), 1350-1353.

Cánovas, C.R., Pérez-López, R., Macías, F., Chapron, S., Nieto, J.M., Pellet-Rostaing, S., 2017. Exploration of Fertilizer Industry Wastes as Potential Source of Critical Raw Materials. Journal of Cleaner Production 143, 497-505.

Capmourteres, V., Adams, J., Berg, A., Fraser, E., Swanton, C., Anand, M., 2018. Precision Conservation Meets Precision Agriculture: A Case Study from Southern Ontario. Agricultural Systems 167, 176-185.

Carroll, K.C., Artiola, J.F., Brusseau, M.L., 2006. Transport of Molybdenum in a Biosolid-amended Alkaline Soil. Chemosphere 65(5), 778-785.

Castro, G.F.d., Ferreira, J.A., Zotarelli, L., Mattiello, E.M., Novais, R.F., Tronto, J., 2020. Layered Double Hydroxides Intercalated with Borate: Effect of Fertilization on Boron Leaching and Successive Sunflower Cultivations. New Journal of Chemistry 44(24), 10042-10049.

Chandra, P.K., Ghosh, K., Varadachari, C., 2009. A New Slow-releasing Iron Fertilizer. Chemical Engineering Journal 155(1), 451-456.

Chaney, R.L., Giordano, P.M., 1977. Microelements as Related to Plant Deficiencies and Toxicities, Soils for Management of Organic Wastes and Waste Waters. pp. 233-279.

Chen, M., Li, Z., Huang, P., Li, X., Qu, J., Yuan, W., Zhang, Q., 2018. Mechanochemical Transformation of Apatite to Phosphoric Slow-release Fertilizer and Soluble Phosphate. Process Safety and Environmental Protection 114, 91-96.

da Silva, R.C., Baird, R., Degryse, F., McLaughlin, M.J., 2018. Slow and Fast-Release Boron Sources in Potash Fertilizers: Spatial Variability, Nutrient Dissolution and Plant Uptake. Soil Science Society of America Journal 82(6), 1437-1448.

Daniel, T.C., Sharpley, A.N., Lemunyon, J.L., 1998. Agricultural Phosphorus and Eutrophication: A Symposium Overview. Journal of environmental quality 27(2), 251-257.

Davies, E.B., 1945. A Case of Molybdenum Deficiency in New Zealand. Nature 156(3961), 392-392.

Eguchi, S., Yamada, Y., 1997. Long-term Field Experiment on the Application of Slow-release Boron Fertilizer Part 2 Behavior of Boron in the Soil, in: Bell, R.W., Rerkasem, B. (Eds.), Boron in Soils and Plants: Proceedings of the International Symposium on Boron in Soils and Plants held at Chiang Mai, Thailand, 7--11 September, 1997. Springer Netherlands, Dordrecht, pp. 49-56.

Elhadj, M.S.Y., Perrin, F.X., 2021. Influencing Parameters of Mechanochemical Intercalation of Kaolinite with Urea. Applied Clay Science 213, 106250.

Essington, M.E., 2015. Soil and Water Chemistry: an Integrative Approach. CRC press.

Everaert, M., Smolders, E., McLaughlin, M.J., Andelkovic, I., Smolders, S., Degryse, F., 2021. Layered Double Hydroxides as Slow-Release Fertilizer Compounds for the Micronutrient Molybdenum. Journal of Agricultural and Food Chemistry 69(48), 14501-14511.

Fageria, N.K., Baligar, V.C., Clark, R.B., 2002. Micronutrients in Crop Production, in: Sparks, D.L. (Ed.) Advances in Agronomy. Academic Press, pp. 185-268.

Fageria, N.K., Baligar, V.C., Li, Y.C., 2008. The Role of Nutrient Efficient Plants in Improving Crop Yields in the Twenty First Century. Journal of Plant Nutrition 31(6), 1121-1157.

Fernandez, V., Brown, P.H., 2013. From Plant Surface to Plant Metabolism: the Uncertain Fate of Foliar-applied Nutrients. Frontiers in Plant Science 4.

Gharekhani, H., Olad, A., Hosseinzadeh, F., 2018. Iron/NPK Agrochemical Formulation from Superabsorbent Nanocomposite Based on Maize Bran and Montmorillonite with Functions of Water Uptake and Slow-release Fertilizer. New Journal of Chemistry 42(16), 13899-13914.

Giraud, R.J., Williams, P.A., Sehgal, A., Ponnusamy, E., Phillips, A.K., Manley, J.B., 2014. Implementing Green Chemistry in Chemical Manufacturing: A Survey Report. ACS Sustainable Chemistry and Engineering 2(10), 2237-2242.

Gouider, M., Feki, M., Sayadi, S., 2014. Treatment of Wastewaters from Phosphate Fertilizer Industry. Environmental Progress and Sustainable Energy 33(2), 463-471.

Gupta, P.K., 2019. Toxic Effects of Metals and Micronutrients, in: Gupta, P.K. (Ed.) Concepts and Applications in Veterinary Toxicology: An Interactive Guide. Springer International Publishing, Cham, pp. 83-119.

Gupta, U.C., Wu, K., Liang, S., 2008. Micronutrients in Soils, Crops, and Livestock. Earth Science Frontiers 15(5), 110-125.

Hawkesford, M., Horst, W., Kichey, T., Lambers, H., Schjoerring, J., Møller, I.S., White, P., 2012. Chapter 6 - Functions of Macronutrients, in: Marschner, P. (Ed.) Marschner's Mineral Nutrition of Higher Plants (Third Edition). Academic Press, San Diego, pp. 135-189.

Hernandez, J.G., Bolm, C., 2017. Altering Product Selectivity by Mechanochemistry. The Journal of Organic Chemistry 82(8), 4007-4019.

Hignett, T.P., McClellan, G.H., 1985. Sources and Production of Micronutrient Fertilizers, in: Vlek, P.L.G. (Ed.) Micronutrients in Tropical Food Crop Production. Springer Netherlands, Dordrecht, pp. 237-260.

Hodge, C.A., 1994. Pollution Control in Fertilizer Production. CRC Press.

Honer, K., Kalfaoglu, E., Pico, C., McCann, J., Baltrusaitis, J., 2017. Mechanosynthesis of Magnesium and Calcium Salt–Urea Ionic Cocrystal Fertilizer Materials for Improved Nitrogen Management. ACS Sustainable Chemistry and Engineering 5(10), 8546-8550.

Honer, K., Pico, C., Baltrusaitis, J., 2018. Reactive Mechanosynthesis of Urea Ionic Cocrystal Fertilizer Materials from Abundant Low Solubility Magnesium- and Calcium-Containing Minerals. ACS Sustainable Chemistry and Engineering 6(4), 4680-4687.

Horie, K., Barón, M., Fox, R.B., He, J., Hess, M., Kahovec, J., Kitayama, T., Kubisa, P., Maréchal, E., Mormann, W., others, 2004. Definitions of Terms Relating to Reactions of Polymers and to Functional Polymeric Materials (IUPAC Recommendations 2003). Pure and Applied Chemistry 76(4), 889-906.

Huang, Y., Chen, Y., Wen, D., Zhao, P., Li, F., Li, L., Du, R., Shi, H., Deng, T., Du, Y., 2022. Biochar-based Molybdenum Slow-release Fertilizer Enhances Nitrogen Assimilation in Chinese Flowering Cabbage (Brassica parachinensis). Chemosphere 303, 134663.

James, S.L., Adams, C.J., Bolm, C., Braga, D., Collier, P., Friščić, T., Grepioni, F., Harris, K.D.M., Hyett, G., Jones, W., others, 2012. Mechanochemistry: Opportunities for New and Cleaner Synthesis. Chemical Society Reviews 41(1), 413-447.

Jiao, W., Chen, W., Chang, A.C., Page, A.L., 2012. Environmental Risks of Trace Elements Associated with Long-term Phosphate Fertilizers Applications: A Review. Environmental Pollution 168, 44-53.

Jones, G.B., Belling, G.B., 1967. The Movement of Copper, Molybdenum, and Selenium in Soils as Indicated by Radioactive Isotopes. Australian Journal of Agricultural Research 18(5), 733-740.

Juhász, Z., Opoczky, L., 1982. Mechanical Activation of Silicates by Fine Grinding. Akadémiai Kiadó, Budapest.

Juhasz, Z.A., 1998. Colloid-chemical Aspects of Mechanical Activation. Particulate Science and Technology 16(2), 145-161.

Kaiser, B.N., Gridley, K.L., Ngaire Brady, J., Phillips, T., Tyerman, S.D., 2005. The Role of Molybdenum in Agricultural Plant Production. Ann Bot 96(5), 745-754.

Kamprath, E.J., Foy, C.D., 1985. Lime-Fertilizer-Plant Interactions in Acid Soils, Fertilizer Technology and Use. pp. 91-151.

Karki, S., Friščić, T., Jones, W., 2009. Control and Interconversion of Cocrystal Stoichiometry in Grinding: Stepwise Mechanism for the Formation of a Hydrogen-bonded Cocrystal. CrystEngComm 11(3), 470-481.

Khan, H.A., Naqvi, S.R., Mehran, M.T., Khoja, A.H., Khan Niazi, M.B., Juchelková, D., Atabani, A., 2021. A Performance Evaluation Study of Nano-biochar as a Potential Slow-release Nano-fertilizer from Wheat Straw Residue for Sustainable Agriculture. Chemosphere 285, 131382.

Kirkby, E., 2012. Chapter 1 - Introduction, Definition and Classification of Nutrients, in: Marschner, P. (Ed.) Marschner's Mineral Nutrition of Higher Plants (Third Edition). Academic Press, San Diego, pp. 3-5.

Konôpka, M., Turanský, R., Reichert, J., Fuchs, H., Marx, D., ifmmode \checkS\else Š\fitich, I., 2008. Mechanochemistry and Thermochemistry are Different: Stress-Induced Strengthening of Chemical Bonds. Physical Review Letters. 100(11), 115503-115503.

Lateef, A., Nazir, R., Jamil, N., Alam, S., Shah, R., Khan, M.N., Saleem, M., 2016. Synthesis and Characterization of Zeolite Based Nano–composite: An Environment Friendly Slow Release ertilizer. Microporous and Mesoporous Materials 232, 174-183.

Lee, P.Y., Koch, C.C., 1987. The Formation and Thermal Stability of Amorphous Ni-Nb Alloy Powder Synthesized by Mechanical Alloying. Journal of Non-Crystalline Solids 94(1), 88-100.

Leukel, S., Tremel, W., 2018. Water-Controlled Crystallization of $CaCO_3$, $SrCO_3$, and $MnCO_3$ from Amorphous Precursors. Crystal Growth and Design 18(8), 4662-4670.

Li, X., Lei, Z., Qu, J., Li, Z., Zhou, X., Zhang, Q., 2017. Synthesizing Slow-release Fertilizers via Mechanochemical Processing for Potentially Recycling the Waste Ferrous Sulfate from Titanium Dioxide Production. Journal of Environmental Management 186, 120-126.

Maine, M.A., Sanchez, G.C., Hadad, H.R., Caffaratti, S.E., Pedro, M.C., Mufarrege, M.M., Di Luca, G.A., 2019. Hybrid Constructed Wetlands for the Treatment of Wastewater from a Fertilizer Manufacturing Plant: Microcosms and Field Scale Experiments. Science of The Total Environment 650, 297-302.

Mendel, R.R., Hänsch, R., 2002. Molybdoenzymes and Molybdenum Cofactor in Plants. Journal of Experimental Botany 53(375), 1689-1698.

Mengel, K., Kirkby, E.A., Kosegarten, H., Appel, T., 2001a. Boron, in: Mengel, K., Kirkby, E.A., Kosegarten, H., Appel, T. (Eds.), Principles of Plant Nutrition. Springer Netherlands, Dordrecht, pp. 621-638.

Mengel, K., Kirkby, E.A., Kosegarten, H., Appel, T., 2001b. Plant Nutrients, in: Mengel, K., Kirkby, E.A., Kosegarten, H., Appel, T. (Eds.), Principles of Plant Nutrition. Springer Netherlands, Dordrecht, pp. 1-13.

Mikula, K., Izydorczyk, G., Skrzypczak, D., Mironiuk, M., Moustakas, K., Witek-Krowiak, A., Chojnacka, K., 2020. Controlled Release Micronutrient Fertilizers for Precision Agriculture – A Review. Science of The Total Environment 712, 136365.

Miller, E.R., Lei, X., Ullrey, D.E., 1991. Trace Elements in Animal Nutrition, Micronutrients in Agriculture. pp. 593-662.

Minjigmaa, A., Temuujin, J., Khasbaatar, D., Oyun-Erdene, G., Amgalan, J., MacKenzie, K.J.D., 2007. Influence of Mechanical Distortion on the Solubility of Fluorapatite. Minerals Engineering 20(2), 194-196.

Mortvedt, J.J., 1985. Micronutrient Fertilizers and Fertilization Practices, in: Vlek, P.L.G. (Ed.) Micronutrients in Tropical Food Crop Production. Springer Netherlands, Dordrecht, pp. 221-235.

Mortvedt, J.J., 1991. Micronutrient Fertilizer Technology, Micronutrients in Agriculture. pp. 523-548.

Mortvedt, J.J., 1994. Needs for Controlled-availability Micronutrient Fertilizers. Fertilizer Research 38(3), 213-221.

Myers, S.S., Wessells, K.R., Kloog, I., Zanobetti, A., Schwartz, J., 2015. Effect of Increased Concentrations of Atmospheric Carbon Dioxide on the Global Threat of Zinc Deficiency: a Modelling Study. The Lancet. Global health 3(10), e639-645.

O'Neill, M.A., Eberhard, S., Albersheim, P., Darvill, A.G., 2001. Requirement of Borate Cross-Linking of Cell Wall Rhamnogalacturonan II for Arabidopsis Growth. Science 294(5543), 846-849.

Ogino, Y., Yamasaki, T., Murayama, S., Sakai, R., 1990. Non-equilibrium Phases Formed by Mechanical Alloying of Cr-Cu alloys. Journal of Non-Crystalline Solids 117-118, 737-740.

Palmer, C.M., Johnson, G.D., 2005. The Activox® Process: Growing Significance in the Nickel Industry. JOM 57(7), 40-47.

Raven, J.A., 1980. Short- and Long-distance Transport of Boric Acid in Plants. New Phytologist 84(2), 231-249.

Ray, D.K., Mueller, N.D., West, P.C., Foley, J.A., 2013. Yield Trends Are Insufficient to Double Global Crop Production by 2050. Plos One 8(6), 1-8.

Riley, M.M., Robson, A.D., Gartrell, J.W., Jeffery, R.C., 1987. The absence of leaching of molybdenum in acidic soils from Western Australia. Soil Research 25(2), 179-184.

Roschangar, F., Sheldon, R.A., Senanayake, C.H., 2015. Overcoming Barriers to Green Chemistry in the Pharmaceutical Industry – the Green Aspiration Level™ Concept. Green Chemistry 17(2), 752-768.

Sabiha, J., Mehmood, T., Chaudhry, M.M., Tufail, M., Irfan, N., 2009. Heavy Metal Pollution from Phosphate Rock Used for the Production of Fertilizer in Pakistan. Microchemical Journal 91(1), 94-99.

Said, A., Zhang, Q., Qu, J., Liu, Y., Lei, Z., Hu, H., Xu, Z., 2018. Mechanochemical Activation of Phlogopite to Directly Produce Slow-release Potassium Fertilizer. Applied Clay Science 165, 77-81.

Saleem, M., Khanif, Y.M., Ishak, Y.M.F., Samsuri, A.W., 2011. Solubility and Leaching of Boron from Borax and Colemanite in Flooded Acidic Soils. Communications in Soil Science and Plant Analysis 42(3), 293-300.

Shaviv, A., 2001. Advances in Controlled-Release Fertilizers, Advances in Agronomy. Academic Press, pp. 1-49.

Shaviv, A., Mikkelsen, R.L., 1993. Controlled-release Fertilizers to Increase Efficiency of Nutrient Use and Minimize Environmental Degradation - A Review. Fertilizer Research 35(1), 1-12.

Shorrocks, V.M., 1997. The Occurrence and Correction of Boron Deficiency. Plant and Soil 193(1), 121-148.

Solihin, Zhang, Q., Tongamp, W., Saito, F., 2010. Mechanochemical Route for Synthesizing $KMgPO_4$ and NH_4MgPO_4 for Application as Slow-Release Fertilizers. Industrial and Engineering Chemistry Research 49(5), 2213-2216.

Solihin, Zhang, Q., Tongamp, W., Saito, F., 2011. Mechanochemical Synthesis of Kaolin–KH_2PO_4 and kaolin–$NH_4H_2PO_4$ Complexes for Application as Slow Release Fertilizer. Powder Technology 212(2), 354-358.

Songkhum, P., Wuttikhun, T., Chanlek, N., Khemthong, P., Laohhasurayotin, K., 2018. Controlled Release Studies of Boron and Zinc from Layered Double Hydroxides as the Micronutrient Hosts for Agricultural Application. Applied Clay Science 152, 311-322.

Stauch, T., Dreuw, A., 2016. Advances in Quantum Mechanochemistry: Electronic Structure Methods and Force Analysis. Chemical Reviews 116(22), 14137-14180.

Stout, P.R., Johnson, C.M., 1956. Molybdenum Deficiency in Horticultural and Field Crops. Soil Science 81(3), 183-190.

Suryanarayana, C., 2001. Mechanical Alloying and Milling. Progress in Materials Science 46(1), 1-184.

Suryanarayana, C., 2004. Mechanical Alloying And Milling. CRC Press.

Suryanarayana, C., Ivanov, E., Boldyrev, V.V., 2001. The Science and Technology of Mechanical Alloying. Materials Science and Engineering: A 304-306, 151-158.

Takacs, L., 2004. M. Carey Lea, the First Mechanochemist. Journal of Materials Science 39(16), 4987-4993.

Tan, Y., Sha, L., Yu, N., Yang, Z., Qu, J., Xu, Z., 2020. Mechanochemical Approach to Synthesize Citric Acid-soluble Fertilizer of Dittmarite ($NH_4MgPO_4 \cdot H_2O$) from Talc/$NH_4H_2PO_4$ Mixture. RSC Advances 10(30), 17686-17693.

Tan, Y., Zou, Z., Qu, J., Ren, J., Wu, C., Xu, Z., 2021. Mechanochemical Conversion of Chrysotile Asbestos Tailing into Struvite for Full Elements Utilization as Citric-acid Soluble Fertilizer. Journal of Cleaner Production 283, 124637.

Thakuria, R., Delori, A., Jones, W., Lipert, M.P., Roy, L., Rodr\'\iguez-Hornedo, N.i., 2013. Pharmaceutical Cocrystals and Poorly Soluble Drugs. International Journal of Pharmaceutics 453(1), 101-125.

Thiessen, P.A., Meyer, K., Heinicke, G., 1967. Grundlagen der Tribochemie: mit 24 Tab. im Text. Akad.-Verlag.

Timilsena, Y.P., Adhikari, R., Casey, P., Muster, T., Gill, H., Adhikari, B., 2015. Enhanced Efficiency Fertilizers: a Review of Formulation and Nutrient Release Patterns. Journal of the Science of Food and Agriculture 95(6), 1131-1142.

Tongamp, W., Zhang, Q., Saito, F., 2008. Mechanochemical Route for Synthesizing Nitrate form of Layered Double Hydroxide. Powder Technology 185(1), 43-48.

Trask, A.V., van de Streek, J., Motherwell, W.D.S., Jones, W., 2005. Achieving Polymorphic and Stoichiometric Diversity in Cocrystal Formation: Importance of Solid-State Grinding, Powder X-ray Structure Determination, and Seeding. Crystal Growth and Design 5(6), 2233-2241.

UN, 2012. World Population Prospects, UN Department of Economic and Social Affairs.

UN, 2015. World Urbanization Prospects.

UN, 2017. World Population Prospects 2017 – Data Booklet. Department of Economic and Social Affairs, Population Division.

Williams, R.J.P., Fraústo da Silva, J.J.R., 2002. The Involvement of Molybdenum in Life. Biochemical and Biophysical Research Communications 292(2), 293-299.

Yao, Y., Gao, B., Chen, J., Zhang, M., Inyang, M., Li, Y., Alva, A., Yang, L., 2013. Engineered Carbon (Biochar) Prepared by Direct Pyrolysis of Mg-accumulated Tomato Tissues: Characterization and Phosphate Removal Potential. Bioresource Technology 138, 8-13.

Yuan, W., Solihin, Zhang, Q., Kano, J., Saito, F., 2014. Mechanochemical Formation of K–Si–Ca–O Compound as a Slow-release Fertilizer. Powder Technology 260, 22-26.

Zhang, Q., Saito, F., 2009. Mechanochemical Synthesis of Slow-Release Fertilizers through Incorporation of Alumina Composition into Potassium/Ammonium Phosphates. Journal of the American Ceramic Society 92(12), 3070-3073.

Zhang, Q., Wang, J., Yin, S., Sato, T., Saito, F., 2004. Synthesis of a Visible-Light Active TiO_2−xSx Photocatalyst by Means of Mechanochemical Doping. Journal of the American Ceramic Society 87(6), 1161-1163.

Chapter 2 Mechanochemical Synthesis of Zinc Borate for Use as a Dual-release B Fertilizer

---

(published in ACS Sustainable Chemistry & Engineering 202. DOI: https://doi.org/10.1021/acssuschemeng.1c07111)

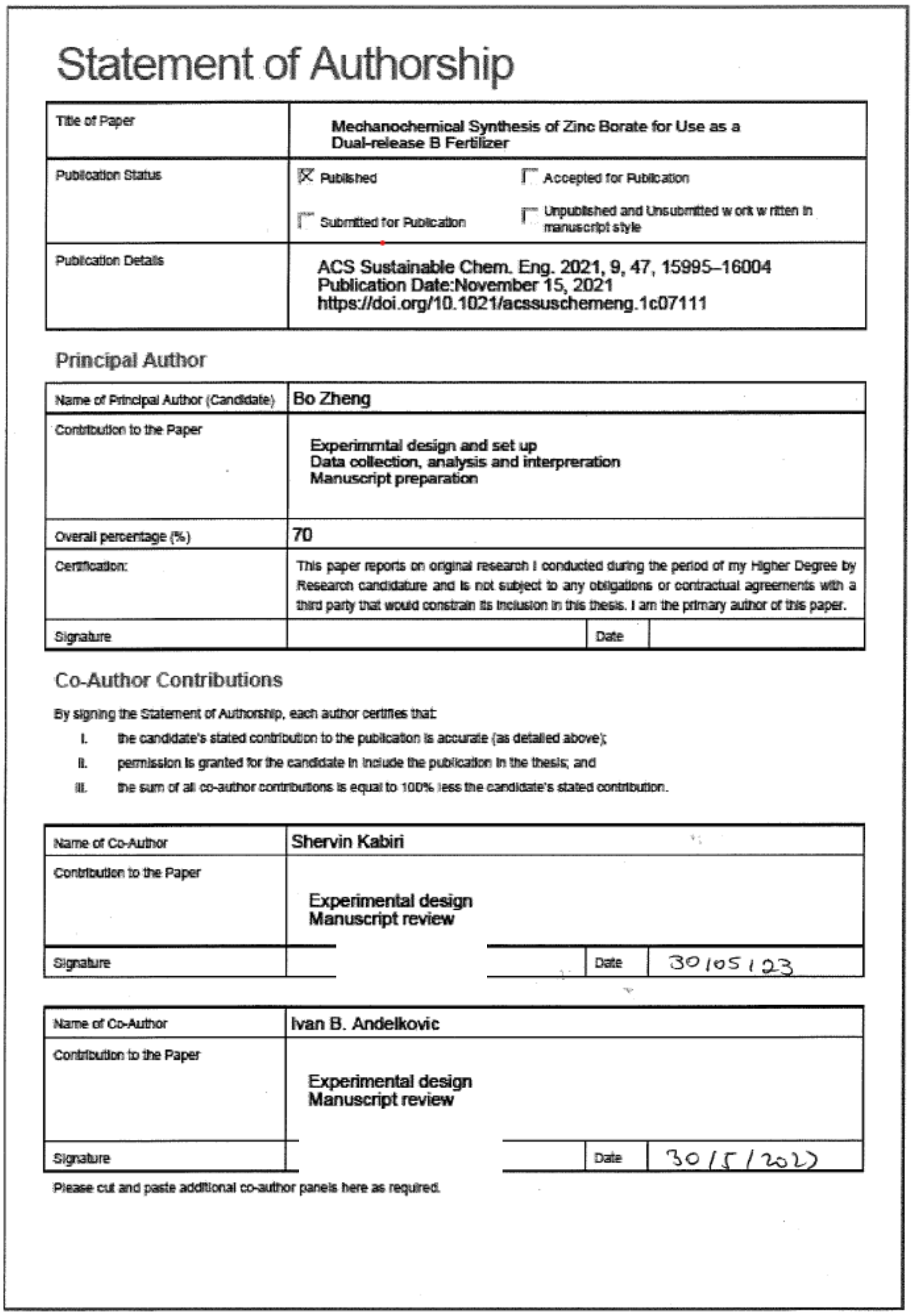

Statement of Authorship

Title of Paper	**Mechanochemical Synthesis of Zinc Borate for Use as a Dual-release B Fertilizer**
Publication Status	☒ Published ☐ Accepted for Publication ☐ Submitted for Publication ☐ Unpublished and Unsubmitted w ork w ritten in manuscript style
Publication Details	**ACS Sustainable Chem. Eng. 2021, 9, 47, 15995–16004** **Publication Date:November 15, 2021** **https://doi.org/10.1021/acssuschemeng.1c07111**

Principal Author

Name of Principal Author (Candidate)	**Bo Zheng**		
Contribution to the Paper	**Experimmtal design and set up** **Data collection, analysis and interpreration** **Manuscript preparation**		
Overall percentage (%)	**70**		
Certification:	This paper reports on original research I conducted during the period of my Higher Degree by Research candidature and is not subject to any obligations or contractual agreements with a third party that would constrain its inclusion in this thesis. I am the primary author of this paper.		
Signature		Date	

Co-Author Contributions

By signing the Statement of Authorship, each author certifies that:

i. the candidate's stated contribution to the publication is accurate (as detailed above);
ii. permission is granted for the candidate in include the publication in the thesis; and
iii. the sum of all co-author contributions is equal to 100% less the candidate's stated contribution.

Name of Co-Author	**Shervin Kabiri**		
Contribution to the Paper	**Experimental design** **Manuscript review**		
Signature		Date	30/05/23

Name of Co-Author	**Ivan B. Andelkovic**		
Contribution to the Paper	**Experimental design** **Manuscript review**		
Signature		Date	30/5/2023

Please cut and paste additional co-author panels here as required.

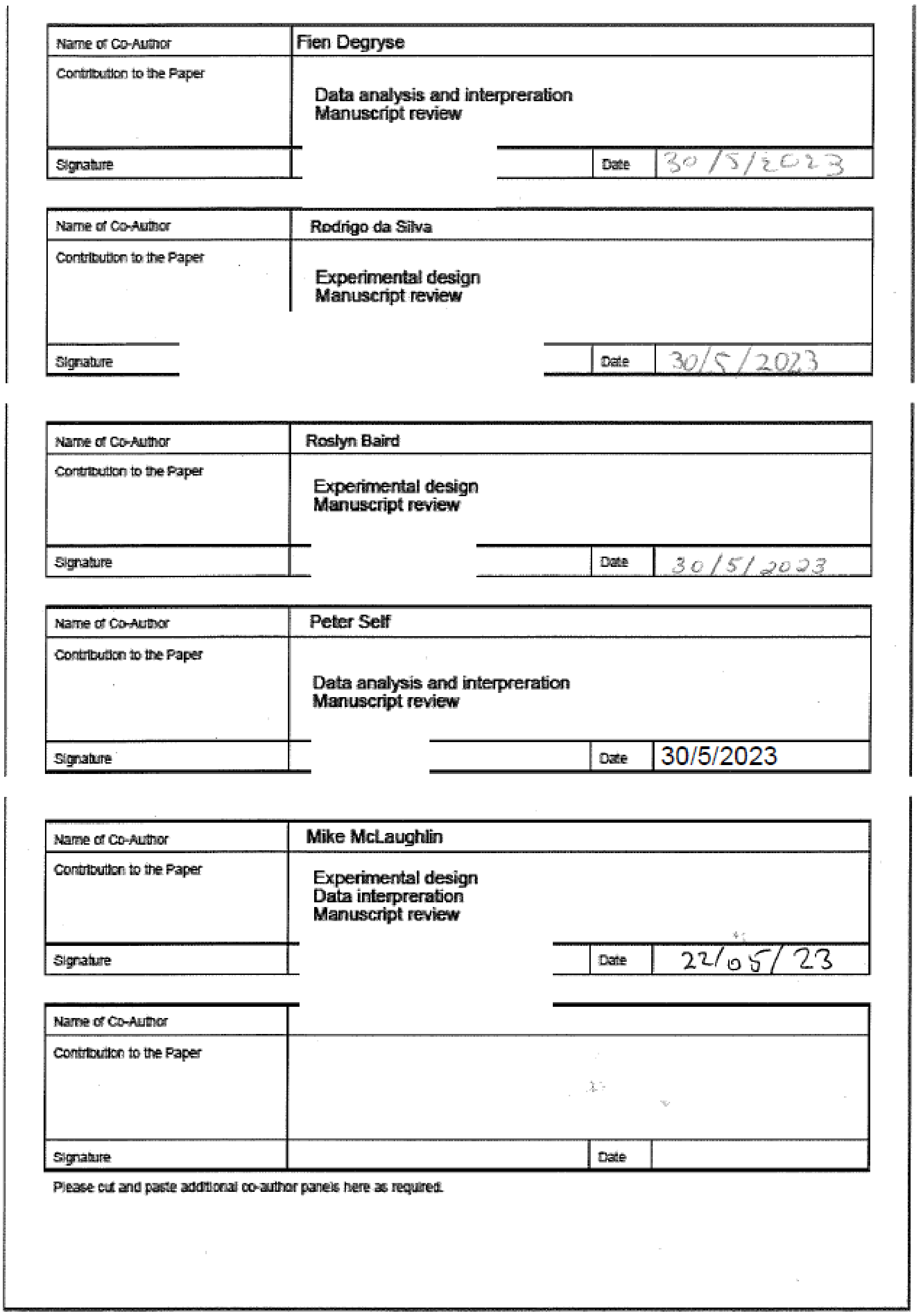

Name of Co-Author	Fien Degryse		
Contribution to the Paper	Data analysis and interpreration Manuscript review		
Signature		Date	30/5/2023

Name of Co-Author	Rodrigo da Silva		
Contribution to the Paper	Experimental design Manuscript review		
Signature		Date	30/5/2023

Name of Co-Author	Roslyn Baird		
Contribution to the Paper	Experimental design Manuscript review		
Signature		Date	30/5/2023

Name of Co-Author	Peter Self		
Contribution to the Paper	Data analysis and interpreration Manuscript review		
Signature		Date	30/5/2023

Name of Co-Author	Mike McLaughlin		
Contribution to the Paper	Experimental design Data interpreration Manuscript review		
Signature		Date	22/05/23

Name of Co-Author			
Contribution to the Paper			
Signature		Date	

Please cut and paste additional co-author panels here as required.

ACS Sustainable Chemistry & Engineering

pubs.acs.org/journal/ascecg

Research Article

Mechanochemical Synthesis of Zinc Borate for Use as a Dual-Release B Fertilizer

Bo Zheng,* Shervin Kabiri, Ivan B. Andelkovic, Fien Degryse, Rodrigo da Silva, Roslyn Baird, Peter Self, and Mike John McLaughlin

Cite This: *ACS Sustainable Chem. Eng.* 2021, 9, 15995−16004

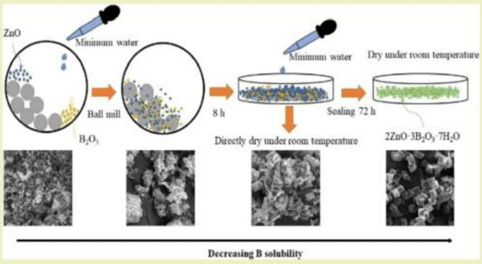

ABSTRACT: This study investigated a mechanochemical method to synthesize a slow-release micronutrient fertilizer containing zinc (Zn) and boron (B). Two reactants ZnO and B_2O_3 were milled in a ball mill for 4 or 8 h with small quantities of water as part of liquid-assisted grinding, with or without a water-assisted reaction (WAR). The products were characterized by X-ray diffraction, Fourier transform infrared spectroscopy, and scanning electron microscopy. Low-solubility zinc borate ($2ZnO\cdot3B_2O_3\cdot7H_2O$), with an octahedral crystal morphology, was successfully synthesized by ball milling and WAR. A column dissolution study showed that the products made by 8 h milling followed by 72 h of WAR exhibited a slow and dual-release pattern of B release, with 26% of the total B released after a 72 h dissolution period. Products made without milling or without WAR showed much faster B release. The proposed synthesis route is a sustainable manufacturing process that is energy efficient and does not generate any noxious effluents, producing a material containing two important micronutrients with a slow release rate.

KEYWORDS: *mechanochemistry, micronutrients, slow release boron fertilizer, zinc borate, fertilizer manufacturing, green synthesis*

INTRODUCTION

Boron (B) and zinc (Zn) are essential micronutrients for crop growth, quality, and yield. Boron is present in soil as $B(OH)_3$ (boric acid) under most conditions and can be easily leached through soil or cause toxicity as it is only weakly bound by organic matter and soil particles.[1,2] The most common forms of B used in fertilizers are hydrated or anhydrous sodium borate, borax, boric acid, or less soluble sources such as colemanite ($Ca_2B_6O_{11}\cdot5H_2O$) and ulexite ($NaCaB_5O_9\cdot8H_2O$).[2] Less soluble B sources are preferred for inclusion in fertilizers to avoid B leaching and possible toxicity due to the narrow window between deficiency and toxicity for this element.[1] However, the solubility of these sources may still vary with particle size and the pH of the co-granulated fertilizer.[3] Other less soluble B sources have been synthesized, such as B frits and BPO_4,[2−5] but these raw materials are not commonly used as fertilizers due to availability and cost issues. Notably, there is still lack of slow-release B products that can be used directly as fertilizers in the field or as a raw material for inclusion in a wide range of macronutrient fertilizers.[3,6]

Zinc is predominantly taken up by plants as Zn^{2+} like other metal cations. However, Zn^{2+} can be readily adsorbed by soil particles and organic matter or precipitated with anions, which makes it less available for plants. The common Zn sources used in the fertilizer industry are ZnO, $ZnSO_4\cdot xH_2O$, and chelated Zn.[7] Zinc oxide has the highest Zn concentration requiring small amounts of raw material for fertilizer formulation and is the cheapest of these Zn sources. Ideally, Zn with high water solubility is preferred for inclusion in fertilizers due to the higher agronomic effectiveness of water-soluble Zn,[7,8] while ZnO has very low solubility. However, the efficiency and residual value of ZnO are not always lower than those of other soluble Zn sources because the availability of Zn^{2+} is influenced by other factors, such as the application method,[8] the macronutrient fertilizer with which it is coated or cogranulated,[9,10] the soil pH,[11] and the application rate.[12,13] In addition, Zn deficiency is common in calcareous soils across the globe,[14] and around 17.3% of the world's population suffers from Zn deficiency.[15] A fertilizer that contains both B and Zn has logistical advantages both for use directly as a fertilizer and as a fertilizer raw material for manufacturing new products.

Mechanochemistry (MC) is recognized as a green method for synthesizing and transforming materials and has been extensively studied in other industries such as alloys and pharmaceuticals.[16,17] Compared to existing chemical synthesis

Received: October 18, 2021
Revised: October 26, 2021
Published: November 15, 2021

methods, MC relies purely on mechanical forces and is therefore cleaner and more efficient. MC can potentially be used by the fertilizer industry for two purposes: (i) to increase the solubility of low-solubility minerals (such as apatite) by decreasing their particle size and increasing reactivity[18−20] and (ii) to synthesize low-solubility compounds through the incorporation of soluble salts into insoluble compounds or matrixes, thereby producing products that are less prone to leaching and/or less toxic. For example, metal oxides or hydroxides such as Al_2O_3,[21] $Mg(OH)_2$,[22] and clay minerals[23,24] were milled with highly soluble macronutrient salts to synthesize low-solubility compounds containing potassium (K) and phosphorus (P) or nitrogen (N). Honer and co-workers applied MC to synthesize urea co-crystals either with low solubility minerals[25,26] or micronutrient salts[27,28] to enhance N efficiency by reducing ammonia (NH_3) emissions. Traditionally, wet chemistry involves large volumes of solution to allow reactants to dissolve, achieve homogeneity, and obtain final products. Liquids (e.g., water) are often also used in MC during grinding. Recent research showed that the liquid in liquid-assisted grinding (LAG) could promote the connection between reactants by increasing the rate of diffusion of molecules during ball milling.[29]

Hydrated zinc borates have been used in many industries as flame retardants and preservatives for bio-composites/wood.[30] The common method for zinc borate synthesis is through hydro-thermal methods, which require excess amounts of reactants, long drying/heating times, and large volumes of solvents.[31,32] In this study, we developed a greener method to synthesize zinc borate for fertilizer use by MC and water-assisted reaction (WAR) without producing unwanted by-products/wastes. The WAR was modified and employed from solvent-assisted reaction[33,34] as a separate step after MC. The use of WAR was inspired by previous studies where a second step of agitation or hydrothermal treatment after ball milling was found to increase grain growth of products.[35−37] Different conditions such as the milling time and water addition were investigated to obtain a product with relatively low B water solubility compared to the raw materials. The synthesized materials were characterized using scanning electron microscopy (SEM), X-ray diffraction (XRD), and Fourier-transform infrared (FTIR) spectroscopy. The kinetics of B and Zn release from the synthesized zinc borate fertilizers were evaluated using a column dissolution technique.

■ MATERIALS AND METHODS

Reagents. Zinc oxide (ZnO, 99.8% analytical grade) was purchased from ChemSupply (SA, Australia), and boric anhydride (B_2O_3, 98%, granulated) was purchased from Sigma-Aldrich (NSW, Australia). Ground colemanite was obtained from Etimine USA, Inc., and disodium tetraborate ($Na_2B_4O_7$) 30-mesh (as Dehybor) was obtained from U.S. Borax Inc. Calcium chloride dihydrate ($CaCl_2 \cdot 2H_2O$) was purchased from Scharlau (Barcelona, Spain). All chemicals were employed without further purification. Reverse osmosis (RO) water was used for all processes.

MC and WAR. Zinc oxide, B_2O_3, and RO water were used as reactants for LAG. The mixtures of the reactants were either manually ground by mortar and pestle to achieve homogeneity (control treatment) or milled for 30 min, 1, 2, 4, or 8 h at 26 Hz. The milling procedure was performed in a mixer mill Retsch MM400 (Haan, Germany) with a 5 min break after 1 h of milling to avoid overheating. In a typical milling procedure, 0.45 g of ZnO, 0.55 g of B_2O_3, and 170 μL of water as LAG to promote homogeneity and to maintain products as free-flowing powders were loaded into a 25 mL stainless steel jar and filled with eleven stainless steel balls with a diameter of 5 mm (~2 g per ball) to achieve a ball to a solid material mass ratio of ~20. On a subset of milled samples (Control, 30 min, 1 h, 2 h, 4 h, and 8 h), WAR was performed (Control-S, 30 min-S, 1 h-S, 2 h-S, 4 h-S, and 8 h-S) (Table 1) by adding 1.5 mL of RO water per 1 g of milled product to achieve a paste-like mixture. The paste-like mixtures were directly air-dried after adding water as a short time WAR (-S treatments) and manually ground by mortar and pestle to homogenize. As the 4 h-S and 8 h-S treatments had lower solubility than other treatments (see results), we performed further WAR for longer time on Control (Control-L) and 4 h (4 h-L) and 8 h (8 h-L) samples by sealing the mixtures in a 50 mL tube for 3 d after adding water and incubating at room temperature around 20−25 °C. Samples were air-dried after 3 d of contact with water and manually ground to homogenize. For comparison, two other reference materials were prepared by mixing ZnO with high and low solubility B sources at the same weight ratio of 1:1.22, that is, 0.45 g of ZnO and 0.55 g of $Na_2B_4O_7$ and colemanite ($Ca_2B_6O_{11} \cdot 5H_2O$).

Table 1. Synthesized Products and Reference Materials Formulation and Parameters for Preparation

treatments	chemicals	milling time (h)	WAR[a]
Control	ZnO, B_2O_3	0	N
30 min	ZnO, B_2O_3	0.5	N
1 h	ZnO, B_2O_3	1	N
2 h	ZnO, B_2O_3	2	N
4 h	ZnO, B_2O_3	4	N
8 h	ZnO, B_2O_3	8	N
Control-S	ZnO, B_2O_3	0	S
30 min-S	ZnO, B_2O_3	0.5	S
1 h-S	ZnO, B_2O_3	1	S
2 h-S	ZnO, B_2O_3	2	S
4 h-S	ZnO, B_2O_3	4	S
8 h-S	ZnO, B_2O_3	8	S
Control-L	ZnO, B_2O_3	0	L
4 h-L	ZnO, B_2O_3	4	L
8 h-L	ZnO, B_2O_3	8	L
Col + ZnO	ZnO, $Ca_2B_6O_{11} \cdot 5H_2O$	0	N
TetB + ZnO	ZnO, $Na_2B_4O_7$	0	N

[a] N—no WAR, S—short time of WAR, and L—long time of WAR.

Water Solubility and Chemical Composition. The solubility of the synthesized products, reactants (ZnO and B_2O_3), and reference materials was assessed by weighing 0.1 g of sample into a 50 mL digestion tube with 10 mL of RO water. Samples were shaken in an end-over-end shaker for 1 h, followed by 10 min centrifugation at 4685*g*. Then, the suspensions were filtered through a 0.2 μm syringe filter prior to analysis using inductively coupled plasma−optical emission spectrometry (ICP−OES, Avio 200, PerkinElmer, Waltham, USA) and pH measurement. The sediment remaining in the centrifuge tubes was digested overnight at room temperature using *aqua regia* (HNO_3/HCl = 1:3 v/v), followed by 45 min heating at 80 °C and 165 min heating at 125 °C on a digestion hot block. The Zn and B concentrations in the digest were also analyzed by ICP−OES to determine the total content of soluble and insoluble Zn and B.

Structural Characterization. The morphology of the synthesized products was analyzed by field emission SEM (FE-SEM, Quanta 450, FEI, USA). XRD patterns of products and reactants were recorded on an X'Pert Pro multi-purpose diffractometer (PANalytical B.V. Almelo, Netherlands) using Fe-filtered Co Kα radiation, an automatic divergence slit, a 2° anti-scatter slit, and a fast X'Celerator Si strip detector. The diffraction patterns were recorded in steps of 0.017° 2 theta with a 0.5 s counting time per step for an overall counting time of approximately 30 min. Phase identification was performed on the XRD data using in-house software (XPLOT) (Microsoft, Redmond, Washington, USA) and HighScore Plus (from PANalytical) search/match software. The relative amounts of the major phases were

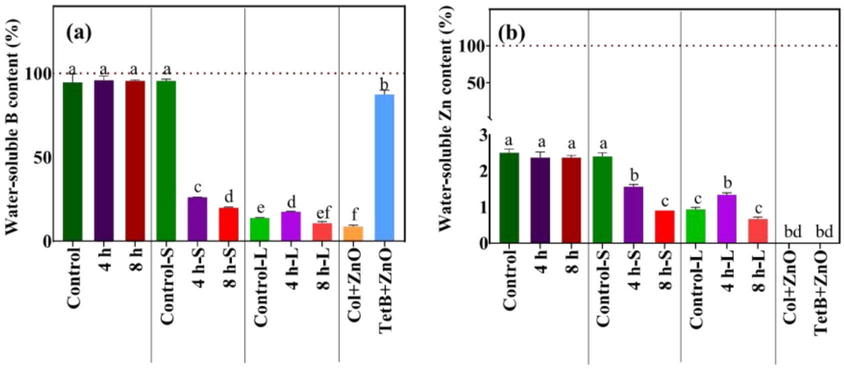

Figure 1. (a) Water soluble B and (b) water soluble Zn as percentages of total B and Zn of the zinc borate products and reference materials after 1 h of shaking. The error bars represent standard errors of three replicates, and different letters indicate significant differences ($P \leq 0.05$, Tukey's HSD).

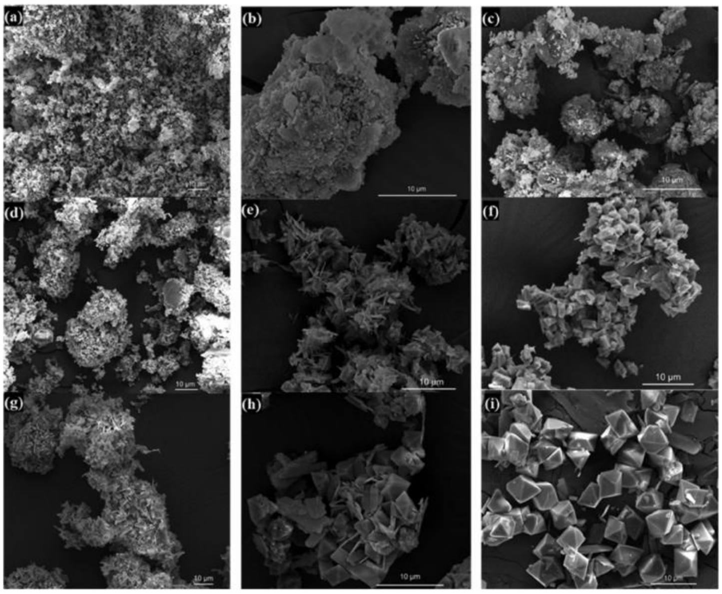

Figure 2. SEM images of (a) Control, (b) 4 h milled, (c) 8 h milled, and (d) the short WAR time control (Control-S), (e) 4 h milled (4 h-S), (f) 8 h milled (8 h-S), and (g) the long WAR time control (Control-L), (h) 4 h milled (4 h-L), and (i) 8 h milled (8 h-L) treatments.

determined by the Rietveld method using the TOPAS software package from Bruker (Bruker BioSpinCorporation, Billerica, Massachusetts, USA). The FTIR measurements were carried out using the attenuated total reflectance (ATR) module on an Alpha FT-IR spectrometer (Bruker Optics, Ettlingen, Germany). The analysis was performed in the middle infrared range (wavelength from 4000 to 400 cm^{-1}) at 4 cm^{-1} resolution and corrected against an air background. The sample was mounted on the platinum platform and covered with a thin layer of foil paper. Each sample was scanned 100 times, and the platform was cleaned by a lint-free tissue and ethanol between treatments.

Column Dissolution Study. Dissolution kinetic experiments were conducted for nine selected products (Control, 4 h, 8 h, Col + ZnO, TetB + ZnO, Control-S, 4 h-S, 8 h-S, Control-L, and 8 h-L) using the column perfusion method described by Baird et al.[38] This is a laboratory method that examines the dynamic release of nutrients from fertilizer formulations by continuously perfusing samples with solution in real time. Previous studies showed good correlation between the pot, leaching, and seeding toxicity experiments using this method.[4,6,39] The 4 h-L was not included as no significant changes in other characteristics were observed between 4 h-S and 4 h-L. Powders were used in this study to avoid any potential effects of granulation due to particle size and/or binders. 0.4 g of powder sample was placed in between 1 g of glass wool in each polypropylene column (150 mm long × 15 mm diameter). The percolating solution (10 mM $CaCl_2$, pH = 6) was introduced to the column from the bottom using a peristaltic pump at a constant rate of 10 mL h^{-1}. The solutions released from the top of the column were collected every hour for 72 h using a fraction collector (SuperFracTM, Pharmacia, USA). At the end of the study, residues, glass wool, and solution remaining in each column were collected and dried in the oven under 90 °C until all liquid vaporized. These residues were digested using hot *aqua regia*, analyzed by ICP–OES, and added to all nutrients released over time to determine the total nutrient in the sample. The nutrient in each hourly sample was expressed as a percentage of this total. All column dissolutions were performed in duplicate. For two materials (8 h-S and Control-S), the morphology (FE-SEM) and the FTIR spectrum of the residues were determined.

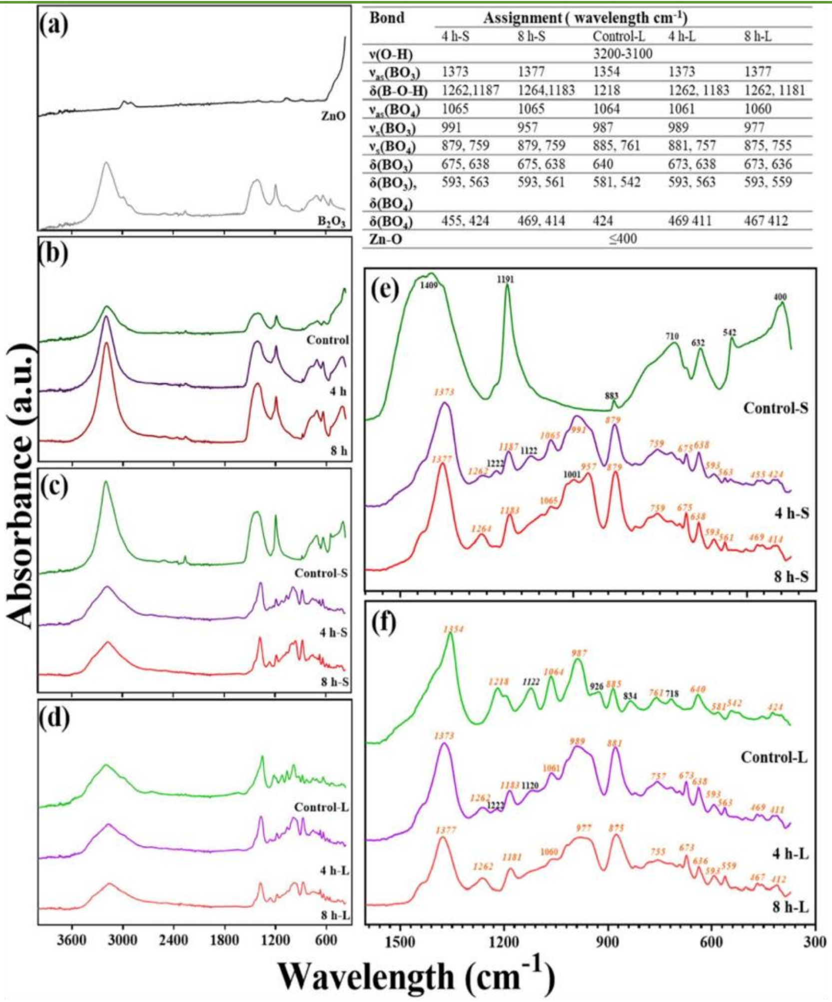

Bond	Assignment (wavelength cm^{-1})				
	4 h-S	8 h-S	Control-L	4 h-L	8 h-L
ν(O-H)			3200-3100		
$\nu_{as}(BO_3)$	1373	1377	1354	1373	1377
δ(B-O-H)	1262,1187	1264,1183	1218	1262, 1183	1262, 1181
$\nu_{as}(BO_4)$	1065	1065	1064	1061	1060
$\nu_s(BO_3)$	991	957	987	989	977
$\nu_s(BO_4)$	879, 759	879, 759	885, 761	881, 757	875, 755
$\delta(BO_3)$	675, 638	675, 638	640	673, 638	673, 636
$\delta(BO_3)$, $\delta(BO_4)$	593, 563	593, 561	581, 542	593, 563	593, 559
$\delta(BO_4)$	455, 424	469, 414	424	469 411	467 412
Zn-O			≤400		

Figure 3. FTIR profiles of (a) reactants, (b) Control, 4 h, and 8 h milled treatments, (c) short-time water-assisted control (Control-S), milled 4 h (4 h-S), and 8 h (8 h-S) treatments, (d) long-time water-assisted control (Control-L), milled 4 h (4 h-L), and 8 h (8 h-L) treatments, (e) fingerprint wavelength range (300−1500 cm^{-1}) of short-time water-assisted treatments with peaks belonging to zinc borate indicated in orange, and (f) long-time water-assisted treatments with peaks belonging to zinc borate indicated in orange. The observed FTIR peak wave numbers and assigned bonds of the synthesized products are summarized in the top right of the figure.

RESULTS AND DISCUSSION

Chemical Composition and Solubility. The synthesized products contained between 11−15% B and 26−34% Zn (Table S1). The variation of B and Zn concentrations in the products is likely due to the amount of hydration on the surface of the products and the amount of crystalline water. The water solubility of the treatments is reported as the percentage of total B and Zn in solution after 1 h shaking (Figure 1a,b). More than 90% of B was dissolved for all treatments without WAR (Figure 1a). Therefore, ball milling alone did not change the solubility of B. A short time of WAR after ball milling significantly decreased B solubility for 4 h-S (26%) and 8 h-S (20%) while the Control-S treatment had B solubility similar to those of the Control (unmilled) and milled (4 h and 8 h) treatments, with more than 90% of the total B being water soluble. B solubility was the lowest in the longer-time water-assisted treatments. Surprisingly, only 14% of B was released from Control-L, which had not been milled prior to the WAR. The solubility of B was around 18 and 11% for 4 h-L and 8 h-L samples, respectively. TetB + ZnO released about 90% of the total B while Col + ZnO only released 10%. The water solubility of Zn followed trends similar to those for B, but solubility was very low for all treatments, less than 3% of the total Zn. The water-soluble Zn was highest in treatments without WAR and lowest in 8 h-S and 8 h-L. The amount of Zn released from Col + ZnO and TetB + ZnO was below the detection limit (<0.4 μg/L, equivalent to 0.0003% of total Zn).

Structural Characterization of Synthesized Products. The SEM images of Control, 4 h, and 8 h samples showed a morphology of agglomerated particles (Figure 2a−c). The agglomeration of 4 h and 8 h samples might be due to cold welding.[40] No identifiable crystal morphology was observed in these treatments. A change in morphology was observed with the WAR. In short, for water-assisted treatments, the SEM image of Control-S (Figure 2d) showed large single particles covered by smaller particles, likely due to recrystallization of B_2O_3 or different particle sizes of reactants. However, 4 h-S and 8 h-S (Figure 2e,f) transformed to a mixture of thick rod-like, layered, and elongated octahedral crystals. The long WAR time induced a transformation in morphology in all treatments with or without milling (Figure 2g–i) where the Control-L treatment transformed to a thin rod-like layered structure and the 4 h-L and 8 h-L treatments were similar in crystal shape to the 4 h-S and 8 h-S treatments but with noticeable increases in crystal size. Most notably, the 8 h-L (Figure 2i) treatment displayed a well-dispersed mixture of octahedral and elongated octahedral crystals with negligible rod-like or layered crystals seen in Control-L. The lower-magnification SEM images (Figure S1a–f) showed that a longer milling time before WAR and a longer WAR time favored the formation of octahedral crystals.

The same characteristic peaks in FTIR spectra of reactants (Figure 3a) could be seen in the spectra of milled samples (Figure 3b). This suggests an absence of breaking and/or formation of new bonds during milling. The short- and long-time WAR significantly changed the spectrum (Figure 3c,d) of all the treatments except for the Control-S treatment, which mainly showed the peaks of the reactants. The FTIR spectrum of the Control-L treatment was different from all other treatments, such as the B−O−H bending and out-of-plane bending of B_3−O and B_4−O. The spectra of 4 h-S, 8 h-S, 4 h-L, and 8 h-L treatments (Figure 3c,d) were in good agreement with the spectrum of zinc borate ($2ZnO·3B_2O_3·7H_2O$) reported in the literature.[31,32] The characteristic peaks of zinc borate are summarized in the table of Figure 3 and highlighted in Figure 3e,f. The detailed wavelength fingerprint range of short and long WAR treatments was slightly different between the treatments milled for 4 h and 8 h (Figure 3e,f), where unhighlighted peaks 1222 and 1122/1120 cm^{-1} might belong to other types of zinc borate (unidentifiable) with different B−O−H bending. Nevertheless, the 4 h-S, 4 h-L, 8 h-S, and 8 h-L treatments contained chemical bonds indicative of zinc borate. The characteristic peaks of trihedral (1373−1377 and 957−991 cm^{-1}) and tetrahedral borate (1060−1065 and 755−881 cm^{-1}) groups are in good agreement with the known ring structure[41] that belongs to $2ZnO·3B_2O_3·7H_2O$.

The XRD pattern (Figure S2) for the ZnO reactant was in good agreement with the theoretical pattern (ICSD 157724), while for B_2O_3, there were a few peaks which were identified as H_3BO_3 (PDF 00-025-0097) due to its partial hydration in the air. The differences between the Control, 4 h, and 8 h treatments were small in terms of the XRD patterns (Figure 4a), and all the observed peaks could be assigned to ZnO and H_3BO_3. The diffraction peaks became broader with an increasing milling time as a consequence of decreasing grain and crystallite size, increasing plastic deformation, and increasing lattice strain, which can be attributed to the generation of crystal defects with extended grinding periods.[42,43] Amirkhanlou et al. suggested that 8 h of milling is optimum for the production of ZnO nanocrystals or nanoparticles, while further milling will not be able to largely change the crystallite size and lattice strain of the ZnO powder.[42] Notably, the ZnO peaks still dominated the spectrum after 8 h of milling (Figure 4a).

The short-time WAR (Figure 4b) treatments produced new compounds, although Control-S still largely remained as the original reactant with identifiable ZnO peaks (Figure S2d), which agrees with the FTIR results. The major component of the 4 h-S and 8 h-S treatments was zinc borate $ZnB_3O_3(OH)_5(H_2O)$ (LPF 1923377) (Figure S2b), also formulated as $2ZnO·3B_2O_3·7H_2O$ in the more recent literature.[31,32,44] Peaks of unreacted ZnO, B_2O_3 as H_3BO_3, and some unidentifiable structures (unlabeled peaks) were detected in the XRD patterns of the 4 h-S and 8 h-S treatments. In the long-time WAR treatments (Figure 4c), Control-L transformed to a new phase without pre-milling where the intensity of the peaks for ZnO was largely decreased, and a few peaks of $2ZnO·3B_2O_3·7H_2O$ and new peaks for other hydrated zinc borate compounds were observed. This is in good agreement with SEM and FTIR results where a new crystal structure and new bonds were observed. Both 4 h-L and 4 h-S treatments showed stronger $2ZnO·3B_2O_3·7H_2O$ peaks compared with the Control-L treatment, such as peaks at 2θ values of 15, 31, and 34°. However, several unidentifiable peaks were still observed in the patterns. Full quantitative analysis was not possible for most of the samples except for the Control, Control-S, 4 h, 8 h, and 8 h-L treatments, as some of the peaks in the XRD patterns of other samples cannot be assigned to a known structure. Quantitative analysis based on the XRD pattern of the 8 h-L sample showed that this sample

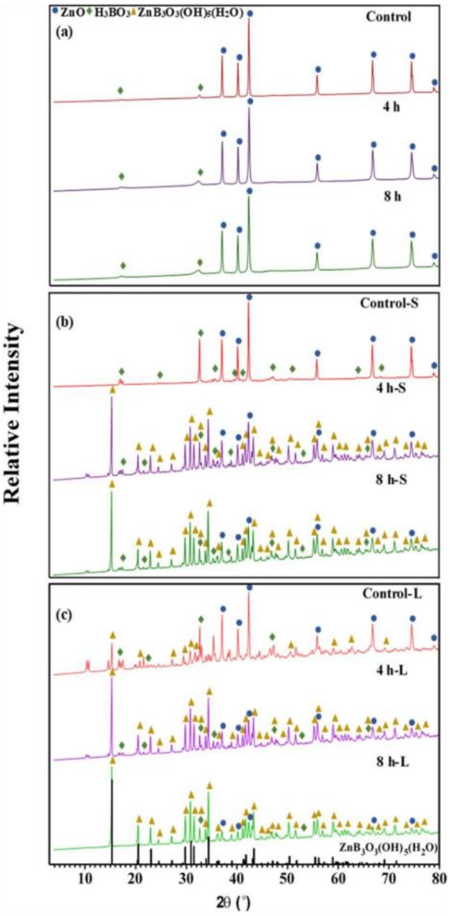

Figure 4. XRD patterns of (a) Control, 4 h, and 8 h milled treatments, (b) short time water-assisted control (Control-S), milled 4 h (4 h-S), and 8 h (8 h-S) treatments, and (c) long time water-assisted control (Control-L), milled 4 h (4 h-L), and 8 h (8 h-L) treatments. Round marks denote the peak allocation to zinc oxide, rhombus marks denote the peak allocation to boric acid, and triangle marks denote the peak allocation to zinc borate $2ZnO·3B_2O_3·7H_2O$.

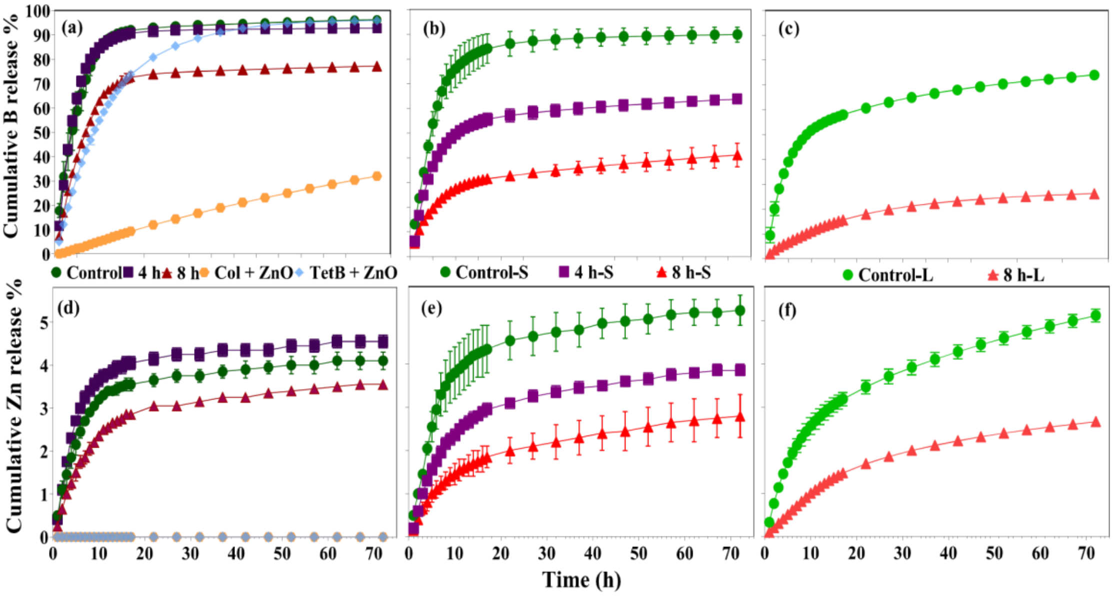

Figure 5. Cumulative B released from (a) non-water-assisted samples and commercial samples, (b) short-time WAR samples, (c) long-time WAR samples and cumulative Zn released from (d) non-water-assisted samples and commercial samples, (e) short-time WAR samples, and (f) long-time WAR samples over 72 h. Error bars represent the standard error (*n* = 2).

consists of 80 to 85 wt.% 2ZnO $3B_2O_3·7H_2O$ with the remainder of the sample being ZnO and H_3BO_3. By comparing the XRD results with the SEM images, it appears that the octahedral crystals can be attributed to the presence of $2ZnO·3B_2O_3·7H_2O$.

Column Dissolution Study. *Boron.* The release profiles of synthesized products were studied and compared with slow- and fast-release B sources (commercial colemanite and sodium tetraborate, respectively) (Figure 5). Colemanite had a consistently slow release rate, which reached 32% cumulative B release over the 72 h monitoring period, while tetraborate showed full release of B over the same period (Figure 5a). The dissolution rate of B decreased with increasing milling time for both milled treatments and treatments having WAR (Figure 5a−c). This was more evident with short and long times for WAR (Figure 5b,c). All synthesized treatments showed an initial rapid release (within 10 h), followed by a subsequent slow release pattern. Control, 4 h, and 8 h treatments reached 85, 85, and 63% of total B release within the first 10 h, respectively, and slowly released another 10% of the total B until the end of the experiment. The B release of the 8 h treatment was lower within the first 10 h and over the whole dissolution period compared to the 4 h and Control treatments, indicating that increasing the milling time before WAR changes the kinetic dissolution characteristics of the product.

Control-S, 4 h-S, and 8 h-S (Figure 5b) treatments showed about 10, 40, and 30% less B release in the first 10 h compared to the respective treatments without WAR (Control, 4 h, and 8 h). After the first 10 h, the Control-S, 4 h-S, and 8 h-S treatments released an additional 10% of the total B over the remaining dissolution period. Control-L (Figure 5c) showed a slower B release compared to other control treatments, while B release after the first 10 h was faster (20% additional B released) than other treatments. Of all the synthesized products, the 8 h-L product (Figure 5c) showed the slowest release kinetics, with only 11% of the total B released in the first 10 h and another 15% of total B released in the subsequent 62 h period. This suggests that the octahedral crystals are likely to have lower solubility compared to the other crystal forms in these products. The dual release behavior of 8 h-L could be beneficial to plant growth, with initial moderate B release minimizing toxicity risks (and leaching losses) and sustained B release supporting plant growth during later high B demand reproductive stages.[45]

Zinc. Dissolution of Zn was consistently negligible over the 72 h period (Figure 5d−f) for the treatments containing colemanite and tetraborate, likely due to the high solution pH imposed by the dissolution of these minerals (Table S1). The same results were also observed in the batch water solubility measurements (Figure 1b) as ZnO has low solubility particularly in the alkaline solution. However, the Zn release profile of synthesized products was similar to the B release profile, where we can see an initial comparatively fast release followed by a slow release period, albeit for a very small percentage of the total Zn in the products. The cumulative Zn release, ranging from 2 to 5% of total Zn, was much lower than that of B (26 to 97% of total B). The cumulative release of Zn was lowest in the 8 h-S and 8 h-L treatments and highest in the Control-S and Control-L treatments. Increased milling time and a longer WAR time decreased the cumulative Zn release, but the differences were negligible compared to cumulative B release due to the low solubility of ZnO. Similar to B release, a different release pattern was observed for Control-L.

Characterization of Residue after Dissolution. The residues of two selected treatments (Control-S and 8 h-S) were collected for characterization by FTIR (Figure 6c) and SEM (Figure 6a,b). The FTIR spectrum of the Control-S residue was identical to that of ZnO (Figure 3a). All absorbance bands assigned to B-related bonds in the Control-S treatment disappeared, which is consistent with the 90% cumulative B release from this material. On the other hand, the FTIR

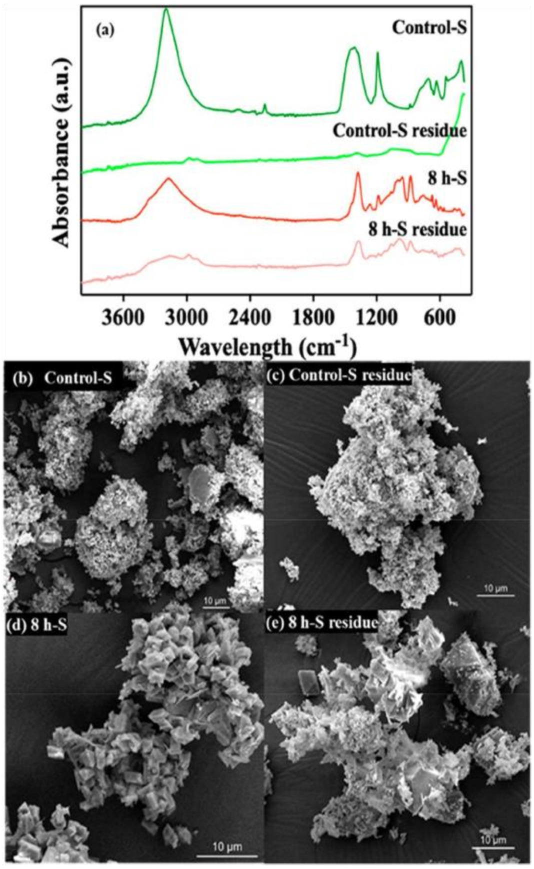

Figure 6. (a) FTIR profiles of Control-S and 8 h-S treatments and the residues collected after column perfusion of the Control-S and 8 h-S treatments and SEM images of (b) Control-S, (c) residues of Control-S, (d) 8 h-S, and (e) residues of 8 h-S. Residues of Control-S and 8 h-S were collected from columns at the end of the column dissolution experiments.

spectrum of the residue from the dissolution of the 8 h-S treatment was similar to the spectrum of the initial 8 h-S treatment. This suggests that the octahedral zinc borate synthesized in the 8 h-S treatment ($2ZnO{\cdot}3B_2O_3{\cdot}7H_2O$) was more resistant to dissolution than the B synthesized in the Control-S treatment. Furthermore, SEM images of the residue from the dissolution of the Control-S showed a fine particle aggregate similar to that before the column dissolution, whereas large amounts of transparent elongated octahedral crystals with different sizes were observed in the residue from the dissolution of the 8 h-S product. The changes of size before and after column dissolution of the 8 h-S product is probably due to Oswald ripening or particle migration and coalescence, whereby small particles migrate to the surface of large particles.[46]

Effects of MC and WAR. The proposed method using both MC and WAR results in a green and simple way to produce zinc borate as a potential fertilizer or fertilizer raw material. As summarized in Table 2, the milling time played an important role in the solubility of both B and Zn to varying extents. The extended 8 h milling time enhanced the size reduction of ZnO[42] and extensively mixed the reactants, thus promoting the growth of octahedral crystals during WAR. The results indicated that without ball milling, the low solubility of octahedral zinc borate cannot be produced by either short (Control-S) or long (Control-L) WAR using the reactants we proposed in this study. The Control-L formed products which had low solubility during the 1 h batch test, but these products were not stable under the conditions of the column perfusion experiment where the products of dissolution were continually removed from the surface of the material. The duration of WAR is essential for the products to age or relax and further increase grain growth as MC is continuously creating defects and accumulating energy in the reactants. Longer WAR might give enough time for the diffusion of B_2O_3 to occur, similar to a solid/vapor reaction,[34] while a short WAR time might minimize the diffusion process with water evaporation; thus, the reaction only takes place in a very short range around the particles. Reactants with less defects or diffusion might recrystallize as ZnO and H_3BO_3 or form unstable hydrated zinc borates. In addition, the residue study indicated that the octahedral zinc borate synthesized in the 8 h-S treatment had the ability to attach into larger crystals rather than be leached out by the eluant. The potential mechanism of $2ZnO{\cdot}3B_2O_3{\cdot}7H_2O$ formation could be summarized in two steps: first, ball milling accumulates in the defect-rich region in the reactants. Second, WAR increased the diffusion and convection of soluble reactants (i.e., B_2O_3), thus promoting the crystallization of stable crystals such as $2ZnO{\cdot}3B_2O_3{\cdot}7H_2O$ to minimize the accumulated mechanochemical energy.

Table 2. Summary of Characteristics of Synthesized Products and Their Solubility

treatments	new bonds[a]	new crystal phases[b]	micromorphology changes[c]	B solubility[d] (% total)
Control	no	no	agglomerated particles	96.2
4 h	no	no		92.7
8 h	no	no		77.2
Control-S	no	no		89.9
4 h-S	yes	yes	thin rods, layers, elongated octahedra	63.8
8 h-S	yes	yes	thin rods, elongated octahedra	41.2
Control-L	yes	yes	thin rods, layers	74.1
4 h-L	yes	yes	thin rods, layers elongated octahedra	n/a
8 h-L	yes	yes	octahedral	26.0

[a] New bonds developed compared to reactants, determined by FTIR absorption peaks. [b] Determined by XRD. [c] Determined by SEM. [d] % total B released after 72 h of column dissolution.

■ CONCLUSIONS

In this study, we provide a new method for the synthesis of a zinc borate material with slow-release B and Zn characteristics using MC and WAR. Conversion of raw materials to zinc borate was not complete but this is desirable for a fertilizer raw material where unreacted and soluble raw materials enhance the rapidly soluble nutrient in the fertilizer, and the synthesized slow release compound provides a slow release component. Column dissolution studies suggested that the zinc borate synthesized after mechanical milling and WAR could be used directly as a dual-release B fertilizer or as a raw material in fertilizer manufacture, with one B component released quickly to avoid early season deficiency and another component released slowly to meet plant demand over an extended period. Moreover, the two micronutrients B and Zn in the synthesized zinc borate are required by plants and needed in fertilizers.

Despite the release of Zn being rather slow and small in magnitude compared to other Zn sources such as $ZnSO_4$, it was higher than ZnO and could potentially be even more available in the presence of plant roots.

Given that the goal of green chemistry and engineering is to minimize the production of polluting and potentially toxic waste streams,[47,48] this synthesis was designed from both agronomic and green manufacturing perspectives to maximize fertilizer efficiency as well as minimize waste production. To achieve waste prevention (principle 1 of green chemistry), Sheldon[49] suggested that the calculation of a simple *E* factor (sEF) and a complete *E* factor (cEF) as full-scale manufacturing *E* factors generally fall between these two metrics. Compared with other methods that synthesized zinc borate before purification (with sEF values ranging from 3.1 to 25.8 and cEF values ranging from 85.1 to 275.8—Table S2), this method could achieve very small *E* factors, sEF = 0.2 and cEF = 1.9. Due to the lack of information in the published methods, the calculation for the previously published methods assumed that either Zn or B reactants were completely reacted or the organic solvents used by these methods for further purification were not included in the calculations. In a recent survey, water usage was the most used metric to assess green chemistry in commercial manufacturing.[50] Water usage in our method was 1.7 g water/g product, while in other methods, water usage could reach 77.5 to 250 g water/g product (Table S2). The successful application of our synthesis method could result in a very small *E* factor, minimal water usage, and high materials/atom economy for the fertilizer industry. The *E* factor could even reach close to 0 as the proposed method could produce fine particles that allow direct application as fertilizers or for coating or incorporation into macronutrient fertilizers. In addition, existing fertilizer coating processes that use water as the atomization and adhesion agent for coating could be potentially used as the WAR, though this requires further study. Other possible treatments can still be explored to further reduce the solubility, such as heating after milling. Further plant-based experiments are also required to compare with other Zn and B sources in terms of agronomic efficiency.

■ ASSOCIATED CONTENT

Supporting Information

The Supporting Information is available free of charge at https://pubs.acs.org/doi/10.1021/acssuschemeng.1c07111.

> Results for water solubility and pH of the treatments milled from 30 min to 8 h; low-magnification SEM images; theoretical XRD pattern of reactants and zinc borate and XRD pattern of initial reactants; and calculated *E* factor of the proposed method compared to other published methods (PDF)

■ AUTHOR INFORMATION

Corresponding Author

Bo Zheng – *Fertilizer Technology Research Centre, School of Agriculture, Food and Wine, The University of Adelaide, Glen Osmond, South Australia 5064, Australia;* orcid.org/0000-0002-5724-0967; Email: bo.zheng@adelaide.edu.au

Authors

Shervin Kabiri – *Fertilizer Technology Research Centre, School of Agriculture, Food and Wine, The University of Adelaide, Glen Osmond, South Australia 5064, Australia*

Ivan B. Andelkovic – *Fertilizer Technology Research Centre, School of Agriculture, Food and Wine, The University of Adelaide, Glen Osmond, South Australia 5064, Australia;* orcid.org/0000-0002-4570-0540

Fien Degryse – *Fertilizer Technology Research Centre, School of Agriculture, Food and Wine, The University of Adelaide, Glen Osmond, South Australia 5064, Australia;* orcid.org/0000-0002-4875-2944

Rodrigo da Silva – *Fertilizer Technology Research Centre, School of Agriculture, Food and Wine, The University of Adelaide, Glen Osmond, South Australia 5064, Australia;* orcid.org/0000-0002-2345-3729

Roslyn Baird – *Fertilizer Technology Research Centre, School of Agriculture, Food and Wine, The University of Adelaide, Glen Osmond, South Australia 5064, Australia;* orcid.org/0000-0002-1269-0323

Peter Self – *CSIRO, Mineral Resources, Glen Osmond, South Australia 5064, Australia*

Mike John McLaughlin – *Fertilizer Technology Research Centre, School of Agriculture, Food and Wine, The University of Adelaide, Glen Osmond, South Australia 5064, Australia*

Complete contact information is available at:
https://pubs.acs.org/10.1021/acssuschemeng.1c07111

Notes

The authors declare no competing financial interest.

■ ACKNOWLEDGMENTS

B.Z. is grateful for the scholarship and support from The University of Adelaide, School of Agriculture, Food and Wine. The authors are thankful for the help and support from Adelaide Microscopy and Ken Neubauer for SEM analysis and to Dr. Les Joseph Janik for assisting with FTIR analysis. The authors acknowledge the support of The Mosaic Company LLC. The authors thank Bogumila Tomczak, Ashleigh Broadbent, and Colin Rivers for their advice and technical support.

■ ABBREVIATIONS

LAG, liquid-assisted grinding; WAR, water-assisted reaction; XRD, x-ray diffraction; FTIR, fourier transform infrared spectroscopy; SEM, scanning electron microscopy; MC, mechanochemistry

■ REFERENCES

(1) Nable, R. O.; Bañuelos, G. S.; Paull, J. G. Boron Toxicity. *Plant Soil* **1997**, *193*, 181–198.

(2) Degryse, F. Boron fertilizers: Use, Challenges and the Benefit of Slow-release Sources—a Review. *J. Boron* **2017**, *2*, 111–122. Retrieved from https://dergipark.org.tr/en/pub/boron/issue/33625/373087/ (accessed Aug 28, 2021)

(3) Abat, M.; Degryse, F.; Baird, R.; McLaughlin, M. J. Slow-release Boron Fertilisers: Co-granulation of Boron Sources with Mono-ammonium Phosphate (MAP). *Soil Res.* **2015**, *53*, 505–511.

(4) Abat, M.; Degryse, F.; Baird, R.; McLaughlin, M. J. Boron Phosphates (BPO_4) as a Seedling-safe Boron Fertilizer Source. *Plant Soil* **2015**, *391*, 153–160.

(5) Hortenstine, C. C.; Ashley, D. A.; Wear, J. I. An Evaluation of Slowly Soluble Boron Materials1. *Soil Sci. Soc. Am. J.* **1958**, *22*, 249–251.

(6) Abat, M.; Degryse, F.; Baird, R.; McLaughlin, M. J. Responses of Canola to the Application of Slow-release Boron Fertilizers and Their Residual Effect. *Soil Sci. Soc. Am. J.* **2015**, *79*, 97–103.

(7) Mengel, K.; Kirkby, E. A.; Kosegarten, H.; Appel, T. Zinc. In *Principles of Plant Nutrition*; Mengel, K.; Kirkby, E. A.; Kosegarten, H.; Appel, T., Eds.; Springer Netherlands: Dordrecht, 2001; pp 585−597.

(8) Mortvedt, J. J.; Gilkes, R. J. Zinc Fertilizers. In *Zinc in Soils and Plants: Proceedings of the International Symposium on 'Zinc in Soils and Plants' Held at the University of Western Australia, 27−28 September, 1993*; Robson, A. D., Ed.; Springer Netherlands: Dordrecht, 1993; pp 33−44.

(9) McBeath, T. M.; McLaughlin, M. J. Efficacy of Zinc Oxides as Fertilisers. *Plant Soil* **2014**, *374*, 843−855.

(10) Montalvo, D.; Degryse, F.; da Silva, R. C.; Baird, R.; McLaughlin, M. J. Agronomic Effectiveness of Zinc Sources as Micronutrient Fertilizer. In *Advances in Agronomy*; Sparks, D. L., Ed.; Academic Press, 2016; Vol. *139*, Chapter 5, pp 215-267.

(11) Milani, N.; McLaughlin, M. J.; Stacey, S. P.; Kirby, J. K.; Hettiarachchi, G. M.; Beak, D. G.; Cornelis, G. Dissolution Kinetics of Macronutrient Fertilizers Coated with Manufactured Zinc Oxide Nanoparticles. *J. Agric. Food Chem.* **2012**, *60*, 3991−3998.

(12) Brennan, R. F.; Bolland, M. D. A. Zinc Sulfate is More Effective at Producing Wheat Shoots than Zinc Oxide in an Alkaline Soil but Both Sources are Equally Effective in an Acid Soil. *Aust. J. Exp. Agric.* **2006**, *46*, 1615−1620.

(13) Brennan, R. F. Residual Value of Zinc Fertiliser for Production of Wheat. *Aust. J. Exp. Agric.* **2001**, *41*, 541−547.

(14) Alloway, B. J. Soil Factors Associated with Zinc Deficiency in Crops and Humans. *Environ. Geochem. Health* **2009**, *31*, 537−548.

(15) Myers, S. S.; Wessells, K. R.; Kloog, I.; Zanobetti, A.; Schwartz, J. Effect of Increased Concentrations of Atmospheric Carbon Dioxide on the Global Threat of Zinc Deficiency: a Modelling Study. *Lancet* **2015**, *3*, e639−e645.

(16) James, S. L.; Adams, C. J.; Bolm, C.; Braga, D.; Collier, P.; Friščić, T.; Grepioni, F.; Harris, K. D. M.; Hyett, G.; Jones, W.; Krebs, A.; Mack, J.; Maini, L.; Orpen, A. G.; Parkin, I. P.; Shearouse, W. C.; Steed, J. W.; Waddell, D. C. Mechanochemistry: Opportunities for New and Cleaner Synthesis. *Chem. Soc. Rev.* **2012**, *41*, 413−447.

(17) Baláž, P.; Achimovičová, M.; Baláž, M.; Billik, P.; Cherkezova-Zheleva, Z.; Criado, J. M.; Delogu, F.; Dutková, E.; Gaffet, E.; Gotor, F. J.; Kumar, R.; Mitov, I.; Rojac, T.; Senna, M.; Streletskii, A.; Wieczorek-Ciurowa, K. Hallmarks of Mechanochemistry: from Nanoparticles to Technology. *Chem. Soc. Rev.* **2013**, *42*, 7571−7637.

(18) Pelovski, Y.; Petkova, V.; Dombalov, I. Thermotribochemical-treatment of Low Grade Natural Phosphates. *J. Therm. Anal. Calorim.* **2007**, *88*, 207−212.

(19) Baláž, P., Applied Mechanochemistry. In *Mechanochemistry in Nanoscience and Minerals Engineering*; Baláž, P., Ed.; Springer Berlin Heidelberg: Berlin, Heidelberg, 2008; pp 297−405.

(20) Chen, M.; Li, Z.; Huang, P.; Li, X.; Qu, J.; Yuan, W.; Zhang, Q. Mechanochemical Transformation of Apatite to Phosphoric Slow-release Fertilizer and Soluble Phosphate. *Process Saf. Environ. Prot.* **2018**, *114*, 91−96.

(21) Zhang, Q.; Solihin, F.; Saito, F. Mechanochemical Synthesis of Slow-Release Fertilizers through Incorporation of Alumina Composition into Potassium/Ammonium Phosphates. *J. Am. Ceram. Soc.* **2009**, *92*, 3070−3073.

(22) Solihin; Zhang, Q.; Tongamp, W.; Saito, F. Mechanochemical Route for Synthesizing $KMgPO_4$ and NH_4MgPO_4 for Application as Slow-Release Fertilizers. *Ind. Eng. Chem. Res.* **2010**, *49*, 2213−2216.

(23) Borges, R.; Prevot, V.; Forano, C.; Wypych, F. Design and Kinetic Study of Sustainable Potential Slow-Release Fertilizer Obtained by Mechanochemical Activation of Clay Minerals and Potassium Monohydrogen Phosphate. *Ind. Eng. Chem. Res.* **2017**, *56*, 708−716.

(24) Solihin; Zhang, Q.; Tongamp, W.; Saito, F. Mechanochemical Synthesis of Kaolin−KH_2PO_4 and Kaolin−$NH_4H_2PO_4$ Complexes for Application as Slow Release Fertilizer. *Powder Technol.* **2011**, *212*, 354−358.

(25) Honer, K.; Kalfaoglu, E.; Pico, C.; McCann, J.; Baltrusaitis, J. Mechanosynthesis of Magnesium and Calcium Salt−Urea Ionic Cocrystal Fertilizer Materials for Improved Nitrogen Management. *ACS Sustainable Chem. Eng.* **2017**, *5*, 8546−8550.

(26) Honer, K.; Pico, C.; Baltrusaitis, J. Reactive Mechanosynthesis of Urea Ionic Cocrystal Fertilizer Materials from Abundant Low Solubility Magnesium- and Calcium-Containing Minerals. *ACS Sustainable Chem. Eng.* **2018**, *6*, 4680−4687.

(27) Casali, L.; Mazzei, L.; Shemchuk, O.; Honer, K.; Grepioni, F.; Ciurli, S.; Braga, D.; Baltrusaitis, J. Smart Urea Ionic Co-crystals with Enhanced Urease Inhibition Activity for Improved Nitrogen Cycle Management. *Chem. Commun.* **2018**, *54*, 7637−7640.

(28) Mazzei, L.; Broll, V.; Casali, L.; Silva, M.; Braga, D.; Grepioni, F.; Baltrusaitis, J.; Ciurli, S. Multifunctional Urea Cocrystal with Combined Ureolysis and Nitrification Inhibiting Capabilities for Enhanced Nitrogen Management. *ACS Sustainable Chem. Eng.* **2019**, *7*, 13369−13378.

(29) Bowmaker, G. A.; Hanna, J. V.; Hart, R. D.; Skelton, B. W.; White, A. H. The Role of Short-range Diffusion in Solvent-assisted Mechanochemical Synthesis of Metal Complexes. *Dalton Trans.* **2008**, *39*, 5290−5292.

(30) Schubert, D. M. Hydrated Zinc Borates and Their Industrial Use. *Molecules* **2019**, *24*, 2419.

(31) Gao, Y.-H.; Liu, Z.-H. Synthesis and Thermochemistry of Two Zinc Borates, $Zn_2B_6O_{11}\cdot 7H_2O$ and $Zn_3B_{10}O_{18}\cdot 14H_2O$. *Thermochim. Acta* **2009**, *484*, 27−31.

(32) Gönen, M.; Balköse, D.; Gupta, R. B.; Ülkü, S. Supercritical Carbon Dioxide Drying of Methanol−Zinc Borate Mixtures. *Ind. Eng. Chem. Res.* **2009**, *48*, 6869−6876.

(33) Bowmaker, G. A.; Hanna, J. V.; Skelton, B. W.; White, A. H. Solvent-assisted Solid-state Synthesis: Separating the Chemical from the Mechanical in Mechanochemical Synthesis. *Chem. Commun.* **2009**, 2168−2170.

(34) Bowmaker, G. A. Solvent-assisted mechanochemistry. *Chem. Commun.* **2013**, *49*, 334−348.

(35) Zhong, L.; Qu, J.; Li, X.; He, X.; Zhang, Q. Simultaneous Synthesis of Ettringite and Absorbate Incorporation by Aqueous Agitation of a Mechanochemically Prepared Precursor. *RSC Adv.* **2016**, *6*, 35203−35209.

(36) Qu, J.; He, X.; Li, X.; Ai, Z.; Li, Y.; Zhang, Q.; Liu, X. Precursor Preparation of Zn−Al Layered Double Hydroxide by Ball Milling for Enhancing Adsorption and Photocatalytic Decoloration of Methyl Orange. *RSC Adv.* **2017**, *7*, 31466−31474.

(37) Qu, J.; He, X.; Chen, M.; Huang, P.; Zhang, Q.; Liu, X. A Facile Mechanochemical Approach to Synthesize Zn-Al Layered Double Hydroxide. *J. Solid State Chem.* **2017**, *250*, 1−5.

(38) Baird, R.; da Silva, R. C.; Degryse, F.; McLaughlin, M. J. A Column Perfusion Test to Assess the Kinetics of Nutrient Release by Soluble, Sparingly Soluble and Coated Granular Fertilizers. *J. Plant Nutr. Soil Sci.* **2019**, *182*, 763−771.

(39) da Silva, R. C.; Baird, R.; Degryse, F.; McLaughlin, M. J. Slow and Fast-Release Boron Sources in Potash Fertilizers: Spatial Variability, Nutrient Dissolution and Plant Uptake. *Soil Sci. Soc. Am. J.* **2018**, *82*, 1437−1448.

(40) Šepelák, V.; Bégin-Colin, S.; Le Caër, G. Transformations in Oxides Induced by High-Energy Ball-Milling. *Dalton Trans.* **2012**, *41*, 11927−11948.

(41) Wu, H.; Yu, H.; Pan, S.; Jiao, A.; Han, J.; Wu, K.; Han, S.; Li, H. New Type of Complex Alkali and Alkaline Earth Metal Borates with Isolated $(B_{12}O_{24})_{12}^{-}$ Anionic Group. *Dalton Trans.* **2014**, *43*, 4886−4891.

(42) Amirkhanlou, S.; Ketabchi, M.; Parvin, N. Nanocrystalline/nanoparticle ZnO Synthesized by High Energy Ball Milling Process. *Mater. Lett.* **2012**, *86*, 122−124.

(43) Damonte, L. C.; Mendoza Zélis, L. A.; Marí Soucase, B.; Hernández Fenollosa, M. A. Nanoparticles of ZnO Obtained by Mechanical Milling. *Powder Technol.* **2004**, *148*, 15−19.

(44) Sawada, H.; Igarashi, H.; Tatebe, A.; Sakao, K. Zinc Borate, and Production Method and Use Thereof. U.S. Patent 6,780,913 B2, 2004.

(45) Dear, B.; Lipsett, J. The Effect of Boron Supply on the Growth and Seed Production of Subterranean Clover. *Aust. J. Agric. Res.* **1987**, *38*, 537−546.

(46) Hansen, T. W.; DeLaRiva, A. T.; Challa, S. R.; Datye, A. K. Sintering of Catalytic Nanoparticles: Particle Migration or Ostwald Ripening? *Acc. Chem. Res.* **2013**, *46*, 1720−1730.

(47) Anastas, P. T., Warner, J. C. *Green Chemistry, Theory and Practice*; Oxford University Press: Oxford, 1998.

(48) Anastas, P. T.; Zimmerman, J. B. Peer Reviewed: Design Through the 12 Principles of Green Engineering. *Environ. Sci. Technol.* **2003**, *37*, 94A−101A.

(49) Sheldon, R. A. The E Factor: Fifteen Years on. *Green Chem.* **2007**, *9*, 1273−1283.

(50) Giraud, R. J.; Williams, P. A.; Sehgal, A.; Ponnusamy, E.; Phillips, A. K.; Manley, J. B. Implementing Green Chemistry in Chemical Manufacturing: A Survey Report. *ACS Sustainable Chem. Eng.* **2014**, *2*, 2237−2242.

Supporting Information

Mechanochemical synthesis of zinc borate for use as a dual-release B fertilizer

Bo Zheng†, Shervin Kabiri†, Ivan B. Andelkovic†, Fien Degryse†, Rodrigo da Silva†, Roslyn Baird†, Peter Self‡, Mike John McLaughlin†*

†Fertilizer Technology Research Centre, School of Agriculture, Food and Wine, The University of Adelaide, Waite Campus PMB 1, Glen Osmond SA 5064, Australia

‡CSIRO, Land and Water, Locked Bag 2, Glen Osmond, SA 5064, Australia

*Corresponding author: bo.zheng@adelaide.edu.au .

Numbers of pages: 6

Number of Tables: 2

Number of Figures: 2

Table S1. Total and water-soluble concentrations of B and Zn in the reactants, reference materials and synthesized products, and equilibrium pH of water suspensions.

Treatments	**Water-soluble B (mg/L)**	**Water-soluble Zn (mg/L)**	**Total B (%)**	**Total Zn (%)**	**pH[a]**
Reactants					
ZnO	-	2 ± 0	-	76 ± 1	8.0
B2O3	2509 ± 47	-	24 ± 0	-	5.7
Reference materials					
Col + ZnO	59 ± 6	ND	7 ± 0	38 ± 0	9.3
TetB + ZnO	950 ± 47	ND	11 ± 1	38 ± 2	9.2
Synthesized products					
Control	1415 ± 76	85 ± 3	15 ± 1	34 ± 2	7.0
30 min[b]	1119 ± 21	65 ± 2	12 ± 0	27 ± 0	7.2
1 h	1132 ± 43	65 ± 1	12 ± 0	26± 0	7.2
2 h	1112 ± 18	64 ± 0	12 ± 0	27 ± 0	7.2
4 h	1239 ± 34	75 ± 5	13 ± 0	31 ± 1	7.2
8 h	1192 ± 8	73 ± 1	12 ± 0	31 ± 2	7.2
Control-S[c]	1121 ± 10	68 ± 2	12 ± 0	28 ± 1	7.1
30 min-S	830 ± 17	50 ± 1	11 ± 0	27± 0	7.2
1 h-S	691 ± 27	50 ± 1	12± 0	27± 0	7.4
2 h-S	483 ± 18	68 ± 2	11± 1	28 ± 2	7.3
4 h-S	340 ± 2	48 ± 2	13 ± 1	30 ± 2	7.6
8 h-S	249 ± 6	28 ± 1	13 ± 1	31 ± 2	7.8
Control-L[d]	166 ± 4	27 ± 1	12 ± 1	28 ± 2	7.8
4 h-L	225 ± 4	39 ± 2	13 ± 1	30 ± 2	7.8
8 h-L	130 ± 10	20 ± 1	12 ± 0	29 ± 1	7.8

[a] Determined after shaking end-over-end for 1 h

[b] Milling time

[c] Short water-assisted reaction time

[d] Long water-assisted reaction time

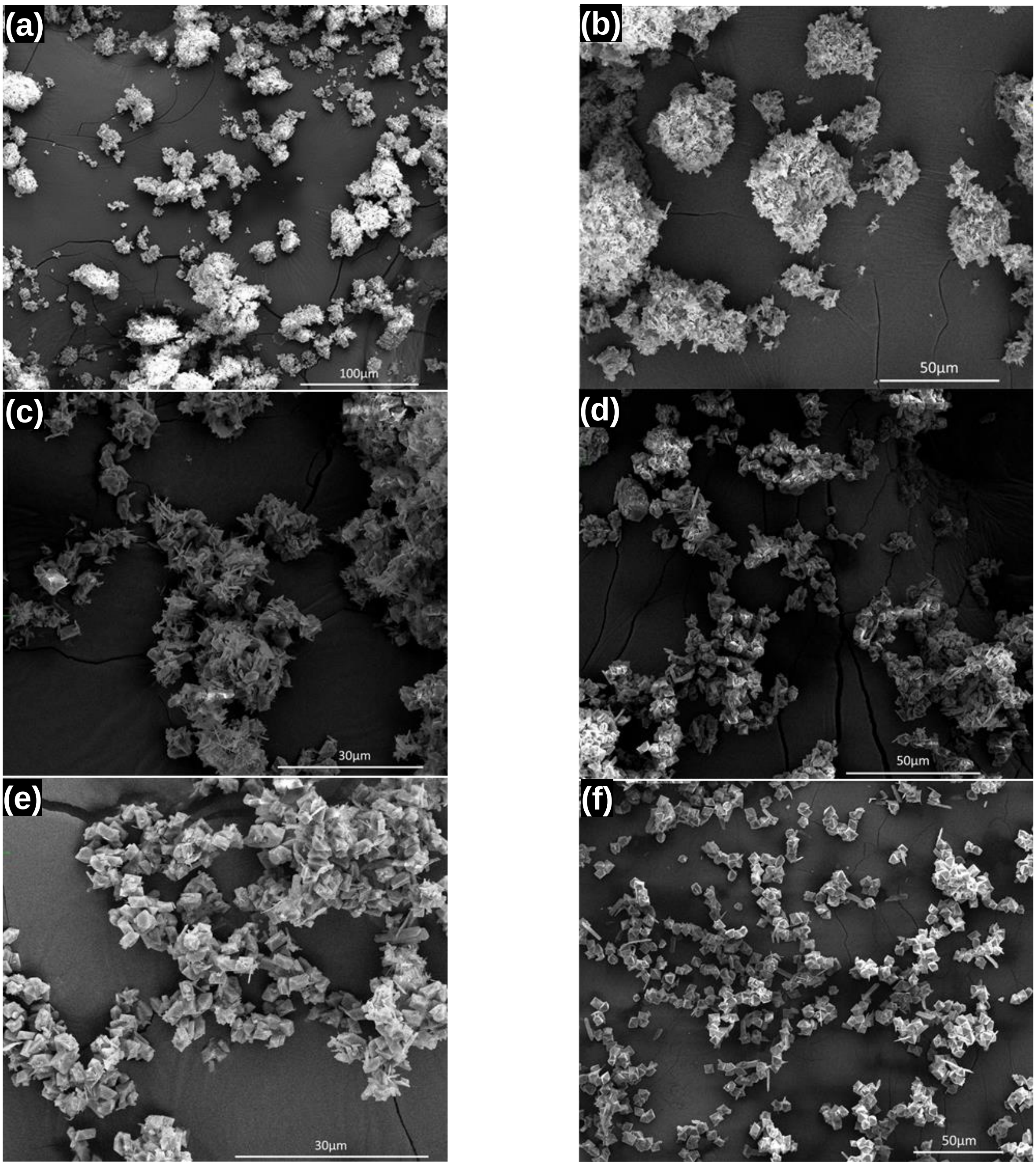

Figure S1. Low magnification SEM images of (a) the short water assisted reaction time control (Control-S), (c) milled 4 h (4 h-S) and (e) 8 h (8 h-S) treatments and the (b) the long water assisted reaction time control (Control-L), (d) milled 4 h (4 h-L) and (f) 8 h (8 h-L) treatments.

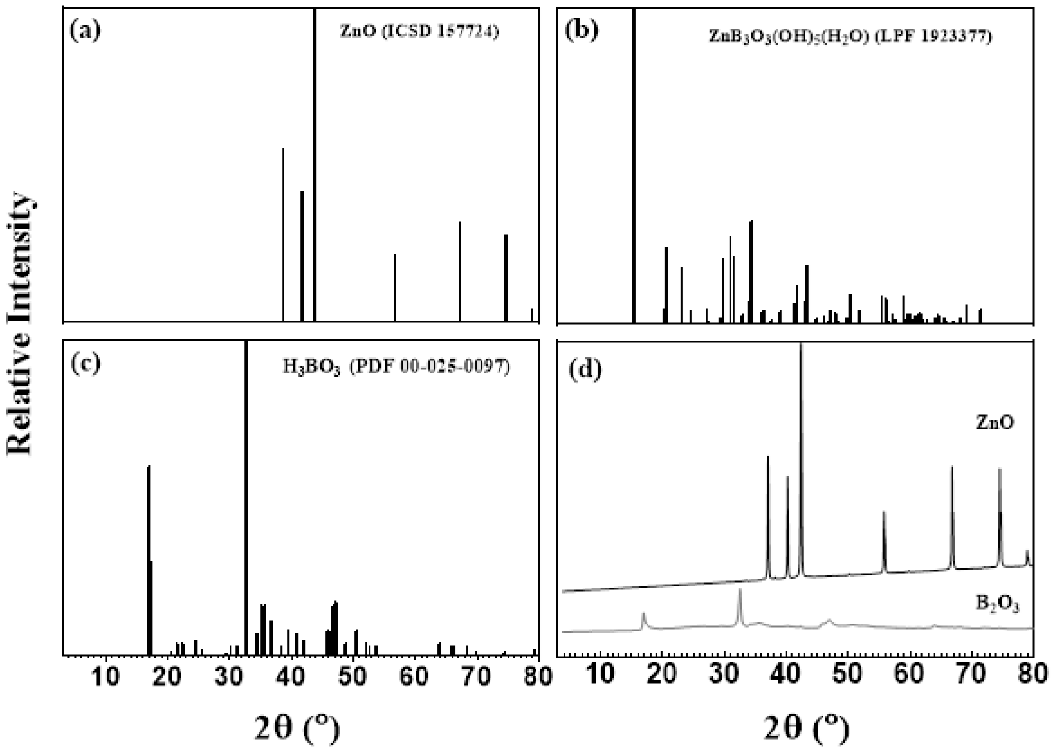

Figure S2. The XRD pattern of (a) the theoretical ZnO, (b) $ZnB_3O_3(OH)_5(H_2O)$, (c) H_3BO_3 and (d) initial reactants ZnO and B_2O_3 used in this study.

Table S2. Production of waste per g of zinc borate in our proposed method compared to other published methods.

Ref	**Waste**	**Weight (g/g zinc borate)**	**% Contribute to sEF**[a]	**% Contribute to cEF**[b]
(Dong and Hu, 1998; Gönen et al., 2009)[c]	Zinc nitrate	≥3.1	100.0	2.0
	Sodium tetraborate	0	0	0
	Ethanol/methanol	50.0	-	32.7
	Water	100.0	-	65.3
	Solvent used for washing and purification: ethanol and water			
E factor (sEF and cEF)			≥3.1	153.1
(Gao and Liu, 2009)[d]	Sodium tetraborate	≥ 7.6	100.0	8.9
	Zinc oxide	0	0	0
	Zinc sulphate	0	0	0
	Water	77.5	-	91.1
	Solvent used for washing and purification: alcohol, ether and water			
E factor (sEF and cEF)			7.6	85.1
(Chen et al., 2009; İpek, 2020)[c]	Zinc nitrate	≥3.1	12.0	1.1
	Sodium tetraborate	0	0	0
	Ammonia (25 wt.%)	22.7	88.0	8.2
	Water	250.0	-	90.6
	Solvent used for washing and purification: water			
E factor (sEF and cEF)			25.8	275.8
This work	Zinc Oxide Boric anhydride	≤0.2	100.0	11.8
	Water	1.7	-	88.2
	Solvent could use for washing and purification: water			
E factor (sEF and cEF)			0.2	1.9

[a] $sEF = \sum m\ (raw\ materials) + \sum m\ (reagents) - m(product)/m(product)$

[b] $sEF = \sum m\ (raw\ materials) + \sum m\ (reagents) + \sum m\ (solvent) + \sum m\ (water) - m(product)/m(product)$

[c] Due to lack of data, the calculation assumed that B-reactant was all reacted

[d] Due to lack of data, the calculation assumed that all Zn-reactants were reacted

References

Dong, J. X.; Hu, Z. S., A Study of the Anti-wear and Friction-reducing Properties of the Lubricant Additive, Nanometer Zinc Borate. *Tribology International* **1998,** *31* (5), 219-223.

Gönen, M.; Balköse, D.; Gupta, R. B.; Ülkü, S., Supercritical Carbon Dioxide Drying of Methanol−Zinc Borate Mixtures. *Industrial & Engineering Chemistry Research* **2009,** *48* (14), 6869-6876.

Gao, Y.-H.; Liu, Z.-H., Synthesis and Thermochemistry of Two Zinc Borates, $Zn_2B_6O_{11}\cdot 7H_2O$ and $Zn_3B_{10}O_{18}\cdot 14H_2O$. *Thermochimica Acta* **2009,** *484* (1), 27-31.

Chen, T.; Deng, J.-C.; Wang, L.-S.; Feng, G., Preparation and Characterization of Nano-Zinc Borate by a New Method. *Journal of Materials Processing Technology* **2009,** *209* (8), 4076-4079.

İpek, Y., Effect of Surfactant Types on Particle Size and Morphology of Flame-retardant Zinc Borate Powder. *Turk J Chem* **2020,** *44* (1), 214-223.

Chapter 3 Agronomic Comparison of Mechanochemically Synthesized Zinc Borate with Other Boron Sources by Coating or Co-compacting with Macronutrient Fertilizers

(Chapter 3 was accepted for publication by Journal of Soil Science and Plant Nutrition)

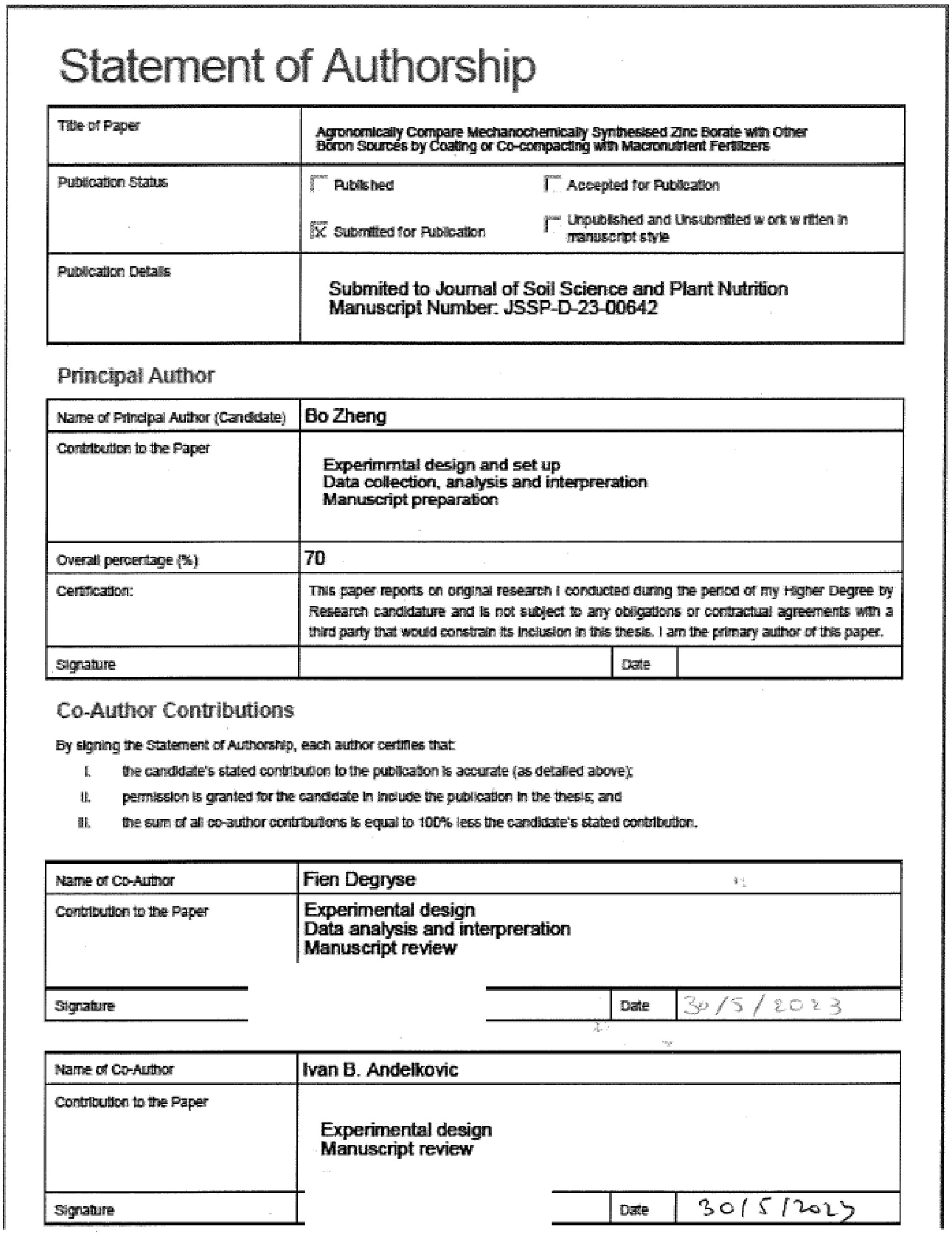

Statement of Authorship

Title of Paper	Agronomically Compare Mechanochemically Synthesised Zinc Borate with Other Boron Sources by Coating or Co-compacting with Macronutrient Fertilizers
Publication Status	☐ Published ☐ Accepted for Publication ☒ Submitted for Publication ☐ Unpublished and Unsubmitted work written in manuscript style
Publication Details	Submited to Journal of Soil Science and Plant Nutrition Manuscript Number: JSSP-D-23-00642

Principal Author

Name of Principal Author (Candidate)	Bo Zheng		
Contribution to the Paper	Experimmtal design and set up Data collection, analysis and interpreration Manuscript preparation		
Overall percentage (%)	70		
Certification:	This paper reports on original research I conducted during the period of my Higher Degree by Research candidature and is not subject to any obligations or contractual agreements with a third party that would constrain its inclusion in this thesis. I am the primary author of this paper.		
Signature		Date	

Co-Author Contributions

By signing the Statement of Authorship, each author certifies that:

i. the candidate's stated contribution to the publication is accurate (as detailed above);
ii. permission is granted for the candidate in include the publication in the thesis; and
iii. the sum of all co-author contributions is equal to 100% less the candidate's stated contribution.

Name of Co-Author	Fien Degryse		
Contribution to the Paper	Experimental design Data analysis and interpreration Manuscript review		
Signature		Date	30/5/2023

Name of Co-Author	Ivan B. Andelkovic		
Contribution to the Paper	Experimental design Manuscript review		
Signature		Date	30/5/2023

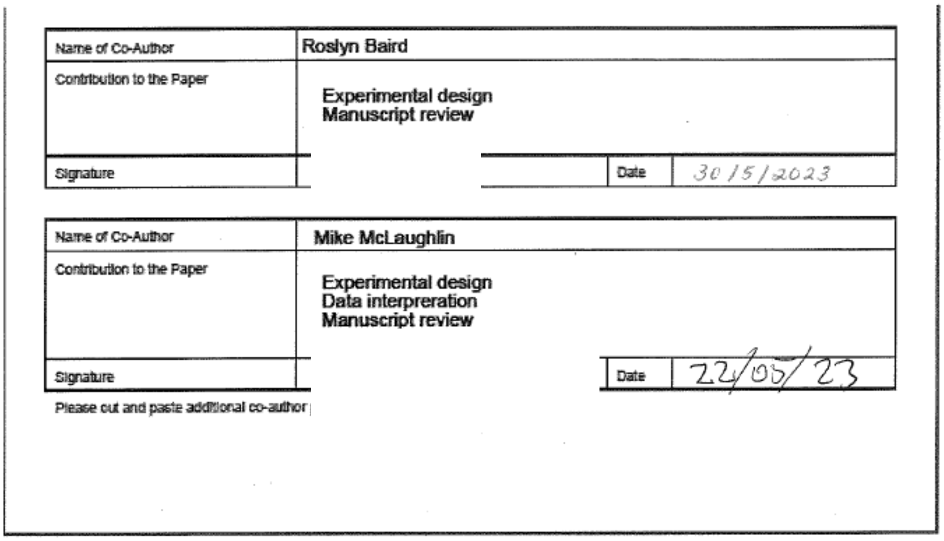

Name of Co-Author	Roslyn Baird		
Contribution to the Paper	Experimental design Manuscript review		
Signature		Date	30/5/2023

Name of Co-Author	Mike McLaughlin		
Contribution to the Paper	Experimental design Data interpreration Manuscript review		
Signature		Date	22/05/23

Please cut and paste additional co-author

Corresponding Author

Bo Zheng- School of Agriculture, Food and Wine, The University of Adelaide, Waite Campus, PMB1, Glen Osmond, South Australia 5064, Australia. 0000-0002-5724-0967

E-mail: bo.zheng@adelaide.edu.au .

Authors

Fien Degryse - Fertilizer Technology Research Centre, School of Agriculture, Food and Wine, University of Adelaide, Waite Campus, PMB1, Glen Osmond, South Australia 5064, Australia. 0000-0002-4875-2944

Ivan B. Andelkovic - Fertilizer Technology Research Centre, School of Agriculture, Food and Wine, University of Adelaide, Waite Campus, PMB1, Glen Osmond, South Australia 5064, Australia. 0000-0002-4570-0540

Roslyn Baird - Fertilizer Technology Research Centre, School of Agriculture, Food and Wine, University of Adelaide, Waite Campus, PMB1, Glen Osmond, South Australia 5064, Australia. 0000-0002-1269-0323

Mike John McLaughlin - Fertilizer Technology Research Centre, School of Agriculture, Food and Wine, University of Adelaide, Waite Campus, PMB1, Glen Osmond, South Australia 5064, Australia. 0000-0001-6796-4144

Abstract

Purpose - Boron (B) is an essential micronutrient required throughout the growth cycle of plants so effectively supplying crops with B using fertilizers is challenging. The purpose of this study was to assess the agronomic effectiveness of mechanochemically synthesized zinc borate as a slow release B source and compare it to commonly used B sources after incorporation with different macronutrient carriers.

Methods - Zinc borate synthesized using a green mechanochemical method as well as commercial B sources (borax, colemanite, and commercial zinc borate) were incorporated with various macronutrient fertilizers (monoammonium phosphate – MAP, muriate of potash – MOP and urea). The fertilizers were evaluated by a) assessing the solubility behaviour of these products; and b) comparing potential leaching losses, plant growth, and plant uptake through a greenhouse study.

Results - The mechanochemically synthesized zinc borate, commercial zinc borate, and colemanite had similar dissolution rates when MAP was the carrier, but both zinc borates dissolved more B than colemanite when MOP and urea were the carriers. In the pot trial, high losses of B in leachates resulted in low B uptake by plants fertilized with soluble sodium tetraborate. All the slow-release B sources had greater B uptake compared to the soluble B treatment.

Conclusions - Our study indicates that mechanochemically synthesized zinc borate with urea as the carrier could be effective in matching plant demand for B and reduce leaching losses in high rainfall environments.

Keywords: mechanochemistry, slow-release boron fertilizer, zinc borate, fertilizer manufacturing, green synthesis, agronomic effectiveness

3.1 INTRODUCTION

Boron (B) is an essential micronutrient for crop growth. Boron fertilization can be challenging due to the narrow window between deficiency and toxicity and the high mobility of B in soil (Mengel et al., 2001). Both B toxicity and deficiency will harm plant growth (Camacho-Cristóbal et al., 2008; Gupta, 1983; Wimmer and Eichert, 2013) and thus decrease crop yield (Findeklee et al., 1997; Pregno and Armour, 1992). Boron deficiency generally occurs in highly weathered, coarse textured, low organic matter and frequently cultivated soils, because B is easily removed from the soil through leaching, runoff, and plant uptake (Shorrocks, 1997). Zinc (Zn) is present in the soil as a cation and is commonly deficient in alkaline and calcareous soils due to strong sorption and fixation (Alloway, 2009). Until now, Zn deficiency remains a global health problem that affects more than 17% of the world's population (Myers et al., 2015).

The most commonly applied B sources are soluble compounds, such as boric acid and sodium borates. However, these soluble sources can cause seedling toxicity and are easily leached from soil. Slow-release sources of B could contribute to a more efficient and precise B application. Existing slow-release B sources are mainly colemanite, ulexite and other sodium/calcium borates (Broschat, 2008). More recently, new slow-release B compounds have been proposed such as boron phosphates (BPO4) (Abat et al., 2015a, c, d), layered double hydroxides with B incorporated (Songkhum et al., 2018), and organic (Svishcheva et al., 2022; Thombare et al., 2021) or hybrid matrices incorporated with B (Xie et al., 2011).

Generally, micronutrients required by plants in small amounts are combined with macronutrients nitrogen (N), phosphorus (P), and/or potassium (K), or applied as foliar liquids to decrease the costs of application and promote the uniform distribution of micronutrients in the field (Gupta, 1993). However, combining slow-release micronutrient sources with macronutrients through coating or co-granulation could change their release behaviour due to new chemical reactions or physical aggregation (Abat et al., 2015d; Milani et al., 2012). It is important to find new slow-release fertilizers that retain their slow-release character when combined with macronutrients, and have potential to achieve better plant growth and agronomic and environmental efficiency. Only a few attempts have been made to address this issue when assessing new slow-release B sources (Abat et al., 2015c, d; da Silva et al., 2018; Samreen et al., 2021).

Mechanochemistry has been proposed as a more sustainable synthesis method than wet chemistry because it relies solely on mechanical forces to decrease particle size, increase particle contact area, accumulate crystal defects and promote reactions without waste streams being produced (Ardila-Fierro and Hernández, 2021; Boldyrev, 2006). Mechanochemical methods such as ball milling, crushing, and shearing are common processes in the fertilizer industry for phosphate rock and other mineral processing and have been widely applied in other industries such as alloy and pharmaceutical production (Baláž, 2008; Baláž et al., 2013). Several studies have assessed the possibility of using mechanochemistry to synthesize slow-release fertilizers. The focus of previous mechanochemically synthesized fertilizer studies was mainly the macronutrients N, P and K. For instance, metal (hydr)oxides (Honer et al., 2018; Julien et al., 2020), LDH (Lei et al., 2018; Solihin et al., 2010), and ionic co-crystals (Barčauskaitė et al., 2020; Honer et al., 2017; Sharma et al., 2019) have been used to incorporate N, clay minerals (Solihin et al., 2011), LDH (Buates and Imai, 2021), metal (hydr)oxides (Zhang and Saito, 2009) to incorporate P, and struvite (Solihin et al., 2010), phlogopite (Said et al., 2018), clay minerals (Borges et al., 2017; Solihin et al., 2011), SiO_2 (Yuan et al., 2014) and LDH

(Lei et al., 2018) to incorporate K. Most of these proposed slow-release fertilizers had low water solubility in static or batch solubility tests. However, very few agronomic comparisons were made to compare mechanochemically synthesized products with commercial products.

Hydrated zinc borates are low-solubility B compounds that are used as flame retardants and preservatives for bio-composites/wood (Schubert, 2019) and could potentially be used as slow-release B and Zn fertilizer sources. The addition of Zn being an added benefit as one of the essential plant micronutrients. Different approaches have been used to synthesize zinc borate, such as hydrothermal methods which produce large amounts of waste streams during manufacturing (Gao and Liu, 2009, Gönen et al., 2009). In a previous study, we used mechanochemistry to synthesize a zinc borate using a ball mill and water-assisted reaction (Zheng et al., 2021). A minor amount of water was used for the synthesis (1.7 mL water per g product) compared to other conventional methods (77.5-250 g water per g product). The B release behaviour of the mechanochemically synthesized zinc borate was compared to commercial colemanite and sodium borate in a column dissolution study in which only 26% of B was released from zinc borate compared to 95% of B from sodium borate over 72 h.

This study aimed to compare the agronomic effectiveness of the mechanochemically synthesized zinc borate with other B sources when coated onto or co-granulated with macronutrient carriers. We hypothesized that a) zinc borate could be synthesized *in situ* during the coating process using water atomization to promote water-assisted reaction; b) some macronutrient carriers may impair the slow-release characteristics while others would be more suited as carriers for B sources; and c) the mechanochemical synthesized zinc borate could be used as a slow-release B source in high rainfall areas for plant growth.

3.2 MATERIAL AND METHODS

3.2.1 Mechanochemical synthesis of zinc borate

Zinc borate was prepared using a mechanochemical method described in the previous study with or without further water-assisted reaction (Zheng et al., 2021). In short, 1.35 g of ZnO and 1.65 g of B_2O_3 were added in 50 mL zirconia jars with six zirconia balls (15 mm diameter, 10 g per ball) to achieve a ball to solid (reactants) mass ratio around 20. A minor volume of water (510 µL) was added for liquid assisted grinding (LAG) to promote homogeneity. In the previous study, we used a Retsch MM400 mixer mill (Haan, Germany), but in this study a planetary mill (PM200, Retsch, Haan, Germany) was used to confirm the repeatability of the synthesis method. The milling procedure was performed for 8 h with a change of direction every 1 h and a 5-min break after 1 h of milling to avoid overheating. A control sample was subsampled 1 min after the milling procedure started. Further water-assisted reaction (WAR) was performed in the same manner as described in the previous study for both a subsampled control and a sample milled for 8 h. The WAR was achieved by adding a small amount of water (1.5 g water per g sample) to the products to make a paste-like sample and the sample was sealed for 72 h before drying under room temperature for the reaction to complete.

3.2.2 Characterization of synthesized zinc borate

The morphology of the samples was confirmed by field emission scanning electron microscopy (FE-SEM, Quanta 450, FEI, USA). X-ray diffraction (XRD) patterns of products were recorded with an X'Pert Pro multipurpose diffractometer (PANalytical B.V. Almelo, Netherlands) using Fe-filtered Co Kα radiation, automatic divergence slit, 2° anti-scatter slit, and fast X'Celerator Si strip detector. The diffraction patterns were recorded in steps of 0.017° 2 theta with a 0.5 s counting time per step for an overall counting time of approximately 30 min. Phase identification was performed on the XRD data using in-house software (XPLOT) (Microsoft, Redmond, Washington, USA) and HighScore Plus (from PANalytical) search / match software. The relative amounts of the major phases were determined by the Rietveld method using the Bruker TOPAS software package (Bruker BioSpin Corporation, Billerica, MA, USA).

3.2.3 Surface morphology and components of coated granules

A previous study indicated that Zn-containing coating material could react with MAP and primarily form $ZnNH_4PO_4$ when using water to assist with a coating (Milani et al., 2012). To confirm the crystal structure of the treatments coated onto MAP, the granules were abraded by rotating 10 g of granules placed in a 75 mL plastic container at 30 rpm for 30s. A fraction of the abraded coating material was sieved through a 1.0-mm sieve and analyzed by XRD to verify the composition of the coating material on the surface of the granules. The surface and cross-sectional morphology of the sample coated with commercial zinc borate (CZB) and mechanochemically synthesized zinc borate with water-assisted reaction (WZB) were evaluated using field emission scanning electron microscopy (FE-SEM, Quanta 450, FEI, USA).

3.2.4 Manufacturing of fertilizer treatments

Macronutrient fertilizers were coated or compacted (for the pot trial) with different sources of B and Zn (Table 3.1) to assess the solubility and plant response of the formulations. The B/Zn sources used were control samples with essentially no milling either without (C) or with water-assisted reaction (WC) and the samples that had been milled for 8 h without (ZB) or with water-assisted reaction (WZB). For comparison, a commercial zinc borate (CZB) from Turkey (Etimine USA. Inc.) was included, as well as a commercial fast-release B source (sodium tetraborate, TB) (U.S. Borax Inc,) and a commercial slow-release source (colemanite (Co) from Turkey (Etimine USA Inc). The Zn sources were zinc oxide (ZnO) and zinc sulfate ($ZnSO_4 \cdot 7H_2O$) (compacted with TB to produce a fast-release B and Zn treatment in the pot experiment). The macronutrient granules, urea, MOP (muriate of potash) and MAP (monoammonium phosphate), were either sieved to achieve a similar size (2.0-3.35 mm) before being coated or were ground, sieved (<250 μm) and co-compacted with the B sources. The target B and Zn concentrations in the fertilizers were 5 g kg^{-1} and 10 g kg^{-1}, respectively.

For the coating procedure, 50 g of sieved macronutrient granules and coating material were added to a Petri dish with a covered lid. The weight of powdered coating material added was around 2.1 g for WC, ZB and WZB, 1.7 g for C, 2.3 g for Co and 2.8 g for TB. The powders and granules were manually shaken before spraying a total of 750 µL deionized (DI) water in three pulses (each 5 s with a flow rate of 3 mL per min) to allow physical and chemical reactions at the granule surface. The coated granules were dried at room temperature for two days and sieved for further study. The coated granules were digested overnight at room temperature using *aqua regia* (HNO_3: HCl =1:3 v/v), followed by 45 min of heating at 80° C and 165 min of heating at 125° C in a digestion block. The digests were analyzed by inductively-coupled plasma optical emission spectroscopy (ICP-OES, Avio 200, Perkin Elmer, Waltham, USA) to determine the total content of Zn and B coated on the granules. Reference materials were used for quality control in all the digestion and ICP tests. The amounts of Zn and B coated onto the granules varied between treatments because ZnO tends to aggregate itself rather than evenly distribute on the surface of the granules. Variation was particularly noticeable for the treatments with colemanite and borax as larger amounts of these materials were required for coating to achieve the same B content compared to zinc borates. Therefore, for the pot experiment, we used compacted fertilizers to achieve more precise B and Zn contents. The compaction was carried out by mixing the micronutrient and macronutrient powders and compacting the powders using a pellet press. The powders were mixed to achieve the same target concentrations as before (5 g B kg^{-1} and 10 g Zn kg^{-1}) and 7 g of the powder was mixed with 0.3 mL of DI water to form a paste. The paste was placed into a 4 cm cylinder and 9.8 MPa pressure was applied to form a large pellet. The pellet was air-dried and cut into smaller pellets of similar size (2-3 mm) and weight (around 40 mg).

3.2.5 Batch solubility

The solubility of the samples was assessed by weighing 0.1 g of the sample in a 50 mL digestion tube with 10 mL of DI water. The samples were shaken in an end-over-end shaker for 1 h followed by 10 min centrifugation at 4685 g. A subsample of supernatant was taken for further analysis and 5 mL of DI water was added to the original 50 mL tube and shaken for 23 h. The suspensions were filtered through a 0.2 µm syringe filter prior to analysis using ICP-OES. To check the mass balance, the sediment remaining in the centrifuge tubes was digested overnight at room temperature using *aqua regia* (HNO_3: HCl =1:3 v/v), followed by 45 min heating at 80° C and 165 min heating at 125° C in a digestion hot block. Concentrations of B and Zn in the digest were analyzed by ICP-OES.

3.2.6 Soil leaching and pot experiment

To assess the plant response under leaching conditions, a pot experiment was performed in a temperature (20° C-day and 15° C-night) and humidity-controlled growth chamber for the first eight weeks and in a glasshouse for the remaining four weeks. Canola (*Brassica napus* L.) was chosen as the test crop because the sensitivity to B deficiency is high (Salisbury, 1999). The soil used in this study was Mt Compass (Entisol), an acidic sandy soil selected for its low B concentration (< 0.3 mg B kg^{-1} soil) and prone to B losses through leaching (Table 3.2). The soil was collected from the topsoil (0-10 cm) at Mount Compass, South Australia and air dried before being sieved to less than 2 mm. Plastic pots with a diameter of 12 cm were used and filled with 1 kg of soil. The soil was wetted and mixed in a plastic bag to reach 50% field capacity 2 days before transfer into the pots.

The fertilizer used in the pot experiment was prepared by compacting 5 g B kg^{-1} (CZB, WZB, Co and TB) and 10 g Zn kg^{-1} (ZnO in Co and $ZnSO_4$ in TB) with MOP and urea. The compacted fertilizer granules had an average weight of around 40 mg per granule. To each pot, 5 granules (totaling 0.2 g fertilizer containing approximately 1 mg B and 2 mg Zn) were equally distributed 3.5 cm below the soil surface 2 days before imposition of the leaching treatment. Treatments were randomized with three replicates for each treatment using a complete block design generated by GenStat 19th edition. The leaching procedure was carried out with artificial rain water (ARW, 5×10^{-4} M $CaCl_2$, $Ca(NO_3)_2$, $MgCl_2$ and 10^{-4} M Na_2SO_4, KCl) with a pH of 5.9. Each pot was slowly leached four times with 350 mL (or a total of four pore volumes) of ARW to mimic a heavy rainfall event and remove the available B from the soil. The leachates of each pot were collected and filtered for measurement of pH and ICP-OES analysis for B concentrations. After the leaching event, the pots were left to dry under ambient conditions for 3 days prior to planting. Canola (*Brassica napus* L.) seeds (antifungal treated) supplied by Seed Service Australia were geminated in an incubator for 3 days. The geminated seeds (five seeds per pot) were transplanted 1.5 cm below the soil surface and thinned to three seedlings after 1 week, two after 2 weeks and one after 3 weeks. All pots received 10 mL basal nutrient solution (5 days after planting and every week during the growth period (11 times in total). In total, all pots received 347 mg N kg^{-1}, 136 mg P kg^{-1}, 124 mg Ca kg^{-1}, 80.6 mg S kg^{-1}, 20.6 mg Mg kg^{-1}, 9.4 mg Fe kg^{-1}, 6.9 mg Mn kg^{-1}, 0.7 mg Cu kg^{-1} and 0.07 mg Mo kg^{-1}. Harvesting was carried out 12 weeks after planting. The plant shoots were cut 1 cm above the soil surface and dried in an oven at 60° C. The weight was recorded, and the samples further ground and digested for ICP-OES analysis of the B and Zn concentrations.

3.2.7 Statistical analysis

Differences in the amounts of B and Zn leached, B uptake and concentration in the plant and plant yield were assessed using one-way ANOVA (analysis of variance), where needed, the data were log-transformed to homogenize variance followed by a post-hoc Duncan's Multiple Range Test at $P \leq 0.05$ using GenStat 19th.

3.3 RESULTS

3.3.1 Micronutrient concentrations and crystal morphology

The crystal phase of the mechanochemically synthesized zinc borate was confirmed by XRD and its morphology was confirmed by SEM (Figure S 3.1). Consistent with the previous study, the 8 h milling followed by WAR successfully synthesized an octahedral crystal of zinc borate with a high conversion rate (Zheng et al., 2021). The Zn and B concentration of coated fertilizers (Table S 3.1) were generally close to the target concentrations. However, in some treatments such as TB, WC and Co there was less than half of the expected concentrations in the granules.

3.3.2 Analysis of abraded material

The XRD results collected from sieving coated MAP showed large amounts of commercial zinc borate were transformed to NH_4ZnPO_4 (Figure S 3.2b). In line with the results, the morphology of the CZB coating changed to a different crystal morphology (plate like) when coated onto MAP compared to MOP and urea (Figure S 3.3 d, e, f). Although WZB was largely maintained as zinc borate during the coating process (Figure S 3.2a, Figure S 3.3g, h, and i), it still dissolved in the batch dissolution test of the MAP granules.

3.3.3 Batch solubility

The batch dissolution test revealed that the B solubility in all treatments was significantly influenced by the macronutrient carrier (Figure 3.1). The lowest B dissolution was observed in the WZB, CZB and Co treatments for both urea and MOP carriers. However, the B solubility of these treatments with MOP as the carrier was more than 2 times higher than with urea. When urea was the carrier, WZB, CZB, Co and ZB released most extractable B within the first hour and a minor amount of B was released in the following 23 h, while they continued to dissolve after 1 h when MOP was the carrier. Significantly higher amounts of dissolved Zn (20-30%) were observed for all MAP treatments compared to the MOP and urea treatments (Figure 3.1b, d and f). The release of Zn was higher with MOP than with urea, although the magnitude of dissolution was very small in both cases.

3.3.4 Leaching of boron and zinc

For the TB treatments with highly soluble B and Zn, more than 60% of the added B was found in the leachates regardless of the macronutrient carrier (Figure 3.2a). Approximately 40-50% of total B leached was in the first leaching event. For the low-solubility B treatments, at most 38% of B leached from the soil, mostly in the first leaching event. Total leached B was higher with MOP than with urea as the carrier. The amount of B in the leachate was higher for WZB than for CZB and Co. The total B leached from WZB was 38% of total B added when incorporated with MOP and 10% with urea.

The concentration of Zn in leachates was highest in the MOP + TB, but still accounted for only 3% of added Zn (Figure 3.2b). Slightly higher Zn release was observed in the MOP treatments compared to the urea treatments. This is likely because the pH of the MOP leachates were all around 4.4, while the urea leachate started off around 6.5 then decreased to around 4.4 for the last two leaching events (Table S 3.3). However, even though the difference was significant in some treatments, Zn leaching was very limited overall.

3.3.5 Plant growth and boron and zinc uptake

Treatments with B added had more vigorous growth and advanced phenology compared to the urea and MOP treatments without any added B (Figure 3.3). Both treatments without added B did not grow above the elongation or rosette stage (BBCH growth stage < 34, the BBCH-scale was introduced by Meier (1997) to describe the phenological development of canola plants) and some replicates almost died in the final 4 weeks, indicating severe B deficiency in this leached acid sandy soil. Symptoms of B deficiency were observed in both vegetative and reproductive growth in most replicates of the TB treatments. Two replicates of the urea + TB treatment did not reach the elongation stage after 12 weeks of growth.

All treatments with added B had significantly higher fresh and dry weight yields than the treatments without B (Figure 3.4). Additionally, no visual signs of B deficiency were observed in the low solubility B treatments. The B concentration of the whole plant in the treatments followed Co = CZB = WZB > TB > N for MOP and Co=CZB> WZB > TB > N for urea. The B uptake of the canola followed the same order as the B concentrations in shoots. Concentrations of Zn in plants were similar in all treatments, while Zn uptake was significantly higher in all B added treatments compare to N due to the higher yield.

3.4 DISCUSSION

3.4.1 Co-compaction resulted in more accurate micronutrient enrichment than coating

When incorporating micronutrients into macronutrients, several methods can be used such as coating, compaction or granulation. The two methods assessed in this study, coating and compaction, indicated that more precise micronutrient incorporation could be achieved through the co-compaction method on a laboratory scale. The lower recovery rate from the coating method is likely caused by poor coating adhesion due to: (a) the coating material having different particle sizes and hydrophobicity; (b) more coating material required for the target % resulting in higher losses; and (c) variation in the porosity, moisture content and shape of the macronutrient granules (Goldszal and

Bousquet, 2001; Iley, 1991). For example, ZnO is generally a hydrophobic compound and thus more likely to aggregate to itself than being evenly coated on the surface of granules. As indicated in Table 3.1, the B concentration in the Co coating material was 40% less than for most other treatments, thus more coating material was required for coating. When there is a large amount of material to be coated, the interaction between the coating particles themselves can be weak, resulting in more loss, and hence concentrations can be below target, particularly where compounds with low B concentration are used. On the other hand, analysis of the compacted fertilizer pellets confirmed that the Zn and B concentrations were close to the target. Concentrations of B and Zn in compacted products were on average 89% of the target concentration for B and 103% for Zn (data not shown), values which are closer to the target compared to those produced by coating (Table S 3.1). Therefore, in the pot trial, only compacted fertilizer products were used.

3.4.2 Water-assisted reaction as part of the coating process was not effective

Our previous results showed that a WAR was essential to obtain a zinc borate with octahedral crystal morphology and low solubility. We hypothesized that this WAR might be carried out as part of the coating process using water atomization. However, when coated onto MOP and urea, the mechanochemically synthesized sample without WAR (ZB) was more soluble than the one synthesized using WAR (WZB), indicating that the water treatment during coating was not as effective in reducing solubility as the separate WAR prior to coating. This lower effectiveness of the WAR during coating might be due to the presence of the macronutrient carrier, potentially absorbing some of the water, reacting with the reagents or lowering the available water. To incorporate this product, the WAR must be completed beforehand, or a different approach must be used. To achieve the targeted micronutrient content, compacting is better than coating in this case. Therefore, in the pot trial, only the zinc borate synthesized using WAR (WZB) was used to compare with other low-solubility or conventional soluble sources.

3.4.3 Urea and MOP are more suitable carriers for zinc borate than MAP

It is important to consider the macronutrient sources used for manufacturing micronutrient-enriched fertilizers, as the macronutrients generally have different pH and ionic strength which could potentially affect the release character of the incorporated micronutrient compounds (da Silva et al., 2018b). All low-solubility B treatments became much more soluble when coated with MAP and almost all B was released within the first hour. Generally, the dissolution of MAP acidified the solution thus promoting the release of B. Similar results were observed in a previous study, where colemanite was more soluble with MAP than with MOP (Abat et al., 2015c). Furthermore, the high concentration of the phosphate and ammonium released from the dissolution of MAP likely drove the dissolution further by removing Zn and Ca (from colemanite) from the solution through precipitation of $CaHPO_4$, $Zn_3(PO_4)_2$ and/or NH_4ZnPO_4. Both urea and MOP showed lower solubility of the slow-release B compounds (zinc borate and colemanite) than MAP, with the lowest solubility for urea. The lower B release from urea compared to the MOP is likely due to the dissolution of urea increasing the pH of the solution.

3.4.4 The mechanochemically synthesized zinc borate is an effective B nutrient fertilizer

The B losses in the leachates generally followed the solubility of the B compounds and were higher for MOP than for urea. Among all the B added treatments after leaching, only TB treatment had a residual B concentration in soil less than 0.5 mg B kg^{-1} which is the concentration suggested by other studies for healthy canola growth (Bullock and Sawyer, 1991; Shorrocks, 1997). We indeed observed impairment of reproductive organs (flower buds or flowers), and incomplete or damaged embryo formation in MOP + TB treatment in the plant trial (Figure 3.3b) that was caused by B deficiency (Dell and Huang, 1997). Except for one replicate of the urea + Co treatment, all replicates of the slow-release B treatments reached the flowering to reproduction stage (BBCH 60-79). In addition, when applying soluble B fertilizers, toxicity should also be considered as a potential risk that harms crop yield (Abat et al., 2015c, Degryse, 2017).

Even though deficiency symptoms were observed in the TB treatments, the crop fresh and dry weights were very similar between the treatments with added B. When considering canola yields in the field, the most important part is the development of seeds as these are used for oil extraction. However, in the pot study, the fresh and dry weights were largely the stem and petioles of the canola before the development of seeds and pods (Major, 1977), and the growth stage varied between treatments at harvest. Therefore, it is more appropriate to compare B concentration in plants and B uptake for the low-solubility B treatments. Notably, the B concentrations in urea + Co and CZB were double that of the urea + WZB treatment. This could be explained by two possible reasons: a) the greater B leaching for the WZB treatments, and b) the WZB with urea as the carrier becoming less available to plants over time. Several studies have concluded or suggested that the critical B concentration in plant tissue for deficiency is around 10 mg kg^{-1} (Asad et al., 1997; Bell, 1997; Huang et al., 1996). Indeed, deficiency symptoms were observed during harvest for the plants with B concentrations less than 10 mg kg^{-1}, namely the N and TB treatments (Figure 4a). In general, several studies have suggested that the appropriate plant B concentration for optimum canola yield is 20-30 mg B kg^{-1} in plant tissue (Bullock and Sawyer, 1991; Malhi et al., 2003) and 12-16 mg kg^{-1} in seed (Ma et al., 2019). These critical concentrations vary with different plant species (Shorrocks, 1997) and even with different genotypes (Stangoulis et al., 2000). In this study, no deficiency was observed for any of the slow-release B source treatments, therefore after heavy leaching, the B supply from the slow-release B source was adequate for canola growth.

Compared to other low-solubility B sources such as colemanite, the zinc borate has an advantage as Zn was also supplied as part of the low-solubility B compound. However, there was no difference in Zn concentration or uptake between the different B treatments, likely due to the low solubility, and hence slow release, of Zn in the treatments with zinc borate. The uptake of Zn was higher for all treatments with B compared to the control, due to the enhanced plant growth in the presence of B (Grewal et al., 1998).

3.5 CONCLUSIONS

In this study, the effectiveness of mechanochemically synthesized zinc borate and other commercial slow- or fast-release B sources was evaluated using two macronutrients as carriers. We concluded that mechanochemically synthesized zinc borate co-compacted with urea or MOP was a more effective B fertilizer than commonly used soluble B sources under leaching conditions. This study highlights the importance of agronomic comparisons of fertilizer formulations, particularly on material engineered through new chemical methods, as the behaviour of the fertilizers will change when incorporated with other nutrients or applied in soil for crop growth. More precise, green and effective manufacturing methods are needed for fertilizer materials that produce fewer waste streams and reduce energy requirements in production to meet Sustainable Development Goals. Mechanochemistry offers an opportunity to transform fertilizer manufacturing methods, but the resultant products need to be evaluated not only for their manufacturing environmental footprint but also for their agronomic and environmental performance and their compatibility with current nutrient delivery systems. Field studies are required to further confirm the effectiveness of this mechanochemically synthesized zinc borate as a B and Zn fertilizer.

3.6 SUPPORTING INFORMATION

Table S 3.1 The B and Zn content of macronutrient fertilizer granules coated with different treatments.

Treatment	**B (mg g^{-1} after coating)**			**Zn (mg g^{-1} after coating)**		
	Urea	**MOP**	**MAP**	**Urea**	**MOP**	**MAP**
WC	3.2 ± 0.3	2.1 ± 0.3	2.0 ± 0.1	9.3 ± 0.6	8.4 ± 0.8	8.4 ± 1.2
WZB	3.2 ± 0.4	4.6 ± 0.2	3.9 ± 0.2	7.8 ± 1.0	10.1 ± 0.6	8.7 ± 0.5
C	2.9 ± 0.1	4.3 ± 0.3	3.8 ± 0.9	9.4 ± 0.2	9.9 ± 0.6	8.9 ± 0.9
ZB	4.5 ± 0.2	4.6 ± 0.2	4.0 ± 0.4	9.5 ± 0.1	9.6 ± 0.5	8.2 ± 1.1
CZB	5.0 ± 0.6	4.5 ± 0.6	6.6 ± 0.6	10.5 ± 0.5	9.8 ± 0.1	9.2 ± 1.0
Co	3.4 ± 0.2	3.0 ± 0.4	3.2 ± 0.4	7.4 ± 0.6	3.8 ± 0.4	3.9 ± 0.2
TB	3.5 ± 0.7	2.4 ± 0.0	2.2 ± 0.1	9.9 ± 0.8	10.1 ± 0.7	9.3 ± 1.0

Table S 3.2 The pH of the coated fertilizers after 24 h dissolution.

Treatments	**Urea**	**MOP**	**MAP**
C	7.8	8.1	4.3
WC	8.3	8.1	4.2
ZB	7.8	8.0	4.3
WZB	8.3	7.9	4.2
CZB	8.1	8.1	4.3
Co	8.9	8.3	4.6
TB	9.9	8.9	4.5

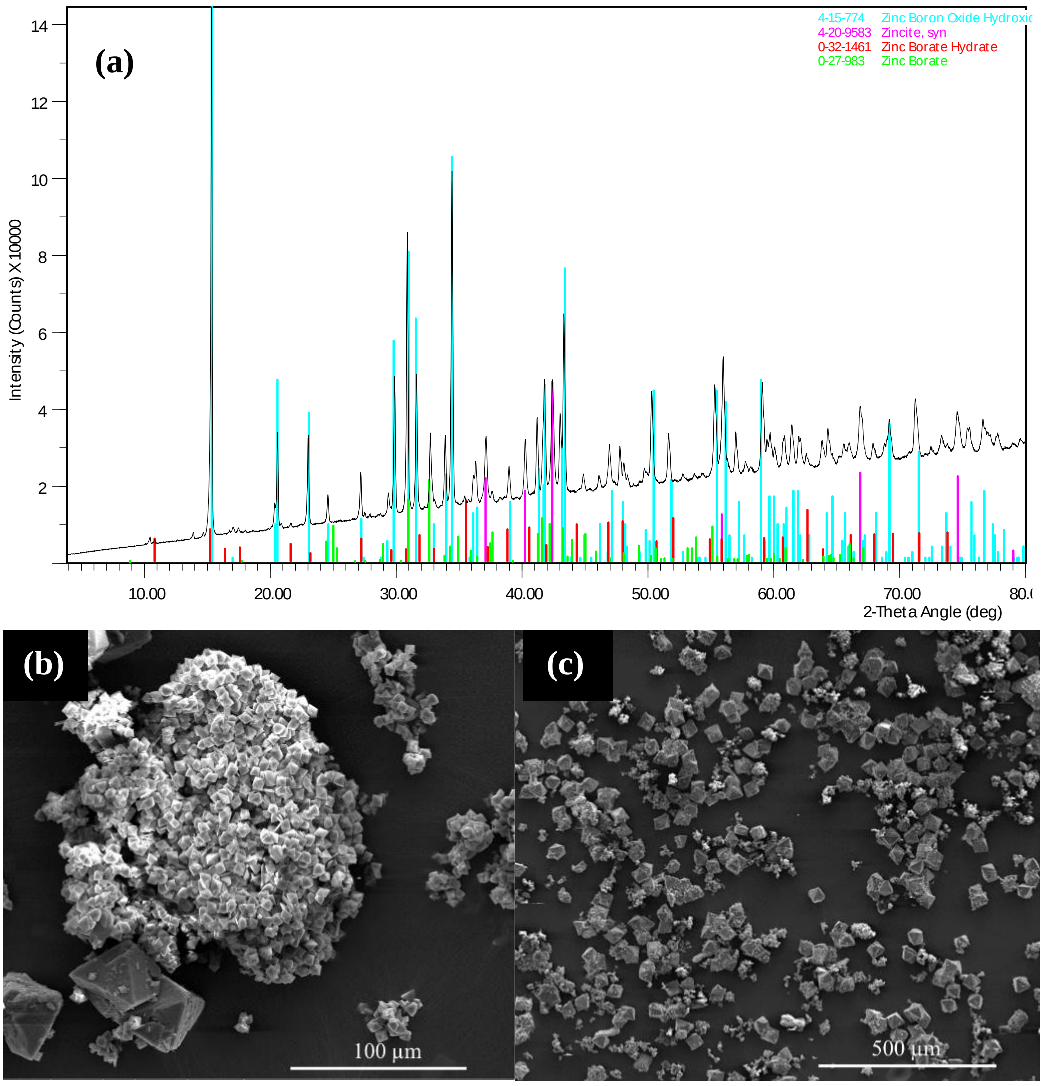

Figure S 3.1 The (a) XRD pattern and (b, c) SEM images of mechanochemical synthesized zinc borate with water assisted reaction (WZB).

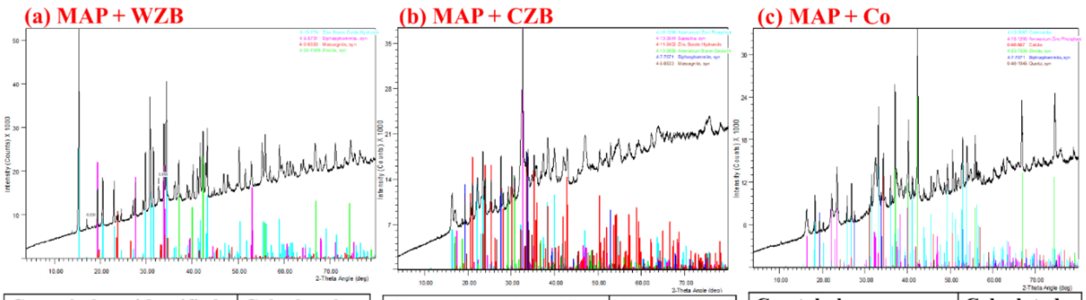

Crystal phase identified	Calculated composition by weight (wt.%)
Zinc Boron Oxide Hydroxide Hydrate - $Zn_2B_6O_{11}\cdot 7H_2O$	72
Biphosphammite - $NH_4(H_2PO_4)$	15
Zincite - ZnO	9
Mascagnite - $(NH_4)_2SO_4$	5

Crystal phase identified	Calculated composition by weight (wt.%)
Ammonium Zinc Phosphate - $(NH_4)Zn(PO_4)$	31
Sassolite - H_3BO_3	31
Zinc Borate Hydroxide - $ZnB_3O_4(OH)_3$	22
Ammonium Boron Oxide Hydroxide Hydrate - $(NH_4)B_5O_6(OH)_4(H_2O)_2$	7
Biphosphammite - $NH_4(H_2PO_4)$	5
Mascagnite - $(NH_4)_2SO_4$	4

Crystal phase identified	Calculated composition by weight (wt.%)
Colemanite- $Ca_2B_6O_{11}\cdot 5H_2O$	41
Ammonium Zinc Phosphate - $(NH_4)Zn(PO_4)$	32
Calcite - $CaCO_3$	9
Zincite- ZnO	9
Biphosphammite - $NH_4(H_2PO_4)$	3
Quartz - SiO_2	1
Clay Minerals (Mica, smectite)	5

Figure S 3.2 The XRD patterns and calculated composition of abraded material from MAP coated with (a) mechanochemically synthesized zinc borate, (b) commercial zinc borate, and (c) colemanite + ZnO.

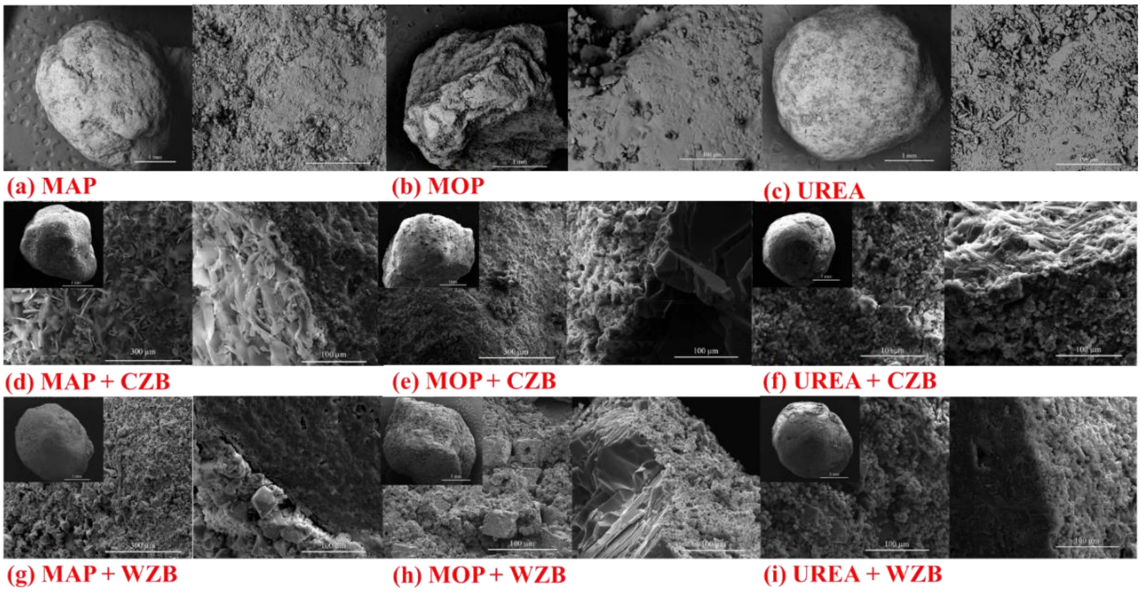

(a) MAP (b) MOP (c) UREA

(d) MAP + CZB (e) MOP + CZB (f) UREA + CZB

(g) MAP + WZB (h) MOP + WZB (i) UREA + WZB

Figure S 3.3 SEM images (of the surface and a cross-section) of MAP, MOP, and urea, either (a-c) uncoated, (d-f) coated with commercial zinc borate (CZB) or (g-i) coated with mechanochemically synthesized zinc borate (WZB).

Table S 3.3 The average pH of the four consecutive leachates (L1-4) collected from the acid sandy soil treated with MOP or urea fertilizer compacted with different B/Zn sources.

B/Zn source	**MOP**				**Urea**			
	L1	L2	L3	L4	L1	L2	L3	L4
None	4.3 ± 0	4.6 ± 0	4.5 ± 0	4.4 ± 0	6.6 ± 0.5	6.2 ± 0.1	4.4 ± 0	4.3 ± 0
TB + $ZnSO_4$	4.3 ± 0.1	4.6 ± 0	4.5 ± 0	4.4 ± 0	6.1 ± 0.2	5.6 ± 0.2	4.4 ± 0.1	4.3 ± 0
Co + ZnO	4.3 ± 0	4.6 ± 0.1	4.5 ± 0.1	4.4 ± 0	6.3 ± 0.4	5.9 ± 0.5	4.4 ± 0	4.4 ± 0.1
CZB	4.4 ± 0	4.6 ± 0.1	4.5 ± 0	4.4 ± 0.1	6.2 ± 0.5	6.4 ± 0.5	4.4 ± 0	4.4 ± 0
WZB	4.3 ± 0	4.6 ± 0	4.5 ± 0	4.4 ± 0	6.5 ± 0.5	5.6 ± 0.2	4.4 ± 0	4.3 ± 0

3.7 DECLARATION OF COMPETING INTEREST

This research did not receive any specific grant from funding agencies in the public, commercial, or not-for-profit sectors.

3.8 ACKNOWLEDGEMENTS

Bo Zheng is grateful for the scholarship and support from The University of Adelaide, School of Agriculture, Food and Wine. We thank the help and support from Adelaide Microscopy and Ken Neubauer for the SEM analysis. The authors acknowledge the support of The Mosaic Company LLC. The authors thank Bogumila Tomczak, Ashleigh Broadbent and Andrea Paparella for their advice and technical support.

3.9 REFERENCES

Abat, M., Degryse, F., Baird, R., McLaughlin, M.J., 2015a. Boron Phosphates (BPO_4) as a Seedling-safe Boron Fertilizer Source. Plant and Soil 391:153-160.

Abat, M., Degryse, F., Baird, R., McLaughlin, M.J., 2015b. Responses of Canola to the Application of Slow-Release Boron Fertilizers and Their Residual Effect. Soil Science Society of America Journal 79:97-103.

Abat, M., Degryse, F., Baird, R., McLaughlin, M.J., 2015c. Slow-release Boron Fertilizers: Co-granulation of Boron Sources with Mono-ammonium Phosphate (MAP). Soil Research 53:505-511.

Alloway, B.J., 2009. Soil Factors Associated with Zinc Deficiency in Crops and Humans. Environmental Geochemistry and Health 31:537-548.

Ardila-Fierro, K.J., Hernández, J.G., 2021. Sustainability Assessment of Mechanochemistry by Using the Twelve Principles of Green Chemistry. ChemSusChem 14:2145-2162.

Baláž, P., 2008. Applied Mechanochemistry, in: Baláž, P. (Ed.) Mechanochemistry in Nanoscience and Minerals Engineering. Springer Berlin Heidelberg, Berlin, Heidelberg, pp 297-405.

Baláž, P., Achimovičová, M., Baláž, M., Billik, P., Cherkezova-Zheleva, Z., Criado, J.M., Delogu, F., Dutková, E., Gaffet, E., Gotor, F.J., Kumar, R., Mitov, I., Rojac, T., Senna, M., Streletskii, A., Wieczorek-Ciurowa, K., 2013. Hallmarks of Mechanochemistry: from Nanoparticles to Technology. Chemical Society Reviews 42:7571-7637.

Barčauskaitė, K., Brazienė, Z., Avižienytė, D., Silva, M., Drapanauskaite, D., Honer, K., Gvildienė, K., Slinksiene, R., Jancaitiene, K., Mazeika, R., Staugaitis, G., Dambrauskas, T., Baltakys, K., Baltrusaitis, J., 2020. Mechanochemically Synthesized Gypsum and Gypsum Drywall Waste Cocrystals with Urea for Enhanced Environmental Sustainability Fertilizers. Journal of Environmental Chemical Engineering 8:103965.

Boldyrev, V.V., 2006. Mechanochemistry and Mechanical Activation of Solids. Russian Chemical Reviews 75:177-189.

Borges, R., Prevot, V., Forano, C., Wypych, F., 2017. Design and Kinetic Study of Sustainable Potential Slow-Release Fertilizer Obtained by Mechanochemical Activation of Clay Minerals and Potassium Monohydrogen Phosphate. Journal of Industrial and Engineering Chemistry 56: 708-716.

Broschat, T.K., 2008. Release Rates of Soluble and Controlled-release Boron Fertilizers. HortTechnology hortte 18:471-474.

Buates, J., Imai, T., 2021. Assessment of Plant Growth Performance and Nutrient Release for Application of Phosphorus-loaded Layered Double Hydroxides as Fertilizer. Environmental Technology and Innovation 22:101505.

Camacho-Cristóbal, J.J., Rexach, J., González-Fontes, A., 2008. Boron in Plants: Deficiency and Toxicity. Journal of Integrative Plant Biology 50:1247-1255.

da Silva, R.C., Baird, R., Degryse, F., McLaughlin, M.J., 2018. Slow and Fast-Release Boron Sources in Potash Fertilizers: Spatial Variability, Nutrient Dissolution and Plant Uptake. Soil Science Society of America Journal 82:1437-1448.

Degryse, F., 2017. Boron Fertilizers: Use, Challenges and the Benefit of Slow-release Sources–A Review. J of Boron 2:111-122.

Findeklee, P., Wimmer, M., Goldbach, H.E., 1997. Early Effects of Boron Deficiency on Physical Cell Wall Parameters, Hydraulic Conductivity and Plasmalemma-bound Reductase Activities in Young *C. pepo* and *V. faba* Roots, in: Bell, R.W., Rerkasem, B. (Eds.), Boron in Soils and Plants: Proceedings of the International Symposium on Boron in Soils and Plants held at Chiang Mai, Thailand, 7–11 September, 1997. Springer Netherlands, Dordrecht, pp 221-227.

Gupta, U.C., 1983. Boron Deficiency and Toxicity Symptoms for Several Crops as Related to Tissue Boron Levels. Journal of Plant Nutrition 6:387-395.

Honer, K., Kalfaoglu, E., Pico, C., McCann, J., Baltrusaitis, J., 2017. Mechanosynthesis of Magnesium and Calcium Salt–Urea Ionic Cocrystal Fertilizer Materials for Improved Nitrogen Management. ACS Sustainable Chemistry and Engineering 5:8546-8550.

Honer, K., Pico, C., Baltrusaitis, J., 2018. Reactive Mechanosynthesis of Urea Ionic Cocrystal Fertilizer Materials from Abundant Low Solubility Magnesium- and Calcium-Containing Minerals. ACS Sustainable Chemistry and Engineering 6:4680-4687.

Julien, P.A., Germann, L.S., Titi, Hatem M., Etter, M., Dinnebier, R.E., Sharma, L., Baltrusaitis, J., Friščić, T., 2020. In Situ Monitoring of Mechanochemical Synthesis of Calcium Urea Phosphate Fertilizer Cocrystal Reveals Highly Effective Water-based Autocatalysis. Chemical Science 11:2350-2355.

Lei, Z., Cagnetta, G., Li, X., Qu, J., Li, Z., Zhang, Q., Huang, J., 2018. Enhanced Adsorption of Potassium Nitrate with Potassium Cation on H_3PO_4 Modified Kaolinite and Nitrate Anion into Mg-Al Layered Double Hydroxide. Applied Clay Science 154:10-16.

Meier, U. 1997. Growth Stages of Mono-and Dicotyledonous Plants, Blackwell Wissenschafts-Verlag.

Mengel, K., Kirkby, E.A., Kosegarten, H., Appel, T., 2001. Boron, in: Mengel, K., Kirkby, E.A., Kosegarten, H., Appel, T. (Eds.), Principles of Plant Nutrition. Springer Netherlands, Dordrecht, pp 621-638.

Milani, N., McLaughlin, M.J., Stacey, S.P., Kirby, J.K., Hettiarachchi, G.M., Beak, D.G., Cornelis, G., 2012. Dissolution Kinetics of Macronutrient Fertilizers Coated with Manufactured Zinc Oxide Nanoparticles. Journal of Agricultural and Food Chemistry. 60:3991-3998.

Myers, S.S., Wessells, K.R., Kloog, I., Zanobetti, A., Schwartz, J., 2015. Effect of Increased Concentrations of Atmospheric Carbon Dioxide on the Global Threat of Zinc Deficiency: a Modelling Study. The Lancet. Global health 3:639-645.. Pregno, L.M., Armour, J.D., 1992. Boron Deficiency and Toxicity in Potato cv. Sebago on an Oxisol of the Atherton Tablelands, North Queensland. Aust. J. Exp. Agric. 32(2), 251-253.

Said, A., Zhang, Q., Qu, J., Liu, Y., Lei, Z., Hu, H., Xu, Z., 2018. Mechanochemical Activation of Phlogopite to Directly Produce Slow-release Potassium Fertilizer. Appl. Clay Sci. 165, 77-81.

Salisbury, P.A., 1999. Canola in Australia: The First Thirty Years. Organising Committee of the 10th International Rapeseed Congress.

Samreen, T., Degryse, F., Baird, R., da Silva, R.C., Zahir, Z.A., Nazir, M.Z., Wakeel, A., Sidra Tul, M., McLaughlin, M., 2021. Development and Testing of Improved Efficiency Boron-Enriched Diammonium Phosphate Fertilizers. J. Soil Sci. Plant Nutr. 21(2),

Sharma, L., Kiani, D., Honer, K., Baltrusaitis, J., 2019. Mechanochemical Synthesis of Ca- and Mg-Double Salt Crystalline Materials Using Insoluble Alkaline Earth Metal Bearing Minerals. ACS Sustain. Chem. Eng. 7(7), 6802-6812.

Shorrocks, V.M., 1997. The Occurrence and Correction of Boron Deficiency. Plant Soil 193(1), 121-148.

Solihin, Zhang, Q., Tongamp, W., Saito, F., 2010. Mechanochemical Route for Synthesizing KMgPO4 and NH4MgPO4 for Application as Slow-Release Fertilziers. Ind. Eng. Chem. Res. 49(5), 2213-2216.

Solihin, Zhang, Q., Tongamp, W., Saito, F., 2011. Mechanochemical Synthesis of Kaolin–KH2PO4 and kaolin–NH4H2PO4 Complexes for Application as Slow Release Fertilizer. Powder Technology 212(2), 354-358.

Songkhum, P., Wuttikhun, T., Chanlek, N., Khemthong, P., Laohhasurayotin, K., 2018. Controlled Release Studies of Boron and Zinc from Layered Double Hydroxides as the Micronutrient Hosts for Agricultural Application. Appl. Clay Sci. 152, 311-322.

Svishcheva, N.B., Uspenskii, S.A., Sedush, N.G., Khaptakhanova, P.A., Kasatova, A.I., Buzin, A.I., Dmitryakov, P.V., Piskarev, M.S., Aleksandrov, A.I., Taskaev, S.Y., 2022. Biodegradable Boron-Containing Poly(Lactic Acid) for Fertilizers with Prolonged Action. Mater. Today Commun. 33, 104514.

Thombare, N., Mishra, S., Shinde, R., Siddiqui, M.Z., Jha, U., 2021. Guar Gum Based Hydrogel as Controlled Micronutrient Delivery System: Mechanism and Kinetics of Boron Release for Agricultural Applications. Biopolymers 112(3), e23418.

Wimmer, M.A., Eichert, T., 2013. Review: Mechanisms for Boron Deficiency-mediated Changes in Plant water Relations. Plant Sci. 203-204, 25-32.

Xie, L., Liu, M., Ni, B., Zhang, X., Wang, Y., 2011. Slow-release Nitrogen and Boron Fertilizer from a Functional Superabsorbent Formulation Based on Wheat Straw and Attapulgite. Chemical Engineering Journal 167(1), 342-348. 10.1016/j.cej.2010.12.082.

Yuan, W., Solihin, Zhang, Q., Kano, J., Saito, F., 2014. Mechanochemical Formation of K–Si–Ca–O Compound as a Slow-release Fertilizer. Powder Technology 260, 22-26.

Zhang, Q., Saito, F., 2009. Mechanochemical Synthesis of Slow-Release Fertilizers through Incorporation of Alumina Composition into Potassium/Ammonium Phosphates. J. Am. Ceram. Soc. 92(12), 3070-3073.

Zheng, B., Kabiri, S., Andelkovic, I.B., Degryse, F., da Silva, R., Baird, R., Self, P., McLaughlin, M.J., 2021. Mechanochemical Synthesis of Zinc Borate for Use as a Dual-Release B Fertilizer. ACS Sustain. Chem. Eng. 9(47), 15995-16004..

Table 3.1 Synthesis methods, source materials and target nutrient contents for the different B and Zn sources.

Treatments	Milling time (h)	WAR[a]	B	Zn	Nutrient concentration	
					B (%)	Zn (%)
Mechanochemical (WZB and ZB) and control (WC and C) treatments						
WC	0.017	Y	B_2O_3	ZnO	12	28
WZB	8	Y			12	29
C	0.017	N			15	34
ZB	8	N			12	31
Commercial B treatments						
CZB			Commercial Zinc borate		10	35
Co			Colemanite	ZnO	8	36
TB			Sodium tetraborate	ZnO in solubility test / $ZnSO_4$ in the pot experiment	6	36/19

[a] WAR= water-assisted reaction

Table 3.2 Characteristics of the Mt Compass soil.

Characteristics	**Value**
pH (H_2O: soil - 5:1)	5.9
pH (0.01 M $CaCl_2$: soil - 5:1)	4.9
Total C (g kg^{-1}) -Total Carbon	5.0
Exchangeable K ($cmol_c$ kg^{-1})	0.2
Exchangeable Ca ($cmol_c$ kg^{-1})	1.5
Exchangeable Mg ($cmol_c$ kg^{-1})	0.3
CEC ($cmol_c$ kg^{-1}) - Cation Exchange Capacity	2.0
Hot water extractable B (mg kg^{-1})	0.2
Clay (g kg^{-1})	43
Silt (g kg^{-1})	9.0
Sand (g kg^{-1})	943
Field capacity (g kg^{-1})	35
Total Zn concentration (mg kg^{-1})	8.0

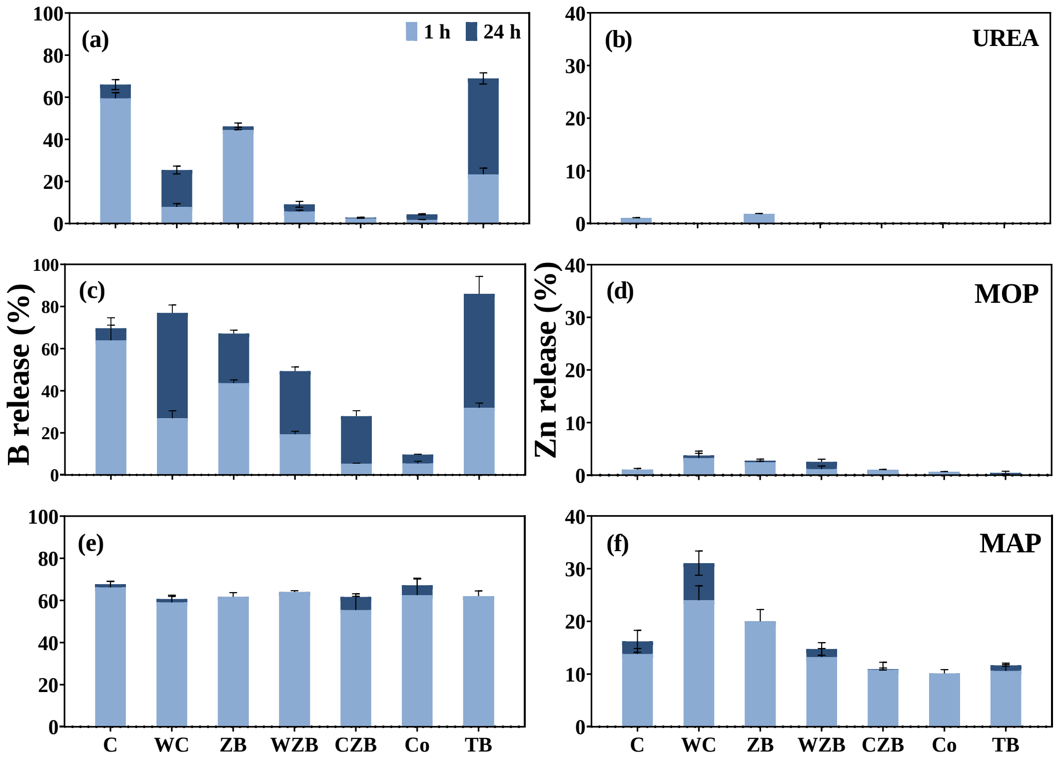

Figure 3.1 The B and Zn release of coated (a, b) urea, (c, d) MOP (muriate of potash), and (e, f) MAP (monoammonium phosphate) with C (ZnO + B_2O_3), WC (ZnO + B_2O_3 and water-assisted reaction), ZB (ZnO + B_2O_3, 8h milling), WZB (ZnO + B_2O_3, 8h milling and water-assisted reaction), CZB (commercial zinc borate), Co (Colemanite + ZnO) and TB (tetraborate + ZnO) after 1 h and 24 h shaking in a batch water-solubility test. The error bars represent the standard deviation of three replicates.

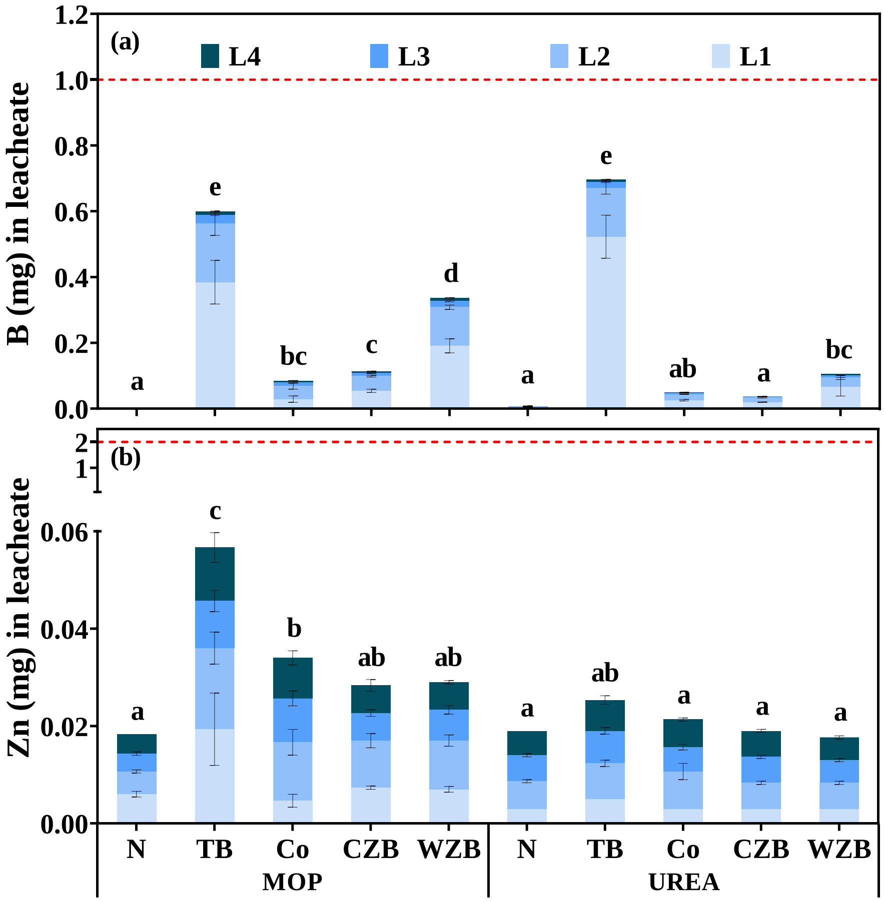

Figure 3.2 (a) B and (b) Zn recovered in leachates from four successive leaching events of pots (L1 to L4) for MOP (muriate of potash) and urea treatments alone (N) or co-compacted with borax + $ZnSO_4$ (TB), colemanite + ZnO (Co), commercial zinc borate (CZB), or mechanochemically synthesized zinc borate (WZB). The error bars represent standard deviation of three replicates and different letters indicate significant differences ($P \leq 0.05$, Duncan's Multiple Range Test). The red line indicates the amount of B and Zn added per pot.

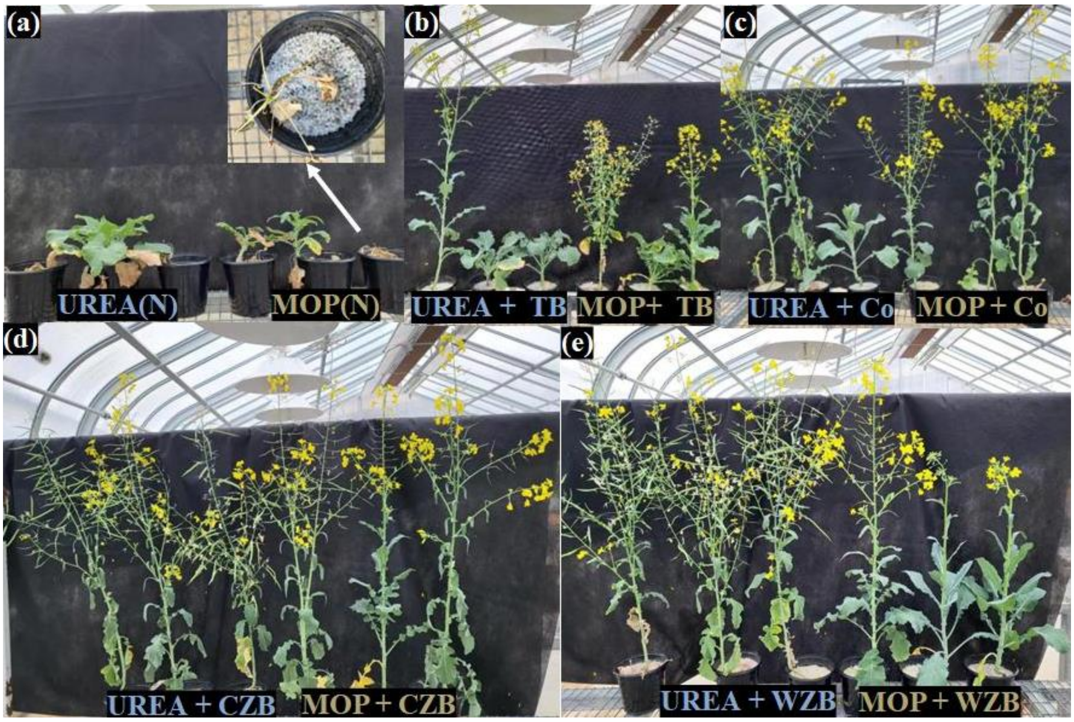

Figure 3.3 Images of canola before harvesting for: a) urea and MOP (muriate of potash) without added B (N), b) Urea and MOP + sodium tetraborate (TB), c) Urea and MOP + Colemanite (Co), d) Urea and MOP + commercial zinc borate (CZB), and e) Urea and MOP + mechanochemically synthesized zinc borate (WZB).

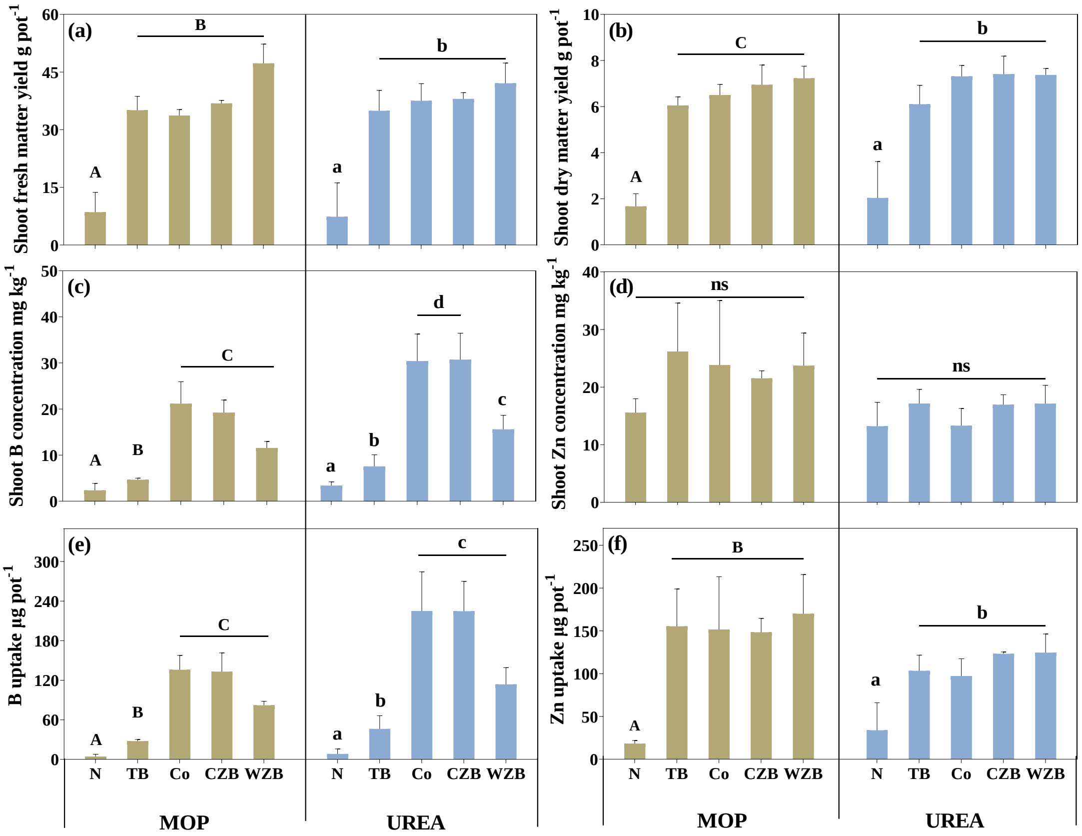

Figure 3.4 The (a) fresh and (b) dry weight; (c) B and (d) Zn concentration of shoots; and (e) B and (f) Zn uptake and (e) fresh and (f) dry weight for canola grown for 12 weeks after leaching, in response to the application of different B (+Zn) sources co-compacted with MOP (muriate of potash) or urea (N: no B; TB: sodium tetraborate; Co: colemanite, CZB: commercial zinc borate; WZB: mechanochemically synthesized zinc borate). The error bars represent the standard deviation of three replicates and different letters indicate significant differences between treatments for a given macronutrient carrier - capital letter assigned to MOP and small letter assigned to urea ($P \leq 0.05$, Duncan's Multiple Range Test).

Chapter 4 Mechanochemical Synthesis of Layered Zn-Mo Compounds as Slow-release Mo Fertilizers

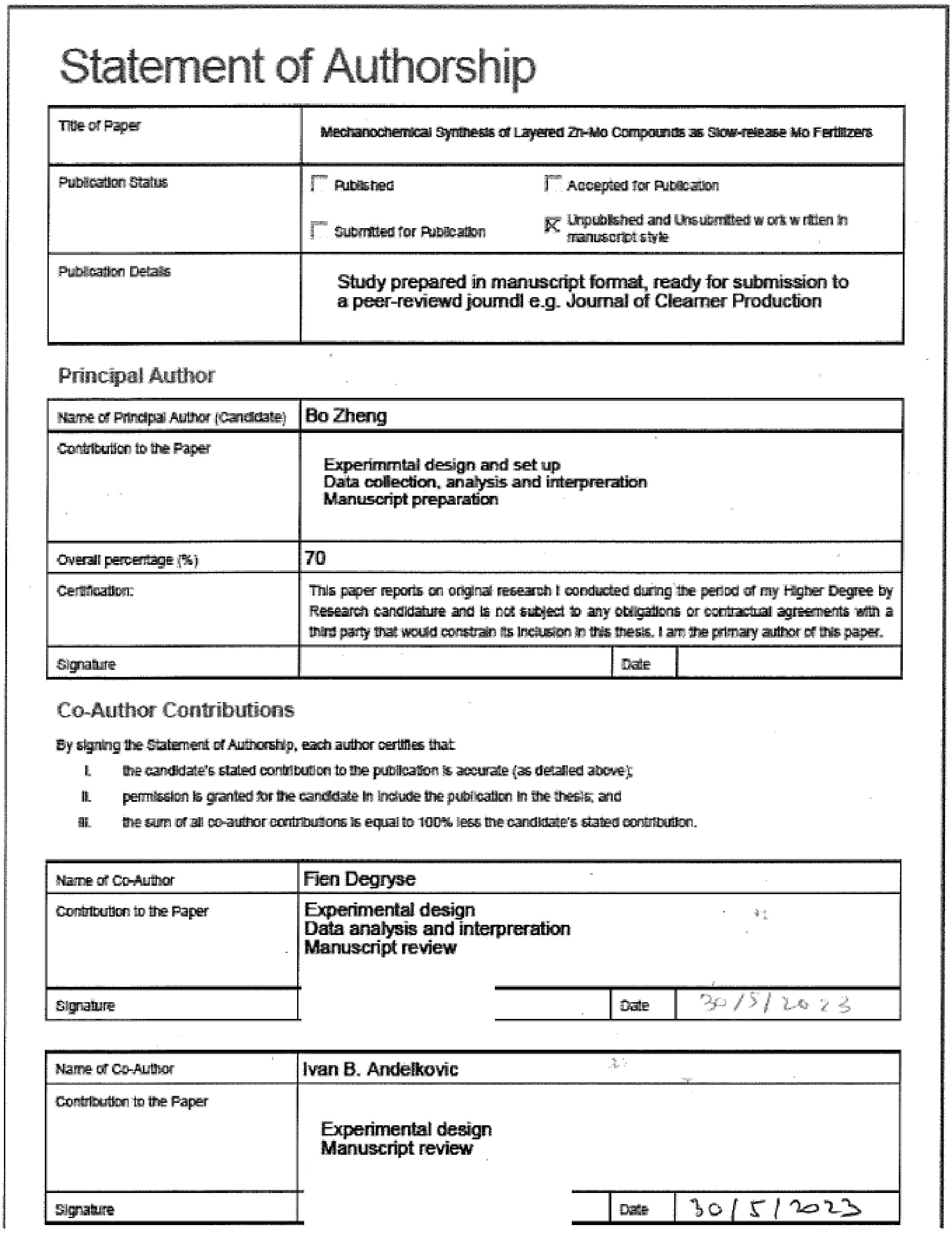

Statement of Authorship

Title of Paper	Mechanochemical Synthesis of Layered Zn-Mo Compounds as Slow-release Mo Fertilizers
Publication Status	☐ Published ☐ Accepted for Publication ☐ Submitted for Publication ☒ Unpublished and Unsubmitted work written in manuscript style
Publication Details	Study prepared in manuscript format, ready for submission to a peer-reviewd journdl e.g. Journal of Clearner Production

Principal Author

Name of Principal Author (Candidate)	Bo Zheng		
Contribution to the Paper	Experimmtal design and set up Data collection, analysis and interpreration Manuscript preparation		
Overall percentage (%)	70		
Certification:	This paper reports on original research I conducted during the period of my Higher Degree by Research candidature and is not subject to any obligations or contractual agreements with a third party that would constrain its inclusion in this thesis. I am the primary author of this paper.		
Signature		Date	

Co-Author Contributions

By signing the Statement of Authorship, each author certifies that:

i. the candidate's stated contribution to the publication is accurate (as detailed above);
ii. permission is granted for the candidate in include the publication in the thesis; and
iii. the sum of all co-author contributions is equal to 100% less the candidate's stated contribution.

Name of Co-Author	Fien Degryse		
Contribution to the Paper	Experimental design Data analysis and interpreration Manuscript review		
Signature		Date	30/5/2023

Name of Co-Author	Ivan B. Andelkovic		
Contribution to the Paper	Experimental design Manuscript review		
Signature		Date	30/5/2023

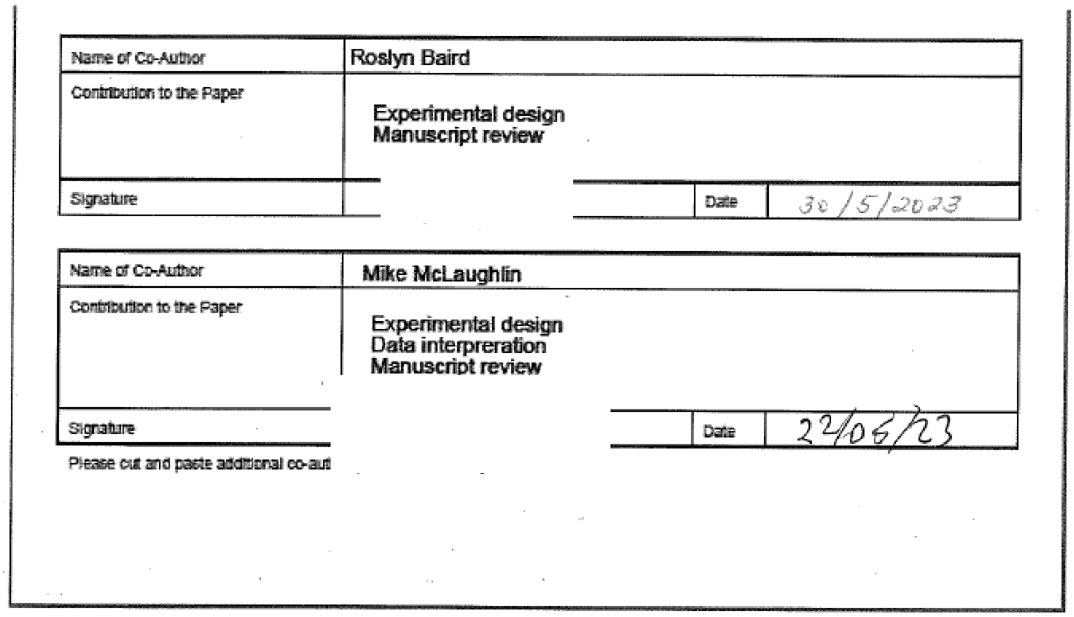

Name of Co-Author	Roslyn Baird		
Contribution to the Paper	Experimental design Manuscript review		
Signature		Date	30/5/2023

Name of Co-Author	Mike McLaughlin		
Contribution to the Paper	Experimental design Data interpreration Manuscript review		
Signature		Date	22/06/23

Please cut and paste additional co-aut

Abstract

This study describes a mechanochemical (MC) technique to synthesize a slow-release fertilizer containing zinc (Zn), molybdenum (Mo) and minor amounts of sulfur (S). The reactants ZnO, MoO_3, and $ZnSO_4 \cdot 7H_2O$ were milled in a ball mill with a two-step operation. The two metal oxide reactants were initially milled for 1 h followed by milling with $ZnSO_4 \cdot 7H_2O$ or a small addition of water for another 2 or 4 h. The products were characterized by X-ray diffraction (XRD), Fourier-transform infrared spectroscopy (FTIR), scanning electron microscopy (SEM), and thermogravimetric analysis (TGA), which confirmed the successful synthesis of a product with low Mo solubility containing mostly Zn and Mo. The product milled with $ZnSO_4 \cdot 7H_2O$ formed a clear layered structure which further slowed the release of Mo. The slow-release character of the product with 1 h + 2 h milling was observed in a column dissolution study; the solubility of Mo was less than half the product made without the second milling step. Furthermore, the products maintained lower solubility in a wider pH range compared to the reactants.

4.1 INTRODUCTION

Zinc (Zn) and molybdenum (Mo) are essential micronutrients for plant metabolism as they are important constituents or activators of various enzymes (Mengel et al., 2001b). Zinc is present in the soil as a cation and is commonly deficient in calcareous soils (Alloway, 2009). Zinc deficiency remains a global health problem that is estimated to affect 17% of the global population (Myers et al., 2015). At the same time, high concentrations of soluble Zn from water-soluble Zn-containing fertilizers can affect microbial functions in soil e.g. Rhizobium (El-Kenawy et al., 1997). Molybdenum is present in the soil as a cation, anion, or complex, with several valences depending on soil conditions (Kaiser et al., 2005). Many greenhouse and field trials have evaluated the importance of Mo application for crop yield, seed quality, and interactions with nitrogen (N) fixation and phosphorus (P) uptake and availability. Molybdenum deficiency is generally more severe in legume plants, as Mo-bonded pterins are an important cofactor of many enzymes in the N fixation system (Adams et al., 1990; Basak et al., 1982; Campo et al., 2009; Mengel et al., 2001; Reddy et al., 1981; Reisenauer, 1963; Zimmer and Mendel, 1999). Commonly used Mo fertilizer compounds are primarily soluble Mo salts such as sodium molybdate dihydrate ($Na_2MoO_4.2H_2O$) and ammonium heptamolybdate tetrahydrate ($(NH_4)_6Mo_7O_{24}.4H_2O$). The micronutrient is generally applied with macronutrients or as a foliar fertilizer (Vieira et al., 1998). Soluble Mo sources are immediately available to plants, but can also be easily leached out of soils or fixed in Mo-retentive soils. Molybdenum deficiency is observed mainly in well-aerated acid soils, as a decrease in soil pH will increase the Mo adsorption onto soil oxides, particularly on Fe oxides (Kaiser et al., 2005). However, alkaline soils in high rainfall areas can also lose plant-available Mo through runoff or leaching (Schulin et al., 2010).

Therefore, slow- or controlled-release Mo fertilizers are preferred, to better synchronize supply with plant demand and further improve fertilizer efficiency. Only a few attempts have been made to synthesize slow-release Mo fertilizers, such as long-chain sodium magnesium polymolybdophosphate (Bandyopadhyay et al., 2008b) with a half-life of more than 21 days and a Mo intercalated Zn-Al layered double hydroxide (LDH) (Everaert et al., 2021a) with a half-life range of 35 to more than 600 h during hydrolysis in water or mimicked soil solution.

Advanced materials, such as layered structures with a charged surface, have been considered as a matrix for carrying nutrients as fertilizers because the charged surface could potentially load the desired elements and release them more slowly. Various attempts have been made to load or incorporate plant nutrients in layered structures, such as clay minerals (montmorillonite, zeolite, etc. + N, P, S, potassium (K), and boron (B) (de Campos Bernardi et al., 2013; Manjaiah et al., 2019; Olad et al., 2018), graphene oxide + P, copper (Cu) and Zn (Kabiri et al., 2017, Andelkovic et al., 2019) and LDH + P, N, B and Mo (Benício et al., 2017, Everaert et al., 2016, Torres-Dorante et al., 2009). Mechanochemistry (MC), which relies solely on mechanical forces, is a cleaner and more efficient method for the synthesis of functional materials. Certain industries, such as alloying, have a long history of utilizing MC and currently the technique is expanding into other important industries, such as pharmaceuticals, lithium-ion batteries, semiconductors, catalysis, and ceramics, where sustainable manufacturing is demanded (James et al., 2012a). Numerous studies have evaluated the possibility of synthesizing or modifying materials with layered structures such as clay minerals (Frost et al., 2002, Yang et al., 2006, Chen et al., 2019, Said et al., 2018), graphite (Posudievsky et al., 2012),

MoS_2 (Wu et al., 2010), layered hydroxide salts (LHS) (Thomas, 2012, Santosa et al., 2020) and LDH (Tongamp et al., 2007, Iwasaki et al., 2012, Zhang and Li, 2013).

Milling as one of the methods used in mechanochemistry is also used in fertilizer manufacturing. The earliest application was simply to decrease the particle size of raw materials used in manufacturing plants, such as phosphate rock, to increase surface area and achieve a higher extraction rate or greater solubility (Baláž, 2008a). Using MC to activate or synthesize layered structure materials as carriers for plant nutrients is one of the earliest approaches to mechanochemically synthesize materials proposed as potential fertilizers. Mechanochemically combined kaolin and potassium dihydrogen phosphate/ammonium dihydrogen phosphate (KH_2PO_4/$NH_4H_2PO_4$) was proposed as a slow-release NPK fertilizer (Zhang and Saito, 2009). Later, other clay minerals such as smectite and glauconite were mechanically intercalated with urea as a slow-release N and K fertilizer (Rudmin et al., 2020). Tongamp et al. (2008) proposed a MC process, using Mg and Al hydroxide and magnesium nitrate hexahydrate ($Mg(NO_3)_2 \cdot 6H_2O$), to synthesize Mg-Al-NO_3 LDH as a slow-release N-fertilizer. They used a two-step milling method, in which they first milled $Mg(OH)_2$ and $Al(OH)_3$ for 1 h and then added hydrated salts for another 2 h milling. A 24 h static solubility test showed a slower N-release pattern for the Mg-Al-NO_3 LDH than for the reactants before ball milling. This two-step milling process has been used in several other studies to mechanochemically synthesize a LDH (Qu et al., 2016a).

Recently, attempts have been made to incorporate Mo into LDH or LHS, where Mo was either part of the layered structure or an intercalated guest anion. A Mo-containing LDH structure was successfully synthesized forming Ni-Mo LDH (Mostafa et al., 2018) and Zn-Mo LDH (Muramatsu et al., 2007) using co-precipitation and urea decomposition methods, respectively. Later, Zn-LHS was synthesized using alkaline precipitation methods and further intercalated with Mo by anion exchange (Abrantes Leal et al., 2020). To date, only one synthesized Mo-containing LDH has been reported as a potential Mo fertilizer. Everaert et al. (2021) loaded molybdate anion into a Zn-Al LDH at different Zn/Al ratios using co-precipitation and anion exchange. The optimum Mo-Zn_2Al LDH compound could be incorporated with urea as a potential slow-release Mo fertilizer.

In this study, we aimed to have Mo as part of the layered structure with Zn using MC synthesis, providing a new material containing both Mo and Zn micronutrients and having slow-release characteristics. To achieve this, we adopted a two-step milling process. In the first step, the metal oxides (ZnO and MoO_3) are milled to create more defects and decrease the particle size. In the second step, either $ZnSO_4 \cdot 7H_2O$ or water was used in minor amounts as a means to provide additional anions to promote the formation of a positively charged layer structure (Qu et al., 2016a). We report the chemical composition, characterization of the structure, and release behaviour of this mechanochemically synthesized fertilizer. The objectives of this study were a) to synthesize a slow-release Mo fertilizer with a one-pot ball milling procedure without further purification and/or waste generation; and b) to evaluate the nutrient release of the synthesized fertilizer.

4.2 MATERIALS AND METHODS

4.2.1 Reagents

Three reactants were used in this study: zinc oxide (ZnO, 99.0% puriss) was purchased from Sigma-Aldrich (NSW, Australia), molybdenum (VI) oxide (MoO_3, 99.5%) was purchased from Merck (VIC, Australia) and zinc sulfate heptahydrate ($ZnSO_4 \cdot 7H_2O$, 100%) was purchased from Acros Organics (NJ, United State). All chemicals were employed without further purification. Reverse osmosis (RO) water was used for all processes.

4.2.2 Mechanochemical Synthesis and Washing Procedure

The synthesis procedure is summarized in Figure 4.1. In general, MoO_3 and ZnO were weighed and added to 50-mL zirconia jars, with four or six zirconia balls (15 mm diameter and 10 g per ball) in each jar to achieve a ball-to-sample weight ratio of around 20. Balls were added to, or extracted from, the milling vessel during processing to keep this ratio constant. Ball milling was carried out in a planetary mill (PM200, Retsch, Haan, Germany) with a 5 min break and a change of direction every 30 min of milling to avoid overheating. After 1 min of milling, a 1 g subsample (labelled ZM1) was taken. After 1 h of dry grinding, another 1 g subsample was taken from the jars (sample ZM2) and then either 200 μL RO water (termed 'ZM' samples) or 1.198 g of $ZnSO_4 \cdot 7H_2O$ and two balls (termed 'ZMS' samples) were added. The subsample ZMS1and ZM2 (1 g per jar) and two balls were taken after 1 min of milling with $ZnSO_4 \cdot 7H_2O$ or water. Subsamples ZM3/ZMS2 and ZM4/ZMS3 were collected after 2 h and 4 h of milling in the same manner. Half of the subsamples ZM1 to 4 and ZMS1 to 3 were further washed with 1 L of flowing RO water and dried at room temperature (resulting in samples W-ZM1-4 and W-ZMS1-3) to remove unreacted soluble reactants and achieve a higher crystallinity in the products for structural characterization.

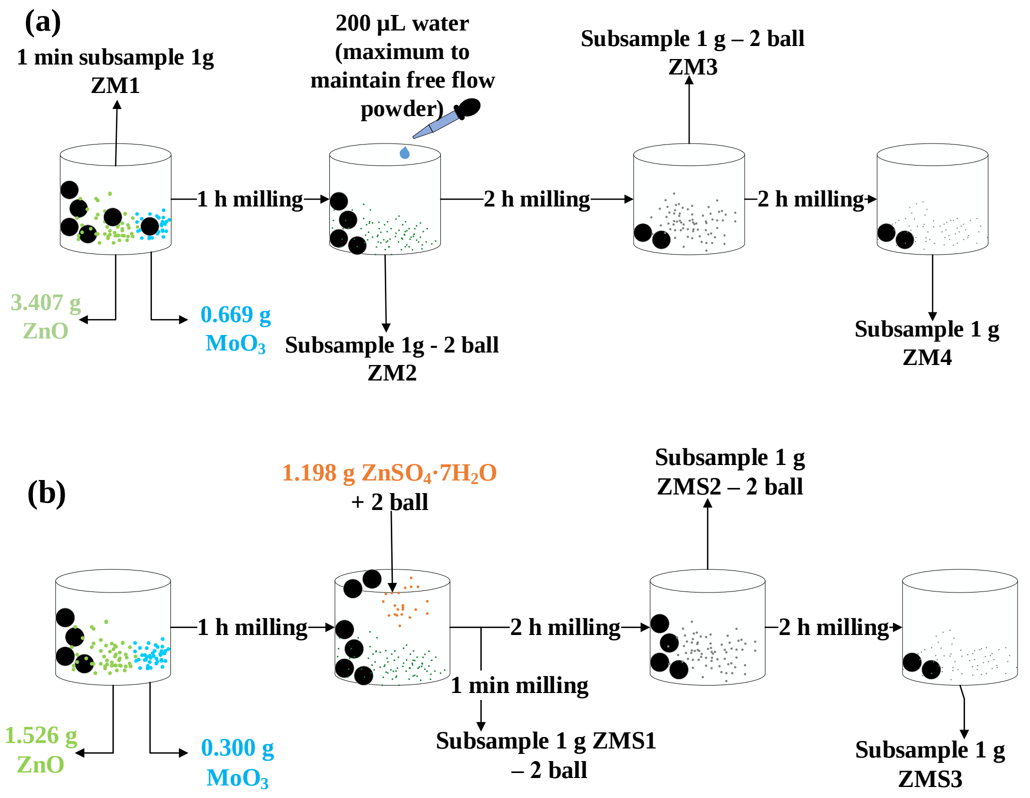

Figure 4.1 Flowchart of the sequential sampling of ZM1-4 (a) and ZMS1-3 (b).

4.2.3 Structural Characterization

The morphology of the samples (including the reactants) was analyzed by field emission scanning electron microscopy (FE-SEM, Quanta 450, FEI, USA). X-ray diffraction (XRD) patterns of products and reactants were recorded with an X'Pert Pro multipurpose diffractometer (PANalytical B.V. Almelo, Netherlands) using Fe-filtered Co Kα radiation, automatic divergence slit, 2° anti-scatter slit, and fast X'Celerator Si strip detector. The diffraction patterns were recorded with a step size of 0.017° 2 theta and a counting time of 0.5 s per step for an overall counting time of approximately 30 min. The relative amounts of the major phases were determined by the Rietveld method using the Bruker TOPAS software package (Bruker BioSpinCorporation, Billerica, MA, USA). Fourier transform infrared (FTIR) spectroscopy measurements were carried out using the attenuated total reflectance (ATR) module on an Alpha FT-IR spectrometer (Bruker

Optics, Ettlingen, Germany). The analysis was performed in the middle infrared range (wavenumber from 4000 to 400 cm^{-1}) at a resolution of 4 cm^{-1} and corrected for an air background. The sample was mounted on a platinum platform and covered with a thin layer of foil paper. Each sample was scanned 100 times and the platform was cleaned with lint-free tissue and ethanol between treatments. The thermal decomposition was carried out in air using a thermogravimetric analyzer (Q500, TA Instruments, USA), heating from room temperature to 900°C at a rate of 10°C min^{-1}.

4.2.4 Water Solubility, Chemical Composition, and Release of Mo

The solubility of the samples was assessed by weighing 0.1 g of the sample into a 50-mL digestion tube with 10 mL of RO water. The samples were shaken on an end-over-end shaker for 1 h followed by 10 min centrifugation at 4685 g. Then 5 mL of the supernatant was taken for further analysis and 5 mL of RO water was added to the original 50-mL tube and shaken for 23 h. The supernatant samples were then filtered through a 0.2-µm syringe filter before analysis using an inductively coupled plasma-optical emission spectrometry (ICP-OES, Avio 200, Perkin Elmer, Waltham, USA) and pH measurement. The sediment remaining in the centrifuge tubes was digested overnight at room temperature using *aqua regia* (HNO_3: HCl =1:3 v/v), followed by 45 min of heating at 80°C and 165 min of heating at 125°C in a digestion hot block. The concentrations of Zn, Mo, and S in the digest were also analyzed by ICP-OES to determine the total content of soluble and insoluble Zn, Mo, and S. References materials were used for quality control in all the digestion and ICP tests.

The Mo release as a function of pH was determined in a titration experiment. The samples (0.03 g of ZMS1, ZMS2, ZM1 and ZM3) were weighed into a 50 mL tube and 30 mL RO water was added. The samples were titrated with either 1 M HCl or 1 M NaOH, with

20 minutes equilibration on a shaker between each titration step. After each equilibration step, the pH was determined and a 1 mL subsample was taken and filtered over a 0.45 µm filter. The samples were diluted and the concentration of dissolved Mo and Zn in the sample was measured by ICP-OES. Reference materials were used for quality control in all the digestion and ICP tests.

4.2.5 Column Dissolution Study

Dissolution kinetic experiments were carried out for ZM1, ZM3, ZMS1 and ZMS2 (unwashed samples) using the column perfusion method described by Baird et al. (2019). This is a laboratory method that examines the dynamic release of nutrients from fertilizer formulations by continuously perfusing samples with a solution. Previous studies have shown a good correlation between pot, leaching, and seedling toxicity experiments with this method (Abat et al., 2015b, Abat et al., 2015c, da Silva et al., 2018a). Powders were used in this study to avoid any potential effects of granulation due to particle size and/or binders. The powdered sample (0.2 g) was placed in between 1 g of glass wool in each polypropylene column (150 mm long × 15 mm diameter). The percolating solution (10 mM $CaCl_2$, pH=6) was introduced into the column from the bottom using a peristaltic pump at a constant rate of 10 mL h^{-1}. The eluates from the top of the column were collected every hour for 72 h using a fraction collector (SuperFracTM, Pharmacia, USA). At the end of the study, residues, glass wool, and the solution remaining in each column were collected and dried in the oven at 90° C until all liquid vaporized. These residues were digested using hot *aqua regia*, analyzed by ICP-OES, and added to all nutrients released over time to establish the total nutrient content of the sample. The nutrient in each sample collected hourly was expressed as a percentage of this total. All column dissolutions were performed in duplicate.

4.3 RESULTS AND DISCUSSION

4.3.1 Structural characterization

4.3.1.1 SEM

Different morphologies were observed between the reactants (Figure 4.2) and the milled samples (Figure 4.2 and Figure S 4.1). The morphology of ZMS1 (Figure 4.3a) was agglomerated particles, most likely due to the introduction of water into the system via $ZnSO_4·7H_2O$ resulting in crystal agglomeration (Qu et al., 2016b). Further milling resulted in the appearance of a lamellar structure in ZMS2 and ZMS3 samples (Figure 4.3b and c). The morphology of the hexagonal platelets and the lamellar structure was very clear after the washing procedure for samples W-ZMS1-3 (Figure 4.3d-g). The crystal morphology of the non-washed milled samples ZMS1, ZMS2, and ZMS3 was not as clear compared to that of the washed samples. This has also been reported in other ball-milling studies, in which agitation (Qu et al., 2017), aging (Stepanova et al., 2022), hydrothermal (Wang et al., 2015, Fahami et al., 2016) or ultrasonic (Szabados et al., 2016) procedures in water after milling were found to increase the crystallinity or the amount of the layered products (Melia et al., 2017). On the other hand, the morphology of W-ZM3 and W-ZM4 (Figure S 4.1a) did not change to clear platelet structures like W-ZMS2 and W-ZMS3 after the washing procedure; therefore, the second step of milling with $ZnSO_4·7H_2O$ is essential to form the lamellar and platelet structure. Other MC experiments also found that introduction of water and a guest anion into the reactants promoted the formation of a layered structure (Qu et al., 2016b, Qu et al., 2016a).

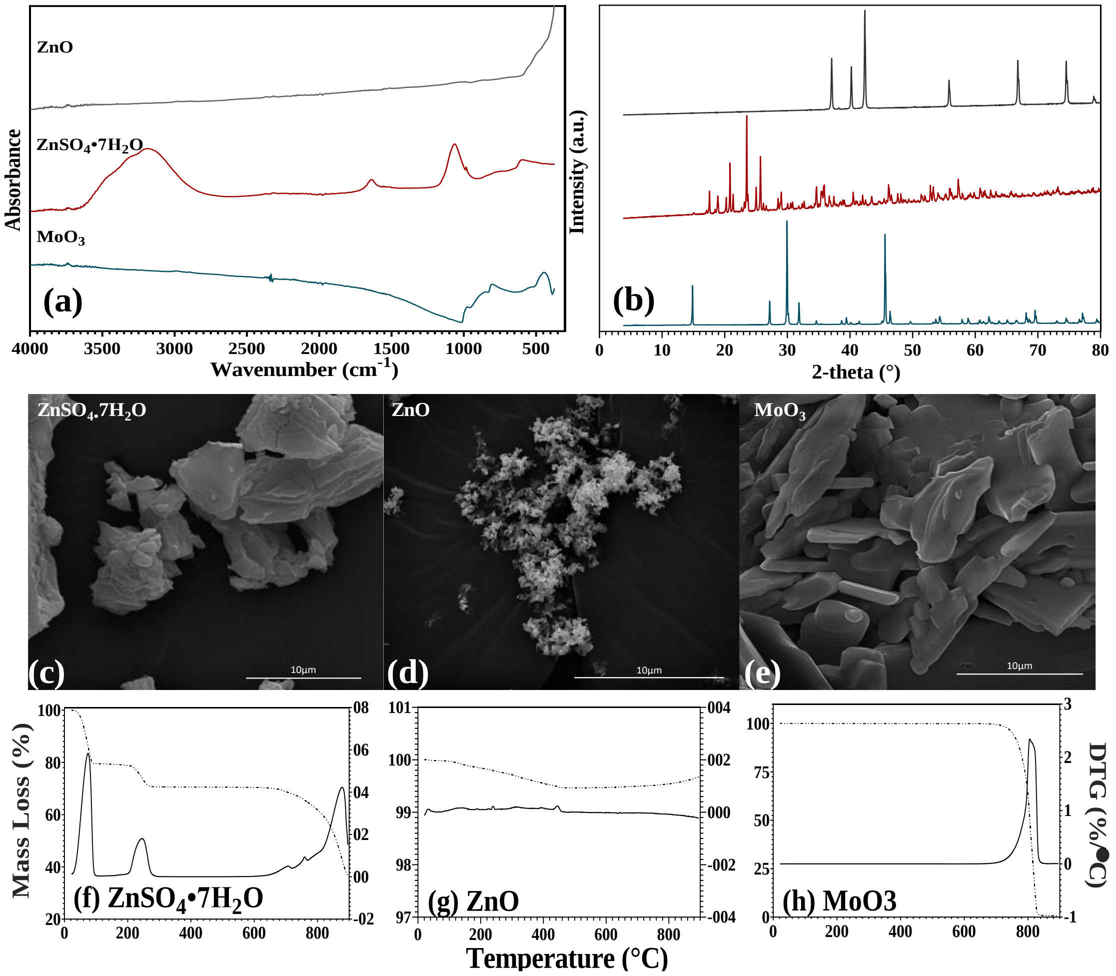

Figure 4.2 FTIR spectra (a), XRD spectra (b), SEM images and TGA results for the reactants $ZnSO_4{\cdot}7H_2O$ (c, f), ZnO (d,g) and MoO_3 (e,h).

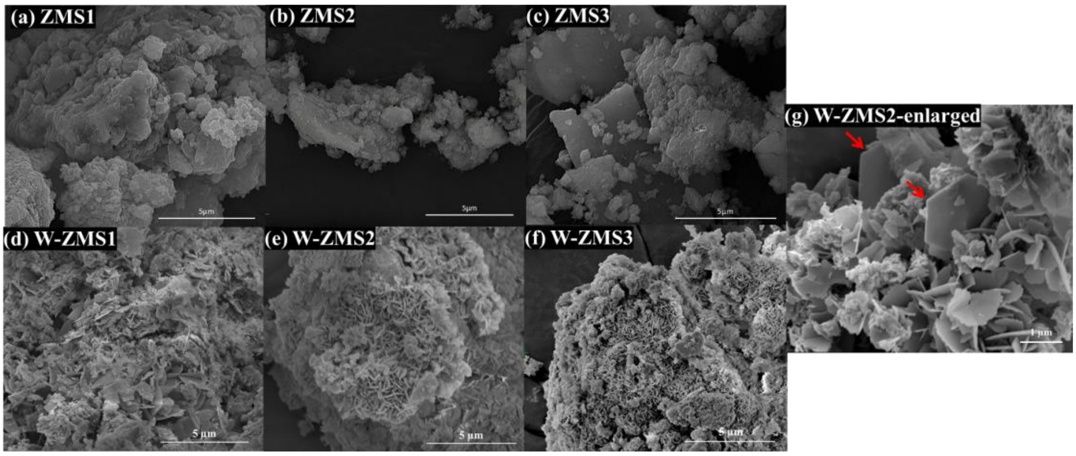

Figure 4.3 SEM images of (a, b, c) ZMS1-3, (d, e, f) W-ZM1-3 and (g) High magnification W-ZMS2. Red arrows indicate clear hexagonal platelets.

4.3.1.2 XRD

In the control samples ZM1 (Figure S 4.2a) and ZMS1 (Figure 4.4a), most of the peaks could be assigned to the initial reactants (Figure 4.2b); ZnO and MoO_3 peaks were observed in ZM1 and ZnO and $ZnSO_4·7H_2O$ peaks in ZMS1. A decrease of peak intensity and broadening in ZM2-4 (Figure S 4.2a) indicated a reduction in crystallite size and an increase in lattice strain due to the additional milling. Peaks (2ϴ= 14, 20, 27, 31, 34, 39, 59, and 71°) assigned to $Zn_5Mo_2O_{11}·5H_2O$ could be identified in ZM3, ZM4 and W-ZM2-4 (indicated by red squares in Figure S 4.2 a, c and in Figure 4.4 c). This suggests that both the washing procedure (in W-ZM2) and the addition of water in the second step (in ZM3-4) could promote the formation of $Zn_5Mo_2O_{11}·5H_2O$.

In the ZMS samples, the peaks assigned to $ZnSO_4·7H_2O$ that were observed in the ZMS1 sample could not be seen in the W-ZMS1 sample, indicating that washing removed the $ZnSO_4·7H_2O$ (Figure 4.4c). These peaks also disappeared after 2 h milling (ZMS2) or 4 h milling (ZMS3). Instead, new peaks were observed at 38, 68, and 72° in ZMS2 and ZMS3 (Figure 4.4a). Further, the peak intensity decreased and many broad new peaks were observed in ZMS2 and ZMS3. The broad peaks ranged from 2ϴ = 10-15°, 25-35°, 45-50°, and 58-62°. This is likely due to the formation of a poorly crystallized layered structure (Temuujin et al., 1998). The washing procedure increased the crystallinity of ZMS2 and ZMS3, with the broad peaks in ZMS2 and ZMS3 becoming individual peaks in W-ZMS2 and W-ZMS3 (Figure 4.4a, c). Many studies have reported that a follow-up step of ageing the mechanochemically activated products in water could greatly accelerate crystallization (Stepanova et al., 2022, Suchanek et al., 2004). However, this was a short washing procedure, thus only slightly promoting crystallinity. In W-ZMS1, peaks were observed that indicated the presence of zinc hydroxide sulfate (ZHS), also known as osakaite, $Zn_4SO_4(OH)_6 \cdot 5H_2O$ (Ohnishi et al., 2007) (purple triangle marked in Figure 4.4c). These osakaite peaks nearly disappeared in W-ZMS2 and W-ZMS3. The d-space of the $2\Theta \sim 9°$ peak representing the space between the layers decreased and shifted from 10.91 Å in W-ZMS1 to 10.88 Å in W-ZMS2 and 10.67 Å in W-ZMS3. This is likely due to the loss of water per unit of ZHS due to the increasing milling time (Stanimirova et al., 2017). The peaks assigned to $Zn_5Mo_2O_{11} \cdot 5H_2O$ could also be identified in W-ZMS1, while after extended milling in the second step, the peaks became slightly different in the W-ZMS2 and W-ZMS3 samples. Peaks around 20, 34, 45, 53, and 64° disappeared and peaks around 15, 27, and 31° were slightly shifted to the left. A new peak around 48° was observed. After fitting the new phase with the ICDD database, no Mo analogue structure could be identified; however, the peaks (indicated by the black arrows in Figure 4.4c) were close to the peaks assigned to $Zn_2CrO_5 \cdot H_2O$ and $4ZnO \cdot CrO_3 \cdot 3H_2O$. A possible explanation could be that extended milling changed $Zn_5Mo_2O_{11} \cdot 5H_2O$ to a less hydrated phase of zinc molybdenum hydroxide (Monma et al., 2009, Wang et al., 2021). Some of the peaks are similar to the ammonium zinc molybdate layered double hydroxide in the literature (Karuppiah et al., 2022). Overall, these results suggest that the layered structure observed in the SEM images of W-ZMS2 and W-ZMS3 was due to formation of a zinc molybdenum oxide and osakaite analogues.

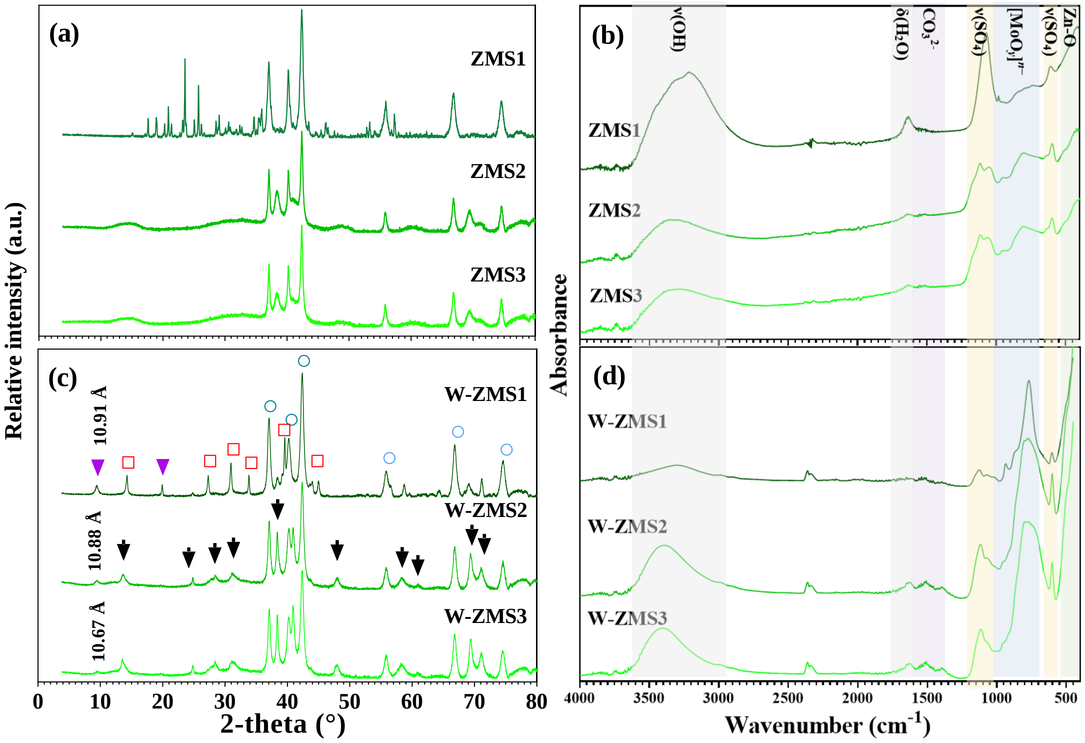

Figure 4.4 XRD pattern of (a) ZMS1-3 (c) washed ZMS1-3 (W-ZMS1, W-ZMS2 and W-ZMS3); The peaks indicated as ○ are assigned to ZnO, those indicated as □ are assigned to $Zn_5Mo_2O_{11}\cdot 5H_2O$ and those indicated as ▼ are assigned to osakaite ($Zn_4SO_4(OH)_6\cdot 5H_2O$); the ⬇ indicates an unidentifiable zinc molybdenum oxide analogue; (b) FTIR spectra of ZMS1-3 (d) washed ZMS1-3 (W-ZMS1, W-ZMS2 and W-ZMS3).

4.3.1.3 FTIR

Broad bands were observed around 3500-3200 cm^{-1} for all samples (Figure 4.4b, d and Figure S 4.2b, d), which could be attributed to the stretching of the OH bond in the crystalline water, interlayer water or in M-OH groups. Another band associated with the OH-bending of water in the layered structure was observed as a weak band close to 1640 cm^{-1}. The bands assigned to the interlayer water or hydroxide group decreased with increasing milling time in ZM3-4 (Figure S 4.2b) and ZMS1-3 (Figure 4.4b). A band attributed to the SO_4^{2-} vibration was observed between 1000-1200 cm^{-1} in ZMS1. This band changed from a single strong peak in ZMS1 to a shoulder peak in ZMS2 and ZMS3, indicating that SO_4^{2-} may have partially transformed to HSO_4^-. A possible explanation for this transformation is due to the loss of structural water, as H^+ of H_2O is used for the protonation of SO_4^{2-} (Stanimirova et al., 2017). The peaks around 600 cm^{-1} are assigned to the antisymmetric deformation mode of SO_4^{2-} in the ZMS 1-3 samples. The absorption bands in all samples within the range of 700-1000 cm^{-1} are due to the vibration of $[MoO_y]^{n-}$ (Liang et al., 2012). The peaks in W-ZMS1 attributed to interlayer water or hydroxide groups attached to the surface and SO_4^{2-} were much weaker than in W-ZMS2 and W-ZMS3 as a result of the formation of fewer layers with fewer bonding sites for hydroxide groups/ interlayer water or anions (Figure 4.4d). Furthermore, minor peaks of carbonate (CO_3^{2-}) were found in W-ZMS2 and W-ZMS3, which were probably intercalated during the washing procedure. These new peaks were not observed in the ZM samples after the washing procedure (Figure S 4.2d), which indicated the new peaks assigned to carbonate in W-ZMS samples are associated with the formation of osakaite. Similar spectra with identifiable peaks have been observed in osakaite and a hemihydrate osakaite metaphase (Stanimirova et al., 2017). Together, the results of XRD and FTIR confirmed that the second step of milling the hydrated salt with the initial metal oxide reactants promoted the formation of osakaite and a zinc molybdenum oxide analogue.

4.3.1.4 TGA

The unwashed products were used for TGA assessments to better understand the reaction of water and $ZnSO_4 \cdot 7H_2O$ during the second step of milling. As shown in Figure 4.5, a three-stage thermal degradation was observed for ZMS1-3, which was attributed to dehydration of surface water (first stage), interlayer water and crystal water (second stage), and sulphate removal (third stage). The first mass loss before 200° C was approximately 2 times greater in ZMS1 (12.9%) than in ZMS2 and ZMS3 (6%). The theoretical and measured crystal water content in $ZnSO_4 \cdot 7H_2O$ is 17.34 wt.% (Figure 4.2f). This change is likely due to two reasons. First, extended grinding may have removed most of the water on the surface of the reactants; and second, part of the water may have been interlaminated into the layered structure or incorporated as a hydroxide group. Therefore, less water was eliminated before 200° C while more water was removed after 200° C for the ZMS2-3 samples. This was further supported by the DTG peaks being divided into 3 peaks for ZMS2 and ZMS3 in the 200-400°C range, compared to a single peak for ZMS1. The third stage is the loss of the interlayer anion SO_4^{2-} or absorbed CO_3^{2-} at temperatures over 400° C (Andersen et al., 2021, Radha and Kamath, 2009). The mass loss of ZMS2 and ZMS3 above 400° C was very close to the calculated amount of SO_4 in the synthesized products i.e. around 11 wt%. The decomposition of the sulphate group was complete at a slightly higher temperature for ZMS2 and ZMS3 than for ZMS1. According to the results from the FTIR, transformation of sulphate to a bisulphate occurred after extended milling generating a crosslink of the O^{2-} between the layers thus increasing the thermal stability of SO_4^{2-} and remaining hydroxide group (Stanimirova et al., 2017). For the ZM samples, ZM1 and ZM2 (Figure S 4.1b) had a profile similar to the ZnO (Figure 4.2g), the water added after first step milling did not make any changes in ZM2 due to lack of second step milling, while TGA profiles of ZM3 and ZM4 indicate incorporation of water into the newly formed crystal structure (Figure S 4.1b). In ZM3 and ZM4, a large degradation was observed with four distinct weight loss peaks ranging from 0-400° C. A similar weight loss for $Zn_5Mo_2O_{11} \cdot 5H_2O$ was reported by Zhai et al. (2017) who observed three weight loss peaks associated with the water and hydroxide groups around 200-300° C.

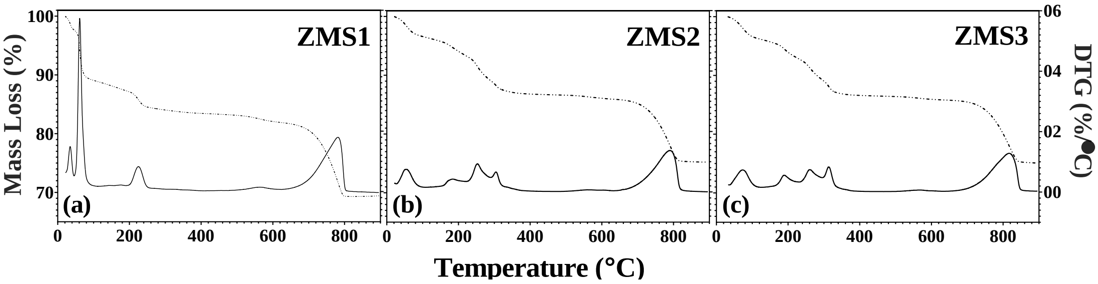

Temperature range (°C)	**ZMS1 Mass loss (wt%)**	**ZMS2 Mass loss (wt%)**	**ZMS3 Mass loss (wt%)**
<200	12.9	5.9	6.1
200-400	3.7	7.3	7.4
>400	14.0	11.6	11.6

Figure 4.5 TGA and DTG curves of (a) S1, (b) S2, and (c) S3 and the calculated mass loss within different temperature ranges.

4.3.2 Solubility of Mo

4.3.2.1 Batch solubility

The batch solubility tests, titrations, and column dissolutions were conducted using products prior to the washing procedure. Sample W-ZMS2 was also included in the batch solubility test for comparison. The chemical composition of ZMS2 and ZMS3 was similar (50-52% Zn, 7% Mo and 5% S) (Table 4.1). The ZM2-4 samples had a higher content of Zn (65-70%) and Mo (10-11%) than the ZMS products. The higher Mo and Zn contents in ZM1 compared to other fully milled samples is likely caused by the short (1 min) milling time limiting sample homogeneity. The freshly added reactants with high water contents formed heterogeneous aggregates, making representative subsampling difficult. The ZMS1-3 and ZM1-4 products had a pH around 6.3 after 1 h of dissolution, which increased to 6.5 after 24 h of dissolution. Molybdenum release was lowest in ZM1 and ZM3 among the ZM samples and in ZMS2 among ZMS samples after 1 h of equilibration. The amount of Mo released after 24 h of water dissolution doubled in ZM1, 3 and 4 compared to the 1-h equilibration, while only a 3-5 % increase was observed in ZMS samples. A higher Mo release was observed in ZM2 than in ZM1, indicating that 1 h ball milling promoted the release of Mo, possibly due to reductions in particle size (increasing sample surface area) resulting in faster dissolution. Interestingly, the amount of Zn and S released after 24 h was lower compared to release after 1 h for the ZMS1 sample. This is likely due to the formation of the zinc hydroxide salt during dissolution in a batch system, which is consistent with other studies that use water agitation procedures to promote the growth of the layered structure after the MC process (Qu et al., 2017). However, milling with minor amounts of water and $ZnSO_4 \cdot 7H_2O$ in the second step decreased Mo solubility. The differences between water-extractable nutrients in ZMS2 and ZMS3 were minor indicating that the 2 h milling after adding $ZnSO_4 \cdot 7H_2O$ was adequate to decrease the solubility of the highly soluble $ZnSO_4 \cdot 7H_2O$. The MoO_3 used as a reactant had the lowest batch solubility (when expressed as % of total Mo) because of the 6- or 10-times higher Mo content in MoO_3 compared to ZM and ZMS samples and because of the lower equilibrium pH of the solution (Table 4.1). The dissolution of MoO_3 in water caused the pH to drop to 3.2 after 1 h and 2.6 after 24 h. At these pH values, MoO_3 is only slightly soluble in water (Oyerinde et al., 2008). When these compounds are added to soil, the soil would buffer the pH and this pH drop would not occur and dissolution products would be sorbed by soil surfaces, resulting in higher inherent solubility.

Table 4.1 Chemical composition of reactants and samples ZM1-4 and ZMS1-3, and equilibrium pH of water suspensions after 1 h and 24 h of shaking.

Treatments	**Nutrient content% (w / w)**			**Water extractable % of total element**						**pH**	
				1 h			**24 h**			**1 h**	**24 h**
	Zn	**Mo**	**S**	**Zn**	**Mo**	**S**	**Zn**	**Mo**	**S**		
ZM1	81 .0 ± 4	11.9 ± 1	/	0.7 ± 0	10.8 ± 2	/	2.5 ± 0	24.0 ± 1	/	6.6	6.8
ZM2	69.6 ± 1	10.7 ± 0	/	3.9 ± 0	32.2 ± 0	/	3. 0 ± 0	30.5 ± 0	/	6.6	6.8
ZM3	64.7 ± 3	9.9 ± 0	/	0.5 ± 0	10.9 ± 0	/	0.8 ± 0	17.6 ± 0	/	6.8	6.8
ZM4	69.7 ± 1	10.7 ± 0	/	1.0 ± 0	13.5 ± 0	/	1.4 ± 0	19.8 ± 0	/	6.8	6.8
ZMS1	51.1 ± 0	6.4 ± 2	6.3 ± 0	19.2 ± 1	28.8 ± 0	44 ± 1	17.5 ± 1	28.8 ± 1	39.2 ± 0	6.2	6.5
ZMS2	51.6 ± 0	6.7 ± 0	4.7 ± 0	9.0 ± 0	17.2 ± 0	33.8 ± 1	10.3 ± 0.2	20.9 ± 0	39.7 ± 1	6.3	6.5
ZMS3	50.4 ± 0	6.5 ± 1	4.6 ± 0	9.7 ± 0	18.4 ± 0	35.1 ± 1	11.0 ±	23.1 ± 0	41.8 ± 1	6.3	6.6
W-ZMS2	50.5 ± 4	5.7 ± 0	3.8 ± 0	3.2 ± 0	9.4 ± 0	13.4 ± 1	5.2 ± 1	14.1± 2	16.5 ± 1	6.2	6.5
ZnO	85.7 ± 2	/	/	0	/	/	0	/	/	7.0	7.4
MoO_3	/	65.9 ± 5	/	/	2.2	/	/	9.2	/	3.2	2.6
$ZnSO_4\cdot 7H_2O$	31.8 ± 0	/	15.6 ± 0	70.0 ± 3	/	69.3 ±1	87.2 ± 3	/	94.6 ± 3	5.3	5.4

The Mo release from ZM1, ZM3, ZMS1 and ZMS2 as a function of pH was determined in an acid and base titration experiment (Figure 4.6 a, b). The pH increased quickly for all samples in the base titration after adding 3.5 mmol base solution g^{-1} sample where pH increased from around 6 to more than 10 (Figure 4.6). On the other hand, a strong acid buffering capacity was observed in the acid titration, with the samples maintaining a pH around 6 until 7 mmol acid solution g^{-1} sample was added. For the ZM samples, the lowest solubility was observed at small acid additions, while for the ZMS samples the lowest Mo solubility was observed at small base additions. During the base titration, both ZM samples had much higher Mo. However, the lower solubility might also be due to the formation of ZHS, where dissolved MoO_4^{2-} might be able to attach or exchange to the surface or interlayer of ZHS (Reichle et al., 1975, Hongo et al., 2010). Increasing pH would also promote the formation of ZHS with a larger plate surface area (Zhang and Yanagisawa, 2007).

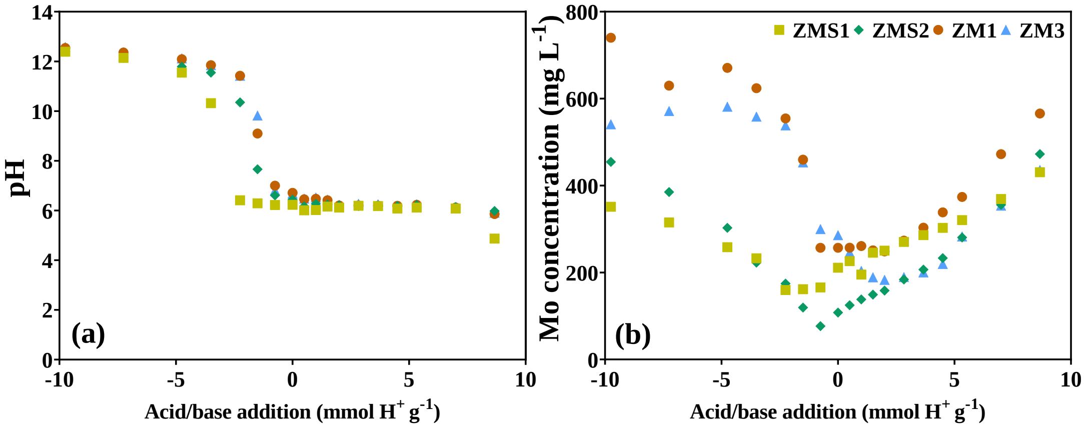

Figure 4.6 The effect of the acid or base titration on (a) equilibrium pH and (b) dissolution of Mo from ZM1, ZM3, ZMS1, ZMS2.

4.3.2.2 Column dissolution

Given that the batch dissolution tests could underestimate the solubility due to precipitation and crystallization of mechanochemically activated products, we further compared the column dissolution results of the unwashed products ZM1-3 and ZMS1-2 (Figure 4.7). The Zn release was consistently low and negligible from both ZM1 and ZM3; only around 5% of the total Zn was released after 72 h of dissolution (Figure 4.7 a, c). This is due to the low solubility of ZnO. The cumulative release of Mo after 72h from ZM1 (42%) was double that of ZM3 (21%) (Figure 4.7b). The total release of Mo (50%), S (89%) and Zn (25%) for ZMS1 was 3.8, 2.9, and 4.7 times higher than for ZMS2, respectively (Figure 4.7d, e). All nutrients in ZMS1 and ZMS2 had a biphasic release behaviour in which 50-80% of the total nutrients leached (after 72 h dissolution) were released within the first 10 h, followed by a slow and steady release until the end of the experiment. The steady release stage was slower in ZMS2 compared to ZMS1. The amount of nutrients released by the end of the experiment was in good agreement with the soluble amount in the batch solubility test for ZM3 and ZMS2, but not for ZM1 and ZMS1. The removal of dissolved Mo and S by the percolation solution doubled the Mo and S release of ZM1 and ZMS1 compared to the release in the batch solubility test.

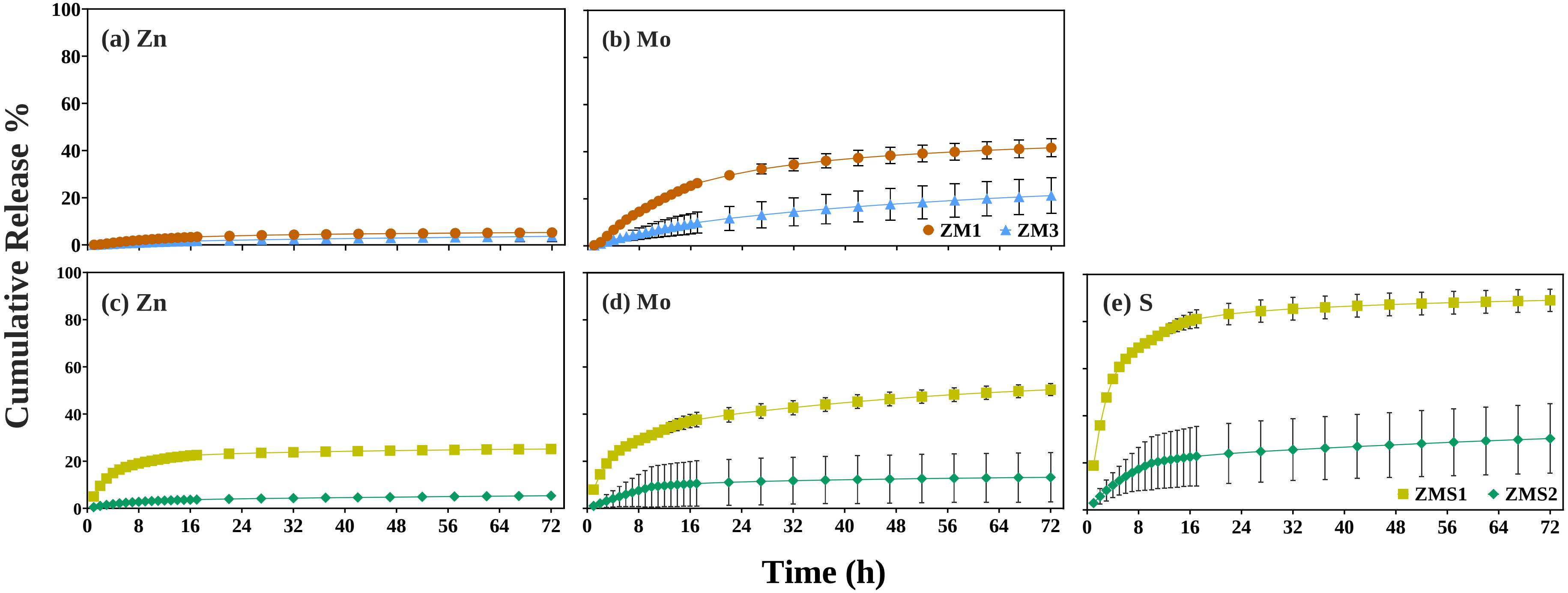

Figure 4.7 Cumulative release of Zn (a and c), Mo (b and d) and S (e) from ZM1, ZM2, ZMS1 and ZMS2 over 72 h of column dissolution. The error bars represent the standard error (n=2).

The biphasic release of nutrients is ideal and might better fit plant nutrient demand have compared to a highly soluble product. The slower release of Zn, Mo and S after the initial flush may be related to the dissolution of the layered structure of ZHS and zinc molybdenum oxide hydroxide in ZMS2 and zinc molybdenum oxide hydroxide in ZM3. The products were tested without any purification process (i.e. washing, or other additional treatments); thus, the initial rapid release may have resulted from unreacted or amorphous reactants. Therefore, this Zn-Mo-S could fall into the category of a rhizosphere-controlled fertilizer whose initial soluble fraction compensates for the soil deficiency and the rest of the insoluble residue could be released by exudation of acids by plant roots (Erro et al., 2007, López-Rayo et al., 2017).

On the basis of above results, we can conclude that a slow-release Zn-Mo-S fertilizer with a layered structure was successfully synthesized by the two-step ball milling process. Although a large amount of layered structure was observed by SEM, the reactants were still present in the synthesized products as was evident from XRD and FTIR results. A possible explanation could be that the reaction is not complete due to the formation of a layered structure that passivates the ZnO surface (Shao et al., 2014). With the objective of this study in mind, the products were not modified or purified further; therefore, the products directly after MC synthesis were used in the column dissolution test. Previous studies have shown a relatively good correlation between pot, leaching, and seedling toxicity experiments with this method in a controlled environment (Abat et al., 2015b, Abat et al., 2015c, da Silva et al., 2018a). In general, the application rate of Mo as fertilizer is 0.01-0.5 kg ha^{-1} for Mo-deficient soil, and that of Zn is 4.5-34 kg ha^{-1} for Zn-deficient soil (Martens and Westermann, 1991). The composition of the synthesized products could fit into the application rate above, reducing the chance of unwanted elemental accumulation in soil or seedling toxicity. Furthermore, MoO_3 is readily soluble in the presence of ammonia, thus products from this study could be better incorporated with macronutrients such as diammonium phosphate or urea.

4.4 CONCLUSIONS

The adapted two-step MC method successfully prepared the desired sparingly soluble fertilizer to contain Mo and Zn for plants. This method used minor water and the final products were produced as dry powders without generating any waste water such as reacting, purifying or leaching solutions. The biphasic release behaviour of these nutrients could potentially satisfy the demands of plants and remedy soil deficiency without causing seedling or bacterial toxicity (e.g. Rhizobium) with soluble Zn or leaching risks for Mo. The dissolution study of the products indicated that ZMS2 could be applied alone as a slow-release fertilizer containing Mo and Zn. The Mo content in the products could be further optimized to achieve a lower or higher initial release rate to satisfy plant demand or compensate for soil deficiency. Further optimization or evaluation of the products to adjust the Mo release could possibly also be achieved by calcination or hydrothermal treatment. Agronomically, a comparison with other Mo fertilizers in plant trials is needed to confirm the effectiveness and residual value of these products.

4.5 REFERENCES

Abat, M., Degryse, F., Baird, R., McLaughlin, M.J., 2015a. Boron Phosphates (BPO_4) as a Seedling-Safe Boron Fertilizer Source. Plant and Soil 391(1), 153-160.

Abat, M., Degryse, F., Baird, R., McLaughlin, M.J., 2015b. Responses of Canola to the Application of Slow-Release Boron Fertilizers and Their Residual Effect. Soil Science Society of America Journal 79(1), 97-103.

Abrantes Leal, D., Wypych, F., Bruno Marino, C.E., 2020. Zinc-Layered Hydroxide Salt Intercalated with Molybdate Anions as a New Smart Nanocontainer for Active Corrosion Protection of Carbon Steel. ACS Applied Materials and Interfaces 12(17), 19823-19833.

Adams, J.F., Burmester, C.H., Mitchell, C.C., 1990. Long-term Fertility Treatments and Molybdenum Availability. Fertilizer Research 21(3), 167-170.

Alloway, B.J., 2009. Soil Factors Associated with Zinc Deficiency in Crops and Humans. Environmental Geochemistry and Health 31(5), 537-548.

Andelkovic, I.B., Kabiri, S., da Silva, R.C., Tavakkoli, E., Kirby, J.K., Losic, D., McLaughlin, M.J., 2019. Optimisation of Phosphate Loading on Graphene oxide–Fe(iii) Composites – Possibilities for Engineering Slow Release Fertilizers. New Journal of Chemistry 43(22), 8580-8589.

Andersen, A.B.A., Henriksen, C., Wang, Q., Ravnsbæk, D.B., Hansen, L.P., Nielsen, U.G., 2021. Synthesis and Thermal Degradation of $MAl_4(OH)_{12}SO_4·3H_2O$ with M = Co^{2+}, Ni^{2+}, Cu^{2+}, and Zn^{2+}. Inorganic Chemistry 60(21), 16700-16712.

Baird, R., da Silva, R.C., Degryse, F., McLaughlin, M.J., 2019. A Column Perfusion Test to Assess the Kinetics of Nutrient Release by Soluble, Sparingly Soluble and Coated Granular Fertilizers. Journal of Plant Nutrition and Soil Science 182, 763-771.

Baláž, P., 2008. Applied Mechanochemistry, in: Baláž, P. (Ed.) Mechanochemistry in Nanoscience and Minerals Engineering. Springer Berlin Heidelberg, Berlin, Heidelberg, pp. 297-405.

Bandyopadhyay, S., Bhattacharya, I., Ghosh, K., Varadachari, C., 2008. New Slow-Releasing Molybdenum Fertilizer. Journal of Agricultural and Food Chemistry 56(4), 1343-1349.

Basak, A., Mandal, L.N., Haldar, M., 1982. Interaction of Phosphorus and Molybdenum in Relation to Uptake and Utilization of Molybdenum, Phosphorus, Zinc, Copper and Manganese by Rice. Plant and Soil 68(2), 261-269.

Benício, L.P.F., Constantino, V.R.L., Pinto, F.G., Vergütz, L., Tronto, J., da Costa, L.M., 2017. Layered Double Hydroxides: New Technology in Phosphate Fertilizers Based on Nanostructured Materials. ACS Sustainable Chemistry and Engineering 5(1), 399-409.

Campo, R.J., Araujo, R.S., Hungria, M., 2009. Molybdenum-enriched Soybean Seeds Enhance N Accumulation, Seed Yield, and Seed Protein Content in Brazil. Field Crops Research 110(3), 219-224.

Chen, Z., Ma, W., Lu, G., Meng, F., Duan, S., Zhang, Z., Wei, L., Pan, Y., 2019. Adsorption of Levofloxacin onto Mechanochemistry Treated Zeolite: Modeling and Site energy Distribution Analysis. Separation and Purification Technology 222, 30-34.

da Silva, R., Baird, R., Degryse, F., McLaughlin, M.J., 2018. Slow and Fast-Release Boron Sources in Potash Fertilizers: Spatial Variability, Nutrient Dissolution and Plant Uptake. Soil Science Society of America Journal 82(6), 1437-1448.

de Campos Bernardi, A.C., Anchão Oliviera, P.P., de Melo Monte, M.B., Souza-Barros, F., 2013. Brazilian Sedimentary Zeolite Use in Agriculture. Microporous and Mesoporous Materials 167, 16-21.

El-Kenawy, Z.A., Angle, J.S., Gewaily, E.M., El-Wafai, N.A., van Berkum, P., Chaney, R.L., Ibekwe, M.A., 1997. Zinc and Cadmium Effects on the Early Stages of Nodulation in White Clover. Agronomy Journal 89(6), 875-880.

Erro, J., Urrutia, O., San Francisco, S., Garcia-Mina, J.M., 2007. Development and Agronomical Validation of New Fertilizer Compositions of High Bioavailability and Reduced Potential Nutrient Losses. Journal of Agricultural and Food Chemistry 55(19), 7831-7839.

Everaert, M., Smolders, E., McLaughlin, M.J., Andelkovic, I., Smolders, S., Degryse, F., 2021. Layered Double Hydroxides as Slow-Release Fertilizer Compounds for the Micronutrient Molybdenum. Journal of Agricultural and Food Chemistry 69(48), 14501-14511.

Everaert, M., Warrinnier, R., Baken, S., Gustafsson, J.-P., De Vos, D., Smolders, E., 2016. Phosphate-Exchanged Mg–Al Layered Double Hydroxides: A New Slow Release Phosphate Fertilizer. ACS Sustainable Chemistry and Engineering 4(8), 4280-4287.

Fahami, A., Al-Hazmi, F.S., Al-Ghamdi, A.A., Mahmoud, W.E., Beall, G.W., 2016. Structural Characterization of Chlorine Intercalated Mg-Al Layered Double Hydroxides: A Comparative Study between Mechanochemistry and Hydrothermal Methods. Journal of Alloys and Compounds 683, 100-107.

Frost, R.L., Kristof, J., Mako, E., Martens, W.N., 2002. Modification of the Hydroxyl Surface of Kaolinite through Mechanochemical Treatment Followed by Intercalation with Potassium Acetate. Langmuir 18(17), 6491-6498.

Hongo, T., Iemura, T., Satokawa, S., Yamazaki, A., 2010. Chromate Adsorption and pH Buffering Capacity of Zinc Hydroxy Salts. Applied Clay Science 48(3), 455-459.

Iwasaki, T., Yoshii, H., Nakamura, H., Watano, S., 2012. Simple and Rapid Synthesis of Ni–Fe Layered Double Hydroxide by A New Mechanochemical Method. Applied Clay Science 58, 120-124.

James, S.L., Adams, C.J., Bolm, C., Braga, D., Collier, P., Friščić, T., Grepioni, F., Harris, K.D.M., Hyett, G., Jones, W., Krebs, A., Mack, J., Maini, L., Orpen, A.G., Parkin, I.P., Shearouse, W.C., Steed, J.W., Waddell, D.C., 2012. Mechanochemistry: Opportunities for New and Cleaner Synthesis. Chemical Society Reviews 41(1), 413-447.

Kabiri, S., Degryse, F., Tran, D.N.H., da Silva, R., McLaughlin, M.J., Losic, D., 2017. Graphene Oxide: A New Carrier for Slow Release of Plant Micronutrients. ACS Applied Materials and Interfaces 9(49), 43325-43335.

Kaiser, B.N., Gridley, K.L., Ngaire Brady, J., Phillips, T., Tyerman, S.D., 2005. The Role of Molybdenum in Agricultural Plant Production. Annals of Botany 96(5), 745-754.

Karuppiah, C., Babulal, S.M., Chen, T.-W., Chen, S.-M., Hsu, L.-F., Al Farraj, D.A., Ramaraj, S.K., Elshikh, M.S., Yang, C.-C., 2022. A Novel Ammonium Zinc Molybdate Layered Double Hydroxide Nanoflakes/vapor Grown Carbon Fibers Nanomaterials Based Electrocatalyst for the Monitoring of Dimetridazole Drug in Real Samples. Journal of Environmental Chemical Engineering 10(5), 108227.

Liang, Y., Liu, P., Li, H.B., Yang, G.W., 2012. ZnMoO4 Micro- and Nanostructures Synthesized by Electrochemistry-Assisted Laser Ablation in Liquids and Their Optical Properties. Crystal Growth and Design 12(9), 4487-4493.

López-Rayo, S., Imran, A., Bruun Hansen, H.C., Schjoerring, J.K., Magid, J., 2017. Layered Double Hydroxides: Potential Release-on-Demand Fertilizers for Plant Zinc Nutrition. Journal of Agricultural and Food Chemistry 65(40), 8779-8789.

Manjaiah, K.M., Mukhopadhyay, R., Paul, R., Datta, S.C., Kumararaja, P., Sarkar, B., 2019. Chapter 13 - Clay Minerals and Zeolites for Environmentally Sustainable Agriculture, in: Mercurio, M., Sarkar, B., Langella, A. (Eds.), Modified Clay and Zeolite Nanocomposite Materials. Elsevier, pp. 309-329.

Martens, D.C., Westermann, D.T., 1991. Fertilizer Applications for Correcting Micronutrient Deficiencies, Micronutrients in Agriculture. pp. 549-592.

Mengel, K., Kirkby, E.A., Kosegarten, H., Appel, T., 2001. Plant Nutrients, in: Mengel, K., Kirkby, E.A., Kosegarten, H., Appel, T. (Eds.), Principles of Plant Nutrition. Springer Netherlands, Dordrecht, pp. 1-13.

Monma, H., Okura, T., Hara, Y., Moriyoshi, Y., 2009. Mechanochemical Properties of Octacalcium PHosphate and Brushite. Phosphorus Research Bulletin 23, 10-14.

Mostafa, M.S., Betiha, M.A., Rabie, A.M., M. Hassan, H., Morshedy, A.S., 2018. New Conduct in the Adsorptive Removal of Sulfur Compounds by New Nickel–Molybdenum Adsorbent. Industrial and Engineering Chemistry Research 57(2), 425-433.

Muramatsu, K., Saber, O., Tagaya, H., 2007. Preparation of New Layered Double Hydroxide, Zn-Mo LDH. Journal of Porous Materials 14(4), 481-484.

Myers, S.S., Wessells, K.R., Kloog, I., Zanobetti, A., Schwartz, J., 2015. Effect of Increased Concentrations of Atmospheric Carbon Dioxide on the Global Threat of Zinc Deficiency: A Modelling Study. The Lancet. Global health 3(10), e639-645.

Ohnishi, M., Kusachi, I., Kobayashi, S., 2007. Osakaite, Zn4SO4 (OH)6·5H2O, a New Mineral Species from the Hirao Mine, Osaka, Japan. Canadian Mineralogist - Can MineralogI 45, 1511-1517.

Olad, A., Zebhi, H., Salari, D., Mirmohseni, A., Reyhani Tabar, A., 2018. Water Retention and Slow Release Studies of a Salep-based Hydrogel Nanocomposite Reinforced with Montmorillonite Clay. New Journal of Chemistry 42(4), 2758-2766.

Oyerinde, O.F., Weeks, C.L., Anbar, A.D., Spiro, T.G., 2008. Solution Structure of Molybdic Acid from Raman Spectroscopy and DFT Analysis. Inorganica Chimica Acta 361(4), 1000-1007.

Posudievsky, O.Y., Khazieieva, O.A., Koshechko, V.G., Pokhodenko, V.D., 2012. Preparation of Graphene Oxide by Solvent-free Mechanochemical Oxidation of Graphite. Journal of Materials Chemistry 22(25), 12465-12467.

Qu, J., He, X., Chen, M., Hu, H., Zhang, Q., Liu, X., 2017a. Mechanochemical Synthesis of Cu-Al and Methyl Orange Intercalated Cu-Al Layered Double Hydroxides. Materials Chemistry and Physics 191, 173-180.

Qu, J., He, X., Chen, M., Huang, P., Zhang, Q., Liu, X., 2017b. A Facile Mechanochemical Approach to Synthesize Zn-Al Layered Double Hydroxide. Journal of Solid State Chemistry 250, 1-5.

Qu, J., Zhang, Q., Li, X., He, X., Song, S., 2016a. Mechanochemical Approaches to Synthesize Layered Double Hydroxides: A Review. Applied Clay Science 119, 185-192.

Qu, J., Zhong, L., Li, Z., Chen, M., Zhang, Q., Liu, X., 2016b. Effect of Anion Addition on the Syntheses of Ca–Al Layered Double Hydroxide via A Two-step Mechanochemical Process. Applied Clay Science 124-125, 267-270.

Radha, S., Kamath, P.V., 2009. Polytype Selection and Structural Disorder Mediated by Intercalated Sulfate Ions Among the Layered Double Hydroxides of Zn with Al and Cr. Crystal Growth and Design 9(7), 3197-3203.

Reddy, G.D., Alston, A.M., Tiller, K.G., 1981. Effects of Fertilizer on Concentrations of Copper, Molybdenum, and Sulfur in Subterrranean Clover (Trifolium Subterraneum). Australian Journal of Experimental Agriculture 21(112), 491-497.

Reichle, R.A., McCurdy, K.G., Hepler, L.G., 1975. Zinc Hydroxide: Solubility Product and Hydroxy-complex Stability Constants from 12.5–75 C. Canadian Journal of Chemistry 53(24), 3841-3845.

Reisenauer, H.M., 1963. Relative Efficiency of Seed-and-Soil-Applied Molybdenum Fertilizer. Agronomy Journal 55(5), 459-460.

Rudmin, M., Banerjee, S., Yakich, T., Tabakaev, R., Ibraeva, K., Buyakov, A., Soktoev, B., Ruban, A., 2020. Formulation of a Slow-release Fertilizer by Mechanical Activation of Smectite/glauconite and Urea Mixtures. Applied Clay Science 196, 105775.

Said, A., Zhang, Q., Qu, J., Liu, Y., Lei, Z., Hu, H., Xu, Z., 2018. Mechanochemical Activation of Phlogopite to Directly Produce Slow-release Potassium Fertilizer. Applied Clay Science 165, 77-81.

Santosa, S.J., Sudiono, S., Wibawani, R.S., 2020. Solvent-free Mechanochemically Synthesized Zn Layered Hydroxide Salts for the Adsorption of Naphtholate AS Dye. Applied Surface Science 506, 144930.

Schulin, R., Johnson, A., Frossard, E., 2010. Trace Element-Deficient Soils, Trace Elements in Soils. pp. 175-197.

Shao, M., Ning, F., Wei, M., Evans, D.G., Duan, X., 2014. Hierarchical Nanowire Arrays Based on ZnO Core−Layered Double Hydroxide Shell for Largely Enhanced Photoelectrochemical Water Splitting. Advanced Functional Materials 24(5), 580-586.

Stanimirova, T., Kerestedjian, T., Kirov, G., 2017. Dehydration and Rehydration of Zn-hydroxy Sulfate Minerals with Interrupted Decorated Hydroxide Sheets. Applied Clay Science 135, 16-26.

Stepanova, L.N., Kobzar, E.O., Leont'eva, N.N., Gulyaeva, T.I., Vasilevich, A.V., Babenko, A.V., Serkova, A.N., Salanov, A.N., Belskaya, O.B., 2022. Study of the Chemical and Phase Transformations in the Mechanochemical Synthesis of the MgAl-Layered Double Hydroxide. Journal of Alloys and Compounds 890, 161902.

Suchanek, W.L., Byrappa, K., Shuk, P., Riman, R.E., Janas, V.F., TenHuisen, K.S., 2004. Mechanochemical-hydrothermal Synthesis of Calcium Phosphate Powders with Coupled Magnesium and Carbonate Substitution. Journal of Solid State Chemistry 177(3), 793-799.

Szabados, M., Mészáros, R., Erdei, S., Kónya, Z., Kukovecz, Á., Sipos, P., Pálinkó, I., 2016. Ultrasonically-enhanced Mechanochemical Synthesis of CaAl - Layered Double Hydroxides Intercalated by a Variety of Inorganic Anions. Ultrasonics Sonochemistry 31, 409-416.

Temuujin, J., Okada, K., MacKenzie, K.J.D., 1998. Role of Water in the Mechanochemical Reactions of MgO–SiO_2 Systems. Journal of Solid State Chemistry 138(1), 169-177.

Thomas, N., 2012. Mechanochemical Synthesis of Layered Hydroxy Salts. Materials Research Bulletin 47(11), 3568-3572.

Tongamp, W., Zhang, Q., Saito, F., 2007. Preparation of Meixnerite (Mg–Al–OH) Type Layered Double Hydroxide by a Mechanochemical Route. Journal of Materials Science 42(22), 9210-9215.

Tongamp, W., Zhang, Q., Saito, F., 2008. Mechanochemical Route for Synthesizing Nitrate form of Layered Double Hydroxide. Powder Technology 185(1), 43-48.

Torres-Dorante, L.O., Lammel, J., Kuhlmann, H., 2009. Use of a Layered Double Hydroxide (LDH) to Buffer Nitrate in Soil: Long-term Nitrate Exchange Properties under Cropping and Fallow Conditions. Plant and Soil 315(1), 257-272.

Vieira, R.F., Cardoso, E.J.B.N., Vieira, C., Cassini, S.T.A., 1998. Foliar Application of Molybdenum in Common Beans. I. Nitrogenase and Reductase Activities in a Soil of High Fertility. Journal of Plant Nutrition 21(1), 169-180.

Wang, X.-F., Liu, S.-Q., Li, S.-P., 2015. Methotrexatum Intercalated Layered Double Hydroxides: Statistical Design, Mechanism Explore and Bioassay Study. Materials Science and Engineering: C 49, 330-337.

Wang, Z., Li, H., Chen, H., Lv, J., Leng, H., Xiao, J., Wang, S., 2021. Effects of Grinding and Dehydration on Kaolin in a Steam Jet Mill. Clay Minerals 56(1), 75-84.

Wu, Z., Wang, D., Sun, A., 2010. Preparation of MoS2 by a Novel Mechanochemical Method. Journal of Alloys and Compounds 492(1), L5-L7.

Yang, H., Du, C., Hu, Y., Jin, S., Yang, W., Tang, A., Avvakumov, E.G., 2006. Preparation of Porous Material from Talc by Mechanochemical Treatment and Subsequent Leaching. Applied Clay Science 31(3), 290-297.

Zhai, B.-g., Ma, Q.-l., Yang, L., Huang, Y.M., 2017. Synthesis and Optical Properties of Tb-doped Pentazinc Dimolybdate Pentahydrate. Results in Physics 7, 3991-4000.

Zhang, Yanagisawa, K., 2007. Hydrothermal Synthesis of Zinc Hydroxide Chloride Sheets and Their Conversion to ZnO. Chemistry of Materials 19(9), 2329-2334.

Zhang, Q., Saito, F., 2009. Mechanochemical Synthesis of Slow-Release Fertilizers through Incorporation of Alumina Composition into Potassium/Ammonium Phosphates. Journal of the American Ceramic Society 92(12), 3070-3073.

Zhang, X., Li, S., 2013. Mechanochemical Approach for Synthesis of Layered Double Hydroxides. Applied Surface Science 274, 158-163.

Zimmer, W., Mendel, R., 1999. Molybdenum Metabolism in Plants. Plant Biology 1(02), 160-168.

Supporting information

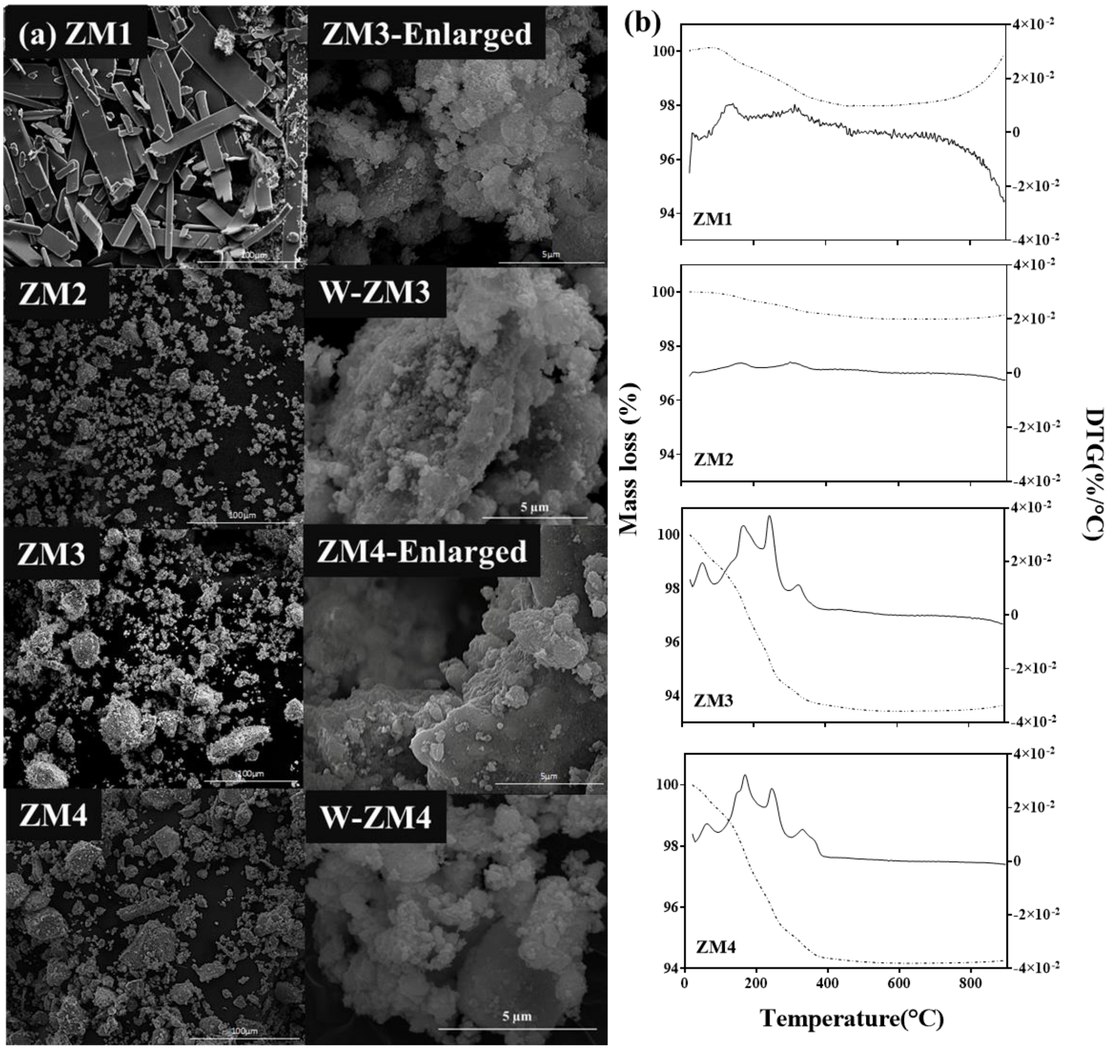

Figure S 4.1 (a) SEM images of ZM1-4 and enlarged ZM3, ZM4, W-ZM3 and W-ZM4; and (b) TGA and DTG curves of ZM1-4.

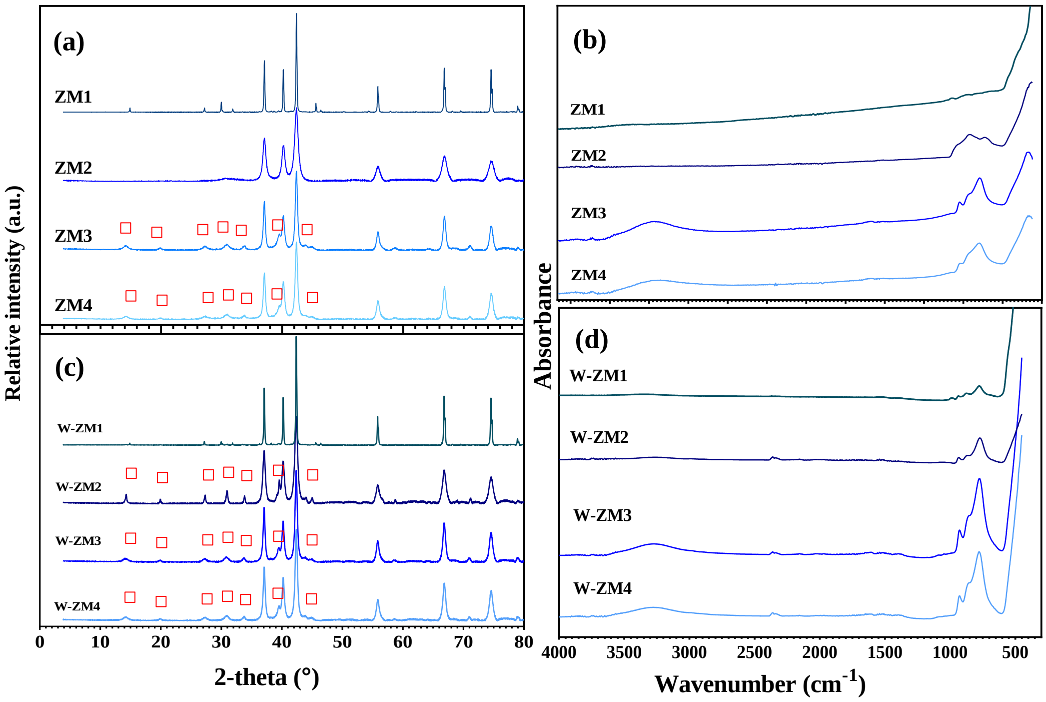

Figure S 4.2 XRD patterns of (a) ZM1-4 products and (b) the washed ZM products (W-ZM1-4); and FTIR spectra of (c) ZM products and (d) W-ZM products. The peaks indicated with a □ are assigned to $Zn_5Mo_2O_{11}\cdot 5H_2O$.

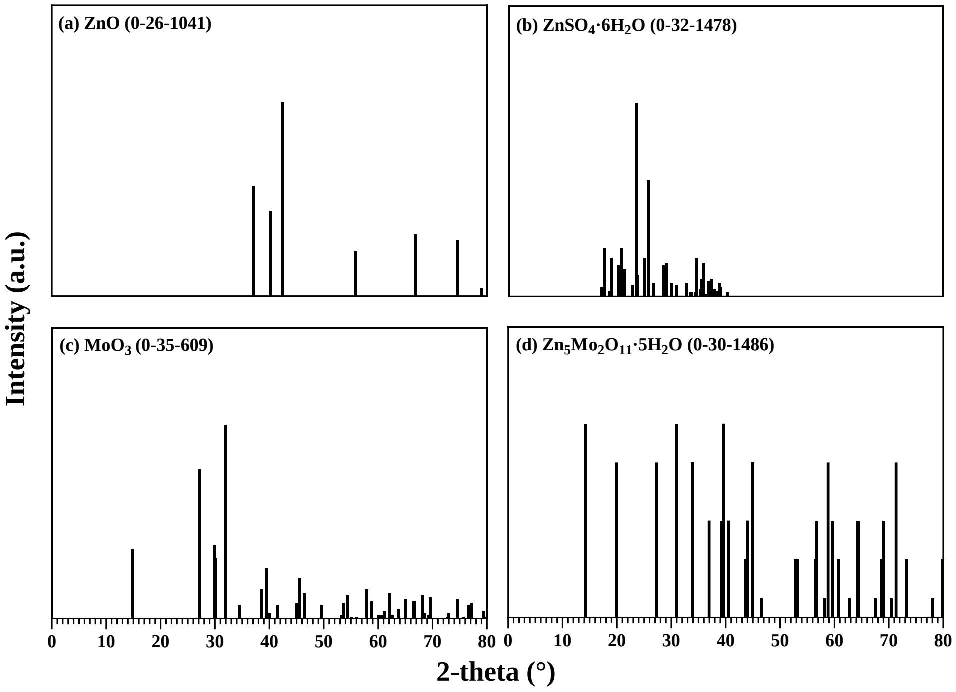

Figure S 4.3 Theoretical XRD patterns of reactants (a) ZnO, (b) $ZnSO_4\cdot 6H_2O$, (c) MoO_3 and (d) $Zn_5Mo_2O_{11}\cdot 5H_2O$.

Chapter 5 Co-granulation of Mechanochemically Processed MoO_3-ZnO Mixtures with Macronutrient Fertilizer Affects Mo Supply to Plants

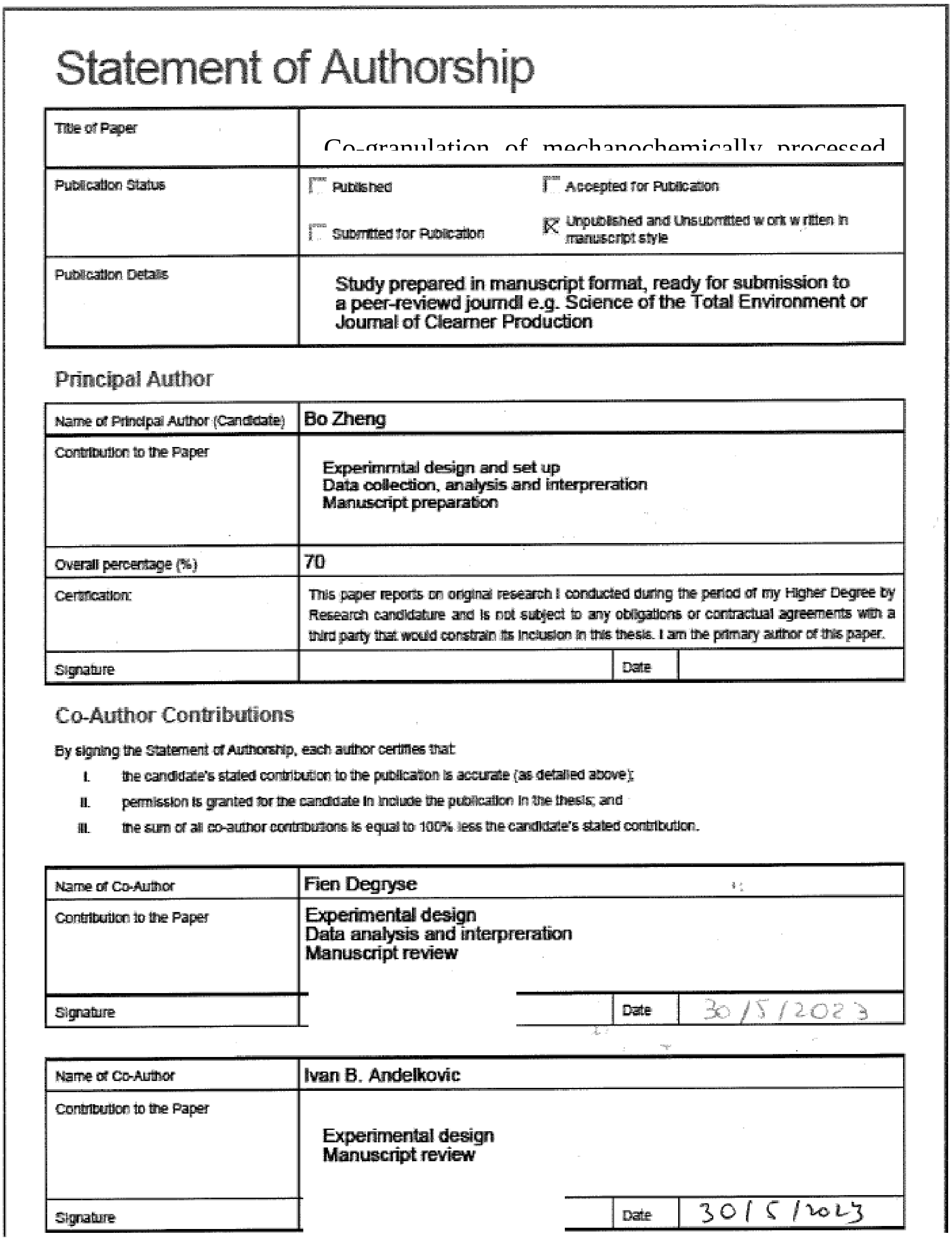

Statement of Authorship

Title of Paper	Co-granulation of mechanochemically processed
Publication Status	☐ Published ☐ Accepted for Publication ☐ Submitted for Publication ☒ Unpublished and Unsubmitted work written in manuscript style
Publication Details	Study prepared in manuscript format, ready for submission to a peer-reviewd journdl e.g. Science of the Total Environment or Journal of Clearner Production

Principal Author

Name of Principal Author (Candidate)	Bo Zheng		
Contribution to the Paper	Experimmtal design and set up Data collection, analysis and interpreration Manuscript preparation		
Overall percentage (%)	70		
Certification:	This paper reports on original research I conducted during the period of my Higher Degree by Research candidature and is not subject to any obligations or contractual agreements with a third party that would constrain its inclusion in this thesis. I am the primary author of this paper.		
Signature		Date	

Co-Author Contributions

By signing the Statement of Authorship, each author certifies that:

i. the candidate's stated contribution to the publication is accurate (as detailed above);
ii. permission is granted for the candidate in include the publication in the thesis; and
iii. the sum of all co-author contributions is equal to 100% less the candidate's stated contribution.

Name of Co-Author	Fien Degryse		
Contribution to the Paper	Experimental design Data analysis and interpreration Manuscript review		
Signature		Date	30/5/2023

Name of Co-Author	Ivan B. Andelkovic		
Contribution to the Paper	Experimental design Manuscript review		
Signature		Date	30/5/2023

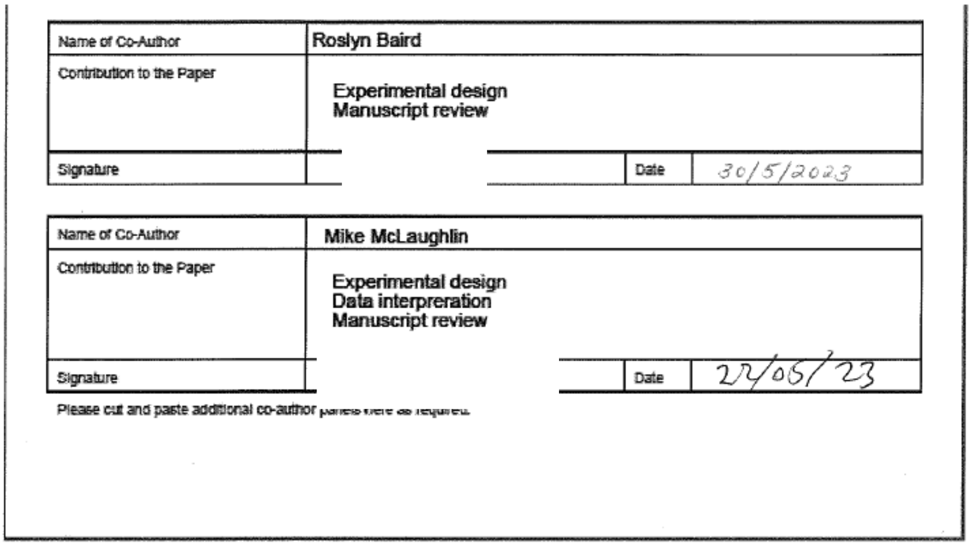

Name of Co-Author	**Roslyn Baird**		
Contribution to the Paper	**Experimental design** **Manuscript review**		
Signature		Date	30/5/2023

Name of Co-Author	**Mike McLaughlin**		
Contribution to the Paper	**Experimental design** **Data interpreration** **Manuscript review**		
Signature		Date	24/05/23

Please cut and paste additional co-author panels here as required.

Abstract

Molybdenum (Mo) is one of the essential micronutrients required for plant growth but is easily leached from neutral and alkaline soils. The use of slow-release Mo sources could potentially reduce leaching losses from soils and increase crop yields. In this study, we assessed mechanochemical synthesis as a green method to produce slow-release Mo sources. Molybdenum compounds (MoO_3 or $(NH_4)_6Mo_7O_{24}\cdot 4H_2O$) were mechanochemically treated (8-h ball milling) with ZnO to achieve compounds with a Mo content of 1-36%. The compounds made with MoO_3 had reduced solubility, while the compounds made with ammonium molybdate were highly soluble and therefore not included for further assessment. Macronutrient pellets were compacted with 4 % Mo and 36 % Mo (characterized as $ZnMoO_4$) for agronomic comparisons. A column dissolution test showed that the 4% Mo compound in a macronutrient carrier (DAP and MAP) only released around 40% of added Mo compared to ~80% for a non-mechanochemically treated control. Column leaching with two soils revealed that the release behaviour of Mo was strongly related to the pH of the leachate, which was affected by both the soil pH and the macronutrient carrier. More Mo was released when co-compacted with diammonium phosphate (DAP) compared to monoammonium phosphate (MAP). The mechanochemically treated compound with 4% Mo showed significantly less leaching than the control without ball milling in both MAP and DAP treatments. In a pot trial with simulated leaching, the treatment with mechanochemically treated 4% Mo showed higher plant uptake than other Mo sources but only significantly so with DAP as carrier. Overall, our results indicate that the mechanochemically treated compound could be used as a slow-release Mo fertilizer in high-rainfall areas.

5.1 INTRODUCTION

Molybdenum (Mo) and zinc (Zn) are essential nutrients for plant growth (Kaiser et al., 2005). The dominant soluble Mo species in the soil is MoO_4^{2-} (molybdate) and is adsorbed by clay minerals and Fe and Al oxides in acid soils (Goldberg et al., 1996, Goldberg et al., 2002). Unlike most other essential cationic micronutrients (e.g. Cu, Zn), Mo availability decreases with decreasing pH (Gustafsson and Tiberg, 2015). In acidic soils, liming usually rectifies Mo deficiency, as absorbed Mo is released into the soil solution (Walker et al., 1955, Anderson, 1956). However, in areas of high rainfall, Mo levels in soil may be low, due to losses through leaching and runoff (He et al., 2005). Currently used Mo fertilizers are commonly soluble molybdates ($Na_2MoO_4.2H_2O$ and $(NH_4)_6Mo_7O_{24}.4H_2O$). Few studies have examined the use of slow-release Mo sources in fertilizers. A 1960s study reports the use of a Mo glassy frit in a field experiment (Henkens and Smilde, 1966) and found a greater residual effect on crop growth compared to a soluble Mo source. Bandyopadhyay et al. (2008) proposed a Mo-containing long-chain magnesium sodium polyphosphate as a slow-release Mo fertilizer and found increased crop yield over the soluble Mo treatment in a field study. More recently, a layered double hydroxide incorporated with Mo was proposed as a slow-release Mo fertilizer, with urea being a potential carrier to allow Mo speciation to be maintained (Everaert et al., 2021).

Until now, Zn deficiency remains a global health problem. It affects more than 17% of the world’s population (Myers et al., 2015). Zinc fertilizers can be applied by themselves, incorporated with macronutrients or by foliar application (Montalvo et al., 2016). Compared to separate soil or foliar applications, incorporating micronutrients with macronutrients is a more efficient way to reduce labour and spreading costs.

Mechanochemistry is a green manufacturing method that has gained much attention in industrial synthesis recently for alloys, semiconductors, ceramics and pharmaceutical applications (Baláž et al., 2013, James et al., 2012a). Recent mechanochemical approaches to fertilizer synthesis have mainly focused on macronutrient NPK fertilizers. Several studies have been carried out to incorporate NPK nutrients into an inorganic matrix such as a clay mineral or LDH (Borges et al., 2017b, Lei et al., 2018, Tongamp et al., 2008, Zhang and Saito, 2009). Recently, mechanochemical methods have been used to combine alkaline metals with urea in organic co-crystals to produce more stable N fertilizers with reduced volatilization losses (Casali et al., 2018; Casali et al., 2019; Honer et al., 2017; Honer et al., 2018). Only one study reported the mechanochemical incorporation of metal or semi-metal in a fertilizer using a ball mill. Yuan et al. (2014) reported an amorphous glass phase of K-Si-Ca-O produced using CaO, SiO_2, and KOH as reactants. The reactants were milled for 2 h and both the milling speed and the SiO_2 content were adjusted to achieve optimal results. The optimal SiO_2 content was chosen to perform a study of the K release rate versus the milling speed. They concluded that a slow-release K fertilizer can be obtained when the milling speed is above 300 rpm. Overall, few attempts have been made to synthesize micronutrient fertilizers using mechanochemistry (Li et al., 2017, Tang et al., 2021) and most mechanochemically synthesized products have only been tested for water solubility to indicate their effectiveness as slow-release fertilizers. However, solubility tests are not a good indicator of agronomic efficiency in soil. Therefore, it is crucial to agronomically compare newly synthesized fertilizers.

Zinc oxide is one of the cheapest and high analysis sources of Zn widely used in the fertilizer industry. Zinc oxide has low water solubility, but its effectiveness as a fertilizer depends largely on the application method, soil pH, and (if applicable) the macronutrient it is incorporated with (McBeath and McLaughlin, 2014). The efficiency of ZnO is similar or close to that of soluble Zn fertilizers such as $ZnSO_4$ when optimum application methods are selected (Hergert et al., 1984; McBeath and McLaughlin, 2014; Montalvo et al., 2016; Rehm et al., 1980). Molybdenum-doped ZnO and $ZnMoO_4$ have been synthesized by different chemical methods using ZnO and MoO_3 (Wu et al., 2015, Wang et al., 2016, Zhang et al., 2015) and have drawn much attention in the materials engineering industry as semiconductors and photocatalysts (Zhao et al., 2020, Yu et al., 2012). One of the products made was mechanochemically synthesized $ZnMoO_4$ (Mancheva et al., 2011, Zazhigalov et al., 2016). In other industries, mechanochemistry has been proposed to prepare complex metal oxides, doped metal oxide, and metal oxide nanoparticles as functional materials (Zdujić et al., 1992, Tsuzuki, 2021).

In this study, we proposed using mechanochemically treated ZnO and MoO_3 as a new slow-release Mo fertilizer. We aimed to incorporate Mo into a ZnO structure or synthesize a new complex metal oxide. In addition to formulation and characterization, the resulting products were thoroughly assessed agronomically by a) incorporating the Mo products into macronutrients (muriate of potash - MOP, MAP and DAP); b) performing column leaching with a 17-day incubation period using two soils; and c) evaluating the effectiveness of the Mo-incorporated fertilizers in a plant uptake experiment with simulating leaching.

5.2 METHODS

5.2.1 Mechanochemical synthesis and characterisation

Zinc oxide (ZnO, 99.0% puriss) from Sigma-Aldrich (NSW, Australia), molybdenum (VI) oxide (MoO_3, 99.5%) from Merck (VIC, Australia) and ammonium molybdate tetrahydrate ($(NH_4)_6Mo_7O_{24}\cdot 4H_2O$) from Chem-Supply (SA, Australia) were used as received.

Different amounts of $(NH_4)_6Mo_7O_{24}\cdot 4H_2O$ (AMT) or MoO_3 were mixed with ZnO to obtain 3 g mixtures in total with Mo concentrations ranging from 1 to circa 35% as indicated in Table S 5.1 and Table 5.1. The mixtures were milled in a 50 mL zirconia jar with six zirconia balls (15 mm diameter and 10 g per ball) to achieve a weight ratio of the ball to the sample of around 20. Ball milling was carried out in a planetary mill (PM200, Retsch, Haan, Germany) for 8 h at a rotation speed of 550 rpm with a break of 5 min and a change of direction every 30 min to avoid overheating. The milled products were characterized by X-ray diffraction (XRD) and Fourier transform infrared (FTIR) spectroscopy. X-ray diffraction patterns of products and reactants were recorded with an X'Pert Pro multipurpose diffractometer (PANalytical B.V. Almelo, Netherlands) using Fe-filtered Co Kα radiation, automatic divergence slit, 2 ° anti-scatter slit, and fast X'Celerator Si strip detector. The diffraction patterns were recorded in steps of 0.017° 2-theta with a counting time of 0.5 s per step for an overall counting time of approximately 30 min. The relative amounts of the major phases were determined by the Rietveld method using the Bruker TOPAS software package (Bruker BioSpin Corporation, Billerica, MA, USA). Fourier transform infrared spectroscopy measurement was carried out using the attenuated total reflectance (ATR) module on an Alpha FT-IR spectrometer (Bruker Optics, Ettlingen, Germany). The analysis was performed in the middle infrared range (wavenumber from 4000 to 400 cm^{-1}) at a resolution of 4 cm^{-1} and corrected for an air background. The sample was mounted on a platinum platform and covered with a thin layer of foil paper. Each sample was scanned 100 times and the platform was cleaned with lint-free tissue and ethanol between treatments. The morphology of the synthesized products was imaged using field emission scanning electron microscopy (FE-SEM, Quanta 450, FEI, USA).

Table 5.1 The mechanochemical treatments of MoO_3 and ZnO milled with different Zn:Mo ratios for 8 h.

Treatments	**MoO_3 (g)**	**ZnO (g)**	**Mo (%)**	**Zn (%)**	**Zn:Mo**
36% Mo	1.64	1.36	36	36	1
10% Mo	0.45	2.55	10	68	7
8% Mo	0.36	2.64	8	71	9
4% Mo	0.18	2.82	4	76	19
2% Mo	0.09	2.91	2	78	39
1% Mo	0.05	2.95	1	79	79

5.2.2 Fertilizer manufacturing, solubility in water, and column dissolution

The compaction of micronutrient and macronutrient powders was carried out using a pellet press. The selected micronutrient samples were the compounds made using MoO_3 and ZnO with 4% or 36% Mo. Also, a mixture of MoO_3 and ZnO (at 4% Mo) without mechanochemical treatment was included for comparison, as well as a mixture of AMT and $ZnSO_4 \cdot 7H_2O$ as a soluble reference treatment. The macronutrient granules MOP (muriate of potash, KCl), MAP (monoammonium phosphate) and DAP (diammonium phosphate) were ground in a commercial grinder, sieved (<250 μm) and mixed with the Mo products (Table 5.2) before adding 1 mL of DI water to 5 g of mixed powder to form a paste. The paste was placed in a 4-cm diameter die and 9.8 MPa pressure was applied using a pellet press (Simplex 12HJ Templeton Kenlyand Co, IL, USA) to form a single pellet. The pellet was air-dried and cut into small pellets of similar size (2-3 mm square) and weights (around 40 mg)

Table 5.2 The amount of micronutrient compound added to macronutrient fertilizers and final Mo and Zn content in the compacted pellets with MAP, MOP and DAP.

Compound	**Amount of Mo/Zn compound added g per 5 g of Macronutrient**		**Theoretical (%)**		**Label in the column leaching and pot trail**
			Mo	Zn	
4% Mo	0.25		0.2	3.8	MC
Control 4% Mo	0.25		0.2	3.8	C
36% Mo	0.027		0.2	0.2	nd[a]
AMT[b] and $ZnSO_4·7H_2O$	0.019	0.91	0.2	3.8	AMT

[a] nd = not determined as not included in the column leaching test.

[b] AMT - $(NH_4)_6Mo_7O_{24}·4H_2O$

The solubility of the samples was evaluated by weighing 0.1 g of the sample in a 50 mL digestion tube with 10 mL of RO water. Samples were shaken on an end-to-end shaker for 1 h followed by 10 min centrifugation at 4685 g and pH was determined. Samples were filtered through a 0.2-µm syringe filter before analysis. The sediment remaining in the centrifuge tubes was digested overnight at room temperature using *aqua regia* (HNO_3: HCl =1:3 v/v), followed by 45 min of heating at 80° C and 165 min of heating at 125° C in hot block digestion. All samples were analyzed by inductively coupled plasma-optical emission spectrometry (ICP-OES, Avio 200, Perkin Elmer, Waltham, USA) to determine the total content of soluble and insoluble Mo and Zn. Reference materials were used for quality control in all the digestion and ICP tests.

Release of Mo and Zn from these products was tested using the column perfusion method described by Baird et al. (2019). This is a laboratory method that examines the dynamic release of nutrients from fertilizer formulations by continuously perfusing samples with a solution in real time. Previous studies have shown a good correlation between pot, leaching, and seeding toxicity experiments with this method (Abat et al., 2015a, b; da Silva et al., 2018). Compacted pellet samples (0.2 g) were placed between 1 g of glass wool in each polypropylene column (150 mm long × 15 mm diameter). The percolating solution (RO water) was introduced into the column from the bottom using a peristaltic pump at a constant rate of 10 mL h^{-1}. The solutions released from the top of the column were collected every hour for 72 h using a fraction collector (SuperFracTM, Pharmacia, USA). At the end of the study, the residues, the glass wool and the solution remaining in each column were collected and dried in the oven at 90° C until all the liquid vaporized. These residues were digested using hot *aqua regia*, analyzed by ICP-OES, and added to all nutrients released over time to establish the total nutrient in the sample. The nutrient release was expressed as a percentage of this total. All column dissolutions were performed in duplicate.

5.2.3 Leaching in soil

A column leaching experiment was performed to examine the release of Mo from the fertilizers in acid soil and in calcareous soil (for soil properties see Table S2). The columns consisted of syringes (120 mm length, 15 mm diameter) that were filled with a layer of glass wool and 30 g of soil. Around 400 mg of fertilizer (or circa 10 granules) was evenly distributed throughout the soil column. Deionized water was introduced to the column from the bottom to the top using a peristaltic pump at a constant rate. The soil was first saturated until no dry soil was observed; then 30 mL of deionized water was added to leach the column from the top on Day 1 and Day 3 followed by six leaching events with 20 mL of DI water every 2 or 3 days. After each leaching, the column was incubated at a constant temperature (25° C). After the final leaching, the soil in each column was dried in the oven and further homogenized by grinding using a mortar and pestle. The soil was then subsampled and digested to determine total Mo concentrations. The collected and filtered leachate after each leaching and digested soil extract were analyzed using ICP-OES.

5.2.4 Pot trial

The pot trial was conducted in a glasshouse using pure sand as a growth medium. Chickpeas were selected due to the high demand for Mo by legumes. Plastic pots (120 mm diameter and 120 mm height) with a few layers of mesh placed at the bottom were filled with 1 kg of washed sand. For each pot, 5 granules (0.2 g of fertilizer containing around 0.4 mg Mo), corresponding to 0.28 kg Mo ha^{-1} soil assuming a bulk density of 1.4 g cm^{-3}, were placed 4.5 cm equidistantly below the soil surface. Leaching was carried out two days later to allow the dissolution of the fertilizer before leaching. The sand naturally contained around 4% water; therefore, no water was added before leaching. Treatments were randomized with 4 replicates of each treatment using a complete block design generated by GenStat 19th edition. The leaching procedure was performed with DI water. Each pot was leached four times with 350 mL (or a total of approximately 4 pore volumes) of water to mimic heavy rainfall events which could remove soluble Mo from the fertilizer and soil. The leachates of each pot were collected and filtered before the determination of solution pH and Mo concentrations by ICP analysis. After the leaching events, the pots were left in ambient conditions for 3 days before planting. The chickpea (anti-fungi treated) was germinated for 2 days in the dark at a constant temperature (25° C). Germinated seeds (3 seeds per pot) were transplanted 2.5 cm below the soil surface and thinned to 1 after 2 weeks. All pots received 10 mL of basal nutrient solution 5 days after planting and every week during the growing period (7 times in total).

Total amounts of nutrients supplied by the basal nutrient solution were 63 mg N kg^{-1}, 198 mg P kg^{-1}, 250 mg K kg^{-1} 90 mg Ca kg^{-1}, 150 mg S kg^{-1}, 15 mg Mg kg^{-1}, 5 mg Mn kg^{-1}, 5 mg Fe kg^{-1}, 0.5 mg Cu kg^{-1}, 0.05 mg B kg^{-1}, and 0.05 mg Co kg^{-1}. Harvesting was carried out at flowering (stage R1) 7 weeks after planting. Plant shoots were cut 1 cm above the soil surface and roots were collected and washed with DI water. Both roots and shoots were oven dried for 72 h at 60° C for dry mass weight and further ground and digested before ICP analysis for Mo content.

For statistical analysis, one-way and two-way ANOVA (analysis of variance) was used for the pot trial followed by Duncan's multiple range test (MRT) to check significant differences using GenStat 19th. Where needed, the data were log-transformed to homogenize variance.

5.3 RESULTS AND DISCUSSION

5.3.1 Solubility of mechanochemically treated Mo-ZnO and characterisation of materials

The batch solubility test was conducted to assess the solubility of the mechanochemically treated MoO_3-ZnO products from both AMT and MoO_3 (1 %, 2 %, 4 %, 8 %, 10 % and 33/36 % Mo). In addition, we also tested the 4% and 36% Mo-Control, which had the same MoO_3-ZnO mixture but without ball milling. The measured total Mo content was close to the expected content for both AMT and MoO_3 treatments (Table S 5.3). Molybdenum release was much higher for the AMT than for the MoO_3 treatments (

Figure **5.1**a). Molybdenum solubility increased with increasing Mo content for both MoO_3 and AMT treatments up to a Mo content of 10%, where all Mo was dissolved for the AMT treatment and ~30% for the MoO_3 treatment. At the highest Mo content (33%), Mo in the AMT treatment was fully dissolved, while the solubility for the MoO_3 (36 % Mo) treatment was lower than the treatment with 10% Mo. This is likely due to the formation of new compounds. The 4% and 36% Mo control treatments (without mechanochemical processing) released more than twice the Mo compared to the mechanochemically treated samples. Given the high solubility of the AMT compounds, only compounds made with MoO_3 were further evaluated. The 4% Mo was selected because of its suitable Zn/Mo ratio for agronomic purposes (ratio similar to that of common Zn/Mo fertilizer rates) and the 36% Mo because newly formed compounds were found in this material (see further)

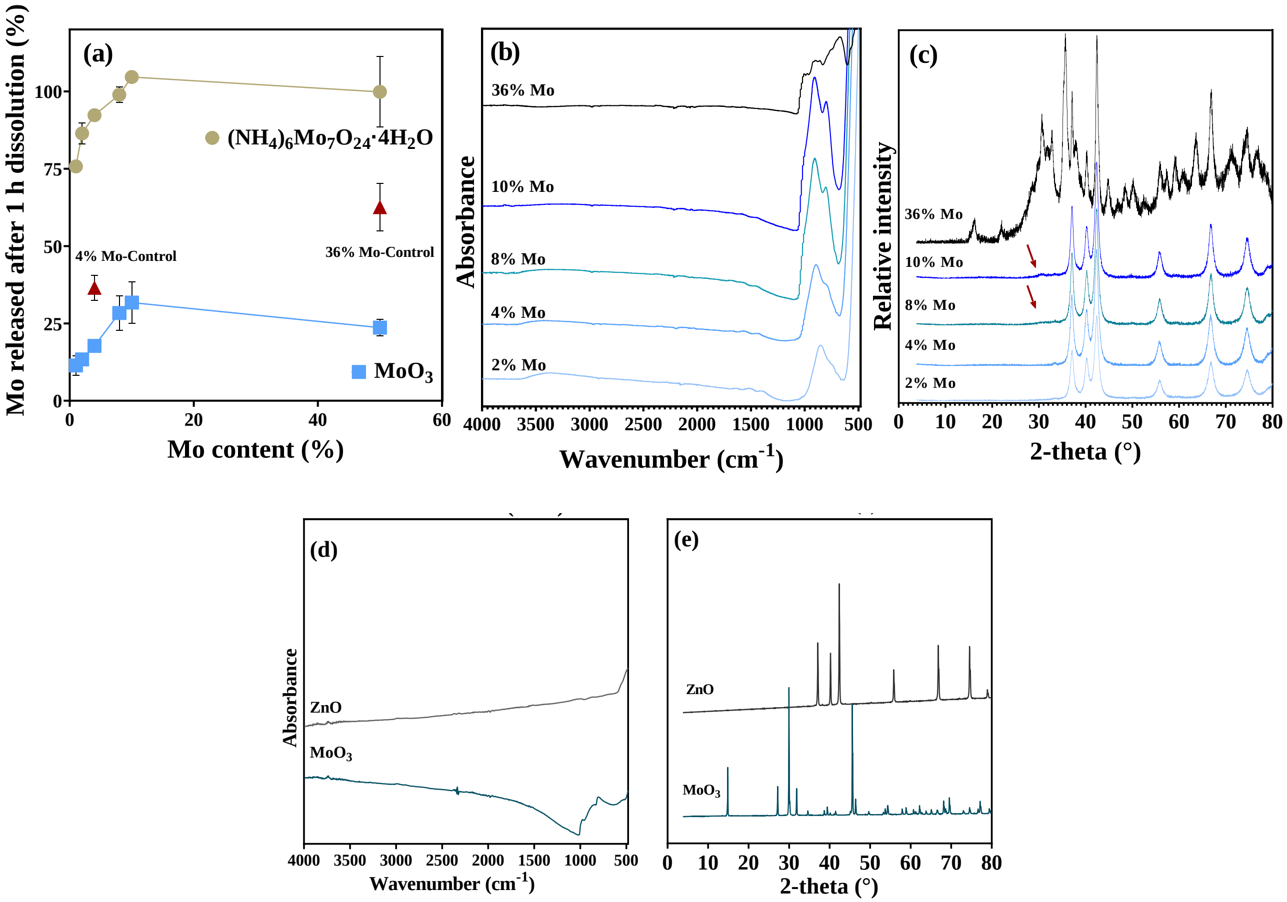

Figure 5.1 a) Solubility of Mo for mechanochemically treated ZnO with different amounts of MoO_3 and $(NH_4)_6Mo_7O_{24}\cdot 4H_2O$ after 1 h equilibration in water; b) FTIR and c) XRD spectrum of mechanochemically treated ZnO with different amounts of MoO_3; d) FTIR and e) XRD of the reactants.

The FTIR spectra of mechanochemically treated samples showed a different pattern compared to the reactants, ZnO and MoO_3 (

Figure **5.1**b, d) as increased Mo content modified the peak intensity and position. The peak at 851 cm^{-1} in the 2 % Mo sample shifted to 899 cm^{-1} at 4 % Mo and split to a shoulder peak at 909 and 806/798 cm^{-1} for the 8 % and 10% formulations. The peaks at 851, 899 and 909 cm^{-1} are likely ascribed to the Mo-O-Mo vibration of Mo^{6+} in $[MoO_4]$ clusters (Chen et al., 2010). The shoulder peaks observed in the 8 and 10 % Mo at 806 and 789 cm^{-1} could be assigned to antisymmetric stretching of Mo-O (Yadav and Sinha, 2019). Characteristic peaks of MoO_3 (

Figure **5.1**d) and Zn-O-Mo (1100-1400 cm^{-1}) were not observed in the 2%-10% Mo samples (Yu et al., 2012). The FTIR spectra of the 36% Mo sample are in line with the FTIR spectra of $ZnMoO_4$ reported in an earlier study (Yadav and Sinha, 2019). It can be concluded that the bond has been altered with increasing Mo content after ball milling.

The X-ray diffraction peaks of the samples agree well with the FTIR results. The six clear peaks in the samples incorporated with 2-10 % MoO_3 could be assigned to the wurtzite phase of ZnO (

Figure **5.1**c), but they were broader than in the control samples (Yu et al., 2012). In the control samples, the peaks assigned to MoO_3 were clearly visible even at lower Mo content (Figure S 5.2a), but these peaks completely disappeared in the mechanochemically treated samples with 2-10% of Mo (

Figure **5.1**e). However, a very broad bump was observed around 2 theta = 31 ° when the percentage of Mo increased to 8 % which was in line with the FTIR results where the shoulder peaks appeared. This could be due to an increase in the Mo concentration that shifted the crystal plane (Ali et al., 2019). When the Mo content increased to 36%, in addition to the identifiable ZnO peaks and minor peaks assigned to MoO_3 (Figure S 5.2b), many new peaks assigned to several zinc molybdates and zinc molybdenum oxide were observed (Figure S 5.1) (Wang et al., 2018). A calculation using the Scherrer equation confirmed the decrease of crystallite size to approximately 1.5 to 2.0 nm for low Mo concentration samples after mechanochemical treatment (data not shown) (Patterson, 1939). .Amirkhanlou et al. (2012) reported mechanochemically synthesized nanocrystalline ZnO could reach a particle size around 60 nm after 8 h ball milling and further milling could not further decrease the particle size. Increasing the pressure within the ball milling jar with oxygen could further reduce the particle size to 5 nm (Glushenkov et al., 2008). Therefore, the much smaller crystallite size of ZnO obtained in this study was likely due to smaller Mo^{6+} (0.065 nm) doped into and replacing Zn^{2+} in the ZnO structure, thus suppressing the growth of ZnO crystals (Yu et al., 2012). Overall, these results indicate that the mechanochemically treated samples at a low Mo inclusion rate successfully penetrated the wurtzite crystalline lattice of ZnO, particularly at 2 and 4 % Mo, where no impurity peaks were observed (Umar et al., 2015), while the crystal structure changed at the highest Mo rate (36%) as a result of new compound formation.

5.3.2 Column dissolution of Mo compacted in MAP, MOP, and DAP

All pelletized samples were macronutrient fertilizers containing a final Mo concentration of 0.2%. Both macronutrients (K and P) were quickly released from the formulations and no difference was observed between Mo treatments (Figure S 5.4 a, c). Total Mo released from DAP and MAP was twice as high in the treatments with the 36% Mo compounds, reaching 80 % and 70 % respectively than in those with the 4% Mo compounds (Figure 5.2 a, b). The Mo release for the 4% Mo treatments was half that of the 4% Mo-Control for both the MAP and DAP treatments. The Mo release from MAP + 4 % Mo was slow and constant, while in DAP + 4 % Mo, a dual release was observed where the release was fast in the initial 10 h (39 %), followed by a minor release (3 %) in the following 62 h. In the MOP treatments, more than 80 % of the total Mo was released after 72 h of dissolution. Total Zn release was negligible in most treatments (<6%) over 72 h, except for MOP + 36 % Mo and MAP + 36 % Mo where 70% and 18% of the total Zn was released, respectively. The lower percentage release of Zn in the 4% Mo treatments was likely due to a) formation of more lower Zn solubility compounds when using MAP and DAP as carriers such as NH_4ZnPO_4 and $Zn_3(PO_4)_2$; (Milani et al., 2012) b) the higher Zn content in the 4% Mo treatments compared to the 36% Mo treatments: c) presence of higher amount of more soluble ZnMoO4 in 36% samples compared to ZnO in 4% samples. Overall, the column dissolution indicated that the DAP + 4% Mo and MAP + 4% Mo behaved as slow-release Mo fertilizers. Leaching in soil and a pot trial were performed to further evaluate the agronomic effectiveness of these two treatments.

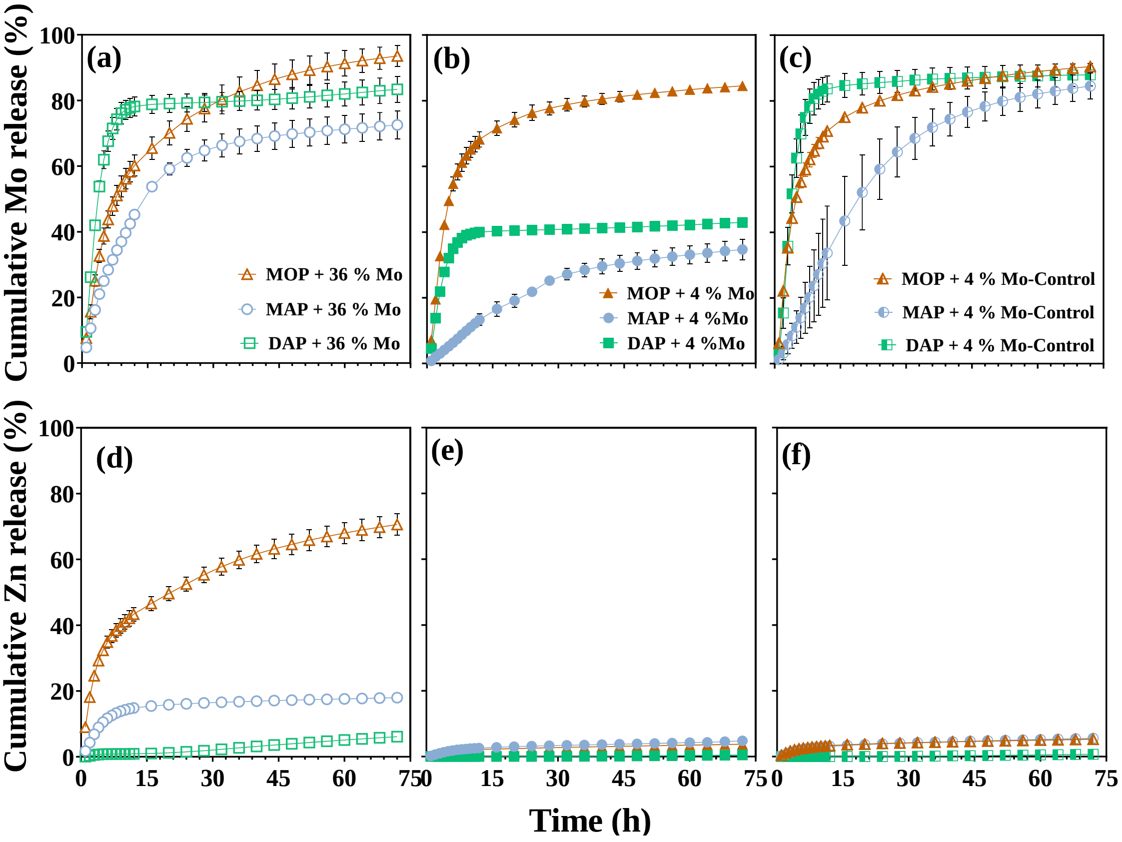

Figure 5.2 The cumulative release over 72 h of (a, b, c) Mo, and (d, e, f) Zn (as % of added) from MAP, MOP and DAP compacted with mechanochemically treated compounds with (a, d) 36 % or (b, e) 4% Mo with or (c, f) compacted with 4% Mo-Control without mechanochemical treatment. Error bars present the standard error of the mean (n = 2).

5.3.3 Molybdenum leaching from fertilizers in soils

Leaching in soil was assessed in two contrasting soils. Four treatments were included in the leaching as indicated in the table of Figure 5.3: a) DAP and MAP alone (no micronutrients added, treatment N) or compacted with b) soluble micronutrients ($(NH_4)_6Mo_7O_{24}\cdot4H_2O$ + $ZnSO_4\cdot7H_2O$, treatment AMT); c) reactants without mechanochemical treatment at 4% Mo (treatment C); and d) mechanochemically treated sample at 4% Mo (treatment MC). For all treatments, Mo incorporated with DAP had a higher Mo release compared to MAP (Figure 5.3). More Mo was leached from the calcareous Streaky Bay soil than from the acid Ngarkat soil except for the DAP + MC treatment. When Mo sources were applied with MAP, the lowest Mo leaching was observed in AMT and MC treatments in both soils, both circa half that of the C treatment. The leached Mo from C was 66% in Ngarkat soil and 93% in Streaky Bay soil at the end of incubation (Figure 5.3 e, f). When Mo sources were applied with DAP, the Mo release was lowest with MC sources compared to C and AMT treatments (Figure 5.3 g, h). Mo leached from MC was approximately 20% lower in Ngarkat soil and 40 % in Streaky Bay soil compared to C and ATM treatments. The Mo release over time in both soils followed the same trend as the pH changes, with an increase in Mo release as the pH of the leachate increased (Figure 5.3a-d). Mo recovered from the residue in the digested soil sample corresponded well with Mo released except for C with DAP in the Ngarkat soil, where no residue was recovered. This may have been due to inhomogeneity of the soil sample or unremovable residues attached to the glass wool. The amount of retained Mo in the soil after leaching was higher for the MC treatment than the other treatments, except with MAP in the Ngarkat soil where AMT and MC retained a similar amount (Figure 5.3 i). The residue of the C treatment was only observed in Ngarkat soil with MAP as the carrier.

Overall, Mo release was affected by the soil, most likely due to differences in the soil pH (Riley et al., 1987). Most treatments had lower Mo recovery in the Streaky Bay soil than in the Ngarkat soil except for MC + DAP. This is consistent with the theory that typical well-drained, near-neutral sandy soils or calcareous soils with organic matter less than 50 g kg^{-1} tend to retain little Mo (Goldberg and Forster, 1998, O'Connor et al., 2001). Moreover, the Mo release from the pellet is also largely affected by the pH induced by the macronutrient carrier. With the same Mo and soil treatment, the Mo release was higher for DAP compared to MAP due to the higher solution pH around DAP granules, except for C treatments where most of the Mo leached out within the first 3 days in the Streaky Bay soil. Due to the lower pH of the leachate in AMT compared to C, the leached Mo was higher for C in all treatments, except the DAP treatments applied in the Streaky Bay soil, where most of Mo leached out by Day 3. Interestingly, the MC and C had a similar pH in the leachate over the 6 leaching events, while the release of Mo was 20-50% lower in MC compared to C treatments regardless of the soil and carriers. The results, therefore, suggest that the MC treatments might be less affected by soil pH compared to the C and AMT treatment.

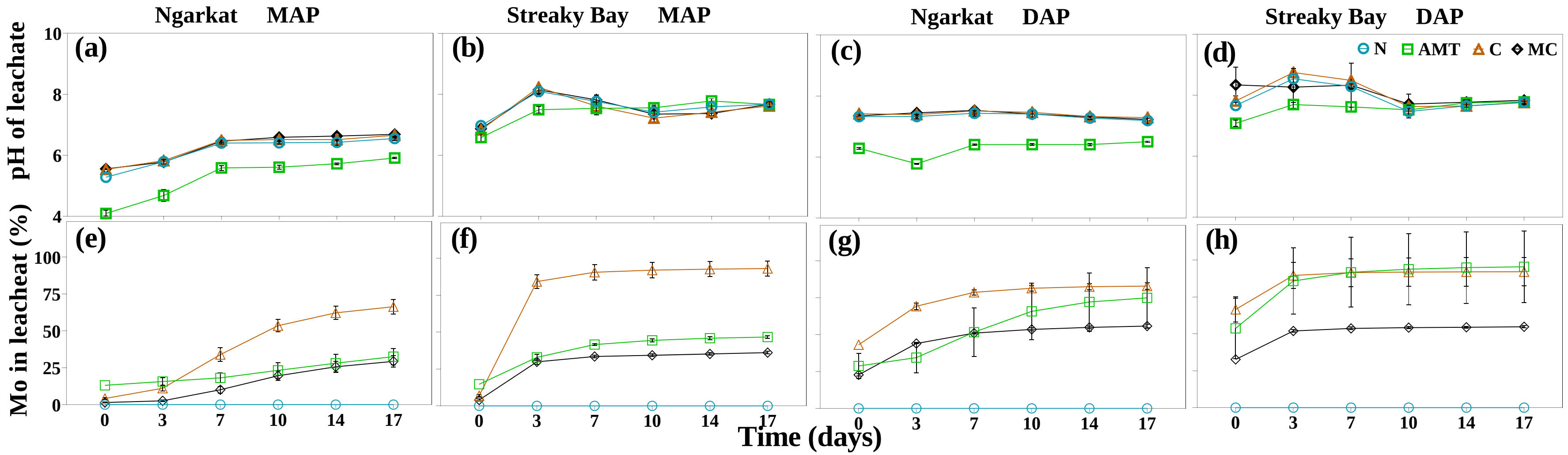

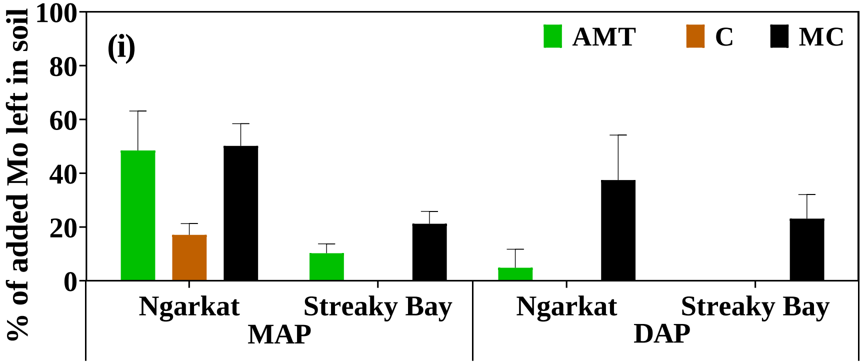

Treatments	**Mo and Zn sources**
N	None
AMT	$(NH_4)_6Mo_7O_{24}\cdot 4H_2O + ZnSO_4\cdot 7H_2O$
C	4% $MoO_3 + ZnO$
MC	Mechanochemically treated 4% $MoO_3 + ZnO$

Figure 5.3 The (a, b, c, d) pH of the leachate and (e, f, g, h) cumulative Mo (% of added Mo) leached from columns at each leaching day from Ngarkat and Streaky Bay soils; the (i) digested residual Mo in the soils after the leaching events. The table indicated the micronutrients added to the treatments and the letter stands for the treatments. Error bars present the standard error of the mean (n = 6).

5.3.4 Pot Trial

More Mo was leached from DAP treatments than from the MAP treatments (Figure 5.4 a, b). The highest recovery of Mo in the leachate was observed in the DAP treatment with C, for which more than 70% of added Mo was found in the leachate (Figure 5.4 b), while only 13% was leached for the corresponding treatment with MAP (Figure 5.4 a). The lowest Mo recovery in leachate was observed in the MAP + MC treatment (5%). When DAP was the carrier, the Mo recovery in leachate from the MC treatment reached 39%. The AMT treatments behaved similarly for both MAP and DAP fertilizers, with 17-25% of the added Mo leached after 4 leaching events. Surprisingly, the Mo leaching from the soluble AMT control treatment was lower than that of the MC treatment for DAP (Figure 5.4 d). This can perhaps be explained by the lower leachate pH for the AMT treatment than for the MC treatment. Furthermore, the pH of leachates was higher for DAP than for MAP across all treatments (Figure 5.4 c, d). In agreement with column leaching, the recovery of Mo in the leachate was closely associated with the pH of the leachate. Leaching of Zn in leachates was observed only in the AMT treatment with MAP as the carrier (Figure S 5.4 a). Despite the use of soluble $ZnSO_4 \cdot 7H_2O$ in the AMT treatment, leaching of Zn from the sandy medium for the AMT treatment with DAP was low, likely due to precipitation of Zn with P compounds, such as NH_4ZnPO_4 and hopeite $(ZnPO_4)_2 \cdot 4H_2O$ (Milani et al., 2012).

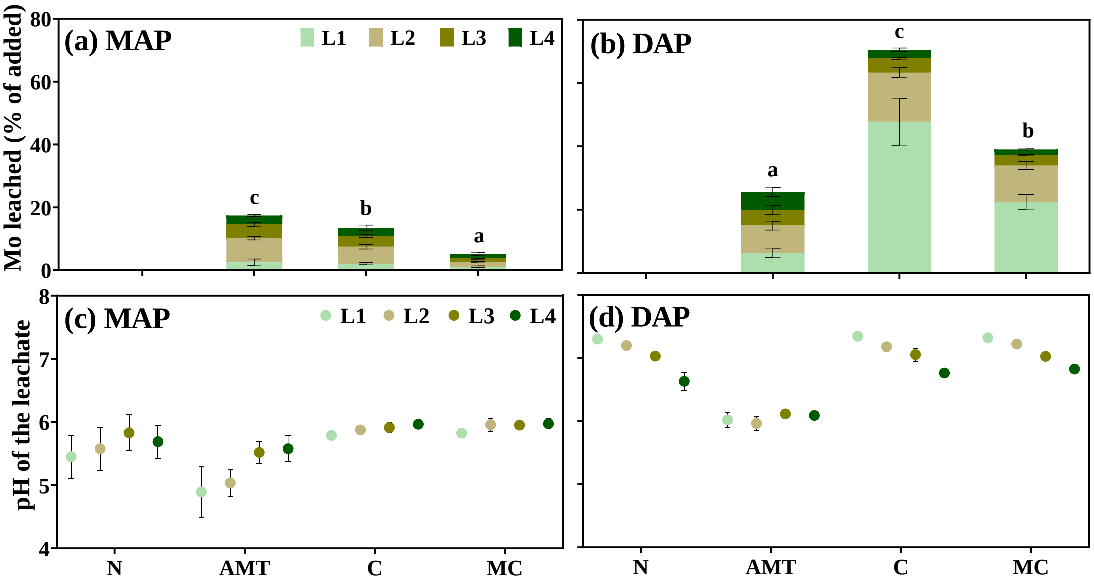

Figure 5.4 (a,b) Amount of Mo recovered in the leachate (as percentage of added) and (c,d) pH of the leachate from MAP or DAP alone (N), or compacted with AMT ($(NH_4)_6Mo_7O_{24}\cdot 4H_2O$ + $ZnSO_4\cdot 7H_2O$), C (4% MoO_3 + ZnO) or MC (mechanochemically treated 4% MoO_3 + ZnO) in the pot experiment collected after 4 consecutive leaching events of one pore volume each (L1 to L4). Error bars present the standard error of the mean (n = 4). Different letters indicate statistical ($P \leq 0.05$) differences between Mo treatments using one-way ANOVA; Duncan's MRT.

The shoot and root dry weights were significantly lower in the DAP+AMT treatment than in the treatment with DAP alone and the shoot dry weight of DAP+MC was significantly higher than the treatment with DAP alone. The lower yield for the DAP+AMT treatment may be due to dissolved Zn^{2+} from $ZnSO_4\cdot 7H_2O$ causing toxicity, (Kaur and Garg, 2021) as the sand had no or minimal cation exchange capacity. In the MAP treatments, there were no significant differences in yield between the treatments (

Figure **5.5** a, d).

For both macronutrient carriers, the effect of Mo addition on Mo concentrations and uptake was much higher in the root than in the shoot (

Figure **5.5** b, c, e and f). The highest shoot Mo concentrations were observed in MAP/DAP + MC and DAP + C treatments (

Figure **5.5** b). The small but detectable Mo shoot concentrations in the N treatments were likely derived from the chickpea seed itself as the pure sand did not contain a detectable amount of Mo. This is in line with other legume growth studies as Mo is essential for N fixation (Rebafka et al., 1993). The root Mo concentration was highest for AMT and MC in the DAP treatments, and highest for MC and C in the MAP treatments (

Figure **5.5** e). The Mo uptake in roots and shoots followed the order MC>C=AMT≥N when DAP was the carrier and MC=C>AMT>N when MAP was the carrier (

Figure **5.5** c, f). The lower Mo uptake observed for the MAP+AMT treatment compared to the other Mo treatments is likely due to a) both AMT and zinc sulphate fertilizer acidifying the soil solution, around roots, thus reducing the Mo uptake (Gammon Jr et al., 1954) and b) Zn^{2+} toxicity. This is supported by the leaching results where AMT treatments had much lower pH than the control and other Mo-added treatments (Figure 5.4 c).

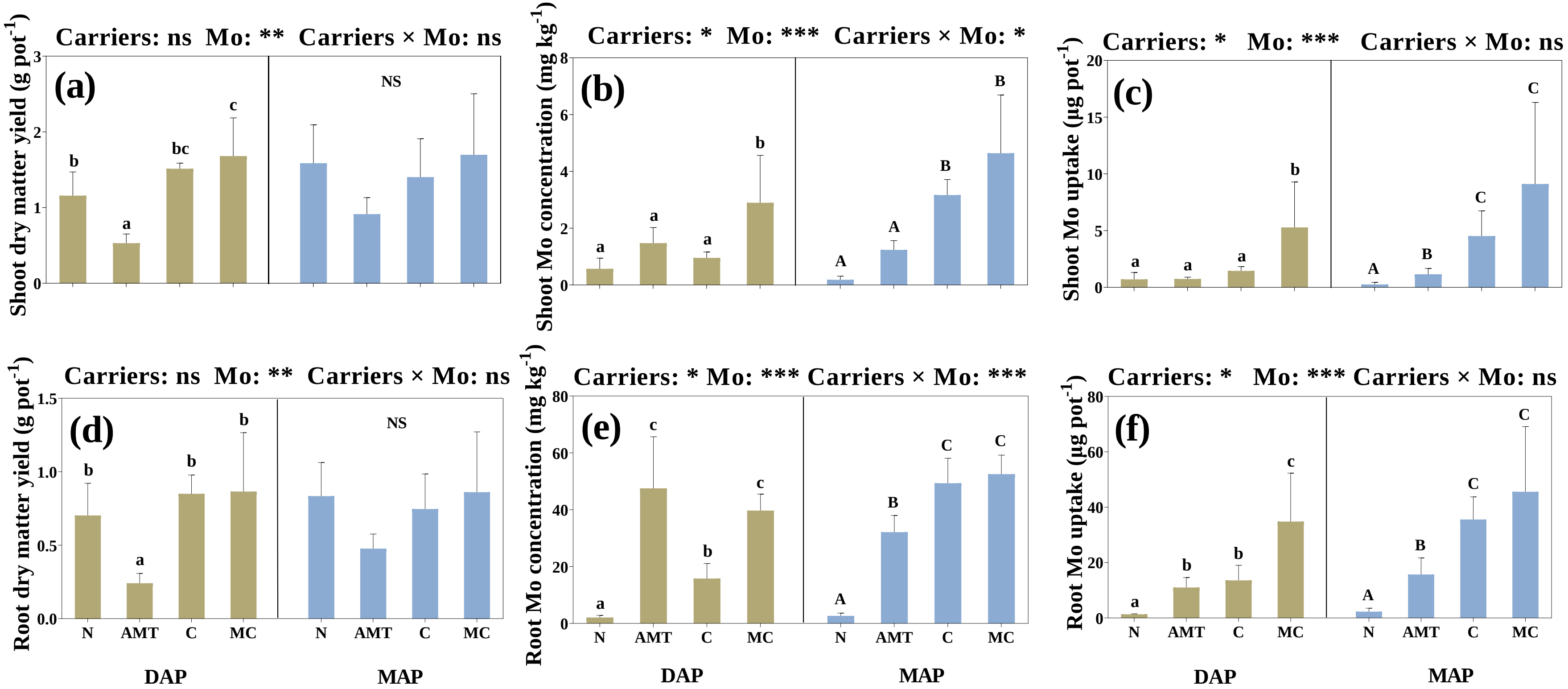

Figure 5.5 (a, d) Shoot and root dry matter yield, (b, e) Mo concentration in the shoots and roots, and (c, f) Mo uptake in shoots and roots of chickpea in response to application of MAP, DAP alone (N) or co-compacted with AMT ($(NH_4)_6Mo_7O_{24}\cdot4H_2O + ZnSO_4\cdot7H_2O$), C (4% MoO_3 + ZnO) or MC (mechanochemically treated 4% MoO_3 + ZnO). Error bars present the standard error of the mean (n = 4). Different letters indicate significant differences between treatments for a given macronutrient carrier - capital letter assigned to MAP and small letter assigned to DAP. Mo treatments (Mo) and their interactions (Carriers × Mo) are indicated by asterisks above each figure (*P ≤ 0.05; **P ≤ 0.01; ***P ≤ 0.001; ns, not significant; using two-way ANOVA; Duncan's MRT).

The availability of Mo is controlled by the pH of the soil solution. Many studies have concluded that liming alone with Mo application can largely promote Mo availability and plant Mo uptake (Hagstrom and Berger, 1963, McBride and Cherney, 2004). In soil, Mo movement or leaching is mainly affected by soil pH. Johansen et al., who conducted a field trial on tropical pasture legumes using MoO_3 and sodium molybdate, reached similar conclusions that soil pH influences Mo movement. Furthermore, they also concluded that there was no difference in residual effects on legume growth between the two Mo sources they applied (Johansen et al., 1977). So, plant uptake of Mo is likely affected by the pH of both the macronutrient carrier and the soil solution, as well as the solubility of the Mo source.

Overall, our results indicate that mechanochemical treatment resulted in slower Mo release and protected Mo against leaching, resulting in higher uptake than for the control (without mechanochemical treatment) when DAP was the carrier. There was no significant difference in plant uptake between the mechanochemical and control treatment when MAP was the carrier, likely because there was less Mo leaching with MAP. However, our experiments were carried out at high fertilizer rates (columns) or with pure sand (pot trial). In field soils with higher pH buffering capacity, the fertilizer carrier would likely have had less effect on the pH and there may have been no Zn toxicity in the soluble reference treatment. Further work is therefore recommended to compare these fertilizer sources in soil systems.

5.4 CONCLUSIONS

The mechanochemical method used in this study did not require water or solvent and did not produce any waste streams. The mechanochemically synthesized Mo-Zn fertilizer was found to be less prone to leaching than currently used Mo fertilizer sources (MoO_3 and $(NH_4)_6Mo_7O_{24}\cdot 4H_2O$). In addition, the lower leaching loss was found to result in higher Mo uptake compared to a non-treated control when DAP was the fertilizer carrier. Therefore, the mechanochemically synthesized Mo-Zn fertilizer has promise as a slow release fertilizer for application in high rainfall areas. To promote this green synthesis method, agronomic comparisons with conventional fertilizers are essential. This study demonstrated the importance of agronomically assessing new fertilizers, especially when examining micronutrients, as micronutrients are required in only small amounts and they are more likely to be affected by other nutrients applied at the same time. The informed selection of macronutrient carriers could greatly change the effectiveness of applied fertilizers. However, pot trials cannot guarantee performance in all agronomic situations. The soils used in this study were sandy soils with a low ability to adsorb Mo, unlike heavier soils where Mo fixation might become a dominant parameter affecting plant Mo uptake. So, further pot and field trials with different soils and climates are required to further evaluate the effectiveness of the synthesized products.

5.5 REFERENCES

Abat, M., Degryse, F., Baird, R., McLaughlin, M.J., 2015a. Boron Phosphates (BPO_4) as a Seedling-safe Boron Fertilizer Source. Plant and Soil 391(1), 153-160.

Abat, M., Degryse, F., Baird, R., McLaughlin, M.J., 2015b. Responses of Canola to the Application of Slow-Release Boron Fertilizers and Their Residual Effect. Soil Science Society of America Journal 79(1), 97-103.

Akiyama, H., Yan, X., Yagi, K., 2010. Evaluation of Effectiveness of Enhanced-Efficiency Fertilizers as Mitigation Options for N_2O and NO Emissions from Agricultural Soils: Meta-analysis. Global Change Biology 16(6), 1837-1846.

Albino, M., Jean-paul, M., Anne-katrin, B., Hugh, E., Fabiana, S., Helena, R.F., 2012. NPK: Will There Be Enough Plant Nutrients to Feed a World of 9 Billion in 2050?

Alloway, B.J., 2009. Soil Factors Associated with Zinc Deficiency in Crops and Humans. Environmental Geochemistry and Health 31(5), 537-548.

Amirkhanlou, S., Ketabchi, M., Parvin, N., 2012. Nanocrystalline/Nanoparticle ZnO Synthesized by High Energy Ball Milling Process. Materials Letters 86, 122-124.

Badruzzaman, M., Pinzon, J., Oppenheimer, J., Jacangelo, J.G., 2012. Sources of Nutrients Impacting Surface Waters in Florida: A Review. Journal of Environmental Management 109, 80-92.

Baird, R., da Silva, R.C., Degryse, F., McLaughlin, M.J., 2019. A Column Perfusion Test to Assess the Kinetics of Nutrient Release by Soluble, Sparingly Soluble and Coated Granular Fertilizers. Journal of Plant Nutrition and Soil Science 182(5), 763-771.

Bandyopadhyay, S., Bhattacharya, I., Ghosh, K., Varadachari, C., 2008. New Slow-Releasing Molybdenum Fertilizer. Journal of Agricultural and Food Chemistry 56(4), 1343-1349.

Blasco, B., Navarro-León, E., Ruiz, J.M., 2018. Chapter 10 - Oxidative Stress in Relation With Micronutrient Deficiency or Toxicity, in: Hossain, M.A., Kamiya, T., Burritt, D.J., Phan Tran, L.-S., Fujiwara, T. (Eds.), Plant Micronutrient Use Efficiency. Academic Press, pp. 181-194.

Capmourteres, V., Adams, J., Berg, A., Fraser, E., Swanton, C., Anand, M., 2018. Precision Conservation Meets Precision Agriculture: A Case Study from Southern Ontario. Agricultural Systems 167, 176-185.

Casali, L., Mazzei, L., Shemchuk, O., Honer, K., Grepioni, F., Ciurli, S., Braga, D., Baltrusaitis, J., 2018. Smart Urea Ionic Co-crystals with Enhanced Urease Inhibition Activity for Improved Nitrogen Cycle Management. Chemical Communications 54(55), 7637-7640.

Casali, L., Mazzei, L., Shemchuk, O., Sharma, L., Honer, K., Grepioni, F., Ciurli, S., Braga, D., Baltrusaitis, J., 2019. Novel Dual-Action Plant Fertilizer and Urease Inhibitor: Urea·Catechol Cocrystal. Characterization and Environmental Reactivity. ACS Sustainable Chemistry & Engineering 7(2), 2852-2859.

Chaney, R.L., Giordano, P.M., 1977. Microelements as Related to Plant Deficiencies and Toxicities, Soils for Management of Organic Wastes & Waste Waters. pp. 233-279.

Chen, T., Deng, J.-C., Wang, L.-S., Feng, G., 2009. Preparation and Characterization of Nano-Zinc Borate by a New Method. Journal of Materials Processing Technology 209(8), 4076-4079.

da Silva, R., Baird, R., Degryse, F., McLaughlin, M.J., 2018. Slow and Fast-Release Boron Sources in Potash Fertilizers: Spatial Variability, Nutrient Dissolution and Plant Uptake. Soil Science Society of America Journal 82(6), 1437-1448.

Daniel, T.C., Sharpley, A.N., Lemunyon, J.L., 1998. Agricultural Phosphorus and Eutrophication: A Symposium Overview. Journal of environmental quality 27(2), 251-257.

Dong, J.X., Hu, Z.S., 1998. A Study of the Anti-wear and Friction-reducing Properties of the Lubricant Additive, Nanometer Zinc Borate. Tribology International 31(5), 219-223.

Everaert, M., Smolders, E., McLaughlin, M.J., Andelkovic, I., Smolders, S., Degryse, F., 2021. Layered Double Hydroxides as Slow-Release Fertilizer Compounds for the Micronutrient Molybdenum. Journal of Agricultural and Food Chemistry 69(48), 14501-14511.

Fageria, N.K., Baligar, V.C., Clark, R.B., 2002. Micronutrients in Crop Production, in: Sparks, D.L. (Ed.) Advances in Agronomy. Academic Press, pp. 185-268.

Fernandez, V., Brown, P.H., 2013. From Plant Surface to Plant Metabolism: the Uncertain Fate of Foliar-applied Nutrients. Frontiers in Plant Science 4.

Gao, Y.-H., Liu, Z.-H., 2009. Synthesis and Thermochemistry of Two Zinc Borates, $Zn_2B_6O_{11}\cdot 7H_2O$ and $Zn_3B_{10}O_{18}\cdot 14H_2O$, Thermochimica Acta 484(1), 27-31.

Gönen, M., Balköse, D., Gupta, R.B., Ülkü, S., 2009. Supercritical Carbon Dioxide Drying of Methanol−Zinc Borate Mixtures. Industrial & Engineering Chemistry Research 48(14), 6869-6876.

Gupta, P.K., 2019. Toxic Effects of Metals and Micronutrients, in: Gupta, P.K. (Ed.) Concepts and Applications in Veterinary Toxicology: An Interactive Guide. Springer International Publishing, Cham, pp. 83-119.

Gupta, U.C., Wu, K., Liang, S., 2008. Micronutrients in Soils, Crops, and Livestock. Earth Science Frontiers 15(5), 110-125.

Hergert, G.W., Rehm, G.W., Wiese, R.A., 1984. Field Evaluations of Zinc Sources Band Applied in Ammonium Polyphosphate Suspension. Soil Science Society of America Journal 48(5), 1190-1193.

Honer, K., Kalfaoglu, E., Pico, C., McCann, J., Baltrusaitis, J., 2017. Mechanosynthesis of Magnesium and Calcium Salt–Urea Ionic Cocrystal Fertilizer Materials for Improved Nitrogen Management. ACS Sustainable Chemistry and Engineering 5(10), 8546-8550.

Honer, K., Pico, C., Baltrusaitis, J., 2018. Reactive Mechanosynthesis of Urea Ionic Cocrystal Fertilizer Materials from Abundant Low Solubility Magnesium- and Calcium-Containing Minerals. ACS Sustainable Chemistry and Engineering 6(4), 4680-4687.

İpek, Y., 2020. Effect of Surfactant Types on Particle Size and Morphology of Flame-retardant Zinc Borate Powder. Turk J Chem 44(1), 214-223.

Jiao, W., Chen, W., Chang, A.C., Page, A.L., 2012. Environmental Risks of Trace Elements Associated with Long-term Phosphate Fertilizers Applications: A Review. Environmental Pollution 168, 44-53.

McBeath, T.M., McLaughlin, M.J., 2014. Efficacy of Zinc Oxides as Fertilisers. Plant and Soil 374(1), 843-855.

Mikula, K., Izydorczyk, G., Skrzypczak, D., Mironiuk, M., Moustakas, K., Witek-Krowiak, A., Chojnacka, K., 2020. Controlled Release Micronutrient Fertilizers for Precision Agriculture – A Review. Science of The Total Environment 712, 136365.

Montalvo, D., Degryse, F., da Silva, R.C., Baird, R., McLaughlin, M.J., 2016. Chapter Five - Agronomic Effectiveness of Zinc Sources as Micronutrient Fertilizer, in: Sparks, D.L. (Ed.) Advances in Agronomy. Academic Press, pp. 215-267.

Mortvedt, J.J., 1985. Micronutrient Fertilizers and Fertilization Practices, in: Vlek, P.L.G. (Ed.) Micronutrients in Tropical Food Crop Production. Springer Netherlands, Dordrecht, pp. 221-235.

Myers, S.S., Wessells, K.R., Kloog, I., Zanobetti, A., Schwartz, J., 2015. Effect of Increased Concentrations of Atmospheric Carbon Dioxide on the Global Threat of Zinc Deficiency: a Modelling Study. The Lancet. Global health 3(10), e639-645.

Rehm, G.W., Wiese, R.A., Hergert, G.W., 1980. Response of Corn To Zinc Source and Rate of Zinc Band Applied with Either Orthophosphate or Polyphosphate. Soil Science 129(1).

Shaviv, A., 2001. Advances in Controlled-Release Fertilizers, Advances in Agronomy. Academic Press, pp. 1-49.

Shaviv, A., Mikkelsen, R.L., 1993. Controlled-release Fertilizers to Increase Efficiency of Nutrient Use and Minimize Environmental Degradation - A Review. Fertilizer Research 35(1), 1-12.

Sheldon, R.A., 2017. The E Factor 25 Years on: the Rise of Green Chemistry and Sustainability. Green Chemistry 19(1), 18-43.

Timilsena, Y.P., Adhikari, R., Casey, P., Muster, T., Gill, H., Adhikari, B., 2015. Enhanced Efficiency Fertilisers: a Review of Formulation and Nutrient Release Patterns. Journal of the Science of Food & Agriculture 95(6), 1131-1142.

Tongamp, W., Zhang, Q., Saito, F., 2008. Mechanochemical Route for Synthesizing Nitrate form of Layered Double Hydroxide. Powder Technology 185(1), 43-48.

Yuan, W., Solihin, Zhang, Q., Kano, J., Saito, F., 2014. Mechanochemical Formation of K–Si–Ca–O Compound as a Slow-release Fertilizer. Powder Technology 260, 22-26.

Zhai, B.-g., Ma, Q.-l., Yang, L., Huang, Y.M., 2017. Synthesis and Optical Properties of Tb-doped Pentazinc Dimolybdate Pentahydrate. Results in Physics 7, 3991-4000.

5.6 SUPPORTING INFORMATION

Table S 5.1 The mechanochemical treatment of AMT and ZnO with different Zn: Mo ratios milled 8h.

	AMT[a]: ZnO treatments				
Treatments	**AMT (g)**	**ZnO (g)**	**Mo %**	**Zn%**	**Zn:Mo**
33% Mo	1.76	1.24	33	33	1.0
10% Mo	0.53	2.47	10	66	6.6
8% Mo	0.42	2.58	8	69	8.6
4% Mo	0.21	2.79	4	75	18.7
2% Mo	0.11	2.89	2	77	38.8
1% Mo	0.05	2.95	1	79	78.9

[a] AMT-$(NH_4)_6Mo_7O_{24}\cdot 4H_2O$

Table S 5.2 The characteristics of the two soils for column leaching.

Characteristics	**Value**	
	Ngarkat	**Streaky Bay**
pH (H_2O: soil -5:1)	6.8	8.6
pH (0.01 M $CaCl_2$: soil - 5:1)	5.3	7.9
Organic carbon (%)	0.7	1.5
Exchangeable K ($cmol_c\ kg^{-1}$)	<0.2	0.6
Exchangeable Ca ($cmol_c\ kg^{-1}$)	2.2	6.3
Exchangeable Mg ($cmol_c\ kg^{-1}$)	0.4	1.4
CEC-Cation Exchange Capacity ($cmol_c\ kg^{-1}$)	3.1	5.8
Clay ($g\ kg^{-1}$)	3	9
Silt ($g\ kg^{-1}$)	1	4
Sand ($g\ kg^{-1}$)	81	15
$CaCO_3$ (%)	<0.2	83

Table S 5.3 Experimentally determined (recovered) and expected Mo and Zn concentration in the mechanochemically synthesized Mo + ZnO treatments.

Treatments	**MoO_3 + ZnO**				**AMT[a] + ZnO**			
	Recovered		**Expected**		**Recovered**		**Expected**	
	Mo%	**Zn%**	**Mo%**	**Zn%**	**Mo%**	**Zn%**	**Mo%**	**Zn%**
36/33% Mo	36.3 ± 2	38.3 ± 2	36	36	30.0 ± 4	29.4 ± 4	33	33
10% Mo	10.1 ± 1	70.1 ± 2	10	68	11.0 ± 1	64.7 ± 5	10	66
8% Mo	8.6 ± 0	74.2 ± 2	8	71	9.0 ± 0	70.1 ± 2	8	69
4% Mo	4.3 ± 0	77.5 ± 1	4	76	4.0 ± 0	74.4 ± 1	4	75
2% Mo	2.1 ± 0	78.1 ± 4	2	78	2.5 ± 0	76.7 ± 5	2	77
1% Mo	1.1 ± 0	77.3 ± 2	1	79	1.3 ± 0	75.8 ± 4	1	79

[a] AMT-$(NH_4)_6Mo_7O_{24}\cdot 4H_2O$

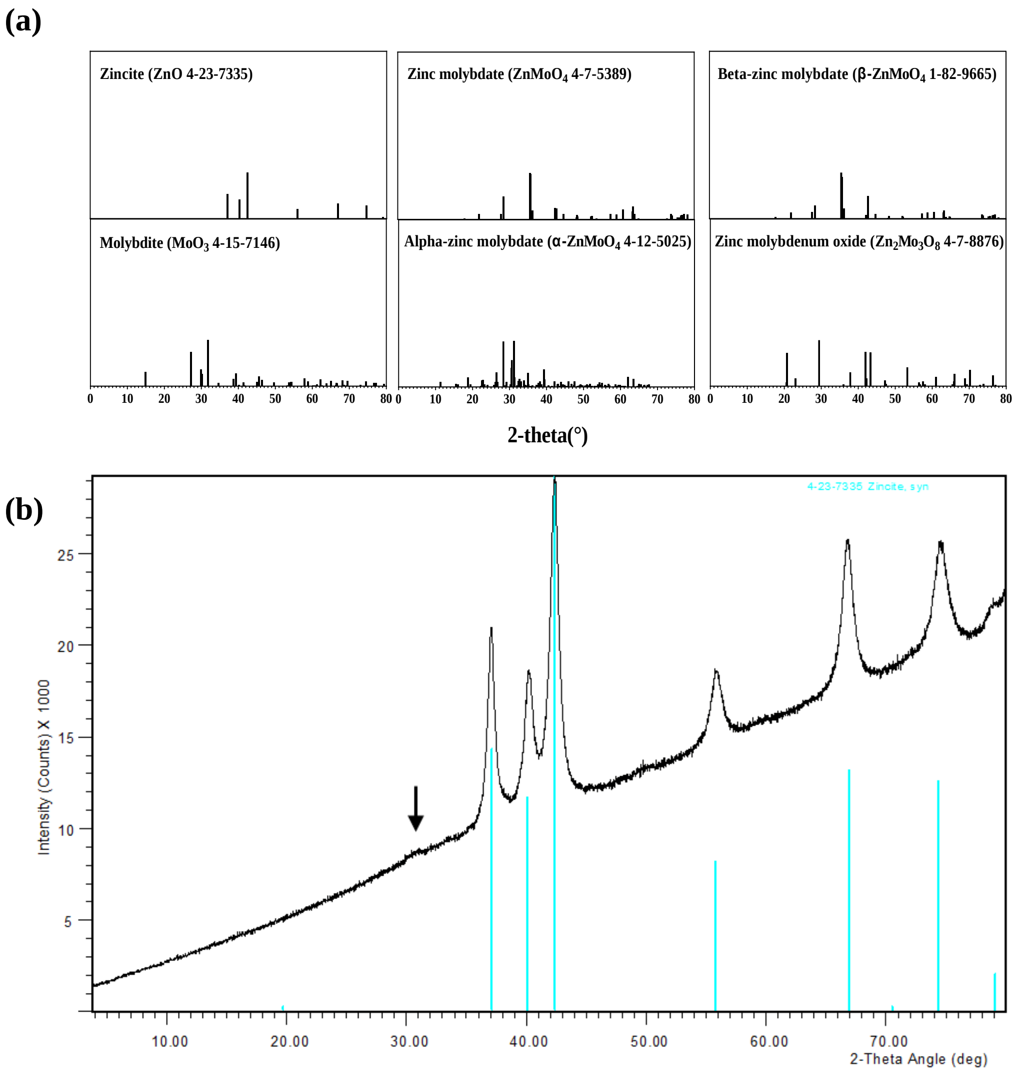

Figure S 5.1 The XRD peaks of the a) theoretical reactants, zinc molybdates and zinc molybdenum oxides; b) XRD pattern of 10% Mo doped ZnO (unstandardized).

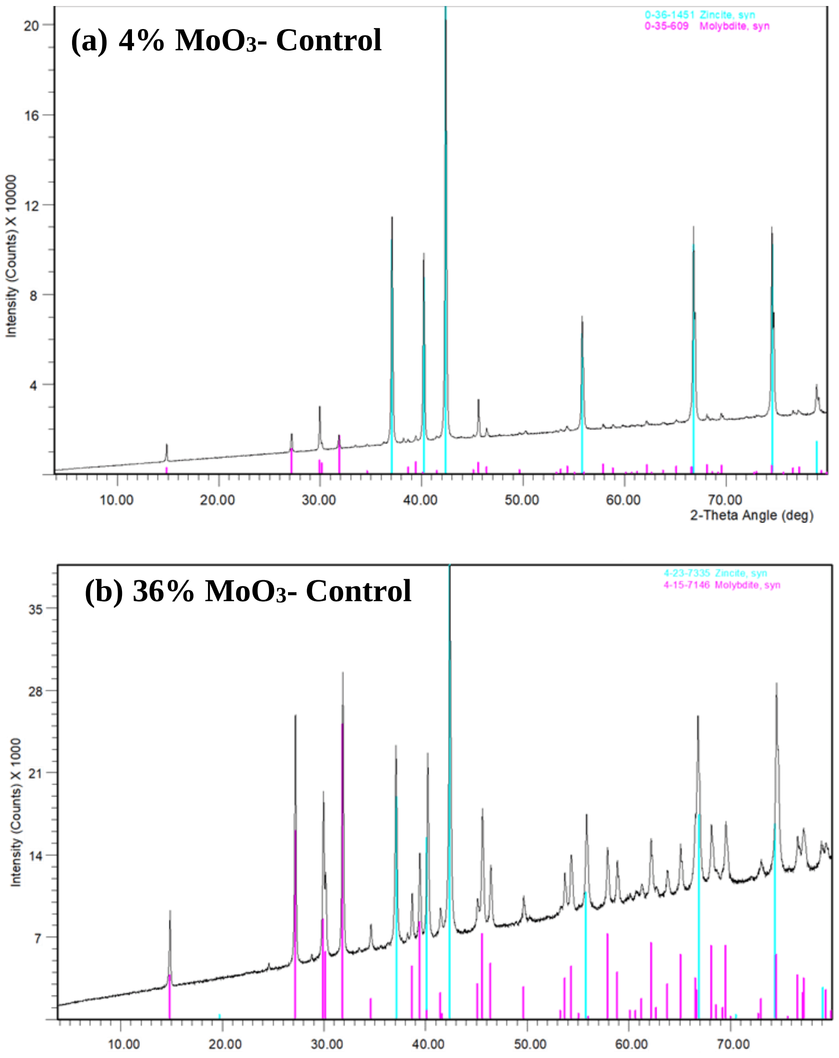

Figure S 5.2 The XRD spectrum of ZnO with (a) 4% and (b) 36% of MoO_3 without mechanochemical treatment as controls.

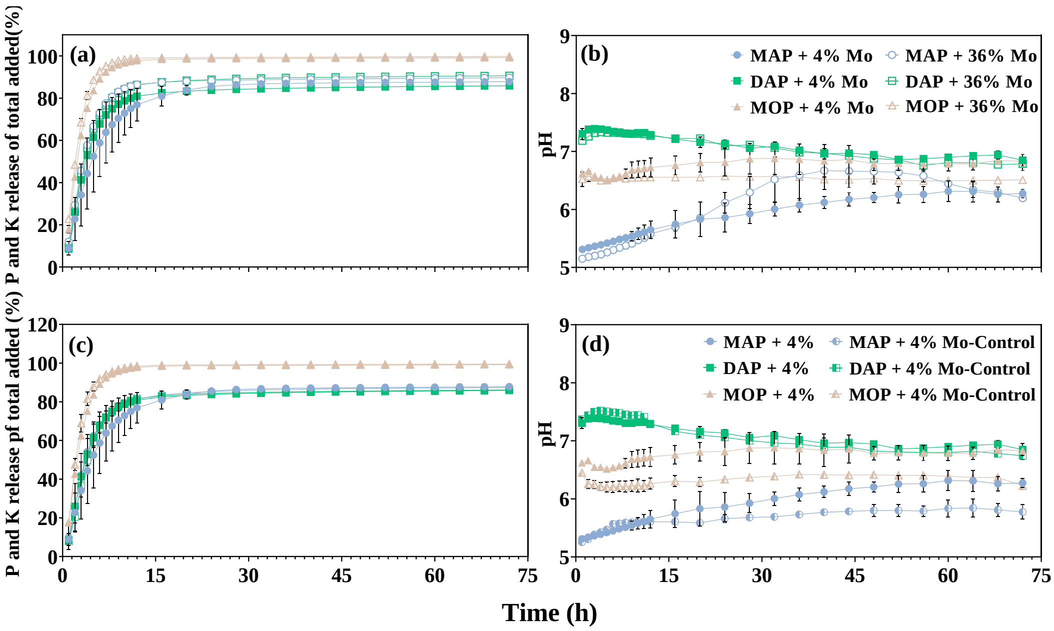

Figure S 5.3 The cumulative release over 72 h of (a, c) P and K (as % of added) and (b, d) pH of the percolation solution at each collection time from MAP, MOP and DAP, compacted with mechanochemically treated 4% and 36% Mo (MoO_3-ZnO) and 4% Mo. The Control was without mechanochemical treatment. Error bars represent standard error of mean (n = 2)

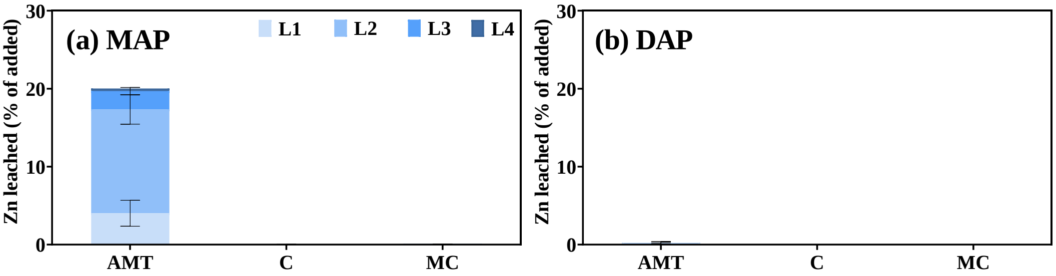

Figure S 5.4 The percentage of total Zn recovered in the leachate from (a) MAP or (b) DAP alone N (no micronutrient source), or compacted with AMT ($(NH_4)_6Mo_7O_{24}\cdot 4H_2O$ + $ZnSO_4\cdot 7H_2O$), C (4% MoO_3 + ZnO) or MC (Mechanochemically treated 4% MoO_3 + ZnO) in the pot experiment collected after 4 consecutive 350 ml leaching events (L1 to L4). Error bars present the standard error of the mean (n = 4).

Chapter 6 Conclusions

6.1 GENERAL CONCLUSIONS AND REFLECTION

Mechanochemistry is an emerging and sustainable synthesis method (Schubert, 2019) that could be beneficial in reducing the carbon footprint and waste stream generation of the fertilizer industry (Ardila-Fierro and Hernández, 2021). Most research in the use of mechanochemistry to synthesize fertilizers has focused on the development of slow-release macronutrient fertilizers. However, micronutrients such as boron (B) and molybdenum (Mo), which have a high risk of leaching or fixation after application, could also benefit from slow release. In addition, mechanochemistry is still in its infancy in the fertilizer industry, and many mechanochemically synthesized materials have been evaluated simply by the solubility of the products rather than using an agronomic approach. Therefore, three gaps could be identified from the literature: a) mechanochemistry has not been used to synthesize B and Mo micronutrient fertilizers; b) the effects of mechanochemical synthesis on the release behaviour of B and Mo micronutrients have not been assessed or compared in the literature; c) there is a lack of agronomic comparison of existing micronutrient fertilizers with mechanochemically synthesized fertilizers.

The main objectives of the present study were to: a) mechanochemically synthesize slow-release B and Mo fertilizers; b) evaluate the release behaviour and identify suitable macronutrient carriers for mechanochemically synthesized B and Mo fertilizers; and c) assess the agronomic effectiveness of the synthesized materials through leaching and pot studies in comparison with existing/commercial B and Mo fertilizers. The major findings of this thesis are summarized below and directions for future work are discussed.

6.2 MAJOR FINDINGS

6.2.1 Mechanochemical synthesis of slow-release micronutrients fertilizer

In Chapters 2, 4 and 5, micronutrient fertilizer formulations were synthesized using mechanochemistry with water-assisted reaction, two-step milling and doping techniques. Three different types of micronutrient fertilizers were synthesized. The products were characterized using methods widely used in chemical engineering, including SEM, FTIR, XRD and TGA. In addition, solubility in water and column dissolution were tested as an initial assessment of the release behaviour.

In Chapter 2, zinc borate was synthesized for the first time as a dual-release B fertilizer using a mechanochemical method employing water-assisted reaction (WAR) with ZnO and B_2O_3 as reactants. The results indicated that the milling time and WAR were essential for synthesizing zinc borate with a high conversion rate, achieved without any waste generation and minimal water use. The water usage in our method was 1.7 g of water per g of product, compared to 77.5 to 250 g of water per g of product for existing methods described in the literature.

In Chapter 4, a layered structure product containing Mo and Zn was synthesized. Slow-release Mo fertilizers could be very beneficial to reduce Mo leaching in alkaline soils and Mo fixation in acidic soils. I first milled ZnO and MoO_3 with minor amounts of water to activate the oxides before adding $ZnSO_4 \cdot 7H_2O$ in the second milling step. This second step was essential to deliver the guest anion and hydroxide groups, in this case, sulphate and crystal water, for the formation of a layered structure. This study aimed to create a slow-release Mo product through incorporation in, or attachment to, the layered compound. The characterization indicated that the products after the washing procedure contain a layered structure compound, identified as zinc hydroxide sulfate (ZHS), together with low solubility zinc molybdenum oxide hydrate ($Zn_5Mo_2O_{11}.5H_2O$) and its less hydrated analogue. Column dissolution indicated that the compounds synthesized after the two-step ball mill could be used as a slow-release Mo source. Compared to reactants containing MoO_3, the product synthesized in this study had a higher pH buffer capacity and maintained its low solubility character over a wider pH range. In other words, this Mo product is less likely to be fixed by acidic soil. However, when coated onto macronutrients, this product lost its slow-release character.

A different approach was therefore used, in Chapter 5, to synthesize a slow-release Mo fertilizer. Different amounts of MoO_3 or $(NH_4)_6Mo_7O_{24}\cdot 4H_2O$ were milled together with ZnO to find the optimum Mo content with the slowest release character. The Mo solubility was lowest with MoO_3 as the reactant, and Mo solubility increased with increasing Mo content up to 10 % Mo and then decreased again for products with 36% Mo. Characterization suggested that when Mo is less than 4%, Mo has likely been doped into ZnO during ball milling, while at the higher Mo contents, transformation to zinc molybdate ($ZnMoO_4$) occurred.

6.2.2 Effect of macronutrient carriers on release behaviour

The performance of the mechanochemically synthesized zinc borate was evaluated against commercial B sources in Chapter 3. Fertilizing crops with B is a challenging practice, as B could be easily leached from soil (Gupta, 1983). Micronutrients are often coated, compacted or co-granulated on macronutrients, to reduce application costs and achieve better field distribution. Thus, we tested various macronutrient carriers to incorporate the mechanochemically synthesized B compounds.

As WAR is an essential step to form zinc borate, we tested whether the WAR could be combined with the coating process. Zinc borate synthesized without or with WAR, commercial zinc borate, colemanite and borax (with ZnO) were used as micronutrient coatings on MAP, MOP and urea by water spraying. However, WAR failed to perform during the coating process. Furthermore, the coating process resulted in a heterogeneous application and all low-solubility B sources lost their slow-release characteristics when coated onto MAP. Therefore, a co-compaction method was used to combine the micronutrients with MOP and urea, for assessment in a leaching and pot study.

Two different mechanochemical approaches were explored in this work for the synthesis of a slow-release Mo fertilizer. In Chapter 4, a two-step method with $ZnSO_4 \cdot 7H_2O$ in the second step was used, and in Chapter 5, a single-step method was employed using oxides only. The former approach aimed to synthesize a layered structure with Mo incorporated or attached to the structure, while the latter aimed to dope Mo into the ZnO structure. These Mo products were incorporated with macronutrients and the release behaviour was tested in a column dissolution study. The results indicated that the Mo products synthesized in Chapter 5 were less soluble than those synthesized in Chapter 4 when combined with macronutrients. This may be due to ion exchange with the layered structure products (Clearfield, 1988, Clearfield, 1995). The layered structure product synthesized in Chapter 4 does not appear to be well-suited for the enrichment of a macronutrient fertilizer but might be effective when applied by itself. Therefore, further leaching and plant studies were only performed with the Mo-doped fertilizers from Chapter 5. These results underline the importance of assessing newly formulated micronutrient fertilizers with the methods applied in agronomic practice. Both the solubility and release pattern of the Mo products dramatically changed after being incorporated with macronutrients.

6.2.3 Agronomic effectiveness of mechanochemically synthesized fertilizer

After mechanochemical synthesis and column dissolution, the most promising fertilizers were further tested in column leaching with soils (Chapter 5) and plant pot trials with simulated leaching (Chapters 3 and 5).

In Chapter 3, I compared canola yield and B uptake with B sources after four heavy leaching events using a sandy soil deficient in B. The plant study confirmed that the mechanochemically synthesized zinc borate could be used as a slow-release B source. Although the concentration and uptake of B per pot were lower in mechanochemically synthesized zinc borate than for the other slow-release B sources, the crop yield was similar for all low-B solubility treatments and higher than with the soluble commercial B source.

In Chapter 5, both the soil column leaching and the pre-planting leaching indicated that MAP was a better macronutrient carrier for all Mo sources than DAP, as the dissolution of DAP largely increased the pH of the leachate and soil solution and hence increased Mo leaching. The mechanochemically treated Mo products had a consistently lower loss of Mo with both carriers compared to the control without mechanochemical treatment. The mechanochemically treated Mo products resulted in higher Mo uptake only when DAP was the carrier. It highlighted the importance of considering the right macronutrient carrier for Mo application with different soils, as soil pH is one of the most important factors controlling Mo availability in practice.

Together, these results emphasize the importance of agronomic evaluation of new potential fertilizers. The mechanochemically synthesized zinc borate and Mo compounds had low solubility alone in the dynamic column dissolution test. However, when applied with other nutrient sources, many other phenomena need to be considered, such as the co-applied macronutrient, the pH and ionic composition of the soil, the climate and the nutrient demand of the plant species.

6.2.4 Water use efficiency, carbon footprint and agricultural sustainability

Overall, mechanochemistry offers an opportunity to transform fertilizer manufacturing methods, but the resultant products need to be evaluated not only for their agronomic and environmental performance and their compatibility with current nutrient delivery systems, but also for their manufacturing footprint. This work presented a novel approach to mechanochemically synthesize B and Mo fertilizers with a low environmental footprint and similar or increased agronomic effectiveness compare to some fertilizer used in the field. For the zinc borate synthesized in Chapter 2, I assessed the sustainability of the manufacturing process using the E factor (Sheldon, 2017) and identified the much lower water usage and waste generated during synthesis compared to conventional manufacturing methods. For the novel Mo-containing compounds I synthesized in Chapters 4 and 5, there was no conventional manufacturing process against which the sustainability of the mechanochemical synthesis could be compared. However, no solid waste or solution was produced during and after the synthesis of these new Mo-containing compounds. In addition, the identified slow-release Mo compounds were used directly after mechanochemical synthesis in fertilizer manufacturing without any further purification.

The strength of my work lies in the connection between green mechanochemical synthesis and agronomic evaluation against commercial products with current fertilizer delivery systems. This work considered the sustainability during fertilizer manufacturing (lower waste streams) and agricultural practice (less leaching and run-off) to promote a greener fertilizer formulation and meet the Sustainable Development Goals (International Fertilizer Industry, 2002).

This study addressed the gaps from several perspectives: a) new formulations of slow-release Mo and B micronutrient fertilizer were proposed; b) evidence was provided to support mechanochemistry as a small-footprint method for fertilizer manufacturing; c) this work revealed the importance of evaluating the agronomic performance of new fertilizer formulations using existing nutrient delivery systems; and d) this work highlighted the importance of agronomic comparison of mechanochemically synthesized fertilizers with traditional fertilizers through soil leaching and plant uptake studies.

6.3 SUGGESTED FUTURE WORK

6.3.1 On mechanochemistry

6.3.1.1 Post-synthesis treatments

In this work, the only post-synthesis treatment carried out was a water-assisted reaction (WAR) on the zinc borates synthesized in Chapter 2. In the literature, various post-synthesis treatments have been described, e.g. hydrothermal treatment, calcination, water agitation, or ultrasonic treatment. These treatments may assist in achieving a higher conversion rate of target compounds, shorter reaction time or more efficient energy utilization. The application of post-synthesis treatments could further optimize the slow-release character of mechanochemically synthesized fertilizers.

6.3.1.2 Scalability of the technology in fertilizer manufacturing

All the products reported in this work were synthesized using laboratory-based mix mills or planetary mills. However, mills used in the fertilizer industry are very different from these laboratory mills. Among the wide range of crushers and mills used in commercial fertilizer plants, the mills used to treat phosphate rock are the most likely to be suited for mechanochemical purposes. Three major mills are used to decrease the particle size of phosphate rock: ring-roller mills (vertical rotating with a horizontal ring), ball mills (horizontal rotating with large steel balls) and table-roller mills (horizontal rotating with spring-loaded rollers). To promote mechanochemistry in fertilizer manufacturing, milling equipment that is already used on an industrial scale in the fertilizer industry should be assessed for its potential for mechanochemical applications.

6.3.2 On agronomic practice

6.3.2.1 Field studies with more plant varieties

The plant trials performed in this study were pot studies in a controlled environment with two plant varieties using simulated leaching and daily watering. The findings are not representative of the much wider climatic conditions, soil types, and plant species presented in agronomic practice. Therefore, field applications with various climates, soil types and plant species are required to further assess newly formulated micronutrient fertilizers.

6.3.2.2 Foliar and seed priming treatments

In this work, we only assessed one method used in the fertilizer industry for micronutrient application, which is incorporated with macronutrients as a fertilizer granule applied before planting. Other common methods used in the fertilizer industry for micronutrient application are foliar and seed priming with soluble salts. These methods are also worth exploring using products synthesized through mechanochemistry, as the particles are generally small, and could be evenly distributed on the surface of seeds or leaves. In addition, processes such as WAR (an essential step for zinc borate synthesis in Chapters 3 and 4) and water agitation could be completed in the solvent before foliar or seed priming applications.

6.3.3 On sustainable practice

6.3.3.1 Using mechanochemically activated material to recycle micronutrients from waste streams

Mechanochemically treated compounds (e.g. serpentine, kaolinite, calcite) have been used as absorbents to recycle useful elements through heavy metal solidification, and wastewater precipitation (Grabias-Blicharz and Franus, 2023, Guo et al., 2010, Nasser and Mingelgrin, 2012). Mechanochemically activated products could potentially be used to recycle the micronutrients from waste streams. For example, the findings of Chapter 2 suggest it might be possible to use mechanochemically activated ZnO to recycle borate from waste streams, as the mechanochemically milled ZnO can react without fully dissolving.

6.3.3.2 Using raw materials to synthesize novel fertilizers

One of the important considerations in this work was to minimize waste when synthesizing or designing new fertilizers. However, all chemicals were purchased from different chemical manufacturers and they would have been extracted, leached or purified with different methods. Therefore, the waste of water or reactants therefore is hard to identify and makes evaluation of sustainability metrics difficult. To maximize the sustainability of mechanochemistry, raw materials such as minerals directly produced by mining could be considered in the future for fertilizer formulations. For example, South Australia could potentially provide Mo minerals such as molybdenite (MoS_2) as potential reactants or fertilizers for further mechanochemical treatment.

6.3.3.3 Cost analysis

For any new technology to be successfully applied in commercial manufacturing, the cost is a big consideration. In this work, sustainability was majorly focused on the waste streams such as water and overused reactants. However, no consideration was made of the cost of the manufacturing process, such as energy and capital costs. As mentioned in the previous section, the chemicals used in this work were purchased from chemical manufacturing which are much more expensive than the chemicals used in fertilizer manufacturing. In further work, a full cost analysis should be carried out as part of a feasibility study.

6.4 REFERENCES

Ardila-Fierro, K.J., Hernández, J.G., 2021. Sustainability Assessment of Mechanochemistry by Using the Twelve Principles of Green Chemistry. ChemSusChem 14(10), 2145-2162.

Clearfield, A., 1988. Role of Ion Exchange in Solid-state Chemistry. Chemical Reviews 88(1), 125-148.

Clearfield, A., 1995. Inorganic Ion Exchangers: A Technology Ripe for Development. Industrial and Engineering Chemistry Research 34(8), 2865-2872.

Grabias-Blicharz, E., Franus, W., 2023. A Critical Review on Mechanochemical Processing of Fly Ash and Fly Ash-derived Materials. Science of The Total Environment 860, 160529.

Guo, X., Xiang, D., Duan, G., Mou, P., 2010. A Review of Mechanochemistry Applications in Waste Management. Waste Management 30(1), 4-10.

International Fertilizer Industry, A., 2002. Industry as a Partner for Sustainable Development, Fertilizer. United Nations Environment Programme.

Li, X., Lei, Z., Qu, J., Li, Z., Zhou, X., Zhang, Q., 2017. Synthesizing Slow-release Fertilizers via Mechanochemical Processing for Potentially Recycling the Waste Ferrous Sulfate from Titanium Dioxide Production. Journal of Environmental Management 186, 120-126.

Nasser, A., Mingelgrin, U., 2012. Mechanochemistry: A Review of Surface Reactions and Environmental Applications. Applied Clay Science 67-68, 141-150.

Said, A., Zhang, Q., Qu, J., Liu, Y., Lei, Z., Hu, H., Xu, Z., 2018. Mechanochemical Activation of Phlogopite to Directly Produce Slow-release Potassium Fertilizer. Applied Clay Science 165, 77-81.

Schubert, D.M., 2019. Hydrated Zinc Borates and Their Industrial Use, Molecules.

Sheldon, R.A., 2017. The E Factor 25 Years on: the Rise of Green Chemistry and Sustainability. Green Chemistry 19(1), 18-43.

Tan, Q., Li, J., 2015. Recycling Metals from Wastes: A Novel Application of Mechanochemistry. Environmental Science and Technology 49(10), 5849-5861.

Tan, Y., Zou, Z., Qu, J., Ren, J., Wu, C., Xu, Z., 2021. Mechanochemical Conversion of Chrysotile Asbestos Tailing into Struvite for Full Elements Utilization as Citric-acid Soluble Fertilizer. Journal of Cleaner Production 283, 12463